6-21-2021 11:15 AM

The Role of Neuronal Nitric Oxide Synthase in Regulating Cerebellar Network Formation Across Murine Development

Vasiliki Tellios, *The University of Western Ontario*

Supervisor: Lu, Wei-Yang, *The University of Western Ontario*

A thesis submitted in partial fulfillment of the requirements for the Doctor of Philosophy degree in Neuroscience

Abstract

The cerebellum is a region of the central nervous system widely known for its role in motor learning and coordination. In the past, mutant mice have been critical in discerning key pathways associated with cerebellar dysfunction and motor deficits. Although a variety of mouse models exist that model the symptoms and pathogenesis of cerebellar ataxia, some have yet to be characterized at the molecular level. Nitric oxide (NO), specifically derived from neuronal nitric oxide synthase (nNOS), is a well-established regulator of synaptic transmission in Purkinje neurons (PNs), governing fundamental processes such as motor learning and coordination. Previous morphological analyses showed similar gross cerebellar structures between neuronal nitric oxide null ($nNOS^{-/-}$) and wild-type (WT) adult male mice, despite prominent ataxic behaviour within $nNOS^{-/-}$ mice. However, a study has yet to characterize potential differences in cerebellar network formation during development in $nNOS^{-/-}$ mice. This thesis study is the first to determine morphological and functional deficits within the cerebellum of $nNOS^{-/-}$ mice using immunostaining, immunoblotting, ex vivo slice culturing, calcium- and sodium-imaging, colourmetric assays and ELISAs. Results from Chapter 2 showed stark PN dendritic abnormalities in $nNOS^{-/-}$ mice compared to WT across development. Specifically, we noted that PN dendritic abnormalities are associated with elevated levels of intracellular calcium via overactivation of metabotropic glutamate receptor type 1 (mGluR1)-initiated store operated calcium entry. Chapter 3 analyses linked the overactivation of mGluR1 in $nNOS^{-/-}$ mice with decreased glutamate uptake via glutamate aspartate transporters (GLAST) on Bergmann glia (BG). Specifically, a lack of NO production resulted in decreased GLAST expression on BG and decreased glutamate uptake. Importantly, Chapter 4 results further demonstrated that the effects of mGluR1 overactivation on PNs specific to $nNOS^{-/-}$ mice resulted in increases in endocannabinoid levels. Specifically, our group noted increases in enzymes downstream of mGluR1 activation and subsequent increases in the endocannabinoid 2-arachidonoylglycerol, as well as decreases in endocannabinoid hydrolyzing enzymes in $nNOS^{-/-}$ cerebella compared to WT. Together, these results are foundational in establishing the $nNOS^{-/-}$ mouse as a model of cerebellar ataxia. Understanding the role of nNOS/NO signaling in cerebellar development may be beneficial in uncovering novel therapeutics for cerebellar disorders.

Keywords

Cerebellum

Neuronal Nitric Oxide Synthase

Nitric Oxide

Purkinje Neuron

Dendritic Morphology

Metabotropic Glutamate Receptor 1

Bergmann Glia

Glutamate/Aspartate Transporter

Excitotoxicity

Endocannabinoids

Lay Abstract

The cerebellum is a brain region associated with the fine-tuning of various movements such as walking, blinking, and balance. In neurodegenerative diseases such as cerebellar ataxia, principal neurons of the cerebellum called Purkinje neurons (PN) begin to malfunction and degenerate, leading to symptoms such as tremors, uncoordinated walking, and loss of balance. Studies on genetically modified mice have helped to gather information on crucial disturbances in cerebellar development that can result in motor deficits similar to those displayed in individuals with cerebellar ataxia. However, some mouse models that present with symptoms of cerebellar ataxia have yet to be characterized at the molecular level. Within the cerebellum, nitric oxide (NO), produced by neuronal nitric oxide synthase (nNOS) is an important gaseous molecule responsible for facilitating PN synaptic firing and motor learning. Despite being abundantly expressed in the cerebellum, previous reports analyzing the nNOS knockout ($nNOS^{-/-}$) mouse revealed no differences in cerebellar anatomy, despite exhibiting deficits in motor behaviour. However, a study has yet to characterize protein-level differences within the cerebellum of $nNOS^{-/-}$ mice across development in comparison to wildtype (WT) mice. The results within this thesis are the first to show differences in $nNOS^{-/-}$ cerebellar development in comparison to WT mice. Specifically, we discovered stark delays in PN dendritic growth in $nNOS^{-/-}$ cerebella across development in comparison to WT. PN dendritic deficits were associated with increases in PN calcium entry caused by overactivation of metabotropic glutamate receptor type 1 (mGluR1) within $nNOS^{-/-}$ mice compared to WT. Overactivation of glutamate receptors is often caused by excess glutamate within the synaptic cleft, and our group showed that $nNOS^{-/-}$ cerebellar astrocytes uptake less glutamate compared to WT cerebellar astrocytes. Specifically, we showed that the glutamate/aspartate transporter (GLAST) is significantly decreased in $nNOS^{-/-}$ cerebella compared to WT across development. Overactivation of mGluR1 is not only responsible for causing increases in intracellular calcium levels within the PN but is also needed for endocannabinoid production. Likewise, our group discovered increases in endocannabinoid concentrations within $nNOS^{-/-}$ cerebella compared to WT. Together, these results are an important first step in understanding the role of nNOS/NO signaling in cerebellar disorders.

Co-Authorship Statement

The following people contributed to the publication of work undertaken as part of this thesis and their contributions are listed under each manuscript:

Candidate: Vasiliki Tellios, The University of Western Ontario
Author 2: Matthew Joseph Elias Maksoud, Robarts Research Institute
Author 3: Ravneet Nagra, The University of Western Ontario
Author 4: Yun-Yan Xiang, Robarts Research Institute
Author 5: Wei-Yang Lu, The University of Western Ontario, Robarts Research Institute

Contribution of work by co-authors for each paper and manuscript.

PAPER 1: Located in Chapter 2
Vasiliki Tellios, Matthew J.E. Maksoud, Yun-Yan Xiang, and Wei-Yang Lu, Nitric Oxide Critically Regulates Purkinje Neuron Dendritic Development Through A Metabotropic Glutamate Receptor Type 1-Mediated Mechanism, Cerebellum. (2020) (4):510-526. 10.1007/s12311-020-01125-7

Author Contributions:
Conceived and designed experiments: Candidate, Author 5
Performed Experiments: Candidate
Contributed technical troubleshooting: Author 2, Author 4
Analyzed the data: Candidate
Wrote the manuscript: Candidate
Revised the manuscript: Author 2, Author 5

PAPER 2: Located in Chapter 3

Vasiliki Tellios, Matthew J.E. Maksoud, and Wei-Yang Lu, The Expression and Function of GLAST in Bergmann Glia Are Critically Regulated by Neuronal Nitric Oxide Synthase-Derived Nitric Oxide, In Preparation.

Author Contributions

Conceived and designed experiments: Candidate, Author 5

Performed the Experiments: Candidate

Contributed technical troubleshooting: Candidate, Author 2

Analyzed the data: Candidate

Contributed with Analysis for Figures 3.8 and 3.9: Author 2

Contributed to organizing data: Candidate, Author 2, Author 5

Wrote the manuscript: Candidate

Revised the manuscript: Author 2, Author 5

PAPER 3: Located in Chapter 4

Vasiliki Tellios, Matthew J.E. Maksoud, Ravneet Nagra, and Wei-Yang Lu, Neuronal Nitric Oxide Synthase Critically Regulates the Endocannabinoid Pathway in the Murine Cerebellum During Postnatal Development, In Preparation.

Author Contributions

Conceived and designed experiments: Candidate, Author 5

Performed the Experiments: Candidate

Contributed with Immunohistochemical Preparation and Analysis: Author 3

Contributed technical troubleshooting: Candidate, Author 2

Analyzed the data: Candidate

Contributed to organizing data: Candidate, Author 2, Author 5

Wrote the manuscript: Candidate

Revised the manuscript: Author 2, Author 5

Acknowledgments

I would like to thank my supervisor, Dr. Wei-Yang Lu, for offering me the opportunity to work on a project that was reflective of my interests. His mentorship style was unparalleled, and I am very appreciative of his support, guidance, and patience as I grew to be a better scientist and an academic.

I owe much of my success within my graduate studies to the support of my lab members. I would like to acknowledge both my colleagues and friends, Matthew Maksoud, Amy Lin, Gurneet Jassal, and Rafael Begazo-Jimenez, for providing a supportive and stimulating atmosphere that made me look forward to coming into the lab every day. I would also like to acknowledge the help of Ravneet Nagra, Dong An and Yimo Wang, who worked diligently and displayed an exceptional passion for research and discovery during their time as undergraduate thesis students. Their presence within the lab sparked my interest in mentorship and my love for teaching and higher education.

I would like to sincerely thank Dr. Yun-Yan Xiang for her dedication to helping me learn lab techniques early on in my graduate school journey. Dr. Xiang helped me create a solid technical foundation of wet lab skills that were consistently used throughout my five years of graduate studies.

I would like to extend my appreciation towards my advisory committee members, Drs. Arthur Brown, Wataru Inoue, and Sean Cregan, for their constant support, guidance, knowledge, and encouragement throughout my graduate school journey. Our discussions within the committee meetings instilled a new sense of inspiration and motivation that renewed my enthusiasm for my project.

Finally, I would like to thank my friends and family for their unfaltering support throughout my academic journey.

Table of Contents

List of Figures

List of Tables

List of Abbreviations

2-AG	2-Arachidonoylglycerol
2W	2 week
7N	7-Nitroindazole
7W	7 week
AEA	N-Arachidonoylethanolamide
AMPAR	α-amino-3-hydroxy-5-methyl-4-isoxazoleproionic acid receptor
AUC	Area Under the Curve
AUI	Arbitrary Unit of Intensity
BC	Basket cell
BG	Bergmann glia
BSA	Bovine Serum Albumen
Ca^{2+}	Calcium Ion
CalB	Calbindin
CaMK	Calcium/Calmodulin-Dependent Protein Kinase
CaMKIIβ	Calcium/Calmodulin-Dependent Protein Kinase -2β
cAMP	Cyclic Adenosine Monophosphate
CB1R	Cannabinoid Receptor 1
CBD	Cannabidiol
CF	Climbing fiber
cGMP	Cyclic Guanosine Monophosphate
CNS	Central Nervous System
Cys	Cysteine
DAG	Diacylglycerol
DAGLα	Diacylglycerol lipase α
DAPI	4’,6-Diamidino-2-Phenylindole
DCN	Deep cerebellar nuclei
DHPG	Dihydroxyphenylglycine
DIV7	Days in vitro 7
DMEM	Dulbecco’s Modified Eagles Medium
E	Embryonic day

EA	Episodic Ataxia
EAAT1	Excitatory Amino Acid Transporter 1
EAAT2	Excitatory Amino Acid Transporter 2
EAAT4	Excitatory Amino Acid Transporter 4
eCB	Endocannabinoid
EGL	External Granular Layer
eNOS	Endothelial Nitric Oxide Synthase
EPSC	Excitatory Post Synaptic Current
ER	Endoplasmic Reticulum
FAAH	Fatty Amino Acid Hydrolase
FBS	Fetal Bovine Serum
fEPSC	Fast Excitatory Post Synaptic Current
GABA	Gamma Aminobutyric Acid
GADPH	Glyceraldehyde 3-Phosphate Dehydrogenase
GC	Golgi Cell
GLAST	Glutamate/Aspartate Transporter
GLT-1	Glutamate Transporter 1
GN	Granule Neuron
GNL	Granule Neuron Layer
GS	Glutamine Synthetase
GTP	Guanosine Triphosphate
HBSS	Hank’s Balanced Salt Solution
HEPES	4-(2-Hydroxyethyl)-1-Piperazineethanesulfonic Acid
IGL	Internal Granular Layer
iNOS	Inducible Nitric Oxide Synthase
IP3	Inositol Triphosphate
IP3R	Inositol Triphosphate Receptor
K^+	Potassium Ion
LC	Lugaro Cell
L-NAME	G-Nitro-L-Arginine-Methyl Ester
LTD	Long-Term Depression
LTP	Long-Term Potentiation

MEM	Minimum Essential Media
MG	Müller glia
mGluR	Metabotropic Glutamate Receptor
mGluR1	Metabotropic Glutamate Receptor Type 1
MGL	Monoacylglycerol Lipase
ML	Molecular Layer
Na^+	Sodium Ion
NADPH	Nicotinamide Adenine Dinucleotide Phosphate
NCX	Sodium/Calcium Exchanger
NCX_i	Sodium/Calcium Exchanger Inhibitor
NDS	Normal Donkey Serum
NMDAR	N-methyl-D-aspartate Receptor
nNOS	Neuronal Nitric Oxide Synthase
$nNOS^{-/-}$	Neuronal Nitric Oxide Synthase Knockout Mouse
NO	Nitric Oxide
NOC-18	Diethylenetriamine NONOate
NOS	Nitric Oxide Synthase
P/S	Penicillin and Streptomycin
PD	Postnatal Day
PBS	Phosphate Buffered Saline
PF	Parallel Fiber
PFA	Paraformaldehyde
PIP2	Phosphatidylinositol 4,5-Biphosphate
PKC	Protein Kinase C
PKG	Protein Kinase G
PKG_i	Protein Kinase G Inhibitor
PLC	Phospholipase C
PM	Plasma Membrane
PN	Purkinje Neuron
PSD	Post Synaptic Density
RGC	Retinal Ganglion Cell
RIPA	Radioimmunoprecipitation Assay

ROI	Region of Interest
SC	Stellate Cell
SCA	Spinocerebellar Ataxia
SEM	Standard Error around the Mean
sEPSC	Slow Excitatory Post Synaptic Current
sGC	Soluble Guanylyl Cyclase
SNAP	S-Nitroso-N-Acetyl-DL-Penicillamine
SNAT	N System of Neutral Amino Acid Transporter
SOCC	Store Operated Calcium Channel
SOCE	Store Operated Calcium Entry
STIM1	Stromal Interaction Molecule
THC	Tetrahydrocannabinol
TRPC	Transient Receptor Potential Canonical
TRPC3	Transient Receptor Potential Canonical Type 3
vGluT1	Vesicular Glutamate Transporter 1
vGluT2	Vesicular Glutamate Transporter 1
WT	Wild-Type

Preface

Before my graduate school journey, I was fortunate enough to gain some wet lab experience while pursuing an undergraduate thesis topic in the field of nitric oxide research, a topic that I understood very little of at the time. As I learned of the ubiquitous nature of this molecule throughout the body and its equivocal role as a therapeutic, the experience piqued my interest in understanding the full potential of nitric oxide. Naturally, when applying to graduate programs, I hoped I could be a part of a research team that specialized in the field of nitric oxide research. Thankfully, I was able to pursue the curiosity I had towards the physiological effects of nitric oxide during my Master's in 2016 within the context of neuroscience. As I worked on my thesis, my attachment to uncovering the role of nitric oxide within neurological processes grew, and I knew I had to transfer to a PhD to pursue this opportunity of discovery. I feel lucky to have had the chance to conduct research in a field I am truly passionate about, and I am excited to see what the future holds for this topic of study.

Chapter 1

1 Introduction

1.1 The Cerebellum: Gross Anatomy and Function

The cerebellum, deriving its name from the Latin meaning “little brain”, has often been described as a distinct subsection of the brain. Treating this region of the brain as other to the cerebral cortex for the most part is understandable, as the cerebellum presents with distinct, organized folia that bear little resemblance to the gyri and sulci of the cerebral cortex. Despite its gross anatomical differences, the cerebellum is closely connected to the cerebrum through efferent tracts that originate within the deep cerebellar nuclei (DCN) and innervate cerebral areas including the prefrontal cortex, motor cortex, and parietal cortex (termed the cerebellarthalamocortical tract), and afferent tracts that originate from the cerebrum and transverse the pontine nucleus to terminate within the DCN (termed the corticopontocerebellar tract)(Fernandez et al., 2020). Foundational lesion studies from the 1900’s determined the overwhelmingly critical role the cerebellum has in motor coordination and fine-tuning motor movements(Glickstein, Strata, & Voogd, 2009). After discovery of the intricate interplay between the cerebellum and the cerebrum, the cerebellum has more recently become a target for functions involving spatial recognition and memory(Buckner, 2013; Klein, Ulmer, Quinet, Mathews, & Mark, 2016), as well as emotion and cognitive function(Habas, 2021).

1.2 Specialized Cerebellar Components: Morphology and Function

The mature cerebellar cortex, unlike the cerebral cortex, presents with a highly organized laminar structure with three distinct layers: the granule neuron layer (GNL), the innermost cell body layer residing overtop cerebellar axonal tracts; the Purkinje neuron (PN) layer, a distinct monolayer consisting of PN somata; and the molecular layer (ML), the layer closest to the pial surface predominantly occupied by PN dendrites and houses

the majority of the synaptic input to the PN as well as the cell bodies of inhibitory interneurons (**Figure 1.1**). The upcoming section will introduce specialized cells residing in the three layers of the cerebellar cortex and their function.

1.2.1 Purkinje Neurons

PNs are highly unique neurons, one of the largest within the CNS, that organize into a discrete monolayer (the PN layer) during development. PNs are GABAergic neurons with elaborate two-dimensional dendritic arbors that extend in the outermost ML. Within the ML, dendritic spines of the PN form mostly excitatory glutamatergic synapses, as well as some inhibitory synapses with neighbouring stellate cells (SCs), and basket cells (BCs) that synapse on the PN axon hillock(M. Hashimoto & Hibi, 2012). Of the neurons present in the cerebellum, PNs constitute the sole output response of this region. PNs extend their myelinated axons primarily towards neurons with the DCN, where they provide inhibitory regulation towards efferents extending to areas of the cerebral cortex(Goodlett & Mittleman, 2017), and to some degree towards vestibular nuclei located within the brainstem(Komuro, Kumada, Ohno, Foote, & Komuro, 2013).

1.2.2 Granule Neurons

Just as PNs are one of the largest neurons within the brain, cerebellar granule neurons (GNs) are one of the smallest and most numerous types of neuron within the CNS(Goodlett & Mittleman, 2017). GNs are densely packed within the GNL and receive synaptic input from mossy fibers, mostly comprising of cerebral input via the corticopontocerebellar tract(Kalinovsky et al., 2011). GNs send small, unmyelinated, glutamatergic axons termed parallel fibers (PFs) from the GNL to the ML, where these fibers run orthogonally to the PN dendritic arbor and boutons originating from one PF can innervate multiple PNs. PF-PN synapses are by far the most numerous within the cerebellum, forming around 200,000 synaptic connections on one PN alone(K. Hashimoto & Kano, 2013; Mishina, Uemura, Yasumura, & Yoshida, 2012).

1.2.3 Climbing Fibers

Climbing fibers (CFs) are glutamatergic axon terminals that originate from the inferior olivary nucleus in the medulla oblongata(Kano, Watanabe, Uesaka, & Watanabe, 2018). CFs are far less numerous in relation to PF terminals, although these synapses form much stronger connections with the PN(K. Hashimoto, Ichikawa, Kitamura, Watanabe, & Kano, 2009). Their synapse point is mainly on the primary branches of the PN and not the dendritic spines, unlike PF terminals. Importantly, in the mature cerebellar cortex, CFs innervate PNs in a 1:1 ratio, where one CF with the strongest synaptic connection will innervate only one PN(Ichikawa et al., 2016; Mishina et al., 2012; Sotelo & Dusart, 2009). In addition to innervating PNs, CF collateral branches extend to the DCN and provide excitatory synaptic input alongside the inhibitory synaptic input originating from PNs(Prestori, Mapelli, & D'Angelo, 2019).

1.2.4 Inhibitory Interneurons: Basket Cells, Stellate Cells, Golgi Cells, and Lugaro Cells

In addition to the glutamatergic synaptic connections via PFs and CFs, PNs are also heavily regulated by inhibitory GABAergic synaptic inputs originating from interneurons that reside in both the ML and GNL. Within the ML, two types of inhibitory interneurons exist – basket cells (BCs) and stellate cells (SCs). BCs reside in the inner ML and provide strong, inhibitory synaptic input towards the PN soma and axon hillock (axon initial segment), creating characteristic pinceau synapses(Buttermore et al., 2012; J. Zhou et al., 2020). BCs hold an important functional role in the regulation of PN synaptic output toward the DCN and subsequently, information transported via the cerebellarthalamocortical tract involved in motor behaviour(Jelitai, Puggioni, Ishikawa, Rinaldi, & Duguid, 2016; Sergaki et al., 2017). On the other hand, SCs occupy the outer ML and make inhibitory synaptic interactions upon PN dendrites(Goodlett & Mittleman, 2017). The influence of inhibitory input that originates from SCs are inherently weaker in comparison to the inhibitory effects of BCs, as SCs provide a more localized inhibitory signal to PNs(Goodlett & Mittleman, 2017). Both BCs and SCs are regulated by excitatory inputs originating from PFs, and inhibitory inputs comprised of PN axon collaterals(Goodlett & Mittleman, 2017).

Two inhibitory interneurons within the GNL are Golgi cells (GCs) and Lugaro cells (LCs). Both GCs and LCs exert inhibitory control via a mixed glycinergic/GABAergic neurotransmitter release(Simat, Parpan, & Fritschy, 2007). Unlike BCs and SCs, both GCs and LCs do not play a large role in regulating PN output activity. GC synaptic output is regulated by excitatory inputs from mossy fibers and PFs, while GC inhibitory innervation is directed toward GN cell bodies(Prestori et al., 2019). LC somata are located just below the PN layer and function to provide inhibitory input towards GCs in the form of collaterals that also comprise of BC and SC innervation(Dumoulin, Triller, & Dieudonné, 2001).

1.2.5 Bergmann Glia

Closely ensheathing glutamatergic synapses on PNs are Bergmann glia (BG) processes – specialized radial glia that are the predominant astrocyte found within the cerebellum. In the mature cerebellum, BG cell bodies reside in the PN layer, and their intricate processes transverse the entirety of the ML and extend to the pial surface(Grosche, Kettenmann, & Reichenbach, 2002). Here, BG processes ensure that glutamate is taken up efficiently by controlling the time-course and extent of PN activation while effectively recycling glutamate from the synaptic cleft(Ullian, Sapperstein, Christopherson, & Barres, 2001). As well, BG protect against excitotoxic insults by preventing prolonged glutamate exposure to PNs (Bordey & Sontheimer, 2003). Finally, BG also regulate metabolic processes by coupling glutamate uptake with increased glucose uptake and lactate formation(Miyazaki et al., 2017).

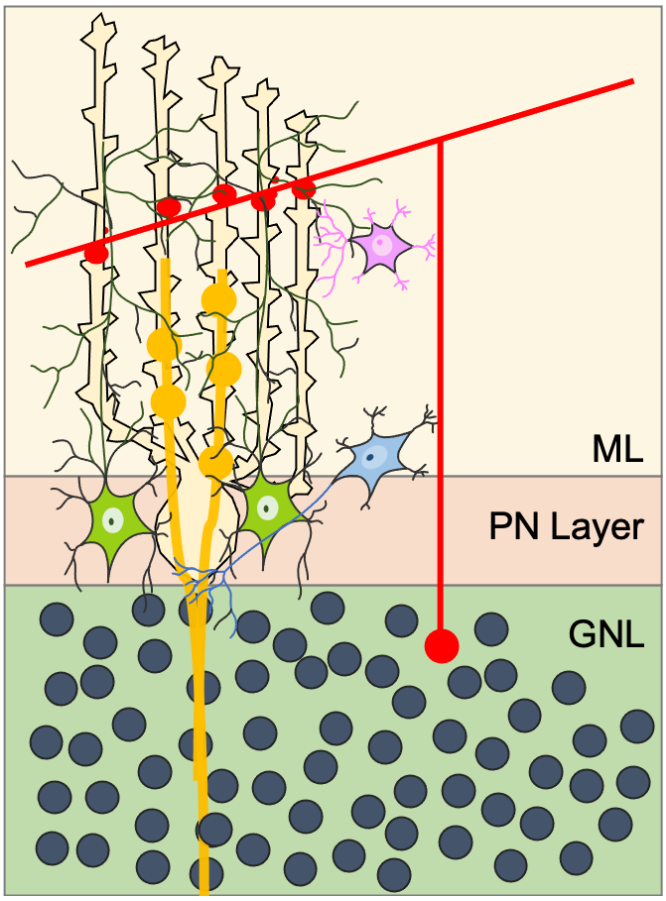

Figure 1.1 Cerebellar Anatomy.

Schematic represents the three prominent layers of the adult cerebellum: the GNL (shaded light green), the PN layer (shaded orange), and the ML (shaded yellow). The GNL houses primarily GNs (represented in dark blue). PFs emerge from GNs to innervate PNs (light yellow) in an orthogonal fashion. CFs (dark yellow), originating from the inferior olive, innervate primary branches of the PN. BCs (blue) reside in the proximal ML and mainly innervate the axon hillock region of the PN, while SCs (pink) reside in the distal ML and provide inhibitory innervation to the distal PN. BG somata (green) reside in the PN layer, while their processes extend into the ML to closely ensheath glutamatergic synapses.

1.3 Murine Cerebellar Development

Like most structures of the CNS, the murine cerebellum is derived from the anterior portion of the neural tube, specifically the rhombencephalon, during embryogenesis, typically around embryonic day 11.5 (E11.5)(Martinez, Andreu, Mecklenburg, & Echevarria, 2013). By E18.5, the first evidence of cerebellar folia along with PN, GN and BG expression are apparent(Sudarov & Joyner, 2007). From then, the cerebellum develops into a bilateral structure comprised of two cerebellar hemispheres connected by the vermis, or the midline of the cerebellum.

All GABAergic neurons of the cerebellum (PNs, BCs, SCs, GCs, and LCs), in addition to BG, originate from progenitor cells within the ventricular zone at approximately E15.5(Martinez et al., 2013; Millen & Gleeson, 2008). By this time point, PNs, in addition to other cerebellar GABAergic neurons, migrate toward the pial surface in a radial manner, to eventually form the PN monolayer by approximately postnatal day 5 (PD5)(Martinez et al., 2013). Additionally, the developing cerebellum also contains a second germinal center that originates from the rhombic lip, termed the external granule layer (EGL)(Wingate, 2001). The EGL is located closest to the pial surface and persists within the cerebellum up until PD14. The EGL gives rise to all glutamatergic neurons of the cerebellum, specifically GNs(Hatten & Heintz, 2005; Martinez et al., 2013).

1.3.1 Early Phase of Purkinje Neuron Development and Synaptic Innervation

PNs begin their development by establishing axonal connections to the DCN and vestibular nuclei during embryogenesis, while an immature form of PN dendritic arborization only begins between PD1-PD3(Kapfhammer, 2004). At this stage, dendrites appear to be disorganized, extending from all directions, both towards and in parallel to the pial surface. This phase of PN dendritic growth is characterized by abundant CF innervation in a pericellular nest formation, where CF boutons are primarily localized on the PN axon hillock(Ichikawa et al., 2011). In this early phase on PN dendritic development, CFs constitute the predominant synaptic innervation to the PN and innervate in a many-to-one fashion(K. Hashimoto et al., 2009). CFs appear in the developing

cerebellum around E19, but do not form synaptic connections with PNs until PD3(Martinez et al., 2013; Morara, Van Der Want, De Weerd, Provinp, & Rosina, 2001). At this phase, the majority of GNs are located in the EGL in an immature state and with small PF extensions(Altman, 1972a). It is also important to note at this phase, precursor inhibitory interneurons are located in the white matter of the cerebellum, where they proliferate before migrating to the internal granular layer (IGL), PN layer, and finally ML by PD7(Kano et al., 2018).

1.3.2 Late Phase of Purkinje Neuron Development and Synaptic Innervation

By PD4-PD7, PNs enter a new phase of dendritic development. The disorganization of dendrites observed in the first week of postnatal development disappear, and the PN begins to orient its dendritic branches towards the pial surface(Hendelman & Aggerwal, 1980). This phase of PN growth, between PD7 – PD28, constitutes the period of rapid dendritic elongation and synaptogenesis(Hendelman & Aggerwal, 1980; Kapfhammer, 2004). Importantly, this phase also marks the development of the planar orientation of PN dendrites(Altman, 1972b). This late phase of rapid PN dendritic elongation also marks a phase for rapid GN migration and maturation, as immature GNs within the EGL differentiate, present with PFs, and migrate to the IGL(Kapfhammer, 2004). Likewise, as the PN dendrites elongate and form synaptic boutons, the sole glutamatergic innervation provided by CFs are slowly displaced by PFs to form PF-PN synapses(Kano et al., 2018). As CF innervation is replaced by PF innervation, redundant CF terminals are eliminated, leaving behind one CF innervating one PN(Mason, Christakos, & Catalano, 1990). Additionally, once the PN dendritic arbor is fully matured (after P28), CF innervation is restricted to the proximal 80% of the PN and strictly innervates the smooth, aspinous dendritic branches of PNs(K. Hashimoto et al., 2009).

At around P14, CF innervation, specifically the pericellular nest formation that was so prominent in the early stages of PN development, has begun to be displaced by BC innervation in the form of pinceau synapses(Ichikawa et al., 2011). These pinceau synapses fully enclose the PN axon hillock by PD28, when the murine cerebellum has

developmentally matured(Ichikawa et al., 2011). Both the early phase and the late phase of PN development are highlighted in **Figure 1.2**.

1.3.3 Bergmann Glia Development

BG, as mentioned previously, are derived from progenitor cells located in the ventricular zone(Martinez et al., 2013). Undifferentiated BG, simply referred to as radial glia, intimately develop alongside immature PNs and GNs. At approximately E15, radial glia begin to extend long laminar processes toward the pial surface(Martinez et al., 2013). Then, radial glia somata migrate from the ventricular zone towards the PN layer around the same time frame as early PN development occurs, between PD0-PD7(Yamada & Watanabe, 2002). In the later phase of PN dendritic development, between PD7-PD28, the unspecialized radial glia differentiate into BG and can be identified by characteristics such as multiple lamellar processes that extend from the soma to the pial surface while also having a close association with PN dendrites(Bellamy, 2006). It is during this time of extensive PN dendritic arborization that BG act as a guide to assist in direction PN dendrites towards the surface. As PN dendrites become more elaborate and synapse-dense, BG processes will transform their lamellar processes from smooth and linear, to fine, elaborate processes that closely ensheath glutamatergic PN synapses(Bellamy, 2006; Yamada et al., 2000).

In addition to guiding PN dendritic development, BG processes are critical in assisting GN migration and maturation from the EGL to the IGL during the second postnatal week(Custer et al., 2006; Miyazaki et al., 2017). During this time, BG processes transverse the entirety of the ML, but also a portion of the IGL to ensure appropriate GN migration between the two layers(Rakic, 1971). As GNs migrate through the ML to the IGL, they form tight interactions with BG lamellar processes that work to guide GNs to the eventual GNL and leave behind developed PFs within the ML(Rakic, 1971; H. Xu et al., 2013).

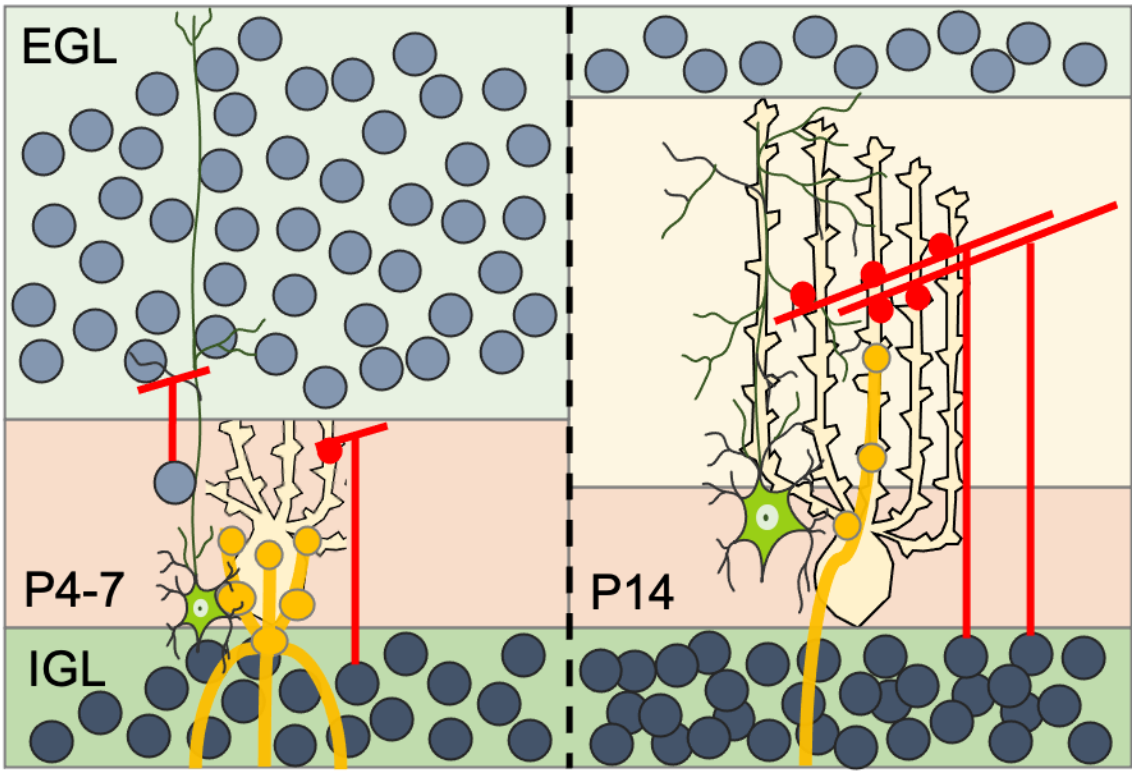

Figure 1.2 Early and Late Stages of PN Development.

(*Left side*): From PD4-7, PNs begin to develop small dendritic branches, and CF innervation dominates the PN, as opposed to PF innervation. The EGL at this point in development is prominent, and BG aide in GN maturation by providing a scaffold to allow for GNs to migrate from the EGL to the IGL. (*Right side*): In the late stage of PN development (PD7 and onward), the PN quickly develops an elaborate dendritic arbor. By PD14, the EGL is nearly, if not totally abolished. Elimination of CF synapses occur, which allows for more PF innervation within the distal PN dendrites. BG process are more elaborate and closely ensheath glutamatergic synapses upon PNs.

1.4 Nitric Oxide Isoforms: Synthesis and Physiological Function

Nitric oxide (NO) is a gaseous molecule differentially produced in a variety of mammalian cells with a diverse range of functions. There are three enzymes that catalyze the production of NO: neuronal nitric oxide synthase (nNOS), endothelial nitric oxide synthase (eNOS), and inducible nitric oxide synthase (iNOS). All three NOS isoforms are classified as oxidoreductases and function as homodimers physiologically(Förstermann & Sessa, 2012). NO is produced by all NOSs enzymatically by utilizing L-arginine and metabolic oxygen as substrates and producing L-citrulline and molecular water as a by-product(Förstermann & Sessa, 2012). All three isoforms of NOS rely on NADPH as a cofactor and reducing agent, and early studies assessing the localization and function of NOS isoforms relied on NADPH-diaphorase expression and activity(D. Stuehr, Pou, & Rosen, 2001).

Both nNOS and eNOS are classified as constitutively expressed NOS isoforms. As well, both isoforms produce NO in a calcium-dependent manner(Förstermann & Sessa, 2012). Briefly, intracellular increases of calcium facilitate binding of calmodulin, which allows for the reductase ability needed to convert L-arginine to NO. Therefore, increases in intracellular calcium levels and/or increases in calmodulin-bound eNOS and nNOS will result in increases in NO production, accordingly(D. J. Stuehr, 1999; D. Stuehr et al., 2001). Interestingly, nNOS – also referred to as brain NOS or NOS1 – was the first physiological NOS isoform to be discovered, fittingly within brain tissue. After this discovery, it is now known that nNOS is also localized in the periphery, specifically within skeletal and cardiac muscle, as well as nitrergic nerves that innervate smooth muscle(Förstermann et al., 1994). Functionally, nNOS-derived NO production within the periphery has been reported to regulate vascular tone by microvascular vasodilation and is more famously known for mediating penile erections(Förstermann et al., 1994; N. Kim, Azadzoi, Goldstein, & Saenz de Tejada, 1991; Melikian, Seddon, Casadei, Chowienczyk, & Shah, 2009). However, nNOS is the predominant NOS isoform in the CNS, localized in both neurons and astrocytes of the cerebrum and cerebellum. Within the CNS, nNOS-derived NO acts as an

unorthodox neurotransmitter that has been implicated in modulating higher-order functions such as memory formation and neurogenesis(L. Zhou & Zhu, 2009). Similar to the periphery, nNOS within the CNS can also contribute to central regulation of blood pressure and vascular tone by affecting brain regions responsible for homeostatic functions, such as the medulla oblongata and the hypothalamus(Toda, Ayajiki, & Okamura, 2009).

As mentioned previously, eNOS is also a constitutively expressed, calcium-dependent NOS isoform. Specifically, eNOS is predominately localized to endothelial cells and to some degree cardio myocytes and kidney tubular epithelial cells(Förstermann et al., 1994). Endothelial NOS produces NO in a similar fashion to nNOS, in that increases in intracellular calcium promotes the binding of calmodulin to the enzyme leading to NO production. However, unlike nNOS, eNOS-derived NO production can be regulated by environmental factors outside of intracellular calcium levels, including phosphorylation of various serine, threonine, and tyrosine residues within the protein, resulting in increased calcium sensitivity and subsequent eNOS activity(Fleming & Busse, 2003; McCabe, Fulton, Roman, & Sessa, 2000). Endothelial NOS is responsible for a variety of physiological functions involving the cardiovascular system, including vasodilation and reduction of vascular inflammation and stimulation of angiogenesis(Murohara et al., 1998; Rapoport, Draznin, & Murad, 1983).

Finally, iNOS differs from eNOS and nNOS in that the enzyme is not constitutively expressed, nor is it usually expressed in physiologically healthy cells. As well, iNOS produces NO in a calcium-independent manner, and is instead regulated by proinflammatory mediators such as bacterial pathogens and inflammatory cytokines(Förstermann & Sessa, 2012). Inducible NOS is primarily localized and utilized by immune cells such as macrophages and microglia, but its expression can be induced in any physiological cell type(Förstermann et al., 1994). While both nNOS and eNOS produce NO in a gradual manner, iNOS produces large amounts of NO in a short period of time(Hallemeesch et al., 2003; B. C. Smith, Fernhoff, & Marletta, 2012). Due to this burst effect of NO characteristic of iNOS, this isoform gives immune cells such as macrophages and microglia their cytotoxic function when interacting with foreign pathogens and various

infection and can cause a pathology when expressed in neurons(Kröncke, Kolb-Bachofen, Berschick, Burkart, & Kolb, 1991).

1.4.1 Nitric Oxide and nNOS in the Cerebellum

Neuronal NOS is of particular importance in the cerebellum, as this isoform is highly expressed within this region compared to any other region within the CNS(Bredt, Hwang, & Snyder, 1990; Campese et al., 2006). In particular, nNOS is localized to GNs, SCs, BCs, and BG, but notably not expressed to any degree within PNs(Schilling, Schmidt, & Baader, 1994; Shimizu-Albergine et al., 2003). Cerebellar NO has been implicated in many homeostatic functions, including synaptogenesis and plasticity, neurotransmitter release, signal transduction, and cell death regulation(Contestabile, 2012; Oldreive, Gaynor, & Doherty, 2012). Unlike what is observed in the cerebral cortex, NO acts as an anterograde messenger, often produced in the presynaptic terminals of PFs, by diffusing into neighbouring PNs to influence cerebellar learning and memory by modulating synaptic plasticity in the form of long-term depression (LTD) or long-term potentiation (LTP)(Contestabile, 2012; Matyash, Filippov, Mohrhagen, & Kettenmann, 2001; Wang et al., 2014). Similarly, nNOS-derived NO can signal endogenously within GNs and plays an important role in GN migration and maturation during cerebellar development(Oldreive et al., 2012). Importantly, nNOS-derived NO within the cerebellum has been previously shown to be critical in promoting PN survival and neuritogenesis during embryonic development in an in vitro environment(Oldreive et al., 2012).

1.4.2 Nitric Oxide Signaling Pathways in the Cerebellum

As a highly diffusible molecule, NO production within the cerebellum can produce a localized response with differential effects on a variety of neighbouring cells. To carry out a myriad of functions within different cell types, NO is known to act through two common signaling mechanisms: the classical NO-cyclic guanosine monophosphate (cGMP)-protein kinase-G (PKG) signaling cascade and protein modification via *S*-nitrosylation of cysteine residues, which will be described in further detail below.

1.4.2.1 Protein Kinase-G Signaling Cascade

Intercellular NO is commonly known to activate soluble guanylyl cyclase (sGC), a cytosolic enzyme that is documented to be the only endogenous receptor that uses NO as a ligand. To active sGC, NO binds to a heme group embedded into the enzyme, which then activates sGC and results in the hydrolysis of guanosine-5'-triphosphate (GTP) into cGMP(Kang, Liu, Wu, & Chen, 2019). Cyclic GMP acts as a secondary messenger that effectively amplifies the original NO response. Considering the highly diffusible, and consequently transient nature of NO, sGC is able to translate the instability of NO into a stable message in the form of cGMP. Additionally, sGC activation results in a 200-fold amplification of the original NO signal, thus preventing the potential cytotoxic effects of NO overproduction(Martin, Berka, Bogatenkova, Murad, & Tsai, 2006). A common downstream effector of cGMP is PKG, a serine/threonine kinase that can phosphorylate a wide variety of proteins within cells(Ariano, Lewicki, Brandwein, & Murad, 1982). Although PNs themselves do not produce NO, they have been reported to express all of the components associated with the sGC-cGMP-PKG pathway, exclusively activated by NO(Ariano et al., 1982). Within PNs, critical proteins that are phosphorylated specifically by PKG include α-amino-3-hydroxy-5-methyl-4-isoxazoleproionic acid receptors (AMPARs) and inositol-3-phospate receptors (IP3Rs), critical for the production of LTD within PNs(Haug, Jensen, Hvalby, Walaas, & Østvold, 1999; Nakazawa, Mikawa, Hashikawa, & Ito, 1995; Shimizu-Albergine et al., 2003). The classical NO-cGMP-PKG pathway is highlighted in **Figure 1.3**.

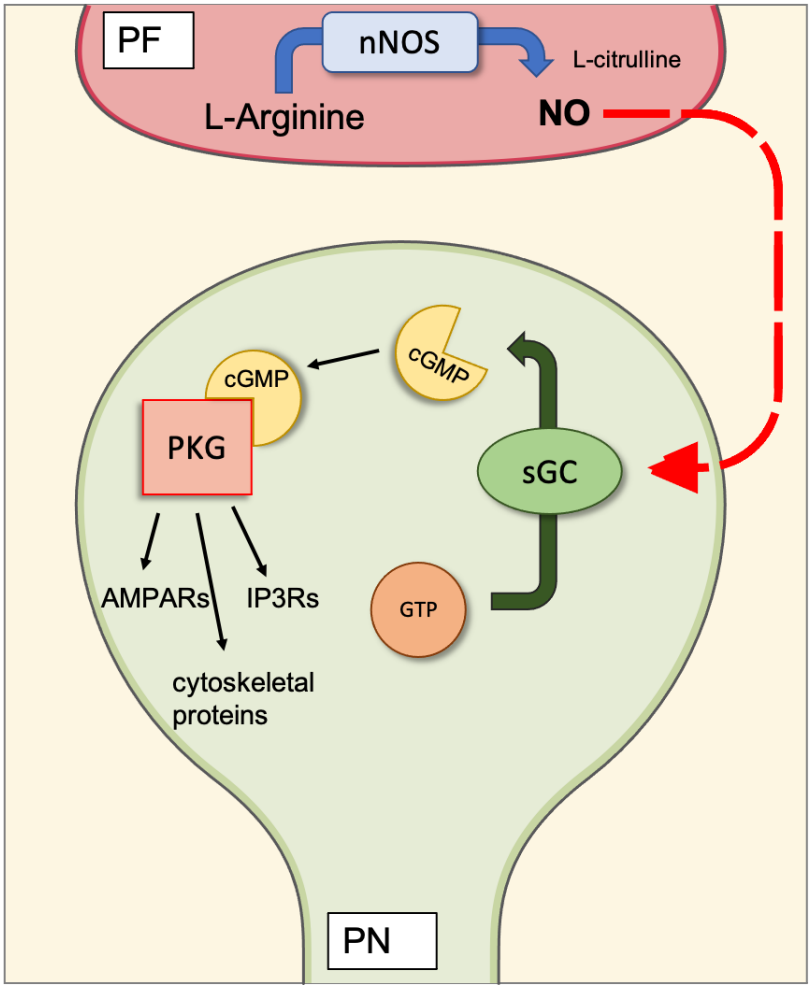

Figure 1.3 Activation of PKG via NO signaling cascade.

L-arginine is catabolized by NOSs, including nNOS, through an oxidoreductase reaction to produce NO and L-citrulline as a by-product. As PNs do not express NOS isoforms, NO diffuses from presynaptic terminals like the PF to bind to sGC, initiating the conversion of GTP to cGMP. Cyclic GMP binds and activates PKG, a protein kinase that is able to phosphorylate serine/threonine residues of proteins such as AMPARs, IP3Rs, and cytoskeletal proteins.

1.4.2.2 Regulation via *S*-Nitrosylation

Due to its robust amplification of NO signaling, the sGC-cGMP-PKG cascade is the classical signaling pathway that results in the indirect cellular effects of NO. However, NO can also directly confer reversible post-translation modifications upon cysteine residues of various proteins in the form of S-nitrosylation(Jaffrey, Erdjument-Bromage, Ferris, Tempst, & Snyder, 2001). The transient nature of NO requires the process of S-nitrosylation to be relatively quick, and unlike the classical PKG pathway, S-nitrosylation requires higher concentrations of NO within the intracellular environment(Stamler, Lamas, & Fang, 2001). In order for S-nitrosylation to occur, the cell itself must be in an optimal redox state, specifically within an oxidative environment(Stamler et al., 2001). Under an oxidative state, cysteine-thiol bonds within proteins transform into thiol radicals that easily react with NO(Gaston, 1999). Within the cerebellum, S-nitrosylation is known to affect stargazin, a regulatory protein known to affect membrane expression levels of AMPARs, as well as cytoskeletal structures, including postsynaptic density-95 (PSD-95)(Ho et al., 2011; Selvakumar, Huganir, & Snyder, 2009).

1.5 Synaptic Plasticity in the Cerebellum

Synaptic plasticity within the cerebellum is defined as cellular changes that underly the storage of motor memories and the development of important functions, including error-driven motor control and learning, as well as movements associated with the vestibulo-ocular reflex(Hirano, 2018; Tanaka, Kawaguchi, Shioi, & Hirano, 2013). In general, there exists a variety of ways in which synaptic plasticity may occur, including receptor sensitization, LTP, LTD, and alterations in synapse morphology(Ito, 1989). The following sections will discuss ways in which PNs display and are affected by synaptic plasticity, with a particular focus on the underlying mechanism associated with PN LTD, as well as associated changes in neuron morphology.

1.5.1 PF-PN Synapse and LTD

PF-PN synaptic function is crucial in governing the development of fine motor skills as well as coordinated movement, both spatially and temporally(Janmaat et al., 2009).

Additionally, it is the site for synaptic plasticity in the form of long term potentiation and depression (LTP/LTD)(Hartmann, Henning, & Konnerth, 2011). The LTD profile functions to weaken the signal of the PF-PN by modulation of cations entering the PN, specifically calcium, which originates from internal stores from the endoplasmic reticulum (ER) or from the extracellular environment(Daniel, Levenes, & Crépel, 1998). LTD is initiated by the release of glutamate from PF terminals and the binding of glutamate to various glutamate receptors located on the PN dendritic spine. In general, glutamate activates ionotropic glutamate receptors, namely AMPARs, to cause a large and transient depolarization, termed the fast excitatory post synaptic current (fEPSC)(Jin, Kim, Kim, Worley, & Linden, 2007). It is crucial to note that PF-PN synapses do not express N-methyl-D-aspartate receptors (NMDARs), and therefore NMDARs do not contribute to the fEPSC within this synapse(Casado, Dieudonné, & Ascher, 2000). As well, glutamate can activate metabotropic glutamate receptors (mGluRs), specifically mGluR1 expressed on PN dendritic spines, to cause a slow and sustained influx of cations into the PN, or a slow EPSC (sEPSC)(Jin et al., 2007).

Notably, NO plays a large role in facilitating LTD at PF-PN synapses(Daniel et al., 1998; Wang et al., 2014). Experimentally, NO blockade via NOS inhibitors within cerebellar slices abolishes the LTD profile at the PF-PN synapse completely(Lev-Ram, Makings, Keitz, Kao, & Tsien, 1995; Linden, Dawson, & Dawson, 1995). However, how NO facilitates cerebellar LTD has remained a controversial topic within scientific literature. The currently favoured model describes NO, specifically produced by PF stimulation, easily diffuses into PN terminals to activate the classical NO-cGMP-PKG pathway, leading to the hyperphosphorylation of PN AMPARs(Hartell, 2002). Therefore, NO production results in decreased AMPAR activity, either through AMPAR desensitization or AMPAR internalization, potentially through either a protein kinase C (PKC)-, or a PKG-dependent mechanism(Blitz, Foster, & Regehr, 2004; Brorson, Manzolillo, Gibbons, & Miller, 1995; Linden et al., 1995; Metzger, Kapfhammer, Metzger, & Kapfhammer, 2003).

1.5.2 CF-PN Synapse and LTD

As mentioned previously, there are two types of excitatory, glutamatergic inputs innervating PNs: PFs and CFs. Although the LTD profile is associated with the PF-PN synapse specifically, it is now known that concurrent CF and PF stimulation upon the PN is needed in order produce a long-lasting depression of signal transmission between PFs and PNs, and not by individual stimulation of PFs and CFs alone(Hirano, 2018; Ito, 2001). Cerebellar LTD is used as a mechanism to refine motor learning behaviours, as CFs often propagate error messages related to motor movement(Maekawa & Simpson, 1973). Therefore, strong activation of CFs work to selectively weaken inappropriate motor signals conveyed by PFs (by up to 50%) when activated together(Hansel, Linden, & D'Angelo, 2001). CF stimulation is necessary for the induction of LTD, as CFs are capable of producing a large calcium influx within the PN (more so than PF stimulation alone), termed the complex spike. To do so, CFs are able to elicit a large influx of calcium within the PN via P/Q type voltage gated calcium channels(Hansel et al., 2001).

1.5.3 Synapse Morphology

In addition to LTD, structural forms of synaptic plasticity exist, in which overactivation and under-activation of synaptic terminals can result in changes to synaptic bouton ultrastructure. Morphological changes in result of synaptic input have been documented many times within neurons of the cerebral cortex and hippocampus(Calabrese, Wilson, & Halpain, 2006; Verpelli et al., 2010). Specifically, it is understood that both dendritic spine density and morphology are constantly changing during development into adulthood in order to reflect changes in learning and memory over time. In general, changes to dendritic spine morphology are often a result of protein synthesis or degradation when building new spines or eliminating unnecessary spines, respectively.

The construction of new spines requires increased presynaptic input and activity, and it is agreed upon that intracellular calcium levels play a key role in synapse reorganization(Wong & Ghosh, 2002). In response to elevated levels of calcium in the postsynaptic terminal, a local change to dendritic spines can occur via calcium-dependent signaling proteins that can alter the dendritic cytoskeleton(Lamont & Weber, 2012). Local,

fast changes to dendritic spines in response to a stimulus such as glutamate can result in an increase in immature synaptic spines, such as filopodia or thin spines, as opposed to canonical, mature, mushroom-type spines(Maiti, Manna, Ilavazhagan, Rossignol, & Dunbar, 2015). Creation of additional thin spines as a result of intracellular calcium levels is often mediated by phosphorylation events through calcium/calmodulin-dependent protein kinases (CaMKs), which are able to alter dendritic structures via modification of cytoskeletal proteins(Wojda, Salinska, & Kuznicki, 2008).

Differences in dendritic spine morphology can determine the efficiency and functionality of the synapse itself. For example, mushroom spines, characterized by a bulbous-shaped synaptic head, followed by a constricted, thinly shaped synaptic neck. Mushroom spines are often referred to as “memory spines”, as they can persist in vivo for months. Their characteristic morphology allows for larger PSDs, which translates to greater densities of glutamate receptors such as AMPARs on the spine membrane(Ashby, Maier, Nishimune, & Henley, 2006; Bourne & Harris, 2007). A bulbous spine head provides room from more synaptic proteins to exist in a localized area, in particular proteins associated with calcium homeostasis. As a result of their long-term stability and persistence, mushroom spines are more likely to exist in a tripartite synaptic formation, with specific inclusion of astrocytic processes ensheathing the entirety of the synapse(Bourne & Harris, 2007; Haber, 2006). In contrast, thin spines are often described as transient, or “learning” spines, as they form quickly and exist for only a few days at a time, before turning into mushroom spines or degenerating completely(Bourne & Harris, 2007). This type of spine morphology is beneficial when accommodating for enhanced or weakened synaptic inputs. As well, both mushroom and thin spines regulate and transmit calcium signals in a different manner. Mushroom spines with long, narrow spine necks retain better control of calcium transients during synaptic activation than thin spines, which impair charge transfer due to their relative lack of post-synaptic proteins and smaller PSDs(Noguchi, Matsuzaki, Ellis-Davies, & Kasai, 2005; Santamaria, Wils, De Schutter, & Augustine, 2006).

1.6 PF-PN Synaptic Transmission

Calcium homeostasis plays an important role in dictating synapse morphology and functionality, ultimately affecting neuronal output and behavioural phenotypes. Therefore, calcium ion dynamics within the cerebellum, particularly within the PN, are highly regulated considering the abundance of synaptic inputs upon the PN. As mentioned in the previous section, mature GNs are stimulated by mossy fiber inputs generating high-frequency bursting action potentials in PFs, thus eliciting calcium influx primarily by slow-acting mGluRs. The upcoming section will describe the mechanism of store-operated calcium entry (SOCE) initiated by mGluRs during PF-PN synaptic transmission (highlighted in **Figure 1.4**).

1.6.1 mGluR1 Signaling Pathway

As highlighted previously, glutamate released from PFs activate two types of glutamate receptors on PNs: ionotropic AMPARs, and metabotropic mGluRs. Metabotropic GluRs differ from ionotropic glutamate receptors in that mGluRs do not form ion channels to mediate calcium entry, but rather propagate an intracellular signaling cascade, indirectly causing calcium entry. In particular, the most abundant mGluR located on PNs are mGluR1s(Knöpfel & Grandes, 2002). As a group I mGluR, mGluR1 is a membrane-bound receptor with seven transmembrane domains that is coupled to Gq proteins(Pandya et al., 2016). When activated, mGluR1 initiates a signaling cascade involving the activation of phospholipase Cβ (PLCβ) that is closely bound to mGluR1 via Gq proteins. PLCβ facilitates the cleavage of phosphatidylinositol-4, 5-bisphosphate (PIP2) into inositol triphosphate (IP3) and diacylglycerol (DAG). IP3 then activates the IP3 receptor on the endoplasmic reticulum (ER) membrane, leading to ER depletion of calcium(Hartmann et al., 2011; Jin et al., 2007; Willard & Koochekpour, 2013). Once calcium exits the ER, calcium sensors on the ER membrane, termed stromal interaction molecule 1 (STIM1), aggregate, oligomerize, and translocate to the plasma membrane (PM)(Ryu et al., 2017). There, the STIM1 complex can interact with the transient receptor potential canonical type 3 (TRPC3) channels, a type of store operated calcium channel (SOCC), causing a large calcium influx into the PN cytosol. This mGluR1-intiated TRPC3

conductance is the main component of the sEPSC, and the predominant form of SOCE in the PN(Hartmann & Konnerth, 2015; G. N. Huang et al., 2006; Yuan, Zeng, Huang, Worley, & Muallem, 2007).

1.6.2 Nitric Oxide and Store-Operated Calcium Entry

Although the NO-cGMP-PKG pathway has been implicated in maintaining the LTD profile within PNs, NO may also play an additional role in modulating calcium homeostasis via SOCE. Recently, it has been noted that NO can potentially regulate the occurrence of SOCE in cells via S-nitrosylation of STIM1(Gui et al., 2018). In particular, NO was shown to modulate Orai-mediated calcium entry in cardiomyocytes by S-nitrosylation of cysteine (Cys) 49 and Cys56 on the STIM1 protein, resulting in suppression of calcium-dependent STIM1 oligomerization(Gui et al., 2018).

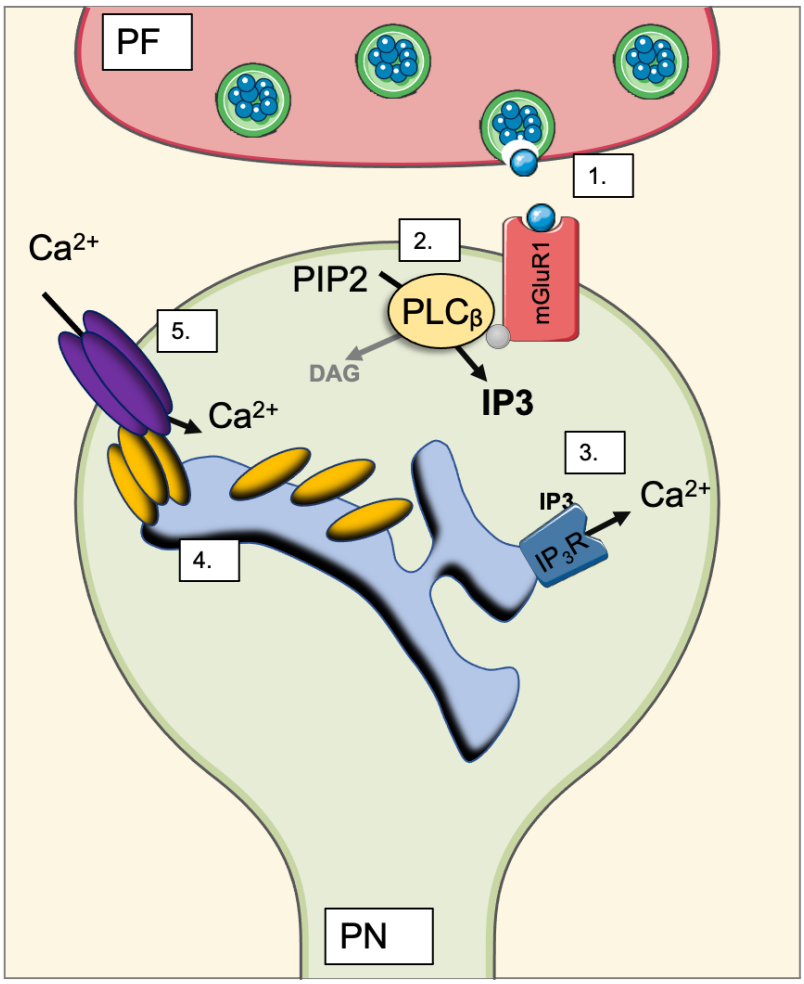

Figure 1.4 mGluR1-initiated SOCE within the PN.

1. Glutamate is released from the PF terminals to activate mGluR1 on the PN membrane. **2.** Activation of mGluR1 induces PLCβ-mediated cleavage of PIP2 into DAG and IP3. **3.** IP3 activates IP3Rs on the ER membrane, allowing the release of calcium into the PN cytosol from internal stores. **4.** Decreased calcium concentrations within the ER lumen will result in STIM1 oligomerization (yellow ovals). **5.** STIM1 oligomers gate the opening of TRPC3 channels (purple ovals) upon the membrane of the PN, allowing extracellular calcium to enter the PN cytosol.

1.7 Glutamate Excitotoxicity and Neurodegeneration

PNs of the cerebellum heavily regulate calcium influx through a variety of mechanisms. As previously described, PNs receive primary glutamatergic input from PFs and when glutamate is released, transient increases of calcium into the PN occur. However, overactivation of glutamate receptors can lead to increased intracellular calcium levels by AMPARs overactivation and by elevated SOCE via mGluR1s(Wojda et al., 2008). As such, pathological increases in calcium often result in neuronal atrophy or even neuronal cell death. Neuronal atrophy is often a measure of deficits in neuron morphology, including synaptic spine morphology, complexity of dendritic arborization, and density/shape of neuronal cell bodies(Mattson, 2007).

In the case of excitotoxicity, pathological increases in intracellular calcium can cause neurodegeneration to occur via activation of calcium-dependent neutral cysteine proteases such as calpains(Vosler, Brennan, & Chen, 2008). Physiologically, calpains function to assist with synaptic plasticity by regulating the expression levels of both AMPA and mGluR1 during LTD/LTP(Bi, Bi, & Baudry, 2000; Slemmer, De Zeeuw, & Weber, 2005; W. Xu et al., 2007). As well, calpain activity is known to remodel cytoskeletal proteins such as α- and β-spectrins to contribute to transient changes to synaptic morphology, and assist with efficient protein trafficking to the PM(Seubert, Baudry, Dudek, & Lynch, 1987; Vosler et al., 2008). Under pathological levels of intracellular calcium, calpains have been documented to degrade cytoskeletal proteins that are crucial in maintaining the integrity of the synapse, which causes the retraction and loss of synaptic spines(Mattson, 1990; Rami, Ferger, & Krieglstein, 1997; Stein-Behrens, Mattson, Chang, Yeh, & Sapolsky, 1994). Beyond cytoskeletal proteolysis, calpains may function to initiate cell death in coordination with caspases, cysteinyl aspartate proteinases often activated during apoptosis(Chan & Mattson, 1999; Mattson, 2007).

Given the dangers of excitotoxicity via overactivation of glutamate receptors, there are multiple ways in which the cerebellum regulates glutamate overexcitation, primarily via glutamate transporters located of BG and to some degree, PNs. The next subsection will discuss how BG can facilitate glutamate uptake to prevent excitotoxicity.

1.7.1 Bergmann Glia: Glutamate Uptake

Although both BG and general astrocytes exist within the cerebellum, BG comprise of over 90% of the astrocytic population, making them the predominant mediators of astrocytic glutamate uptake within the cerebellum(Martínez-Lozada, Hernández-Kelly, Aguilera, López-Bayghen, & Ortega, 2011). PNs also contribute to glutamate uptake as well, as they express excitatory amino acid transporter 4 (EAAT4), although they contribute about 10% of the total glutamate clearance within the cerebellum, preventing long-term spillover of glutamate from the synaptic cleft to adjacent synapses(Danbolt, Furness, & Zhou, 2016; Y. H. Huang, 2004). BG are incredibly efficient in uptaking glutamate from the synaptic cleft, as they form elaborate projections that closely ensheath 67% and 94% of PF and CF synaptic area, respectively(Bellamy, 2006; Xu-Friedman, Harris, & Regehr, 2001). BG uptake glutamate via excitatory amino acid transporter 1/glutamate aspartate transporters (EAAT1/GLAST), and the following section will describe the function and activity of GLAST within the cerebellum.

1.7.2 GLAST Function and Activity

In contrast to unspecialized cortical astrocytes, radial astrocytes such as BG abundantly express GLAST as opposed to glutamate transporter-1 (GLT-1/EAAT2)(Perego et al., 2000). In particular, GLAST is an important cerebellar glutamate transporter that has a 6-fold greater expression level relative to GLT-1, making it the predominant glutamate transporter in the cerebellum(Lehre & Danbolt, 1998; Takatsuru et al., 2006). GLAST functions as a homotrimer on the PM of BG, where uptake of glutamate (as well as L- and D-aspartate with a similar efficiency) into the cell is co-transported with three sodium ions and one hydrogen ion, while one potassium ion is transported to the extracellular space(Bauer et al., 2012). Once glutamate is transported into the BG, glutamate is then recycled to glutamine via glutamine synthetase (GS), then released into the extracellular space through the N system of neutral amino acid transporters 3 and 5 (SNAT3/5)(Martínez-Lozada et al., 2011). Glutamine is then taken up by glutamatergic terminals such as PFs and CFs by SNAT1/2 to be converted back into glutamate, in a process named the glutamate/glutamine shuttle (**Figure 1.5**).

A significant component dictating GLAST functionality is the frequency and magnitude of calcium transients that occur within the BG in the presence of glutamate. It is well known that PF activity can evoke increases in intracellular calcium within BGs(Bazargani & Attwell, 2016; Metea & Newman, 2006; Ortega, Eshhar, & Teichberg, 1991), and this is postulated to occur by a few mechanisms. Firstly, BG are known to express calcium-permeable AMPARs (AMPARs that lack expression of the GluR2 subunit). Therefore, activation of these AMPARs on BG are able to induce localized, transient calcium influxes(Burnashev et al., 1992; Iino et al., 2001). Calcium transients within BG during glutamate uptake are critical, as studies that have abolished calcium transients mediated by AMPARs have reported BG process retraction as well as decreases in GLAST transcription(Ishiuchi et al., 2007; López-Bayghen, Espinoza-Rojo, & Ortega, 2003; Martínez, García, Aguilera, & Ortega, 2014).

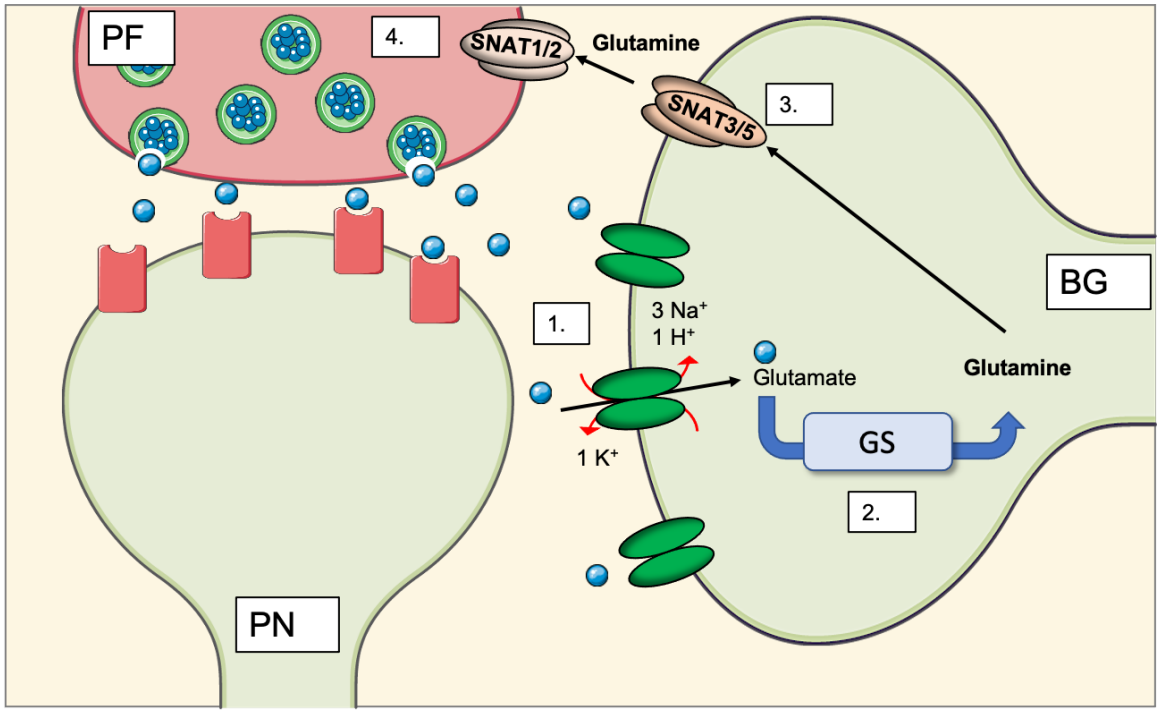

Figure 1.5 The glutamate-glutamine shuttle.

1. Glutamate (blue circles) released from glutamatergic terminals, such as PFs, enter the synaptic cleft to interact with glutamate receptors on the PN membrane. On astrocytes such as BG, glutamate is taken up by GLAST into the BG cytosol along with three sodium ions and one hydrogen ion, while transporting one potassium ion into the extracellular space. **2.** Glutamate is recycled into glutamine through GS. **3.** Glutamine is shuttled outside of the BG into the extracellular space by transport proteins such as SNAT3/5. **4.** Glutamine is then taken up by presynaptic terminals via SNAT1/2 and enzymatically converted into glutamate (within glutamatergic boutons) or GABA (within GABAergic boutons).

1.7.3 NCX and GLAST Coupling and Activity

Importantly, glutamate uptake itself can indirectly act as a driver of calcium entry, as sodium ions co-transported with glutamate via GLAST influences the activity of the sodium/calcium exchanger (NCX) located within BG as well as cortical astrocytes(S. Kirischuk, Kirchhoff, Matyash, Kettenmann, & Verkhratsky, 1999; Sergei Kirischuk, Kettenmann, & Verkhratsky, 2007). The NCX is a solute carrier electrogenic transporter located on the PM of astrocytes, and functions to adjust astrocytic membrane potentials according to the extracellular environment. The NCX exists in two conformations: the forward mode and the reverse mode. In the forward mode, the NCX works to transport three sodium ions into the BG cytosol, while transporting one calcium ion into the extracellular space(Rose, Ziemens, & Verkhratsky, 2020). The forward mode of the NCX is the most likely conformation when the BG is at rest. Conversely, the reverse mode of the NCX, in which one calcium ion is transported into the BG cytosol, while three sodium ions are transported into the extracellular space, is thought to be induced by increases in sodium transients, caused by increased GLAST activity and concurrent sodium ion influx(Sergei Kirischuk et al., 2007; Rose et al., 2020).

1.7.4 Nitric Oxide and Glutamate Uptake Regulation

The effects of NO within the CNS are not limited to neurons; supporting cells such as astrocytes are also under the influence of NO signaling. A recent study has determined that increases in NO concentrations are proportional to increases in GLAST functionality, measured as relative D-aspartate uptake, in cultured BG(Balderas et al., 2014). Similarly, glutamate uptake activity within cultured BG has been shown to increase BG expression of nNOS, suggesting an intricate interplay between glutamate concentrations, nNOS expression, and GLAST activity(Tiburcio-Félix et al., 2019).

NO may indirectly affect GLAST function by modulation of the calcium transients within BG during glutamate uptake. As described earlier, the NCX is coupled closely with GLAST function in order to produce an increase in intracellular calcium. Interestingly, multiple studies have demonstrated the ability of NO to cause a reversal in the NCX,

resulting in increased calcium influx into the BG(Asano et al., 2002; Secondo et al., 2011; Takuma, Ago, & Matsuda, 2013).

1.8 eCB Signaling Pathway

Although glutamate remains central to the induction of cerebellar LTD at PF-PN synapses, the weakened signal of PFs during LTD can also be attributed to a retrograde signaling cascade that works to inhibit the release of PF-derived glutamate. Within the cerebellum, the endocannabinoid (eCB) pathway is the predominant way in which PF activation can be dampened or suppressed for prolonged periods of time. The following sections will describe the production and mechanism of action of the most prominent cerebellar eCB.

1.8.1 2-AG synthesis via mGluR1 Signaling

In addition to the mGluR1-initiated SOCE component during PF-PN synaptic transmission, there is a concurrent signaling cascade initiated by mGluR1 primarily involved with the synthesis of cerebellar eCBs. As discussed previously, mGluR1 activation by glutamate that originates from PFs or CFs results in the production of IP3 and DAG from PIP2 via PLCβ activity. While IP3 acts as a secondary messenger stimulating SOCE within the PN, DAG is enzymatically converted by DAG lipase α (DAGLα) to 2-arachidonoylglycerol (2-AG), the highest-expressed eCB within the cerebellum(Bisogno et al., 2003; P. K. Safo & Regehr, 2005). 2-AG is a lipid messenger able to easily diffuse across the PM, and transverses across the synaptic cleft to retroactively signal cannabinoid-1 receptors (CB1Rs) located on presynaptic terminals, predominately BCs, SCs, and PFs(Kawamura, 2006; Maejima et al., 2005). Termination of the signal occurs via degradation of 2-AG by lipid hydrolases, including monoacylglycerol lipase (MGL) and fatty amino acid hydrolase (FAAH)(Di Marzo & Maccarrone, 2008; Gulyas et al., 2004; Schlosburg et al., 2010). This 2-AG signaling cascade is described and illustrated in **Figure 1.6.**

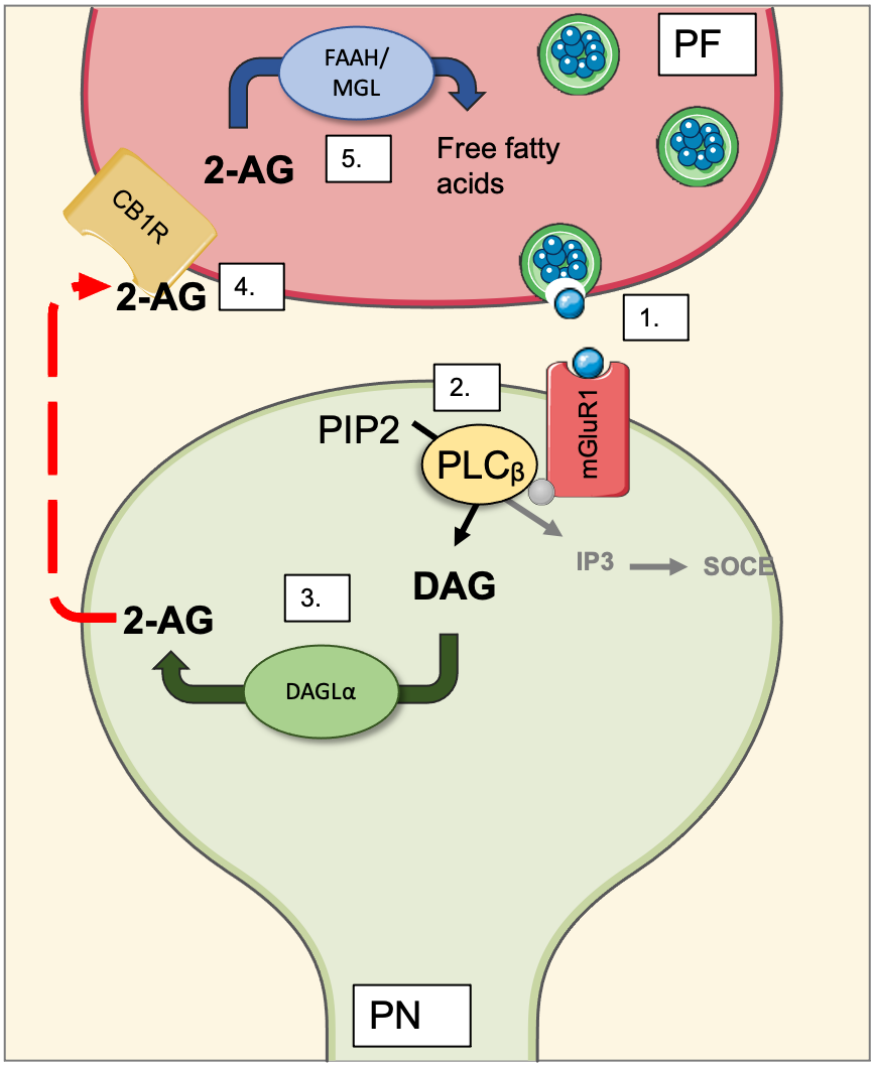

Figure 1.6 mGluR1-initiated 2-AG synthesis.

1. Glutamate released from PFs activate mGluR1s on the PN membrane. **2.** Activation of mGluR1 induces PLCβ-mediated cleavage of PIP2 into DAG and IP3. **3.** DAG is enzymatically catabolized by DAGLα into 2-AG, a prominent eCB within the cerebellum. **4.** 2-AG retroactively activates CB1Rs on presynaptic terminals. **5.** 2-AG is hydrolyzed into free fatty acids within the presynaptic terminal such as FAAH and MGL.

1.8.2 CB1R Activation and Function

In accordance with high levels of 2-AG within the cerebellum, there is also an abundance of CB1Rs that are highly expressed within the molecular layer of the cerebellum(Herkenham et al., 1990). CB1Rs bind to eCBs such as 2-AG and N-arachidonoylethanolamide (AEA), as well as exogenous cannabinoids, including Δ-9-tetrahydrocannabinol (THC) and to a weaker extent, cannabidiol (CBD)(Steinmetz & Freeman, 2016). As a Gi/o protein-coupled receptor, CB1R activation is responsible for inhibiting adenylyl cyclase and cyclic adenylyl monophosphate (cAMP) production, suppression of neurotransmitter release, including GABA from interneurons and glutamate from PFs respectively, and induction of morphological changes in neurons though cAMP-dependent pathways(Carey et al., 2011; P. Safo, Cravatt, & Regehr, 2006; Tapia et al., 2017). More specifically, CB1R activation within the cerebellum may also facilitate cerebellar learning and memory consolidation, as well as contribute to the PF-PN LTD profile(P. K. Safo & Regehr, 2005; Steinmetz & Freeman, 2016). During development, CB1R signaling plays an important role in modulating synaptic strength, as overstimulation of CB1Rs during this time may dampen PN synaptic maturation(Barnes et al., 2020).

1.8.3 Nitric Oxide and CB1R Activity

Multiple sources have described the interaction between CB1R activation and subsequent modulation of nNOS-derived NO production, however, the exact mechanism behind this interaction has yet to be fully elucidated. Interestingly, chronic CB1R activation can subsequently decrease NO production and nNOS expression, through inhibition of voltage-gated calcium channels. Specifically, CB1R-deficient mice exhibit greater NOS activity within the cerebrum compared to WT mice, which suggests a CB1R-dependent suppression of NO production(H. K. Sun et al., 2006). Contrastingly, there has been evidence suggesting CB1R activation leads to an increase in NO production in specific cell types. For example, N18TG2 neuroblastoma cells displayed elevated NO production in the presence of CB1R agonists(Jones, Carney, Vrana, Norford, & Howlett, 2008). However, there is little evidence reported that delineates the interaction between NO and CB1R within the cerebellum. Both CB1R and NO are needed in order to induce PF-PN LTD, as

one study revealed that LTD induction requires CB1R activation first, followed by NO production downstream of CB1R activation(P. K. Safo & Regehr, 2005).

1.9 Cerebellar Disorders and Implications

Cerebellar dysfunctions have increasingly begun to be included in a variety of neurological disorders, including autism, Alzheimer's disease, and Parkinson's disease(Fatemi et al., 2012; Jacobs et al., 2018; Lopez et al., 2020). The following section will describe canonical clinical cerebellar disorders and their association with PN function, PF-PN synaptic transmission, and cerebellar calcium dynamics.

1.9.1 Genetic: Spinocerebellar Ataxia and Episodic Ataxia

Spinocerebellar ataxias (SCA) are a group of rare hereditary ataxias that lead to degenerative changes within the cerebellum and in some cases, the spinal cord(Geschwind, Perlman, Figueroa, Treiman, & Pulst, 1997). Over 40 SCAs have been identified thus far, each with their characteristic genetic mutation, with a global prevalence rate of 0.3-3 per 100,000 per capita(Geschwind et al., 1997; Manto, 2005). Symptoms of the disease along with the perceived severity can vary depending on the type of SCA as well as age of onset, and mainly include uncoordinated gait, impaired hand and eye movements, as well as poor speech formation and cognitive deficits(Bürk et al., 1999, 2003; Manto, 2005). At the physiological level, the cerebellum often shows increased atrophy as well as degeneration and loss of PNs(Iizuka, Matsuzaki, Konno, & Hirai, 2016; Konno et al., 2014). In human SCAs, mutations in *ATXN*, *SPTBN2*, *CACNA1A*, *ITPR1* and *TRPC3* – genes encoding ataxin-1, β-III-spectrin, CaV2.1, IP3 receptor, and TRPC3 – are affected in SCA1, 5, 6, 15 and 41 respectively, and are crucial in maintaining PN viability and functionality(Armbrust et al., 2014; Becker, 2014; Coutelier et al., 2015; Cvetanovic, 2015; Jin et al., 2007; Y. Kim et al., 2012). Specifically, these gene mutations are similar in that they eventually alter calcium ion dynamics within the PN, consequently resulting in PN degeneration and loss(Kasumu & Bezprozvanny, 2012; Reitstetter & Yool, 1998; Yang & Lisberger, 2014).

Episodic ataxias (EAs) are similar to SCAs in that they are both neurological conditions originating in the cerebellum that affect movement coordination(Choi et al., 2017). EAs are also relatively rare disorders, affecting less than 1 in 100,000

individuals(Choi et al., 2017). Unlike SCAs, which present with chronic symptoms, EAs are characterized by transient, periodic bouts of ataxia, along with secondary symptoms including seizures and slurred speech(Orsucci, Raglione, Mazzoni, & Vista, 2019). Like SCAs, there are multiple types of EAs, presenting with various genetic mutations, including CACNA1A and SLC1A3 – genes encoding for CaV2.1 and GLAST, respectively(Iwama et al., 2018; Jen & Wan, 2018).

1.9.2 Chronic Alcohol Abuse

Chronic alcohol use has been implicated in inducing a pathological phenotype within the cerebellum. In general, chronic alcohol users present with physical symptoms that include tremors, uncoordinated gait, and deficits in maintaining upright posture and balance. Excessive alcohol consumption over long periods of time can result in cerebellar atrophy, measured by smaller grey matter areas and lower cerebellar volumes compared to those who abstain from drinking alcohol(Cardenas, Hough, Durazzo, & Meyerhoff, 2020; Cservenka, 2016). Nonmotor behaviours are also affected with chronic alcohol use, including impairments in executive functioning, working memory, attention shifting, and verbal tasks(Cardenas et al., 2020).

There is a significant correlation between cerebellar symptoms associated with chronic alcohol use and changes to NO production, although the exact effect chronic alcohol use has on NO levels remains controversial. Multiple studies have mentioned chronic alcohol use results in increased NO production and leads to cytotoxic and neurodegenerative effects(Lancaster, 1995; H. Sun et al., 2006). Contrastingly, studies have also deemed chronic alcohol use to cause decreases in nNOS-derived NO production both systemically and within the cerebrum(Afshar et al., 2016; Spanagel et al., 2002).

1.9.3 Chronic Cannabis Abuse

As more and more countries move towards legalization of cannabis, scientific studies have begun to assess the effects of long-term cannabis use on brain structure and neurocognition. With relation to the cerebellum, chronic cannabis use has been linked to alterations in cerebellar structure, specifically decreases in white matter volume and

increases in grey matter volume, along with deficits in decision making, memory, and associative learning(Blithikioti et al., 2019). Interestingly, studies have observed deficits in psychomotor tasks specifically in adolescent cannabis users, suggesting a link between cannabis use and cerebellar development(Blithikioti et al., 2019). As well, a study has linked cannabis use to cerebellar NO levels, in that THC-induced ataxias are correlated with decreases in NO production(A. D. Smith & Dar, 2007).

1.9.4 Nitric Oxide and Ataxic Models

Considering the importance that physiological levels of NO has on regulating synaptic transmission and glutamate uptake, there is little data available as to how a lack of NO production can affect cerebellar neuronal development and function. Two critical studies have noted that various cerebellar mutant mice with prominent ataxic behaviours also present with decreased NOS activity(Abbott & Nahm, 2004; Rhyu et al., 2003). This is important to consider, as it has been reported that nNOS expression is significantly decreased in the cerebella of aged rats, which corresponds to a decrease in learning and memory test performance(Yu, Juang, Lee, Liu, & Cheng, 2000). Despite this link, it is uncertain as to how a lack of NO can influence cerebellar pathologies.

1.10 Rationale, Hypothesis, and Aims

1.10.1 Rationale

It is undisputed that NO, and specifically nNOS, has a critical role to play in maintaining cerebellar homeostasis and PN function in a variety of ways, including maintenance of LTD, regulation of glutamate uptake, while also contributing to the eCB pathway. However, previous studies examining adult nNOS knockout ($nNOS^{-/-}$) mice noted the absence of gross CNS abnormalities, despite this model exhibiting behavioural deficits related to both aggression and locomotor activities associated with the cerebellum(P. L. Huang, Dawson, Bredt, Snyder, & Fishman, 1993; Kriegsfeld et al., 1999; Nelson et al., 1995). In addition to the lack of molecular research associated with the $nNOS^{-/-}$ mouse model, previous research has not determined whether an absence of nNOS expression can result in aberrant postnatal development, as most studies using the $nNOS^{-/-}$ model specifically study adult ages.

Although the $nNOS^{-/-}$ mouse model has been relatively understudied, some studies have noted the link between mutant mice exhibiting a cerebellar ataxic phenotype and decreases in NOS activity(Abbott & Nahm, 2004; Rhyu et al., 2003). Interestingly, cerebellar ataxic phenotypes often affect proteins associated with the production of the LTD response, namely components of the mGluR1 pathway as well as the calcium response within the PN. Given the lack of data on the $nNOS^{-/-}$ cerebellar phenotype throughout development, as well as the close connection between the presence of NO and synaptic function/plasticity within the cerebellum, I set out to characterize the role and mechanisms of NO signaling in regulating the morphology and protein expressions at the PF-PN synapse throughout postnatal development.

1.10.2 Hypothesis

It is hypothesized that the absence of nNOS-derived NO signaling during postnatal development in the murine cerebellum negatively impacts cerebellar network formation. Specifically, I hypothesize that the absence of nNOS/NO signaling in the murine cerebellum will result in an excitotoxic phenotype characterized by aberrant PN growth,

development, and synapse formation, through overactivation of mGluR1 on PNs, reduced glutamate uptake by BG, and altered eCB signaling.

1.10.3 Aims

To test this hypothesis, I carried out *in vivo* experiments in WT and nNOS$^{-/-}$ mice, *ex vivo* experiments using WT and nNOS$^{-/-}$ cerebellar slice cultures, and *in vitro* experiments using primary astrocyte cultures isolated from WT and nNOS$^{-/-}$ pups for the following aims:

Aim 1:

To characterize the morphological development of PF-PN synapses in WT and nNOS$^{-/-}$ mice with a focus on mGluR1 mediated SOCE.

Aim 2:

To characterize BG morphology and examine the function of GLAST in BGs of WT and nNOS$^{-/-}$ mice during postnatal development.

Aim 3:

To characterize the mGluR1-mediated eCB pathway in WT and nNOS$^{-/-}$ cerebella during postnatal development.

1.11 References

Abbott, L. C., & Nahm, S. (2004). Neuronal nitric oxide synthase expression in cerebellar mutant mice. *Cerebellum (London, England)*, *3*(3), 141–151. https://doi.org/10.1080/14734220410031927

Afshar, M., Poole, J. A., Cao, G., Durazo, R., Cooper, R. C., Kovacs, E. J., & Sisson, J. H. (2016). Exhaled Nitric Oxide Levels Among Adults With Excessive Alcohol Consumption. *Chest*, *150*(1), 196–209. https://doi.org/10.1016/j.chest.2016.02.642

Altman, J. (1972a). Postnatal development of the cerebellar cortex in the rat. II. Phases in the maturation of Purkinje cells and of the molecular layer. *Journal of Comparative Neurology*, *145*(4), 399–463. https://doi.org/10.1002/cne.901450402

Altman, J. (1972b). Postnatal development of the cerebellar cortex in the rat. III. Maturation of the components of the granular layer. *Journal of Comparative Neurology*, *145*(4), 465–513. https://doi.org/10.1002/cne.901450403

Ariano, M. A., Lewicki, J. A., Brandwein, H. J., & Murad, F. (1982). Immunohistochemical localization of guanylate cyclase within neurons of rat brain. *Proceedings of the National Academy of Sciences of the United States of America*, *79*(4 I), 1316–1320. https://doi.org/10.1073/pnas.79.4.1316

Armbrust, K. R., Wang, X., Hathorn, T. J., Cramer, S. W., Chen, G., Zu, T., … Ranum, L. P. W. (2014). Mutant β-III spectrin causes mGluR1α mislocalization and functional deficits in a mouse model of spinocerebellar ataxia type 5. *The Journal of Neuroscience : The Official Journal of the Society for Neuroscience*, *34*(30), 9891–9904. https://doi.org/10.1523/JNEUROSCI.0876-14.2014

Asano, S., Matsuda, T., Takuma, K., Kim, H. S., Sato, T., Nishikawa, T., & Baba, A. (2002). Nitroprusside and Cyclic GMP Stimulate Na^{+}-Ca^{2+} Exchange Activity in Neuronal Preparations and Cultured Rat Astrocytes. *Journal of Neurochemistry*, *64*(6), 2437–2441. https://doi.org/10.1046/j.1471-4159.1995.64062437.x

Ashby, M. C., Maier, S. R., Nishimune, A., & Henley, J. M. (2006). Lateral diffusion drives constitutive exchange of AMPA receptors at dendritic spines and is regulated by spine morphology. *The Journal of Neuroscience*, *26*(26), 7046–7055. https://doi.org/10.1523/JNEUROSCI.1235-06.2006

Balderas, A., Guillem, A. M., Martínez-Lozada, Z., Hernández-Kelly, L. C., Aguilera, J., & Ortega, A. (2014). GLAST/EAAT1 regulation in cultured Bergmann glia cells: Role of the NO/cGMP signaling pathway. *Neurochemistry International*, *73*(1), 139–145. https://doi.org/10.1016/j.neuint.2013.10.011

Barnes, J. L., Mohr, C., Ritchey, C. R., Erikson, C. M., Shiina, H., & Rossi, D. J. (2020). Developmentally Transient CB1Rs on Cerebellar Afferents Suppress Afferent Input, Downstream Synaptic Excitation, and Signaling to Migrating Neurons. *The Journal of Neuroscience : The Official Journal of the Society for Neuroscience*, *40*(32), 6133–6145. https://doi.org/10.1523/JNEUROSCI.1931-19.2020

Bauer, D. E., Jackson, J. G., Genda, E. N., Montoya, M. M., Yudkoff, M., & Robinson, M. B. (2012). The glutamate transporter, GLAST, participates in a macromolecular complex that supports glutamate metabolism. *Neurochemistry International*, *61*(4), 566–574. https://doi.org/10.1016/j.neuint.2012.01.013

Bazargani, N., & Attwell, D. (2016). Astrocyte calcium signaling: the third wave. *Nature Neuroscience*, *19*(2), 182–189. https://doi.org/10.1038/nn.4201

Becker, E. B. E. (2014). The Moonwalker Mouse: New Insights into TRPC3 Function, Cerebellar Development, and Ataxia. *Cerebellum*, *13*(5), 628–636. https://doi.org/10.1007/s12311-014-0564-5

Bellamy, T. C. (2006). Interactions between Purkinje neurones and Bergmann glia. *Cerebellum*, *5*(2), 116–126. https://doi.org/10.1080/14734220600724569

Bi, X., Bi, R., & Baudry, M. (2000). Calpain-mediated truncation of glutamate ionotropic receptors. Methods for studying the effects of calpain activation in brain tissue. *Methods in Molecular Biology*, *144*, 203–217. https://doi.org/10.1385/1-59259-050-

0:203

Bisogno, T., Howell, F., Williams, G., Minassi, A., Cascio, M. G., Ligresti, A., … Doherty, P. (2003). Cloning of the first sn1-DAG lipases points to the spatial and temporal regulation of endocannabinoid signaling in the brain. *Journal of Cell Biology*, *163*(3), 463–468. https://doi.org/10.1083/jcb.200305129

Blithikioti, C., Miquel, L., Batalla, A., Rubio, B., Maffei, G., Herreros, I., … Balcells-Oliveró, M. (2019). Cerebellar alterations in cannabis users: A systematic review. *Addiction Biology*, *24*(6), 1121–1137. https://doi.org/10.1111/adb.12714

Blitz, D. M., Foster, K. A., & Regehr, W. G. (2004). Short-term synaptic plasticity: A comparison of two synapses. *Nature Reviews Neuroscience*. Nature Publishing Group. https://doi.org/10.1038/nrn1475

Bordey, A., & Sontheimer, H. (2003). Modulation of glutamatergic transmission by Bergmann glial cells in rat cerebellum in situ. *Journal of Neurophysiology*, *89*(2), 979–988. https://doi.org/10.1152/jn.00904.2002

Bourne, J., & Harris, K. M. (2007). Do thin spines learn to be mushroom spines that remember? *Current Opinion in Neurobiology*, *17*(3), 381–386. https://doi.org/10.1016/j.conb.2007.04.009

Bredt, D. S., Hwang, P. M., & Snyder, S. H. (1990). Localization of nitric oxide synthase indicating a neural role for nitric oxide. *Nature*, *347*(6295), 768–770. https://doi.org/10.1038/347768a0

Brorson, J., Manzolillo, P., Gibbons, S., & Miller, R. (1995). AMPA receptor desensitization predicts the selective vulnerability of cerebellar Purkinje cells to excitotoxicity. *The Journal of Neuroscience*, *15*(6), 4515–4524. https://doi.org/10.1523/JNEUROSCI.15-06-04515.1995

Buckner, R. L. (2013). The cerebellum and cognitive function: 25 years of insight from anatomy and neuroimaging. *Neuron*, *80*(3), 807–815. https://doi.org/10.1016/j.neuron.2013.10.044

Bürk, K., Globas, C., Bösch, S., Gräber, S., Abele, M., Brice, A., … Klockgether, T. (1999). Cognitive deficits in spinocerebellar ataxia 2. *Brain : A Journal of Neurology*, *122 (Pt 4*, 769–777. https://doi.org/10.1093/brain/122.4.769

Bürk, K., Globas, C., Bösch, S., Klockgether, T., Zühlke, C., Daum, I., & Dichgans, J. (2003). Cognitive deficits in spinocerebellar ataxia type 1, 2, and 3. *Journal of Neurology*, *250*(2), 207–211. https://doi.org/10.1007/s00415-003-0976-5

Burnashev, N., Khodorova, A., Jonas, P., Helm, P. J., Wisden, W., Monyer, H., … Sakmann, B. (1992). Calcium-permeable AMPA-kainate receptors in fusiform cerebellar glial cells. *Science*, *256*(5063), 1566–1570. https://doi.org/10.1126/science.1317970

Buttermore, E. D., Piochon, C., Wallace, M. L., Philpot, B. D., Hansel, C., & Bhat, M. A. (2012). Pinceau organization in the cerebellum requires distinct functions of neurofascin in purkinje and basket neurons during postnatal development. *Journal of Neuroscience*, *32*(14), 4724–4742. https://doi.org/10.1523/JNEUROSCI.5602-11.2012

Calabrese, B., Wilson, M. S., & Halpain, S. (2006). Development and regulation of dendritic spine synapses. *Physiology*, *21*(1), 38–47. https://doi.org/10.1152/physiol.00042.2005

Campese, V. M., Sindhu, R. K., Ye, S., Bai, Y., Vaziri, N. D., & Jabbari, B. (2006). Regional expression of NO synthase , NAD (P) H oxidase and superoxide dismutase in the rat brain. *Brain Research*, *1134*, 27–32. https://doi.org/10.1016/j.brainres.2006.11.067

Cardenas, V. A., Hough, C. M., Durazzo, T. C., & Meyerhoff, D. J. (2020). Cerebellar Morphometry and Cognition in the Context of Chronic Alcohol Consumption and Cigarette Smoking. *Alcoholism: Clinical and Experimental Research*, *44*(1), 102–113. https://doi.org/10.1111/acer.14222

Carey, M. R., Myoga, M. H., McDaniels, K. R., Marsicano, G., Lutz, B., Mackie, K., &

Regehr, W. G. (2011). Presynaptic CB1 Receptors Regulate Synaptic Plasticity at Cerebellar Parallel Fiber Synapses. *Journal of Neurophysiology*, *105*(2), 958–963. https://doi.org/10.1152/jn.00980.2010

Casado, M., Dieudonné, S., & Ascher, P. (2000). Presynaptic N-methyl-D-aspartate receptors at the parallel fiber-Purkinje cell synapse. *Proceedings of the National Academy of Sciences of the United States of America*, *97*(21), 11593–11597. https://doi.org/10.1073/pnas.200354297

Chan, S. L., & Mattson, M. P. (1999). Caspase and calpain substrates: Roles in synaptic plasticity and cell death. *Journal of Neuroscience Research*, *58*(1), 167–190. https://doi.org/10.1002/(SICI)1097-4547(19991001)58:1<167::AID-JNR16>3.0.CO;2-K

Choi, K. D., Kim, J. S., Kim, H. J., Jung, I., Jeong, S. H., Lee, S. H., … Choi, J. H. (2017). Genetic Variants Associated with Episodic Ataxia in Korea. *Scientific Reports*, *7*(1), 1–11. https://doi.org/10.1038/s41598-017-14254-7

Contestabile, A. (2012). Role of nitric oxide in cerebellar development and function: Focus on granule neurons. *Cerebellum*, *11*(1), 50–61. https://doi.org/10.1007/s12311-010-0234-1

Coutelier, M., Blesneac, I., Monteil, A., Monin, M. L., Ando, K., Mundwiller, E., … Stevanin, G. (2015). A recurrent mutation in CACNA1G alters Cav3.1 T-type calcium-channel conduction and causes autosomal-dominant cerebellar ataxia. *American Journal of Human Genetics*, *97*(5), 726–737. https://doi.org/10.1016/j.ajhg.2015.09.007

Cservenka, A. (2016). Neurobiological phenotypes associated with a family history of alcoholism. *Drug and Alcohol Dependence*, *158*, 8–21. https://doi.org/10.1016/j.drugalcdep.2015.10.021

Custer, S. K., Garden, G. A., Gill, N., Rueb, U., Libby, R. T., Schultz, C., … La Spada, A. R. (2006). Bergmann glia expression of polyglutamine-expanded ataxin-7 produces

neurodegeneration by impairing glutamate transport. *Nature Neuroscience*, *9*(10), 1302–1311. https://doi.org/10.1038/nn1750

Cvetanovic, M. (2015). Decreased Expression of Glutamate Transporter GLAST in Bergmann Glia Is Associated with the Loss of Purkinje Neurons in the Spinocerebellar Ataxia Type 1. *Cerebellum*, *14*(1), 8–11. https://doi.org/10.1007/s12311-014-0605-0

Danbolt, N. C., Furness, D. N., & Zhou, Y. (2016). Neuronal vs glial glutamate uptake: Resolving the conundrum. *Neurochemistry International*, *98*, 29–45. https://doi.org/10.1016/j.neuint.2016.05.009

Daniel, H., Levenes, C., & Crépel, F. (1998). Cellular mechanisms of cerebellar LTD. *Trends in Neurosciences*, *21*(9), 401–407. https://doi.org/10.1016/S0166-2236(98)01304-6

Di Marzo, V., & Maccarrone, M. (2008). FAAH and anandamide: is 2-AG really the odd one out? *Trends in Pharmacological Sciences*, *29*(5), 229–233. https://doi.org/10.1016/j.tips.2008.03.001

Dumoulin, A., Triller, A., & Dieudonné, S. (2001). IPSC Kinetics at Identified GABAergic and Mixed GABAergic and Glycinergic Synapses onto Cerebellar Golgi Cells. *The Journal of Neuroscience*, *21*(16), 6045–6057. https://doi.org/10.1523/JNEUROSCI.21-16-06045.2001

Fatemi, S. H., Aldinger, K. A., Ashwood, P., Bauman, M. L., Blaha, C. D., Blatt, G. J., … Welsh, J. P. (2012). Consensus Paper: Pathological Role of the Cerebellum in Autism. *The Cerebellum*, *11*(3), 777–807. https://doi.org/10.1007/s12311-012-0355-9

Fernandez, L., Rogasch, N. C., Do, M., Clark, G., Major, B. P., Teo, W. P., … Enticott, P. G. (2020, April 1). Cerebral Cortical Activity Following Non-invasive Cerebellar Stimulation—a Systematic Review of Combined TMS and EEG Studies. *Cerebellum*. Springer. https://doi.org/10.1007/s12311-019-01093-7

Fleming, I., & Busse, R. (2003). Molecular mechanisms involved in the regulation of the endothelial nitric oxide synthase. *American Journal of Physiology. Regulatory,*

Integrative and Comparative Physiology, *284*(1), R1-12. https://doi.org/10.1152/ajpregu.00323.2002

Förstermann, U., Closs, E. I., Pollock, J. S., Nakane, M., Schwarz, P., Gath, I., & Kleinert, H. (1994). Nitric oxide synthase isozymes. Characterization, purification, molecular cloning, and functions. *Hypertension*, *23*(6 Pt 2), 1121–1131. https://doi.org/10.1161/01.hyp.23.6.1121

Förstermann, U., & Sessa, W. C. (2012). Nitric oxide synthases: regulation and function. *European Heart Journal*, *33*(7), 829–837, 837a-837d. https://doi.org/10.1093/eurheartj/ehr304

Gaston, B. (1999). Nitric oxide and thiol groups. *Biochimica et Biophysica Acta*, *1411*(2–3), 323–333. https://doi.org/10.1016/s0005-2728(99)00023-7

Geschwind, D. H., Perlman, S., Figueroa, C. P., Treiman, L. J., & Pulst, S. M. (1997). The prevalence and wide clinical spectrum of the spinocerebellar ataxia type 2 trinucleotide repeat in patients with autosomal dominant cerebellar ataxia. *American Journal of Human Genetics*, *60*(4), 842–850. Retrieved from http://www.ncbi.nlm.nih.gov/pubmed/9106530

Glickstein, M., Strata, P., & Voogd, J. (2009). Cerebellum: history. *Neuroscience*, *162*(3), 549–559. https://doi.org/10.1016/j.neuroscience.2009.02.054

Goodlett, C. R., & Mittleman, G. (2017). The Cerebellum. In *Conn's Translational Neuroscience* (pp. 191–212). Elsevier. https://doi.org/10.1016/B978-0-12-802381-5.00016-6

Grosche, J., Kettenmann, H., & Reichenbach, A. (2002). Bergmann glial cells form distinct morphological structures to interact with cerebellar neurons. *Journal of Neuroscience Research*, *68*(2), 138–149. https://doi.org/10.1002/jnr.10197

Gui, L., Zhu, J., Lu, X., Sims, S. M., Lu, W.-Y., Stathopulos, P. B., & Feng, Q. (2018). S-Nitrosylation of STIM1 by neuronal nitric oxide synthase inhibits store-operated Ca^{2+} entry. *Journal of Molecular Biology*. https://doi.org/10.1101/304022

Gulyas, A. I., Cravatt, B. F., Bracey, M. H., Dinh, T. P., Piomelli, D., Boscia, F., & Freund, T. F. (2004). Segregation of two endocannabinoid-hydrolyzing enzymes into pre- and postsynaptic compartments in the rat hippocampus, cerebellum and amygdala. *European Journal of Neuroscience*, *20*(2), 441–458. https://doi.org/10.1111/j.1460-9568.2004.03428.x

Habas, C. (2021). Functional Connectivity of the Cognitive Cerebellum. *Frontiers in Systems Neuroscience*, *15*, 27.

Haber, M. (2006). Cooperative Astrocyte and Dendritic Spine Dynamics at Hippocampal Excitatory Synapses. *Journal of Neuroscience*, *26*(35), 8881–8891. https://doi.org/10.1523/JNEUROSCI.1302-06.2006

Hallemeesch, M. M., Janssen, B. J. A., de Jonge, W. J., Soeters, P. B., Lamers, W. H., & Deutz, N. E. P. (2003). NO production by cNOS and iNOS reflects blood pressure changes in LPS-challenged mice. *American Journal of Physiology-Endocrinology and Metabolism*, *285*(4), E871–E875. https://doi.org/10.1152/ajpendo.00004.2002

Hansel, C., Linden, D. J., & D'Angelo, E. (2001). Beyond parallel fiber LTD: the diversity of synaptic and non-synaptic plasticity in the cerebellum. *Nature Neuroscience*, *4*(5), 467–475. https://doi.org/10.1038/87419

Hartell, N. A. (2002). Parallel fiber plasticity. *The Cerebellum*, *1*(1), 3–18. https://doi.org/10.1080/147342202753203041

Hartmann, J., Henning, H. A., & Konnerth, A. (2011). mGluR1/TRPC3-mediated synaptic transmission and calcium signaling in mammalian central neurons. *Cold Spring Harbor Perspectives in Biology*, *3*(4), 1–16. https://doi.org/10.1101/cshperspect.a006726

Hartmann, J., & Konnerth, A. (2015). TRPC3-dependent synaptic transmission in central mammalian neurons. *Journal of Molecular Medicine*, *93*(9), 983–989. https://doi.org/10.1007/s00109-015-1298-7

Hashimoto, K., Ichikawa, R., Kitamura, K., Watanabe, M., & Kano, M. (2009).

Translocation of a “Winner” Climbing Fiber to the Purkinje Cell Dendrite and Subsequent Elimination of “Losers” from the Soma in Developing Cerebellum. *Neuron*, *63*(1), 106–118. https://doi.org/10.1016/j.neuron.2009.06.008

Hashimoto, K., & Kano, M. (2013). Synapse elimination in the developing cerebellum. *Cellular and Molecular Life Sciences*, *70*(24), 4667–4680. https://doi.org/10.1007/s00018-013-1405-2

Hashimoto, M., & Hibi, M. (2012). Development and evolution of cerebellar neural circuits. *Development Growth and Differentiation*, *54*(3), 373–389. https://doi.org/10.1111/j.1440-169X.2012.01348.x

Hatten, M. E., & Heintz, N. (2005). Large-scale genomic approaches to brain development and circuitry. *Annual Review of Neuroscience*, *28*, 89–108. https://doi.org/10.1146/annurev.neuro.26.041002.131436

Haug, L. S., Jensen, V., Hvalby, Ø., Walaas, S. I., & Østvold, A. C. (1999). Phosphorylation of the inositol 1,4,5-trisphosphate receptor by cyclic nucleotide-dependent kinases in vitro and in rat cerebellar slices in situ. *Journal of Biological Chemistry*, *274*(11), 7467–7473. https://doi.org/10.1074/jbc.274.11.7467

Hendelman, W. J., & Aggerwal, A. S. (1980). The Purkinje neuron: I. A Golgi study of its development in the mouse and in culture. *Journal of Comparative Neurology*, *193*(4), 1063–1079. https://doi.org/10.1002/cne.901930417

Herkenham, M., Lynn, A. B., Little, M. D., Johnson, M. R., Melvin, L. S., de Costa, B. R., & Rice, K. C. (1990). Cannabinoid receptor localization in brain. *Proceedings of the National Academy of Sciences*, *87*(5), 1932–1936. https://doi.org/10.1073/pnas.87.5.1932

Hirano, T. (2018). Regulation and Interaction of Multiple Types of Synaptic Plasticity in a Purkinje Neuron and Their Contribution to Motor Learning. *Cerebellum (London, England)*, *17*(6), 756–765. https://doi.org/10.1007/s12311-018-0963-0

Ho, G. P. H., Selvakumar, B., Mukai, J., Hester, L. D., Wang, Y., Gogos, J. A., & Snyder,

S. H. (2011). S-Nitrosylation and S-Palmitoylation Reciprocally Regulate Synaptic Targeting of PSD-95. *Neuron*, *71*(1), 131–141. https://doi.org/10.1016/j.neuron.2011.05.033

Huang, G. N., Zeng, W., Kim, J. Y., Yuan, J. P., Han, L., Muallem, S., & Worley, P. F. (2006). STIM1 carboxyl-terminus activates native SOC, I(crac) and TRPC1 channels. *Nature Cell Biology*, *8*(9), 1003–1010. https://doi.org/10.1038/ncb1454

Huang, P. L., Dawson, T. M., Bredt, D. S., Snyder, S. H., & Fishman, M. C. (1993). Targeted disruption of the neuronal nitric oxide synthase gene. *Cell*, *75*(7), 1273–1286. https://doi.org/10.1016/0092-8674(93)90615-w

Huang, Y. H. (2004). Climbing Fiber Activation of EAAT4 Transporters and Kainate Receptors in Cerebellar Purkinje Cells. *Journal of Neuroscience*, *24*(1), 103–111. https://doi.org/10.1523/JNEUROSCI.4473-03.2004

Ichikawa, R., Hashimoto, K., Miyazaki, T., Uchigashima, M., Yamasaki, M., Aiba, A., … Watanabe, M. (2016). Territories of heterologous inputs onto Purkinje cell dendrites are segregated by mGluR1-dependent parallel fiber synapse elimination. *Proceedings of the National Academy of Sciences*, *113*(8), 2282–2287. https://doi.org/10.1073/pnas.1511513113

Ichikawa, R., Yamasaki, M., Miyazaki, T., Konno, K., Hashimoto, K., Tatsumi, H., … Watanabe, M. (2011). Developmental Switching of Perisomatic Innervation from Climbing Fibers to Basket Cell Fibers in Cerebellar Purkinje Cells. *Journal of Neuroscience*, *31*(47), 16916–16927. https://doi.org/10.1523/JNEUROSCI.2396-11.2011

Iino, M., Goto, K., Kakegawa, W., Okado, H., Sudo, M., Ishiuchi, S., … Ozawa, S. (2001). Glia-synapse interaction through Ca^{2+}-permeable AMPA receptors in Bergmann glia. *Science*, *292*(5518), 926–929. https://doi.org/10.1126/science.1058827

Iizuka, A., Matsuzaki, Y., Konno, A., & Hirai, H. (2016). Plasticity of the developmentally arrested staggerer cerebellum in response to exogenous RORα. *Brain Structure and*

Function, *221*(6), 2879–2889. https://doi.org/10.1007/s00429-015-1077-9

Ishiuchi, S., Yoshida, Y., Sugawara, K., Aihara, M., Ohtani, T., Watanabe, T., … Ozawa, S. (2007). Ca^{2+}-permeable AMPA receptors regulate growth of human glioblastoma via Akt activation. *Journal of Neuroscience*, *27*(30), 7987–8001. https://doi.org/10.1523/JNEUROSCI.2180-07.2007

Ito, M. (1989). Long-Term Depression. *Annual Review of Neuroscience*, *12*(1), 85–102. https://doi.org/10.1146/annurev.ne.12.030189.000505

Ito, M. (2001). Cerebellar Long-Term Depression: Characterization, Signal Transduction, and Functional Roles. *Physiological Reviews*, *81*(3), 1143–1195. https://doi.org/10.1152/physrev.2001.81.3.1143

Iwama, K., Iwata, A., Shiina, M., Mitsuhashi, S., Miyatake, S., Takata, A., … Matsumoto, N. (2018). A novel mutation in SLC1A3 causes episodic ataxia. *Journal of Human Genetics*, *63*(2), 207–211. https://doi.org/10.1038/s10038-017-0365-z

Jacobs, H. I. L., Hopkins, D. A., Mayrhofer, H. C., Bruner, E., Van Leeuwen, F. W., Raaijmakers, W., & Schmahmann, J. D. (2018). The cerebellum in Alzheimer's disease: Evaluating its role in cognitive decline. *Brain*, *141*(1), 37–47. https://doi.org/10.1093/brain/awx194

Jaffrey, S. R., Erdjument-Bromage, H., Ferris, C. D., Tempst, P., & Snyder, S. H. (2001). Protein S-nitrosylation: A physiological signal for neuronal nitric oxide. *Nature Cell Biology*, *3*(2), 193–197. https://doi.org/10.1038/35055104

Janmaat, S., Frédéric, F., Sjollema, K., Luiten, P., Mariani, J., & van der Want, J. (2009). Formation and maturation of parallel fiber-Purkinje cell synapses in the staggerer cerebellum ex vivo. *Journal of Comparative Neurology*, *512*(4), 467–477. https://doi.org/10.1002/cne.21910

Jelitai, M., Puggioni, P., Ishikawa, T., Rinaldi, A., & Duguid, I. (2016). Dendritic excitation-inhibition balance shapes cerebellar output during motor behaviour. *Nature Communications*, *7*(1), 1–13. https://doi.org/10.1038/ncomms13722

Jen, J. C., & Wan, J. (2018). Episodic ataxias. In *Handbook of Clinical Neurology* (Vol. 155, pp. 205–215). Elsevier B.V. https://doi.org/10.1016/B978-0-444-64189-2.00013-5

Jin, Y., Kim, S. J., Kim, J., Worley, P. F., & Linden, D. J. (2007). Long-Term Depression of mGluR1 Signaling. *Neuron*, *55*(2), 277–287. https://doi.org/10.1016/j.neuron.2007.06.035

Jones, J. D., Carney, S. T., Vrana, K. E., Norford, D. C., & Howlett, A. C. (2008). Cannabinoid receptor-mediated translocation of NO-sensitive guanylyl cyclase and production of cyclic GMP in neuronal cells. *Neuropharmacology*, *54*(1), 23–30. https://doi.org/10.1016/j.neuropharm.2007.06.027

Kalinovsky, A., Boukhtouche, F., Blazeski, R., Bornmann, C., Suzuki, N., Mason, C. A., & Scheiffele, P. (2011). Development of Axon-Target Specificity of Ponto-Cerebellar Afferents. *PLoS Biology*, *9*(2), e1001013. https://doi.org/10.1371/journal.pbio.1001013

Kang, Y., Liu, R., Wu, J. X., & Chen, L. (2019). Structural insights into the mechanism of human soluble guanylate cyclase. *Nature*, *574*(7777), 206–210. https://doi.org/10.1038/s41586-019-1584-6

Kano, M., Watanabe, T., Uesaka, N., & Watanabe, M. (2018). Multiple Phases of Climbing Fiber Synapse Elimination in the Developing Cerebellum. *Cerebellum (London, England)*, *17*(6), 722–734. https://doi.org/10.1007/s12311-018-0964-z

Kapfhammer, J. P. (2004). Cellular and molecular control of dendritic growth and development of cerebellar Purkinje cells. *Progress in Histochemistry and Cytochemistry*, *39*(3), 131–182. https://doi.org/10.1016/j.proghi.2004.07.002

Kasumu, A., & Bezprozvanny, I. (2012). Deranged calcium signaling in purkinje cells and pathogenesis in spinocerebellar ataxia 2 (SCA2) and other ataxias. *Cerebellum*, *11*(3), 630–639. https://doi.org/10.1007/s12311-010-0182-9

Kawamura, Y. (2006). The CB1 Cannabinoid Receptor Is the Major Cannabinoid Receptor

at Excitatory Presynaptic Sites in the Hippocampus and Cerebellum. *Journal of Neuroscience*, *26*(11), 2991–3001. https://doi.org/10.1523/JNEUROSCI.4872-05.2006

Kim, N., Azadzoi, K. M., Goldstein, I., & Saenz de Tejada, I. (1991). A nitric oxide-like factor mediates nonadrenergic-noncholinergic neurogenic relaxation of penile corpus cavernosum smooth muscle. *Journal of Clinical Investigation*, *88*(1), 112–118. https://doi.org/10.1172/JCI115266

Kim, Y., Wong, A. C. Y., Power, J. M., Tadros, S. F., Klugmann, M., Moorhouse, A. J., … Housley, G. D. (2012). Alternative Splicing of the TRPC3 Ion Channel Calmodulin/IP3 Receptor-Binding Domain in the Hindbrain Enhances Cation Flux. *Journal of Neuroscience*, *32*(33), 11414–11423. https://doi.org/10.1523/JNEUROSCI.6446-11.2012

Kirischuk, S., Kirchhoff, F., Matyash, V., Kettenmann, H., & Verkhratsky, A. (1999). Glutamate-triggered calcium signalling in mouse Bergmann glial cells in situ: Role of inositol-1,4,5-trisphosphate-mediated intracellular calcium release. *Neuroscience*, *92*(3), 1051–1059. https://doi.org/10.1016/S0306-4522(99)00067-6

Kirischuk, Sergei, Kettenmann, H., & Verkhratsky, A. (2007). Membrane currents and cytoplasmic sodium transients generated by glutamate transport in Bergmann glial cells. *Pflugers Archiv European Journal of Physiology*, *454*(2), 245–252. https://doi.org/10.1007/s00424-007-0207-5

Klein, A. P., Ulmer, J. L., Quinet, S. A., Mathews, V., & Mark, L. P. (2016). Nonmotor Functions of the Cerebellum: An Introduction. *American Journal of Neuroradiology*, *37*(6), 1005–1009. https://doi.org/10.3174/ajnr.A4720

Knöpfel, T., & Grandes, P. (2002). Metabotropic glutamate receptors in the cerebellum with a focus on their function in Purkinje cells. *The Cerebellum*, *1*(1), 19–26. https://doi.org/10.1007/BF02941886

Komuro, Y., Kumada, T., Ohno, N., Foote, K. D., & Komuro, H. (2013). Migration in the

Cerebellum. In *Cellular Migration and Formation of Neuronal Connections* (pp. 281–297). Elsevier. https://doi.org/10.1016/B978-0-12-397266-8.00030-2

Konno, A., Shuvaev, A. N., Miyake, N., Miyake, K., Iizuka, A., Matsuura, S., … Hirai, H. (2014). Mutant ataxin-3 with an abnormally expanded polyglutamine chain disrupts dendritic development and metabotropic glutamate receptor signaling in mouse cerebellar Purkinje cells. *Cerebellum*, *13*(1), 29–41. https://doi.org/10.1007/s12311-013-0516-5

Kriegsfeld, L. J., Eliasson, M. J., Demas, G. E., Blackshaw, S., Dawson, T. M., Nelson, R. J., & Snyder, S. H. (1999). Nocturnal motor coordination deficits in neuronal nitric oxide synthase knock-out mice. *Neuroscience*, *89*(2), 311–315. https://doi.org/S0306-4522(98)00614-9 [pii]

Kröncke, K. D., Kolb-Bachofen, V., Berschick, B., Burkart, V., & Kolb, H. (1991). Activated macrophages kill pancreatic syngeneic islet cells via arginine-dependent nitric oxide generation. *Biochemical and Biophysical Research Communications*, *175*(3), 752–758. https://doi.org/10.1016/0006-291X(91)91630-U

Lamont, M. G., & Weber, J. T. (2012). The role of calcium in synaptic plasticity and motor learning in the cerebellar cortex. *Neuroscience and Biobehavioral Reviews*, *36*(4), 1153–1162. https://doi.org/10.1016/j.neubiorev.2012.01.005

Lancaster, F. E. (1995). Alcohol and the brain: what's NO got to do with it? *Metabolic Brain Disease*, *10*(2), 125–133. https://doi.org/10.1007/BF01991860

Lehre, K. P., & Danbolt, N. C. (1998). The Number of Glutamate Transporter Subtype Molecules at Glutamatergic Synapses: Chemical and Stereological Quantification in Young Adult Rat Brain. *The Journal of Neuroscience*, *18*(21), 8751–8757. https://doi.org/10.1523/JNEUROSCI.18-21-08751.1998

Lev-Ram, V., Makings, L. R., Keitz, P. F., Kao, J. P. Y., & Tsien, R. Y. (1995). Long-term depression in cerebellar Purkinje neurons results from coincidence of nitric oxide and depolarization-induced Ca^{2+} transients. *Neuron*, *15*(2), 407–415.

https://doi.org/10.1016/0896-6273(95)90044-6

Linden, D., Dawson, T., & Dawson, V. (1995). An evaluation of the nitric oxide/cGMP/cGMP-dependent protein kinase cascade in the induction of cerebellar long-term depression in culture. *The Journal of Neuroscience*, *15*(7), 5098–5105. https://doi.org/10.1523/JNEUROSCI.15-07-05098.1995

López-Bayghen, E., Espinoza-Rojo, M., & Ortega, A. (2003). Glutamate down-regulates GLAST expression through AMPA receptors in Bergmann glial cells. *Molecular Brain Research*, *115*(1), 1–9. https://doi.org/10.1016/S0169-328X(03)00136-0

Lopez, A. M., Trujillo, P., Hernandez, A. B., Lin, Y. C., Kang, H., Landman, B. A., … Claassen, D. O. (2020). Structural Correlates of the Sensorimotor Cerebellum in Parkinson's Disease and Essential Tremor. *Movement Disorders*, *35*(7), 1181–1188. https://doi.org/10.1002/mds.28044

Maejima, T., Oka, S., Hashimotodani, Y., Ohno-Shosaku, T., Aiba, A., Wu, D., … Kano, M. (2005). Synaptically driven endocannabinoid release requires Ca^{2+}-assisted metabotropic glutamate receptor subtype 1 to phospholipase Cbeta4 signaling cascade in the cerebellum. *The Journal of Neuroscience : The Official Journal of the Society for Neuroscience*, *25*(29), 6826–6835. https://doi.org/10.1523/JNEUROSCI.0945-05.2005

Maekawa, K., & Simpson, J. I. (1973). Climbing fiber responses evoked in vestibulocerebellum of rabbit from visual system. *Journal of Neurophysiology*, *36*(4), 649–666. https://doi.org/10.1152/jn.1973.36.4.649

Maiti, P., Manna, J., Ilavazhagan, G., Rossignol, J., & Dunbar, G. L. (2015). Molecular regulation of dendritic spine dynamics and their potential impact on synaptic plasticity and neurological diseases. *Neuroscience and Biobehavioral Reviews*, *59*, 208–237. https://doi.org/10.1016/j.neubiorev.2015.09.020

Manto, M. (2005). The wide spectrum of spinocerebellar ataxias (SCAs). *The Cerebellum*, *4*(1), 2–6. https://doi.org/10.1080/14734220510007914

Martin, E., Berka, V., Bogatenkova, E., Murad, F., & Tsai, A. L. (2006). Ligand selectivity of soluble guanylyl cyclase: Effect of the hydrogen-bonding tyrosine in the distal heme pocket on binding of oxygen, nitric oxide, and carbon monoxide. *Journal of Biological Chemistry*, *281*(38), 27836–27845. https://doi.org/10.1074/jbc.M601078200

Martínez-Lozada, Z., Hernández-Kelly, L. C., Aguilera, J., López-Bayghen, E., & Ortega, A. (2011). Signaling through EAAT-1/GLAST in cultured Bergmann glia cells. *Neurochemistry International*, *59*(6), 871–879. https://doi.org/10.1016/j.neuint.2011.07.015

Martínez, D., García, L., Aguilera, J., & Ortega, A. (2014). An acute glutamate exposure induces long-term down regulation of GLAST/EAAT1 uptake activity in cultured bergmann glia cells. *Neurochemical Research*, *39*(1), 142–149. https://doi.org/10.1007/s11064-013-1198-6

Martinez, S., Andreu, A., Mecklenburg, N., & Echevarria, D. (2013). Cellular and molecular basis of cerebellar development. *Frontiers in Neuroanatomy*, *7*(JUNE), 18. https://doi.org/10.3389/fnana.2013.00018

Mason, C. A., Christakos, S., & Catalano, S. M. (1990). Early climbing fiber interactions with Purkinje cells in the postnatal mouse cerebellum. *Journal of Comparative Neurology*, *297*(1), 77–90. https://doi.org/10.1002/cne.902970106

Mattson, M. P. (1990). Antigenic changes similar to those seen in neurofibrillary tangles are elicited by glutamate and Ca^{2+} influx in cultured hippocampal neurons. *Neuron*, *4*(1), 105–117. https://doi.org/10.1016/0896-6273(90)90447-N

Mattson, M. P. (2007). Calcium and neurodegeneration. *Aging Cell*, *6*(3), 337–350. https://doi.org/10.1111/j.1474-9726.2007.00275.x

Matyash, V., Filippov, V., Mohrhagen, K., & Kettenmann, H. (2001). Nitric oxide signals parallel fiber activity to Bergmann glial cells in the mouse cerebellar slice. *Molecular and Cellular Neuroscience*, *18*(6), 664–670. https://doi.org/10.1006/mcne.2001.1047

McCabe, T. J., Fulton, D., Roman, L. J., & Sessa, W. C. (2000). Enhanced electron flux and reduced calmodulin dissociation may explain “calcium-independent” eNOS activation by phosphorylation. *Journal of Biological Chemistry*, *275*(9), 6123–6128. https://doi.org/10.1074/jbc.275.9.6123

Melikian, N., Seddon, M. D., Casadei, B., Chowienczyk, P. J., & Shah, A. M. (2009). Neuronal nitric oxide synthase and human vascular regulation. *Trends in Cardiovascular Medicine*, *19*(8), 256–262. https://doi.org/10.1016/j.tcm.2010.02.007

Metea, M. R., & Newman, E. A. (2006). Calcium signaling in specialized glial cells. *Glia*, *54*(7), 650–655. https://doi.org/10.1002/glia.20352

Metzger, F., Kapfhammer, J. P., Metzger, F., & Kapfhammer, J. P. (2003). Protein kinase C: its role in activity-dependent Purkinje cell dendritic development and plasticity. *Cerebellum*, *2*, 206–214. https://doi.org/10.1080/14734220310016150

Millen, K. J., & Gleeson, J. G. (2008). Cerebellar development and disease. *Current Opinion in Neurobiology*, *18*(1), 12–19. https://doi.org/10.1016/j.conb.2008.05.010

Mishina, M., Uemura, T., Yasumura, M., & Yoshida, T. (2012). Molecular mechanism of parallel fiber-Purkinje cell synapse formation. *Frontiers in Neural Circuits*, *6*(November), 90. https://doi.org/10.3389/fncir.2012.00090

Miyazaki, T., Yamasaki, M., Hashimoto, K., Kohda, K., Yuzaki, M., Shimamoto, K., … Watanabe, M. (2017). Glutamate transporter GLAST controls synaptic wrapping by Bergmann glia and ensures proper wiring of Purkinje cells. *Proceedings of the National Academy of Sciences*, *114*(28), 7438–7443. https://doi.org/10.1073/pnas.1617330114

Morara, S., Van Der Want, J. J. L., De Weerd, H., Provinp, L., & Rosina, A. (2001). Ultrastructural analysis of climbing fiber-purkinje cell synaptogenesis in the rat cerebellum. *Neuroscience*, *108*(4), 655–671. https://doi.org/10.1016/S0306-4522(01)00433-X

Murohara, T., Asahara, T., Silver, M., Bauters, C., Masuda, H., Kalka, C., … Isner, J. M.

(1998). Nitric oxide synthase modulates angiogenesis in response to tissue ischemia. *Journal of Clinical Investigation*, *101*(11), 2567–2578. https://doi.org/10.1172/JCI1560

Nakazawa, K., Mikawa, S., Hashikawa, T., & Ito, M. (1995). Transient and persistent phosphorylation of AMPA-type glutamate receptor subunits in cerebellar Purkinje cells. *Neuron*, *15*(3), 697–709. https://doi.org/10.1016/0896-6273(95)90157-4

Nelson, R., Demas, G., Huang, P., Fishman, M., Dawson, V., Dawson, T., & Snyder, S. (1995). Behavioural abnormalities in male mice lacking neuronal nitric oxide synthase. *Nature*, *378*(6555), 383–386. https://doi.org/10.1038/378383a0

Noguchi, J., Matsuzaki, M., Ellis-Davies, G. C. R., & Kasai, H. (2005). Spine-neck geometry determines NMDA receptor-dependent Ca^{2+} signaling in dendrites. *Neuron*, *46*(4), 609–622. https://doi.org/10.1016/j.neuron.2005.03.015

Oldreive, C. E., Gaynor, S., & Doherty, G. H. (2012). Effects of nitric oxide on the survival and neuritogenesis of cerebellar Purkinje neurons. *Journal of Molecular Neuroscience : MN*, *46*(2), 336–342. https://doi.org/10.1007/s12031-011-9590-7

Orsucci, D., Raglione, L. M., Mazzoni, M., & Vista, M. (2019). Therapy of episodic ataxias: case report and review of the literature. *Drugs in Context*, *8*, 1–6. https://doi.org/10.7573/dic.212576

Ortega, A., Eshhar, N., & Teichberg, V. I. (1991). Properties of kainate receptor/channels on cultured Bergmann glia. *Neuroscience*, *41*(2–3), 335–349. https://doi.org/10.1016/0306-4522(91)90331-H

Pandya, N. J., Klaassen, R. V., van der Schors, R. C., Slotman, J. A., Houtsmuller, A., Smit, A. B., & Li, K. W. (2016). Group 1 metabotropic glutamate receptors 1 and 5 form a protein complex in mouse hippocampus and cortex. *PROTEOMICS*, *16*(20), 2698–2705. https://doi.org/10.1002/pmic.201500400

Perego, C., Vanoni, C., Bossi, M., Massari, S., Basudev, H., Longhi, R., & Pietrini, G. (2000). The GLT-1 and GLAST glutamate transporters are expressed on

morphologically distinct astrocytes and regulated by neuronal activity in primary hippocampal cocultures. *Journal of Neurochemistry*, *75*(3), 1076–1084. https://doi.org/10.1046/j.1471-4159.2000.0751076.x

Prestori, F., Mapelli, L., & D'Angelo, E. (2019). Diverse Neuron Properties and Complex Network Dynamics in the Cerebellar Cortical Inhibitory Circuit. *Frontiers in Molecular Neuroscience*, *12*, 267. https://doi.org/10.3389/fnmol.2019.00267

Rakic, P. (1971). Neuron-glia relationship during granule cell migration in developing cerebellar cortex. A Golgi and electonmicroscopic study in Macacus rhesus. *Journal of Comparative Neurology*, *141*(3), 283–312. https://doi.org/10.1002/cne.901410303

Rami, A., Ferger, D., & Krieglstein, J. (1997). Blockade of calpain proteolytic activity rescues neurons from glutamate excitotoxicity. *Neuroscience Research*, *27*(1), 93–97. https://doi.org/10.1016/S0168-0102(96)01123-6

Rapoport, R. M., Draznin, M. B., & Murad, F. (1983). Endothelium-dependent relaxation in rat aorta may be mediated through cyclic GMP-dependent protein phosphorylation. *Nature*, *306*(5939), 174–176. https://doi.org/10.1038/306174a0

Reitstetter, R., & Yool, A. J. (1998). Morphological consequences of altered calcium-dependent transmembrane signaling on the development of cultured cerebellar Purkinje neurons. *Developmental Brain Research*, *107*(1), 165–167. https://doi.org/10.1016/S0165-3806(98)00017-0

Rhyu, I. J., Nahm, S. S., Hwang, S. J., Kim, H., Suh, Y. S., Oda, S. I., … Abbott, L. C. (2003). Altered neuronal nitric oxide synthase expression in the cerebellum of calcium channel mutant mice. *Brain Research*, *977*(2), 129–140. https://doi.org/10.1016/S0006-8993(03)02403-X

Rose, C. R., Ziemens, D., & Verkhratsky, A. (2020). On the special role of NCX in astrocytes: Translating Na^+-transients into intracellular Ca^{2+} signals. *Cell Calcium*, *86*, 102154. https://doi.org/10.1016/j.ceca.2019.102154

Ryu, C., Jang, D. C., Jung, D., Kim, Y. G., Shim, H. G., Ryu, H.-H., … Kim, S. J. (2017).

STIM1 regulates somatic Ca $^{2+}$ signals and intrinsic firing properties of cerebellar Purkinje neurons. *The Journal of Neuroscience*, *37*(37), 3973–16. https://doi.org/10.1523/JNEUROSCI.3973-16.2017

Safo, P., Cravatt, B., & Regehr, W. (2006). Retrograde endocannabinoid signaling in the cerebellar cortex. *The Cerebellum*, *5*(2), 134–145. https://doi.org/10.1080/14734220600791477

Safo, P. K., & Regehr, W. G. (2005). Endocannabinoids control the induction of cerebellar LTD. *Neuron*, *48*(4), 647–659. https://doi.org/10.1016/j.neuron.2005.09.020

Santamaria, F., Wils, S., De Schutter, E., & Augustine, G. J. (2006). Anomalous Diffusion in Purkinje Cell Dendrites Caused by Spines. *Neuron*, *52*(4), 635–648. https://doi.org/10.1016/j.neuron.2006.10.025

Schilling, K., Schmidt, H. H., & Baader, S. L. (1994). Nitric oxide synthase expression reveals compartments of cerebellar granule cells and suggests a role for mossy fibers in their development. *Neuroscience*, *59*(4), 893–903.

Schlosburg, J. E., Blankman, J. L., Long, J. Z., Nomura, D. K., Kinsey, S. G., Nguyen, P. T., … Cravatt, B. F. (2010). Chronic monoacylglycerol lipase blockade causes functional antagonism of the endocannabinoid system. *Nature Publishing Group*, *13*(9). https://doi.org/10.1038/nn.2616

Secondo, A., Molinaro, P., Pannaccione, A., Esposito, A., Cantile, M., Lippiello, P., … Annunziato, L. (2011). Nitric oxide stimulates NCX1 and NCX2 but inhibits NCX3 isoform by three distinct molecular determinants. *Molecular Pharmacology*, *79*(3), 558–568. https://doi.org/10.1124/mol.110.069658

Selvakumar, B., Huganir, R. L., & Snyder, S. H. (2009). S-nitrosylation of stargazin regulates surface expression of AMPA-glutamate neurotransmitter receptors. *Proceedings of the National Academy of Sciences*, *106*(38), 16440–16445. https://doi.org/10.1073/pnas.0908949106

Sergaki, M. C., López-Ramos, J. C., Stagkourakis, S., Gruart, A., Broberger, C., Delgado-

García, J. M., & Ibáñez, C. F. (2017). Compromised Survival of Cerebellar Molecular Layer Interneurons Lacking GDNF Receptors GFRα1 or RET Impairs Normal Cerebellar Motor Learning. *Cell Reports*, *19*(10), 1977–1986. https://doi.org/10.1016/j.celrep.2017.05.030

Seubert, P., Baudry, M., Dudek, S., & Lynch, G. (1987). Calmodulin stimulates the degradation of brain spectrin by calpain. *Synapse*, *1*(1), 20–24. https://doi.org/10.1002/syn.890010105

Shimizu-Albergine, M., Rybalkin, S. D., Rybalkina, I. G., Feil, R., Wolfsgruber, W., Hofmann, F., & Beavo, J. A. (2003). Individual cerebellar Purkinje cells express different cGMP phosphodiesterases (PDEs): In vivo phosphorylation of cGMP-specific PDE (PDE5) as an indicator of cGMP-dependent protein kinase (PKG) activation. *Journal of Neuroscience*, *23*(16), 6452–6459. https://doi.org/10.1523/jneurosci.23-16-06452.2003

Simat, M., Parpan, F., & Fritschy, J.-M. (2007). Heterogeneity of glycinergic and gabaergic interneurons in the granule cell layer of mouse cerebellum. *The Journal of Comparative Neurology*, *500*(1), 71–83. https://doi.org/10.1002/cne.21142

Slemmer, J. E., De Zeeuw, C. I., & Weber, J. T. (2005). Don't get too excited: Mechanisms of glutamate-mediated Purkinje cell death. *Progress in Brain Research*, *148*, 367–390. https://doi.org/10.1016/S0079-6123(04)48029-7

Smith, A. D., & Dar, M. S. (2007). Behavioral cross-tolerance between repeated intracerebellar nicotine and acute Δ9-tetrahydrocannabinol-induced cerebellar ataxia: Role of cerebellar nitric oxide. *Journal of Pharmacology and Experimental Therapeutics*, *322*(1), 243–253. https://doi.org/10.1124/jpet.107.120634

Smith, B. C., Fernhoff, N. B., & Marletta, M. A. (2012). Mechanism and kinetics of inducible nitric oxide synthase auto- S -nitrosation and inactivation. *Biochemistry*, *51*(5), 1028–1040. https://doi.org/10.1021/bi201818c

Sotelo, C., & Dusart, I. (2009). Intrinsic versus extrinsic determinants during the

development of Purkinje cell dendrites. *Neuroscience*, *162*(3), 589–600. https://doi.org/10.1016/j.neuroscience.2008.12.035

Spanagel, R., Siegmund, S., Cowen, M., Schroff, K. C., Schumann, G., Fiserova, M., … Putzke, J. (2002). The neuronal nitric oxide synthase gene is critically involved in neurobehavioral effects of alcohol. *Journal of Neuroscience*, *22*(19), 8676–8683. https://doi.org/10.1523/jneurosci.22-19-08676.2002

Stamler, J. S., Lamas, S., & Fang, F. C. (2001). Nitrosylation. the prototypic redox-based signaling mechanism. *Cell*, *106*(6), 675–683. https://doi.org/10.1016/s0092-8674(01)00495-0

Stein-Behrens, B., Mattson, M. P., Chang, I., Yeh, M., & Sapolsky, R. (1994). Stress exacerbates neuron loss and cytoskeletal pathology in the hippocampus. *Journal of Neuroscience*, *14*(9), 5373–5380. https://doi.org/10.1523/jneurosci.14-09-05373.1994

Steinmetz, A. B., & Freeman, J. H. (2016). Cannabinoid modulation of memory consolidation within the cerebellum. *Neurobiology of Learning and Memory*, *136*, 228–235. https://doi.org/10.1016/j.nlm.2016.11.002

Stuehr, D. J. (1999). Mammalian nitric oxide synthases. *Biochimica et Biophysica Acta (BBA) - Bioenergetics*, *1411*(2–3), 217–230. https://doi.org/10.1016/S0005-2728(99)00016-X

Stuehr, D., Pou, S., & Rosen, G. M. (2001). Oxygen reduction by nitric-oxide synthases. *The Journal of Biological Chemistry*, *276*(18), 14533–14536. https://doi.org/10.1074/jbc.R100011200

Sudarov, A., & Joyner, A. L. (2007). Cerebellum morphogenesis: The foliation pattern is orchestrated by multi-cellular anchoring centers. *Neural Development*, *2*(1), 26. https://doi.org/10.1186/1749-8104-2-26

Sun, H. K., Seok, J. W., Xiao, O. M., Ledent, C., Jin, K., & Greenberg, D. A. (2006). Role for neuronal nitric-oxide synthase in cannabinoid-induced neurogenesis. *Journal of*

Pharmacology and Experimental Therapeutics, *319*(1), 150–154. https://doi.org/10.1124/jpet.106.107698

Sun, H., Molacek, E., Zheng, H., Fang, Q., Patel, K. P., & Mayhan, W. G. (2006). Alcohol-induced impairment of neuronal nitric oxide synthase (nNOS)-dependent dilation of cerebral arterioles: Role of NAD(P)H oxidase. *Journal of Molecular and Cellular Cardiology*, *40*(2), 321–328. https://doi.org/10.1016/j.yjmcc.2005.11.004

Takatsuru, Y., Takayasu, Y., Iino, M., Nikkuni, O., Ueda, Y., Tanaka, K., & Ozawa, S. (2006). Roles of glial glutamate transporters in shaping EPSCs at the climbing fiber-Purkinje cell synapses. *Neuroscience Research*, *54*(2), 140–148. https://doi.org/10.1016/j.neures.2005.11.002

Takuma, K., Ago, Y., & Matsuda, T. (2013). The glial sodium-calcium exchanger: a new target for nitric oxide-mediated cellular toxicity. *Current Protein & Peptide Science*, *14*(1), 43–50. https://doi.org/10.2174/1389203711314010007

Tanaka, S., Kawaguchi, S. Y., Shioi, G., & Hirano, T. (2013). Long-term potentiation of inhibitory synaptic transmission onto cerebellar Purkinje neurons contributes to adaptation of vestibulo-ocular reflex. *Journal of Neuroscience*, *33*(43), 17209–17220. https://doi.org/10.1523/JNEUROSCI.0793-13.2013

Tapia, M., Dominguez, A., Zhang, W., Puerto, A. Del, Ciorraga, M., Benitez, M. J., … Garrido, J. J. (2017). Cannabinoid receptors modulate neuronal morphology and ankyring density at the axon initial segment. *Frontiers in Cellular Neuroscience*, *11*, 5. https://doi.org/10.3389/fncel.2017.00005

Tiburcio-Félix, R., Cisneros, B., Hernández-Kelly, L. C. R., Hernández-Contreras, M. A., Luna-Herrera, J., Rea-Hernández, I., … Ortega, A. (2019). Neuronal Nitric Oxide Synthase in Cultured Cerebellar Bergmann Glia: Glutamate-Dependent Regulation. *ACS Chemical Neuroscience*, *10*(6), 2668–2675. https://doi.org/10.1021/acschemneuro.8b00656

Toda, N., Ayajiki, K., & Okamura, T. (2009). Control of systemic and pulmonary blood

pressure by nitric oxide formed through neuronal nitric oxide synthase. *Journal of Hypertension*, *27*(10), 1929–1940. https://doi.org/10.1097/HJH.0b013e32832e8ddf

Ullian, E. M., Sapperstein, S. K., Christopherson, K. S., & Barres, B. A. (2001). Control of synapse number by glia. *Science*, *291*(5504), 657–661. https://doi.org/10.1126/science.291.5504.657

Verpelli, C., Piccoli, G., Zibetti, C., Zanchi, A., Gardoni, F., Huang, K., … Sala, C. (2010). Synaptic Activity Controls Dendritic Spine Morphology by Modulating eEF2-Dependent BDNF Synthesis. *Journal of Neuroscience*, *30*(17), 5830–5842. https://doi.org/10.1523/JNEUROSCI.0119-10.2010

Vosler, P. S., Brennan, C. S., & Chen, J. (2008). Calpain-mediated signaling mechanisms in neuronal injury and neurodegeneration. *Molecular Neurobiology*, *38*(1), 78–100. https://doi.org/10.1007/s12035-008-8036-x

Wang, D.-J., Su, L.-D., Wang, Y.-N., Yang, D., Sun, C.-L., Zhou, L., … Shen, Y. (2014). Long-Term Potentiation at Cerebellar Parallel Fiber-Purkinje Cell Synapses Requires Presynaptic and Postsynaptic Signaling Cascades. *Journal of Neuroscience*, *34*(6), 2355–2364. https://doi.org/10.1523/JNEUROSCI.4064-13.2014

Willard, S. S., & Koochekpour, S. (2013). Glutamate, glutamate receptors, and downstream signaling pathways. *International Journal of Biological Sciences*, *9*(9), 948–959. https://doi.org/10.7150/ijbs.6426

Wingate, R. J. T. (2001, February 1). The rhombic lip and early cerebellar development. *Current Opinion in Neurobiology*. Elsevier Ltd. https://doi.org/10.1016/S0959-4388(00)00177-X

Wojda, U., Salinska, E., & Kuznicki, J. (2008). Calcium ions in neuronal degeneration. *IUBMB Life*, *60*(9), 575–590. https://doi.org/10.1002/iub.91

Wong, R. O. L., & Ghosh, A. (2002). Activity-dependent regulation of dendritic growth and patterning. *Nature Reviews Neuroscience*, *3*(10), 803–812. https://doi.org/10.1038/nrn941

Xu-Friedman, M. A., Harris, K. M., & Regehr, W. G. (2001). Three-dimensional comparison of ultrastructural characteristics at depressing and facilitating synapses onto cerebellar Purkinje cells. *Journal of Neuroscience*, *21*(17), 6666–6672. https://doi.org/10.1523/jneurosci.21-17-06666.2001

Xu, H., Yang, Y., Tang, X., Zhao, M., Liang, F., Xu, P., … Fan, X. (2013). Bergmann glia function in granule cell migration during cerebellum development. *Molecular Neurobiology*, *47*(2), 833–844. https://doi.org/10.1007/s12035-013-8405-y

Xu, W., Wong, T. P., Chery, N., Gaertner, T., Wang, Y. T., & Baudry, M. (2007). Calpain-Mediated mGluR1α Truncation: A Key Step in Excitotoxicity. *Neuron*. https://doi.org/10.1016/j.neuron.2006.12.020

Yamada, K., Fukaya, M., Shibata, T., Kurihara, H., Tanaka, K., Inoue, Y., & Watanabe, M. (2000). Dynamic transformation of Bergmann glial fibers proceeds in correlation with dendritic outgrowth and synapse formation of cerebellar Purkinje cells. *Journal of Comparative Neurology*, *418*(1), 106–120. https://doi.org/10.1002/(SICI)1096-9861(20000228)418:1<106::AID-CNE8>3.0.CO;2-N

Yamada, K., & Watanabe, M. (2002). Cytodifferentiation of Bergmann glia and its relationship with Purkinje cells. *Anatomical Science International / Japanese Association of Anatomists*. https://doi.org/10.1046/j.0022-7722.2002.00021.x

Yang, Y., & Lisberger, S. G. (2014). Purkinje-cell plasticity and cerebellar motor learning are graded by complex-spike duration. *Nature*, *510*(7506), 529–532. https://doi.org/10.1038/nature13282

Yu, W., Juang, S., Lee, J., Liu, T., & Cheng, J. (2000). Decrease of neuronal nitric oxide synthase in the cerebellum of aged rats. *Neuroscience Letters*, *291*(1), 37–40. https://doi.org/10.1016/s0304-3940(00)01377-x

Yuan, J. P., Zeng, W., Huang, G. N., Worley, P. F., & Muallem, S. (2007). STIM1 heteromultimerizes TRPC channels to determine their function as store-operated channels. *Nature Cell Biology*, *9*(6), 636–645. https://doi.org/10.1038/ncb1590

Zhou, J., Brown, A. M., Lackey, E. P., Arancillo, M., Lin, T., & Sillitoe, R. V. (2020). Purkinje cell neurotransmission patterns cerebellar basket cells into zonal modules defined by distinct pinceau sizes. *ELife*, *9*. https://doi.org/10.7554/eLife.55569

Zhou, L., & Zhu, D.-Y. (2009). Neuronal nitric oxide synthase: structure, subcellular localization, regulation, and clinical implications. *Nitric Oxide : Biology and Chemistry*, *20*(4), 223–230. https://doi.org/10.1016/j.niox.2009.03.001

Chapter 2

This chapter was published in the journal *Cerebellum*, volume 19, issue 4, pages 510-526. It has been reproduced with permission from Springer.

2 Nitric Oxide Critically Regulates Purkinje Neuron Dendritic Development Through a Metabotropic Glutamate Receptor Type 1-Mediated Mechanism.

2.1 Abstract

Nitric oxide (NO), specifically derived from neuronal nitric oxide synthase (nNOS), is a well-established regulator of synaptic transmission in Purkinje neurons (PNs), governing fundamental processes such as motor learning and coordination. Previous phenotypic analyses showed similar cerebellar structures between neuronal nitric oxide null ($nNOS^{-/-}$) and wild-type (WT) adult male mice, despite prominent ataxic behavior within $nNOS^{-/-}$ mice. However, a study has yet to characterize PN molecular structure and their excitatory inputs during development in $nNOS^{-/-}$ mice. This study is the first to explore morphological abnormalities within the cerebellum of $nNOS^{-/-}$ mice, using immunohistochemistry and immunoblotting. This study sought to examine PN dendritic morphology and the expression of metabotropic glutamate receptor type 1 (mGluR1), vesicular glutamate transporter type 1 and 2 (vGluT1 and vGluT2), stromal interaction molecule 1 (STIM1), and calpain-1 within PNs of WT and $nNOS^{-/-}$ mice at postnatal day 7 (PD7), 2 weeks (2W), and 7 weeks (7W) of age. Results showed a decrease in PN dendritic branching at PD7 in $nNOS^{-/-}$ cerebella, while aberrant dendritic spine formation was noted in adult ages. Total protein expression of mGluR1 was decreased in $nNOS^{-/-}$ cerebella across development, while vGluT2, STIM1, and calpain-1 were significantly increased. Ex vivo treatment of WT slices with NOS inhibitor L-NAME increased calpain-1 expression, whereas treating $nNOS^{-/-}$ cerebellar slices with NO donor NOC-18 decreased calpain-1. Moreover, mGluR1 agonist DHPG increased calpain-1 in WT, but not in $nNOS^{-/-}$ slices. Together, these results indicate a novel role for nNOS/NO signaling in PN development, particularly by regulating an mGluR1-initiated calcium signaling mechanism.

2.2 Introduction

Mutant mice have been crucial in discerning key pathways associated with cerebellar development and pathogenesis. Although many have been identified and characterized in terms of cerebellar morphology, a number of mutant mice that exhibit ataxic behaviors have yet to be characterized at the molecular level. A well-known modulator of synaptic trans-mission and function within the cerebellum is nitric oxide (NO), produced primarily by neuronal nitric oxide synthase (nNOS). The cerebellar cortex expresses the highest levels of nNOS, and therefore produces higher concentrations of NO than any other region of the brain(Blanco et al., 2010). In addition, NO is known to play a crucial role in the modulation of the long-term depression (LTD) profile of cerebellar Purkinje neurons (PNs), responsible for encoding motor learning and coordination across development(Daniel, Levenes, & Crépel, 1998). Moreover, a study characterizing the expression level and functionality of nNOS/NO production noted a significant downregulation in nNOS mRNA and activity in cerebellar mutant mice, including leaner, staggerer, nervous, and Purkinje cell degeneration mice(Abbott & Nahm, 2004). Accordingly, in vivo deletion of nNOS in mice ($nNOS^{-/-}$) results in an ataxic phenotype with significant motor impairments and tremors(Huang, Dawson, Bredt, Snyder, & Fishman, 1993; Kriegsfeld et al., 1999; Nelson et al., 1995). Despite these already established behavioral deficits, preliminary gross anatomical analyses of the adult $nNOS^{-/-}$ mouse brain revealed no noticeable abnormalities in cerebellar morphology, which included length of dendritic arborization and overall cerebellar volume(Huang et al., 1993).

Under physiological conditions, endogenous NO signaling regulates calcium influx into PNs by modulating excitatory parallel fiber (PF) and climbing fiber (CF) inputs. Both PF and CF inputs determine the LTD profile of the PN(Lev-Ram, Makings, Keitz, Kao, & Tsien, 1995). Calcium influx and efflux is heavily regulated within the physiological PN, and chronic increases in cytosolic calcium concentrations have been reported to cause a number of cerebellar pathologies, including a variety of spinocerebellar ataxias (SCAs) as well as severe cognitive delays(Kasumu & Bezprozvanny, 2012; Liu et al., 2009; Toru et al., 2000). Specifically, activation of metabotropic glutamate receptor type 1 (mGluR1), localized on dendritic spines of PNs, stimulates the production of inositol triphosphate

(IP3) via phospholipase-C (PLC) activity(Hartmann, Henning, & Konnerth, 2011; Jin, Kim, Kim, Worley, & Linden, 2007). IP3 then binds to its endogenous receptor on the endoplasmic reticulum (ER), resulting in calcium efflux from the ER to the cytosol(Willard & Koochekpour, 2013). The low concentration of calcium in the ER causes stromal interaction molecule 1 (STIM1) oligomerization and transient receptor potential canonical type 3 (TRPC3) channel activity, mediating store operated calcium entry(Hartmann et al., 2008, 2014; Schilling, Schmidt, & Baader, 1994; Yoshida et al., 2006). Importantly, a recent paper explained the crucial interaction between STIM1 and NO, which functions to prevent the influx of calcium through store-operated mechanisms(Gui et al., 2018).

Although both ionotropic and metabotropic glutamate receptors are important for the facilitation of calcium entry into the PN, many studies have noted the importance of mGluRs, specifically mGluR1, in the development of cerebellar pathologies and ataxias. For example, overactivation of mGluR1 in an SCA1 mouse model led to decreased PN dendritic branching(Power, Morales, & Empson, 2016). Conversely, decreased expression of mGluR1 on PNs has led to deficits, specifically related to LTD(Conquet et al., 1994). Particularly within human SCAs, a variety of genes associated with the mGluR1 pathway are mutated that can cause symptoms such as tremor, loss of balance, and fine movement control. For example, the genes *ITPR1*, *TRPC3*, and *GRM1* encoding IP3R, TRPC3, and mGluR1 are affected in SCA15, SCA41, and SCA44, respectively, resulting in altered calcium influx within the PN(Fogel, Hanson, & Becker, 2015; Rossi et al., 2010; van de Leemput et al., 2007).

Considering the importance of nNOS/NO signaling in the physiological development of the cerebellum(Kriegsfeld et al., 1999) and the lack of characterization of PN development in the absence of nNOS/NO signaling(Huang et al., 1993), this study sought to examine general morphological differences in PN dendritic structures across postnatal development between wild-type (WT) and $nNOS^{-/-}$ mice. Specifically, the present study aimed to delineate potential structural changes in dendrite and synapse phenotype in $nNOS^{-/-}$ cerebella, alterations in synaptic proteins associated with the mGluR1 pathway, and a potential mechanism in which NO may influence dendritic morphology.

2.3 Materials and Methods

2.3.1 Animals

WT (C57BL/6J, Stock No. 000664) and nNOS$^{-/-}$ mice (B6.129S4-Nos1^{tm1Plh}, Stock No. 002986) were purchased from the Jackson Laboratory. All experiments were conducted in accordance with Animal Use Protocol (#2018-106) ap-proved by the Animal Care and Veterinary Services at the University of Western Ontario. Timepoints for cerebellar collection occurred at postnatal day 7 (PD7), 2 weeks (2W), and 7 weeks (7W) of age on male mice.

2.3.2 Immunohistochemical Preparation

Whole brains were isolated from WT and nNOS$^{-/-}$ mice and immediately placed in 4% paraformaldehyde (PFA) for 48h. Brains were subsequently transferred to a 30% sucrose solution for at least 48 h. Brains were sagittally sectioned at a thickness of 40 μm using a vibratome, placed in a cryoprotectant solution, and stored in − 20 °C until stained. Slices were first washed with phosphate buffered saline solution (PBS), then permeabilized using a 0.25%Triton-X solution for 5 min. Slices were then blocked with a 10% normal donkey serum (NDS) solution for 1 h and incubation with the following primary antibodies overnight in 4 °C: 1:500 goat anti-calbindin (CalB) (Santa Cruz Biotechnology, Dallas, TX), 1:800 rabbit anti-mGluR1 (Novus Biologicals, Oakville, ON), 1:500 guinea pig anti-vesicular glutamate trans-porter type 1 (vGluT1), 1:500 guinea pig anti-vesicular gluta-mate transporter type 2 (vGluT2) (Synaptic Systems, Goettingen, Germany), 1:200 rabbit anti-STIM1 (Proteintech Group Inc., Rosemont, IL), or 1:500 rabbit anti-calpain-1 (Abcam, Toronto, ON). Slices were washed and then incubated with the appropriate secondary antibodies for 2 h: anti-rabbit Cy3, anti-goat AlexaFluor 488, or anti-guinea pig AlexaFluor 488 (Jackson Immunoresearch, Burlington, ON). Slices were mounted on cover glass using Fluoromount-G (Electron Microscopy Solutions, Hatfield, PA), and images were taken using the Olympus FV1000 confocal microscope at ×60 magnification using an oil immersion objective.

2.3.3 Western Blotting

2.3.3.1 Total Protein Isolation

Cerebella were isolated from WT and nNOS$^{-/-}$ mice and stored at −80 °C. Cerebellar lysates were obtained by homogenizing the cerebellar tissues using a glass homogenizer in radioimmunoprecipitation assay (RIPA) lysis buffer, supplemented with 0.1% apoprotein and 0.1% leupeptin. Once homogenized, lysates were centrifuged for 30 min at 4 °C. The supernatant was collected, and protein was measured using a Bradford reagent mix (Bio-Rad, Hercules, CA).

2.3.3.2 PM Protein Isolation

PM protein fractions were isolated using the commercially available Mem-PER Plus Membrane Protein Extraction Kit (ThermoFisher Scientific, Rockford, USA) following the manufacturer's instructions.

Samples were later prepared using ×2 sample buffer and loaded onto 8% or 10% polyacrylamide gels for electrophoresis and run for 2 h at 100 V. Gels were then wet transferred onto nitrocellulose membranes for 2 h at 80 V. Blots were blocked in 5% bovine serum albumin (BSA) for 1 h before incubation with the following primary antibodies overnight: 1:800 rabbit anti-mGluR1 (142 kDa), 1:500 guinea pig anti-vGluT1 (62 kDa), 1:800 rabbit anti-STIM1 (90 kDa), 1:500 guinea pig anti-vGluT2 (64 kDa), 1:500 rabbit anti-β-III-spectrin (270 kDa) (Proteintech Group Inc., Rosemont, IL), 1:500 mouse anti-calpain-1 (80 kDa) (Santa Cruz Biotechnology, Dallas, TX), 1:200 guinea pig anti-GluR1 (AMPA subunit, 100 kDa), or 1:10,000 anti-glyceraldehyde-3-phosphate dehydrogenase (GAPDH, 40 kDa) (Abcam, Toronto, ON) for total protein comparisons, and sodium/potassium adenosine triphosphatase (Na^+/K^+ ATPase, 100 kDa) (Abcam, Toronto, ON) for PM protein comparisons. After three washes in tris-buffered saline solution, the appropriate secondary horseradish-peroxidase antibodies (Jackson Immunoresearch, Burlington, ON) were incubated on the membranes for 1.5 h. Protein was visualized using enhanced chemiluminescence substrate (Bio-Rad, Hercules, CA) and imaged using the Bio-Rad VersaDoc system. All proteins were normalized to the housekeeping protein

GAPDH or Na^+/K^+ ATPase. Densitometric analyses were quantified using FIJI open source software.

2.3.4 Ex Vivo Organotypic Cerebellar Slice Cultures

Cerebella were obtained from 10 to 12 postnatal day (PD) 0 WT and $nNOS^{-/-}$ pups and dissected in Hank's balanced salt solution (HBSS) containing 15 mM 4-(2-hydroxyehtyl)-1-piperazineethanesulfonic acid (HEPES), 0.5% glucose, and 2% sucrose and maintained at pH 7.3 and 315 mOsm. Once isolated, the cerebella were sliced at a thickness of 350 μm using a tissue chopper and carefully isolated and plated on 35-mm membrane inserts (Milipore Ltd., Etobicoke, ON). The bottom half of the insert was exposed to cerebellar slice culture media containing minimum essential medium (MEM) supplemented with 5 mg/ml glucose, 25% heat-inactivated horse serum, 25 mM HEPES, 1 mM glutamine, and 100 U/ml penicillin and streptomycin. Slice cultures were maintained for 7 days in vitro (DIV7), and half of the medium was refreshed every 2 days. WT slice cultures were treated with either NOS inhibitor N(G)-nitro-L-arginine methyl ester (L-NAME, 100 μM) (Santa Cruz Biotechnology, Dallas, TX), mGluR1 agonist dihydroxyphenylglycine (DHPG, 10 μM), and mGluR1 antagonist LY367385 (10 μM) (Tocris Bioscience, Oakville, ON). $nNOS^{-/-}$ cultures were treated with a slow NO donor, diethylenetriamine NONOate (NOC-18, 300 μM) (Santa Cruz Biotechnology, Dallas, TX). Cultured cerebellar slices were either used for western blotting or immunohistochemistry.

2.3.5 Ex Vivo Slice Culture Immunohistochemistry

Organotypic cerebellar slice cultures were established and maintained as previously described. Once slices reached DIV7, slices were incubated in 4% PFA solution for 2 h at 4 °C, washed with PBS, and later left to permeabilize in 0.25%Triton-X solution for 4 h. Slices were then left in 5% NDS blocking solution for 2 h before addition of primary anti-goat CalB (1:500) overnight. Secondary antibodies were incubated for 2 h, and slides were mounted. Images were taken using the Olympus FV1000 confocal microscope and a ×60 oil immersion objective.

2.3.6 Image Analysis

2.3.6.1 Strahler Analysis

PD7 PN dendrites were analyzed using the Strahler analysis plugin available on FIJI opensource software(Schindelin et al., 2012). Briefly, confocal images labeled with CalB were made binary, thresholded, and skeletonized. Each PN was analyzed separately, and all parameters remained consistent across WT and nNOS$^{-/-}$ images. Individual PN somata were identified for each image, and the Strahler analysis plugin was used to identify the total number of dendritic branches per cell. Total branch number per cell was averaged from multiple images across four biological replicates.

2.3.6.2 Dendritic Thickness

Dendritic thickness reports the diameter of the largest primary, aspinous dendrites per confocal image representing CalB from 7W WT and nNOS$^{-/-}$ mice using FIJI. Briefly, the five largest branches were identified per image and measured in micro-meters (μm) using the straight line tool. Dendritic thickness was averaged from multiple images across four biological replicates.

2.3.6.3 Spine Morphology

Spine morphology and characterization was determined using NeuronStudio. Briefly, spine head, neck, and length of spine parameters were set using the default settings, which remained unchanged between WT and nNOS$^{-/-}$ images. The spine classification tool would use the head-to-neck diameter ratio as well as the length of the spine to classify each spine as either mushroom, thin or stubby. The number of mushroom, thin or stubby spine type, was averaged across multiple dendritic branches of 10 μm in length over four biological replicates.

2.3.6.4 Particle Tracking

The number of PN dendritic spines as well as mGluR1, STIM1, and vGluT2 clusters were determined using the Particle Tracker 2D/3D plugin available on FIJI. Parameters for the radius of particle detection, the non-particle discrimination cutoff, and absolute intensity values remained consistent across WT and nNOS$^{-/-}$ samples for each

target protein analyzed. The total number of PN dendritic spines and mGluR1 clusters were determined within non-overlapping ROIs of 300 × 300 μm located specifically within the distal dendritic region of the molecular layer (top 50% of the dendritic area) and averaged across multiple images over four biological replicates. The average number of STIM1 clusters within each PN soma was deter-mined using the image analysis method highlighted in **Figure 2.S1**. The localization and number of vGluT2 clusters for both WT and nNOS$^{-/-}$ cerebella were determined using the Particle Tracker 2D/3D, as shown in **Figure 2.S2.**

2.3.6.5 Integrated Density Analysis

Calpain-1 fluorescence intensity within PN somata of 7W WT and nNOS$^{-/-}$ cerebella was measured using FIJI. Briefly, an ROI of the PN soma, determined using the CalB stain, was made and overlayed on the corresponding calpain-1 image. Then, integrated density—measured in arbitrary units of in-tensity (AUIs)—was graphed for each WT and nNOS$^{-/-}$ PN soma. Integrated density was averaged from multiple cells across four biological replicates.

2.3.7 Statistical Analysis

Statistical analyses were performed using an unpaired, two-tailed t test for all results comparing WT to nNOS$^{-/-}$ mice. Results obtained from organotypic slice cultures were analyzed using a one-way ANOVA corrected with a Tukey's post hoc test. Significance was determined using a threshold of $P = 0.05$. All values were reported as mean ± standard error of the mean (SEM).

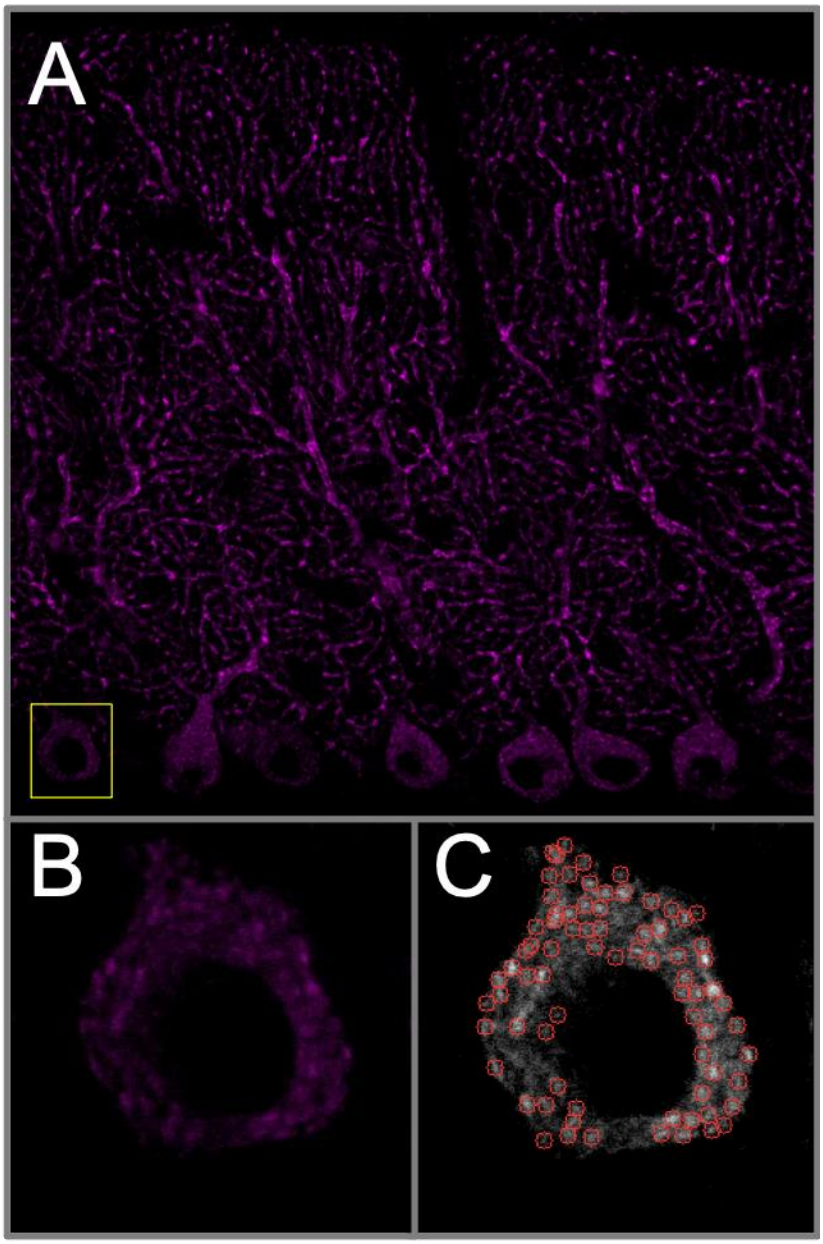

Figure 2.S1 Analysis of STIM1 particles within the PN soma.

Depicted is a representative image of WT 7W cerebellar tissue stained for STIM1, which is selective for PNs. (**A**) First, a rectangular region of interest (ROI) is created to encompass the entirety of the PN soma. (**B**) Next, the ROI is duplicated, and any background staining not associated with PN soma is removed. (**C**) The Particle Tracker 2D/3D plugin is run using FIJI and identifies the number of STIM1 clusters (visualized by the red circles), and a total number of particles is reported by the plugin.

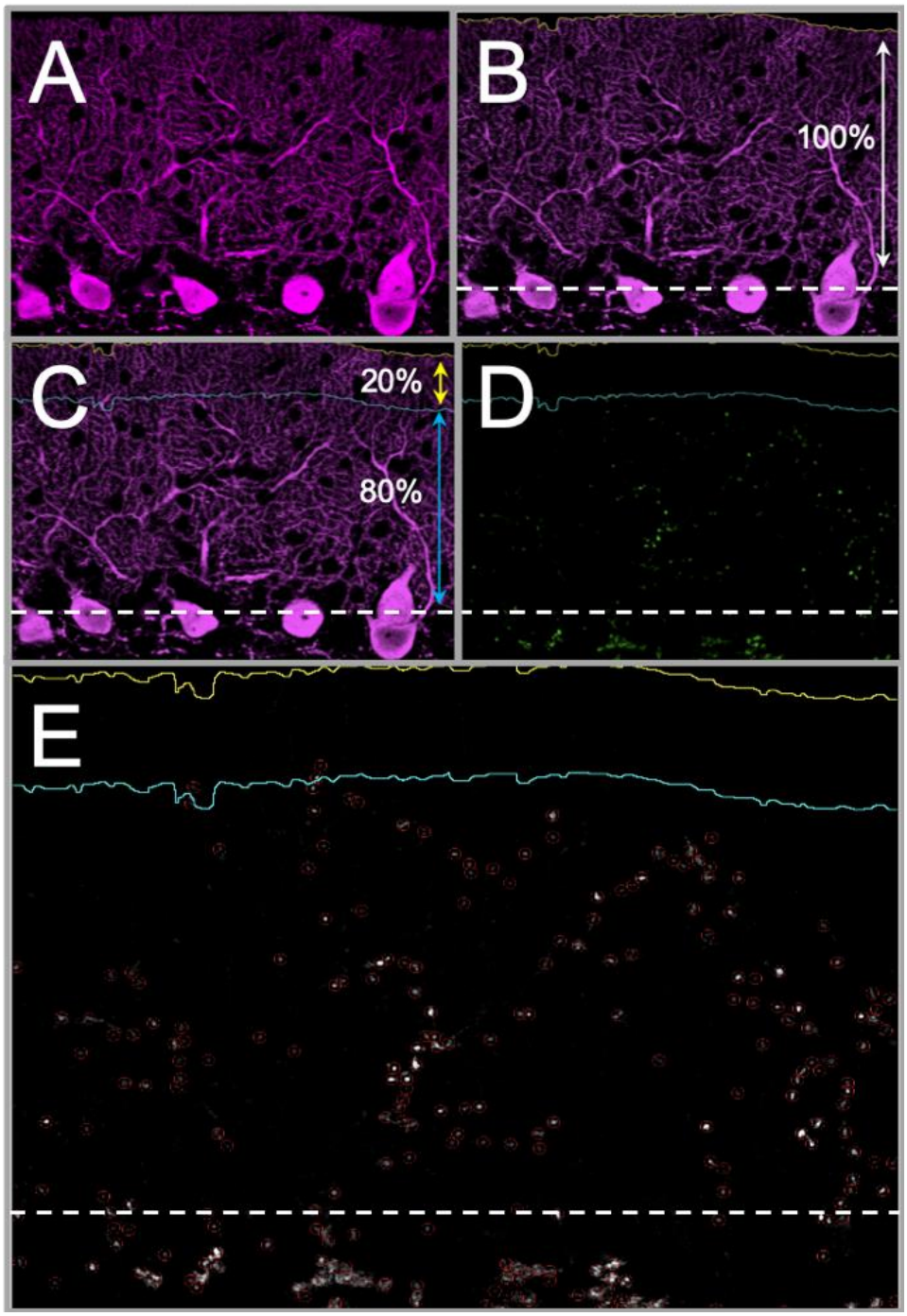

**** Figure legend on next page ****

Figure 2.S2 Method of determining number and localization of vGluT2 clusters.

(**A**) Depicted is a representative image of WT 7W CalB staining. (**B**) The distal border of the PN dendrites (closest to the pial surface) is determined using the freehand line selection tool in FIJI. A straight line is drawn where the proximal dendrites begin. The area in between the white dotted line and the yellow line denotes 100% of the molecular layer. (**C**) The length of this region is determined, and 20% of the length is calculated, the border of which is represented with a blue line. The area between the blue line and the dotted line denotes the bottom 80% of the molecular layer (where climbing fibers are expected to innervate PNs). (**D**) These borders determined on the CalB staining are then applied to the respective vGluT2 stain. (**E**) The Particle Tracker 2D/3D is run, giving the total number of particles detected. Particles detected above the blue line are considered as vGluT2 clusters occupying the upper 20% of the molecular layer, while particles detected between the blue line and white dotted line represents vGluT2 clusters occupying the lower 80% of the molecular layer.

2.4 Results

2.4.1 PN Dendritic Branching and Spine Density Are Reduced in the Cerebella of Young and Adult nNOS$^{-/-}$ Mice.

We first investigated whether nNOS$^{-/-}$ mice displayed alterations in PN morphology during early postnatal development. Despite previous gross anatomical analyses showing no obvious structural changes in the cerebellum of adult nNOS$^{-/-}$ mice(Huang et al., 1993), confocal images of PD7 cerebella showed dramatically less dendritic branching ubiquitously across all PNs in nNOS$^{-/-}$ mice compared with age-matched WT controls (**Figure 2.3a**), while the total number of PN cell somata remained the same between WT and nNOS$^{-/-}$ mice (**Figure 2.3b**). In accordance with this trend, a Strahler analysis quantifying the number of terminal branches per PN showed a significantly lower number of terminal branches for individual PNs of nNOS$^{-/-}$ mice compared with WT (**Figure 2.3c, d**).

We next investigated whether the alteration in nNOS$^{-/-}$ PN morphology carried on into adulthood. Confocal images displaying CalB-immunoreactive PN structures showed dramatically different PN branching between WT and nNOS$^{-/-}$ mice (**Figure 2.4a**), while image analyses revealed no significant difference in soma number or PN dendritic length in nNOS$^{-/-}$ mice compared with WT at 7W (**Figure 2.4b, c**). However, primary aspiny PN dendrites in nNOS$^{-/-}$ cerebella were significantly thicker compared with WT mice (**Figure 2.4d**). Additionally, PN dendritic spine morphology was significantly affected in nNOS$^{-/-}$ mice. Specifically, analysis of spine type determined a significant shift from predominantly mushroom-type spines found on WT PNs to predominantly thin-type spines found on nNOS$^{-/-}$ PNs (**Figure 2.4e–g**), while stubby spines remained un-changed between WT and nNOS$^{-/-}$ (data not shown). In general, the overall number of spines on PN dendrites was significantly less in nNOS$^{-/-}$ mice compared with WT controls (**Figure 2.4h**).

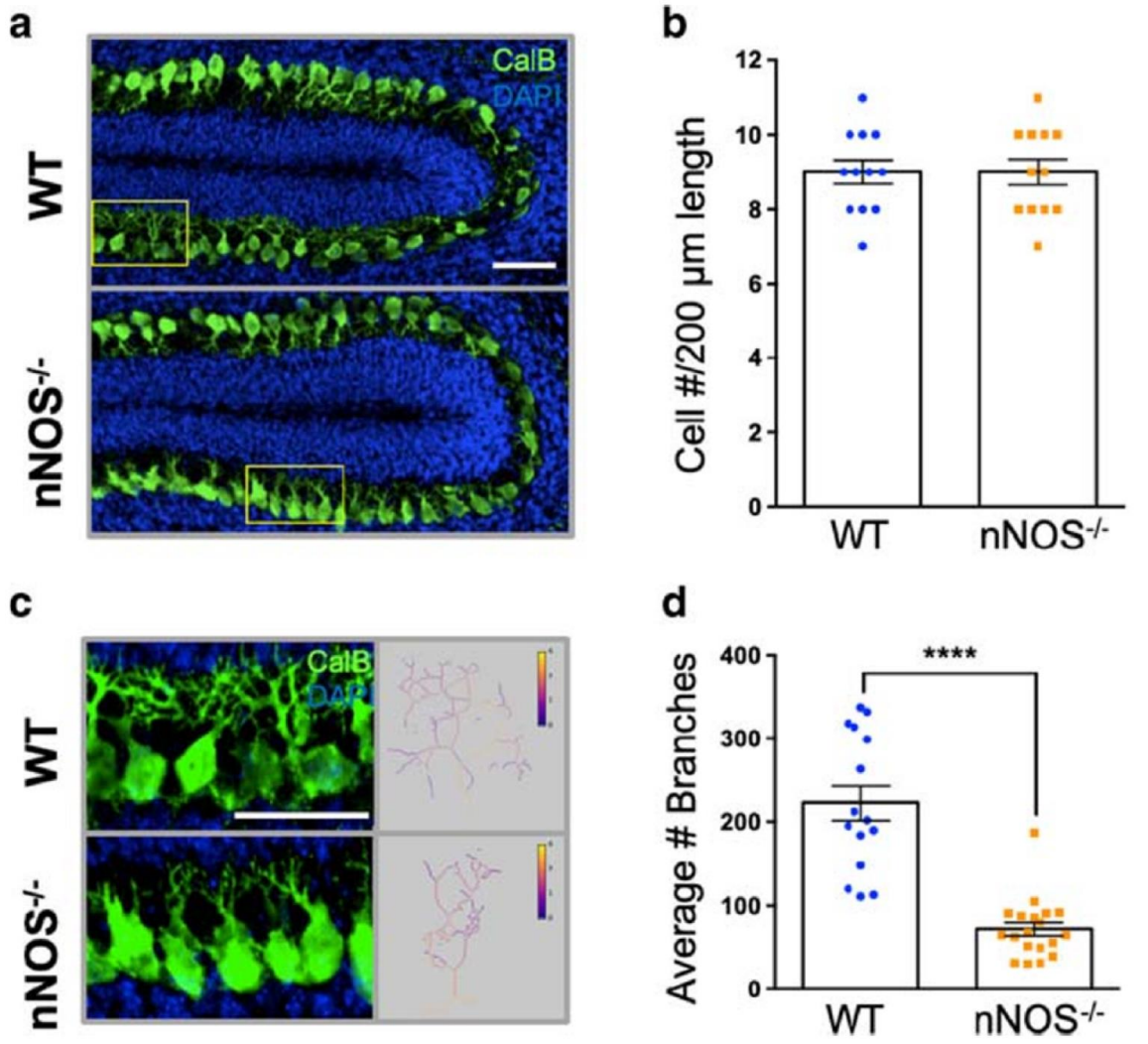

Figure 2.3 PN dendritic branching is robustly altered in PD7 nNOS$^{-/-}$ cerebella.

A) Representative confocal images of WT and nNOS$^{-/-}$ PNs expressing CalB (green) and nuclei stained by DAPI (blue). Scale bars represent 100 µm. **B**) Bar graph represents the number of PN cell somata per 200 µmlength. N = 4 biological replicates per group; WT n =12 cells, nNOS$^{-/-}$ n = 12 cells. P = 0.99. **C**) Enlarged representation of WT and nNOS$^{-/-}$ PNs and sub-sequent Strahler analysis profile, indicating degrees of branching and branch number. Scale bar represents 50 µm. **D**) Bar graph represents average number of PN branches as determined using a Strahler analysis. N = 4 biological replicates per group; WT n =15 cells, nNOS$^{-/-}$ n = 19 cells. P < 0.0001. All data are represented as mean ± SEM.

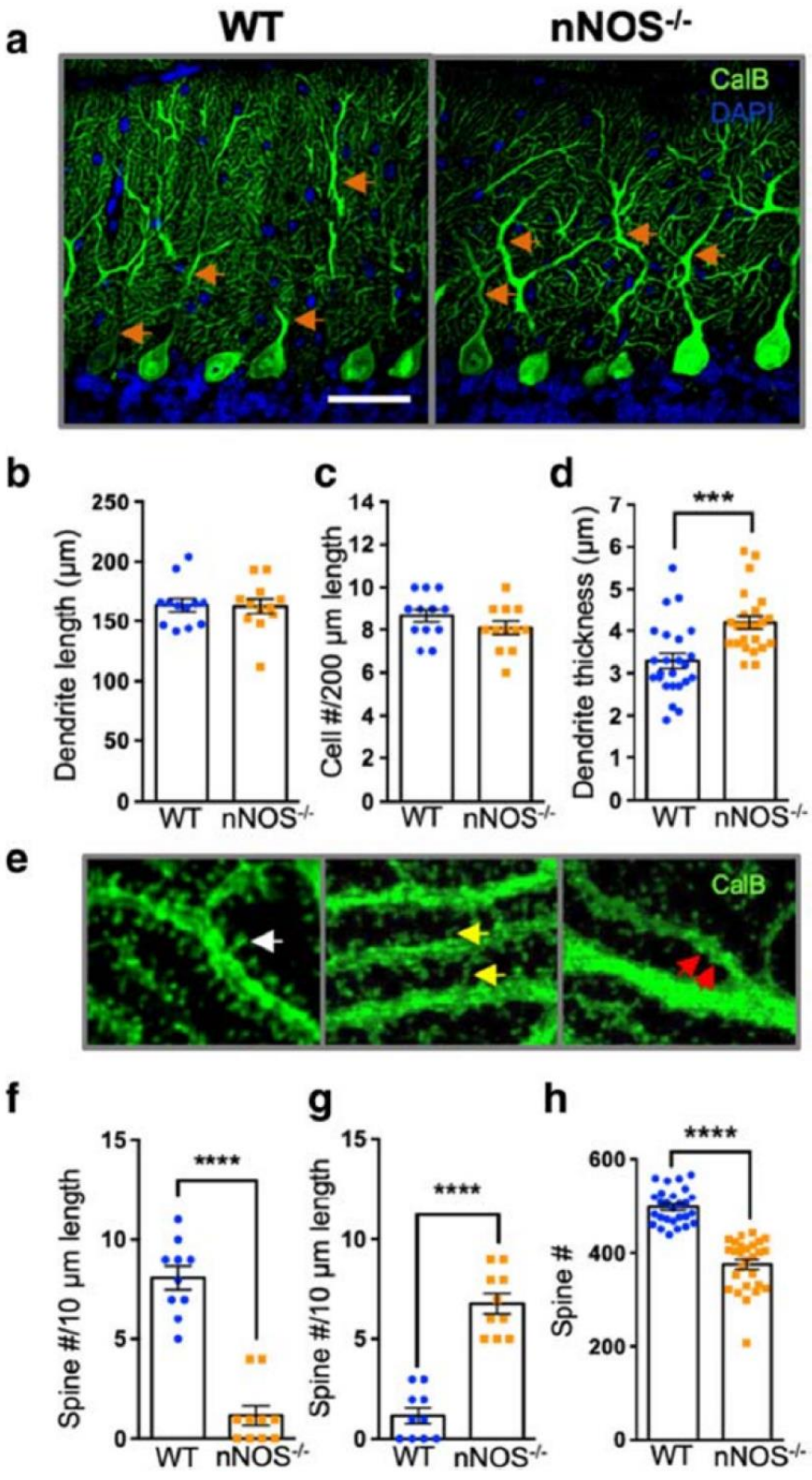

**** Figure legend on next page ****

Figure 2.4 Alterations in PN dendritic branching and synapse morphology in nNOS$^{-/-}$ cerebella at 7W.

A) Representative confocal images of WT and nNOS$^{-/-}$ PNs using CalB (green) at 7W. Orange arrows depict aspinous primary branches. Scale bar represents 50 μm. **B**) Bar graph represents length of dendrites, from PN cell soma to pial surface. N = 4 biological replicates per group; WT n = 12 images, nNOS$^{-/-}$ n = 12 images. P = 0.9028. **C**) Bar graph represents number of PN cell somata per 200-μm length. N = 4 biological replicates per group; WT n = 12 images, nNOS$^{-/-}$ n =12 images. P = 0.1988. **D**) Bar graph represents average thickness of primary aspinous dendrites. N = 4 biological replicates per group; WT n = 25 branches, nNOS$^{-/-}$ n = 25 branches. P = 0.0003. **E**) Representative confocal images of mushroom spines (white arrows), thin spines (yellow arrows), and stubby spines (red arrows). Classification of spine morphology was performed using NeuronStudio. **F**) Bar graph represents number of mushroom spines between WT and nNOS$^{-/-}$ mice at 7W. N = 4 biological replicates per group; WT n = 10 images, nNOS$^{-/-}$ n = 10 images. P < 0.0001. **G**) Bar graph represents number of thin spines between WT and nNOS$^{-/-}$ mice at 7W. N = 4 biological replicates per group; WT n = 10 images, nNOS$^{-/-}$ n = 10 images. P < 0.0001. H) Bar graph represents total spine number per 300 × 300 μm ROI between WT and nNOS$^{-/-}$ mice at 7W. N =4; WT n = 27, nNOS$^{-/-}$ n = 27. P < 0.0001. All data are represented as mean ± SEM.

2.4.2 mGluR1 Expression Is Reduced in the Cerebella of Young and Adult nNOS$^{-/-}$ Mice.

We also characterized the postsynaptic component of glutamatergic synapses, first with a focus on mGluR1 protein expression. Immunohistochemistry revealed that immunofluorescent clusters of mGluR1 in the cerebella of PD7 mice were primarily located on the tip of PN dendritic spines, while some mGluR1 clusters were localized to the PN soma. Notably, overall mGluR1 expression levels were significantly lower in PD7 nNOS$^{-/-}$ cerebella compared with age-matched WT mice (**Figure 2.5a, b**). The observed decrease in mGluR1 protein expression in PD7 nNOS$^{-/-}$ cerebella was consistent at 2W, as determined using western blot (**Figure 2.5c, d**).

Again, nNOS$^{-/-}$ cerebella continued to express lower levels of mGluR1 at 7W (**Figure 2.6**). Specifically, the number of mGluR1 clusters was significantly less in nNOS$^{-/-}$ cerebella (**Figure 2.6a, b**), and total expression levels of mGluR1 were significantly lower in nNOS$^{-/-}$ cerebella at 7W, determined by western blot (**Figure 2.6c**). Interestingly, the PM expression of mGluR1 in cerebellar samples revealed significantly more mGluR1 expression on the membrane in nNOS$^{-/-}$ mice compared with WT at 7W (**Figure 2.6d**). To ensure that the mGluR1 pathway in particular is affected, PM expression of the GluR1 subunit of AMPARs, the main ionotropic glutamate receptor on PNs, was assayed using western blot, and no significant differences were noted between WT and nNOS$^{-/-}$ mice at 7W (**Figure 2.6e**).

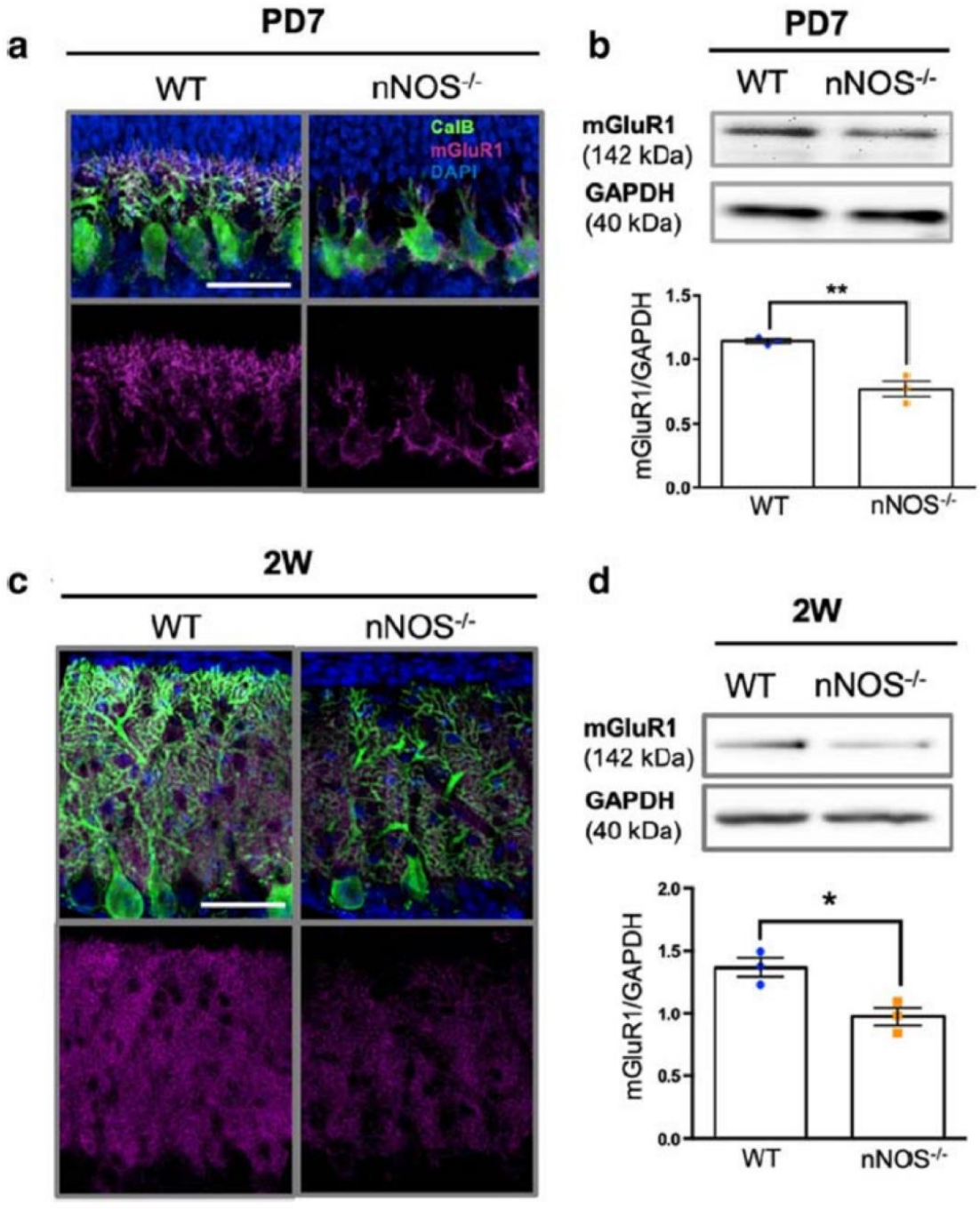

**** Figure legend on next page ****

Figure 2.5 mGluR1 expression is decreased in nNOS$^{-/-}$ PNs at PD7 and 2W.

A) Representative confocal images of WT and nNOS$^{-/-}$ cerebella stained with CalB (green), DAPI (blue), and mGluR1 (magenta) at PD7. Scale bar represents 50 μm. **B**) Representative western blot of total mGluR1 (142 kDa) protein expression for PD7 WT and nNOS$^{-/-}$ cerebella, along with bar graph representing N = 3 biological replicates per group. All mGluR1 bands were normalized to GAPDH (40 kDa) expression. P = 0.0046. **C**) Representative confocal images of WT and nNOS$^{-/-}$ cerebella stained with CalB (green), mGluR1 (magenta), and DAPI (blue) at 2W. Scale bar represents 50 μm. **D**) Representative western blot of total mGluR1 protein expression for 2W WT and nNOS$^{-/-}$ cerebella, along with bar graph representing N = 3 biological replicates per group. All mGluR1 bands were normalized to GAPDH expression. P =0.0211. All data are represented as mean ± SEM.

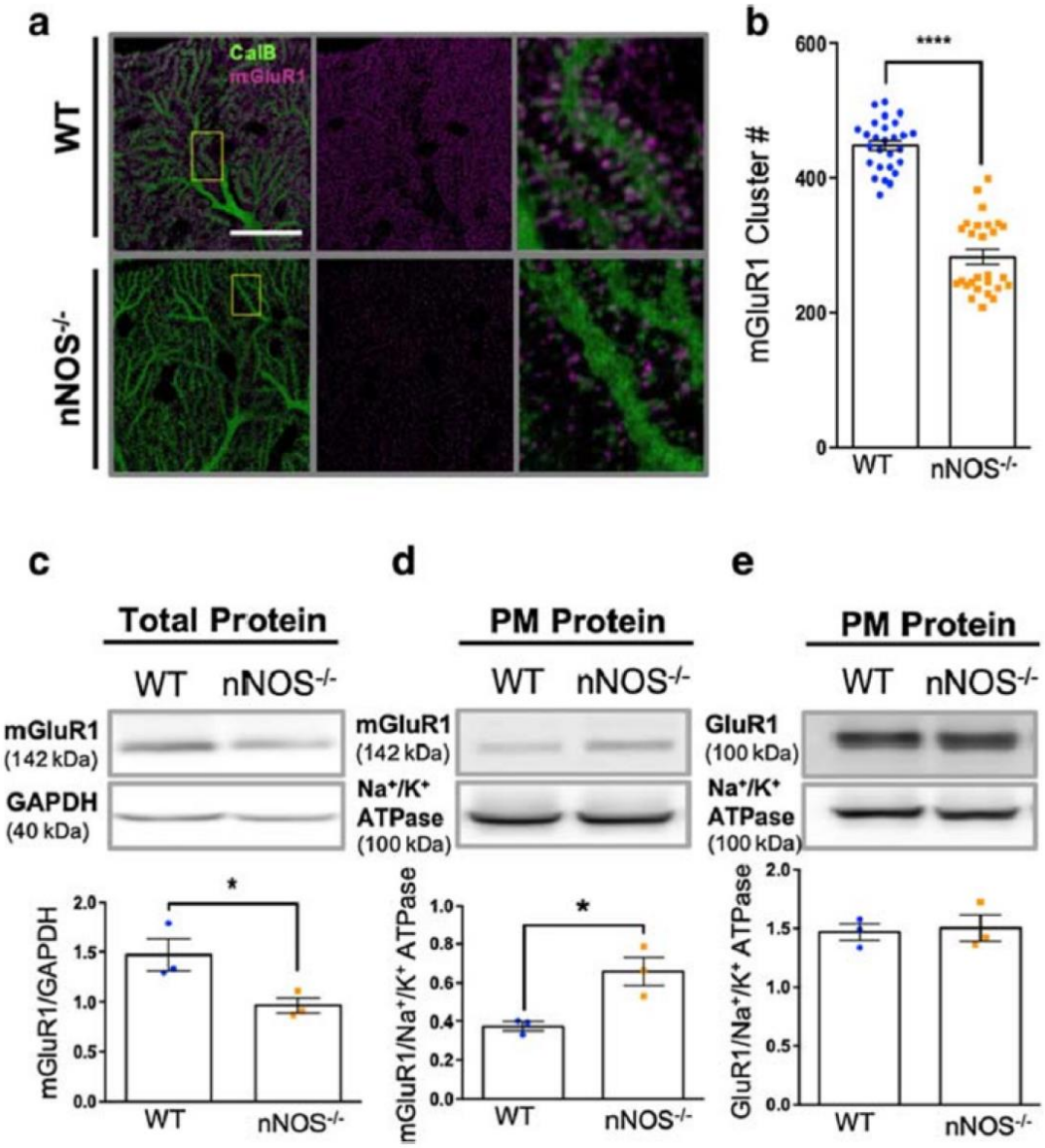

**** Figure legend on next page ****

Figure 2.6 Total mGluR1 expression is decreased, but PM mGluR1 is increased in the PNs of nNOS$^{-/-}$ at 7W.

A) Representative confocal images of WT and nNOS$^{-/-}$ cerebella stained with CalB (green) and mGluR1 (magenta) at 7W. Images in the right panel are magnified insets of the left panel (area depicted with a yellow box). Scale bar represents 25 μm. **B**) Bar graph reports number of mGluR1 clusters per 300 × 300 μm ROI between WT and nNOS$^{-/-}$ cerebella. N = 4 biological replicates per treatment; WT n =27 images, nNOS$^{-/-}$ n =27 images. P < 0.0001. **C**) Representative western blot of total mGluR1 protein ex-pression (142 kDa) for 7W WT and nNOS$^{-/-}$ cerebella, along with bar graph representing N = 3 biological replicates per group. Total mGluR1 protein expression was normalized to GAPDH (40 kDa) expression. P = 0.0434. **D**) Representative western blot of PM expression of mGluR1 within WT and nNOS$^{-/-}$ cerebellar tissues at 7W, along with bar graph representing N = 3 biological replicates per group. PM mGluR1 protein expression was normalized to Na^+/K^+ ATPase (100 kDa). P = 0.0205. **E**) Representative western blot of PM expression of GluR1 (100 kDa) within WT and nNOS$^{-/-}$ cerebellar tissues at 7W, along with bar graph representing N = 3 biological replicates per group. PM mGluR1 protein expression was normalized to Na^+/K^+ ATPase. P = 0.8098. All data are represented as mean ± SEM.

2.4.3 vGluT1 Expression Is Reduced in PD7 nNOS$^{-/-}$ Cerebella, but Not at 2W or 7W.

To determine whether alterations also occurred in the presynaptic compartment of PF-PN synapses in nNOS$^{-/-}$ mice, PF terminals were selectively labeled with vGluT1 and analyzed using confocal microscopy. At PD7, vGluT1 expression was significantly lower in nNOS$^{-/-}$ cerebella, as determined by western blot (**Figure 2.7a, b**). By 2W, this difference was no longer noticeable (**Figure 2.7c**), and western blotting at this time point showed no significant difference in protein levels between nNOS$^{-/-}$ and age-matched WT controls (**Figure 2.7d**). This same trend was noticed at 7W, where immunohistochemical staining and western blots did not reveal a significant difference in vGluT1 expression (**Figure 2.7e, f**).

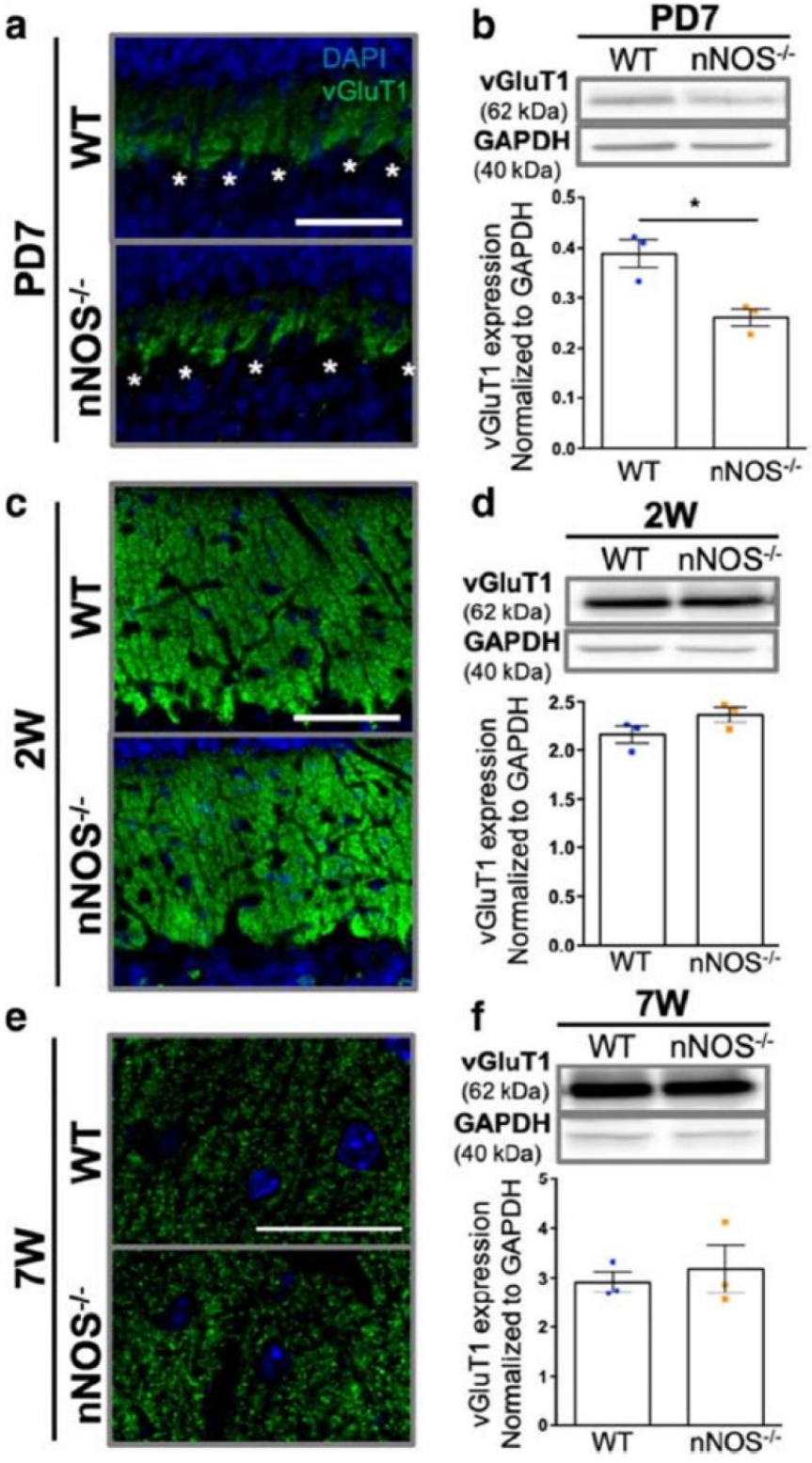

**** Figure legend on the next page ****

Figure 2.7 Expression of vGluT1 is decreased at PD7 in nNOS$^{-/-}$, but this difference is ameliorated by 2W and 7W.

A) Representative confocal images displaying vGluT1 expression (green) and surrounding DAPI (blue) at PD7 in WT and nNOS$^{-/-}$ cerebella. White asterisks represent PN cell somata. Scale bar represents 50 μm. **B**) Representative western blot of vGluT1 (62 kDa) protein expression in PD7 WT and nNOS$^{-/-}$ cerebellar tissue. Expression of vGluT1 was normalized to total GAPDH (40 kDa) protein expression. Bar graph represents N = 3 biological replicates per group. P = 0.0179. **C**) Representative confocal images displaying vGluT1 expression (green) and DAPI (blue) at 2W in WT and nNOS$^{-/-}$ cerebella. Scale bar represents 50 μm. **D**) Representative western blot of vGluT1 protein expression in 2W WT and nNOS$^{-/-}$ cerebellar tissue. Bar graph represents N =3. P = 0.6491. **E**) Representative confocal images showing vGluT1 expression (green) and surrounding DAPI (blue) at 7W in WT and nNOS$^{-/-}$ cerebella. Scale bar represents 25 μm. **F**) Representative western blot of vGluT1 protein expression in 7W WT and nNOS$^{-/-}$ cerebellar tissue. Bar graph represents N = 3 biological replicates per group. P = 0.6347. All data are represented as mean ± SEM.

2.4.4 vGluT2 Expression Is Increased in 7W nNOS$^{-/-}$ Cerebella.

Considering another crucial glutamatergic synapse on PNs arises from climbing fiber (CF) innervation, we immuno-stained vGluT2—a specific marker for CF boutons—to determine whether the CF-PN synapse is affected in nNOS$^{-/-}$ mice. Western blots using cerebellar tissue from WT and nNOS$^{-/-}$ PD7 and 2W mice revealed no significant difference in vGluT2 expression (**Figure 2.8a, b**). However, immunoblots of 7W cerebella revealed a nearly two-fold increase in vGluT2 expression in nNOS$^{-/-}$ mice compared with WT (**Figure 2.8c**). Interestingly, further analysis of fluorescently labeled vGluT2 in 7W nNOS$^{-/-}$ cerebella revealed more vGluT2 clusters within the upper 20% area, closest to the pial surface (**Figure 2.8d, e**). A significant difference in clustering was not noted in the lower 80% of the molecular layer (**Figure 2.8f**), and no significant differences in vGluT2 staining within the granule cell layer (denoting mossy fiber innervation) were detected (data not shown).

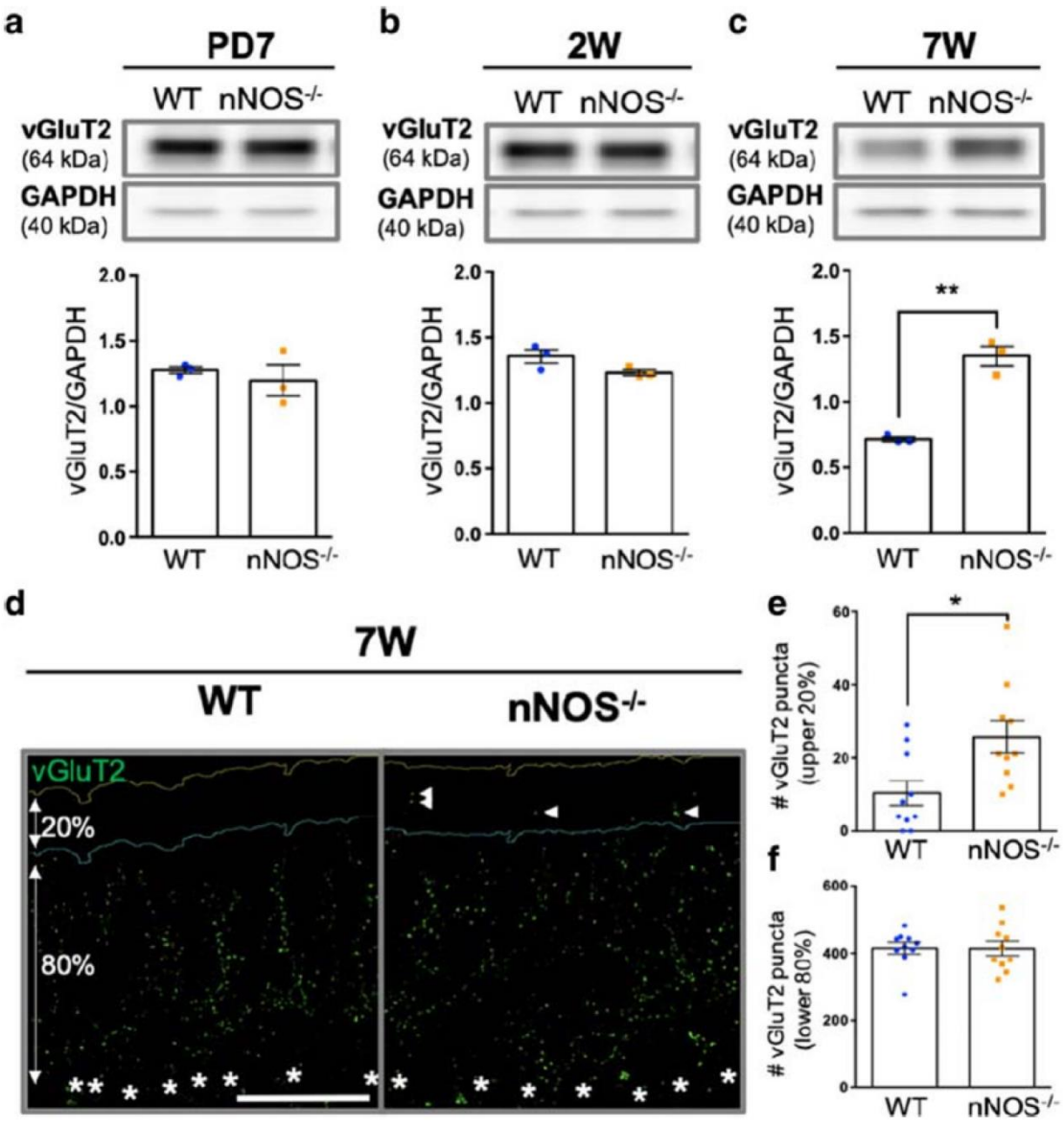

**** Figure legend on next page ****

Figure 2.8 vGluT2 expression is elevated in 7W nNOS$^{-/-}$ cerebella, but not in PD7 or 2W.

A) Representative western blot of WT and nNOS$^{-/-}$ PD7 cerebellar tissue denoting vGluT2 (64 kDa) expression. Bar graph depicts N = 3 biological replicates per group. vGluT2 protein expression was normalized to total GAPDH (40 kDa) protein expression. P = 0.5433. **B**) Representative western blot of WT and nNOS$^{-/-}$ 2W cerebellar tissue denoting vGluT2 expression. Bar graph depicts N = 3 biological replicates per group. P = 0.0984. **C**) Representative western blot of WT and nNOS$^{-/-}$ 7W cerebellar tissue denoting vGluT2 protein expression. Bar graph depicts N = 3 biological replicates per group. vGluT2 protein ex-pression was normalized to GAPDH expression for each sample. P = 0.0012. **D**) Representative image of 7W WT and nNOS$^{-/-}$ CF synapses visualized by vGluT2 (green). Yellow line denotes edge of the molecular layer. Blue line denoted border between upper 20% and lower 80% of the molecular layer. White asterisks represent PN cell somata. Scale bar rep-resents 50 μm. **E**) Bar graph depicts total number of vGluT2 clusters localized within the upper 20% of the molecular layer per image analyzed. N = 4 biological replicates per group; WT n = 10 images, nNOS$^{-/-}$ n = 10 images. P = 0.0134. **F**) Bar graph depicts total number of vGluT2 clusters localized within the lower 80% of the molecular layer per image. N = 4 biological replicates per group; WT n =10 images, nNOS$^{-/-}$ n =10 images. P = 0.9658. All data are represented as mean ± SEM.

2.4.5 STIM1 Expression and Cluster Density Is Increased in nNOS$^{-/-}$ Cerebella.

The specific alterations in mGluR1 expression in nNOS$^{-/-}$ cerebella led us to investigate whether localization and expression of STIM1, an ER calcium sensor implicated downstream of mGluR1 signaling(Hartmann et al., 2014), was changed in the PNs of nNOS$^{-/-}$ mice. Immunohistochemistry showed that at PD7, STIM1 immunoreactive clustering was significantly more abundant within the PN soma of nNOS$^{-/-}$ mice compared with PNs of WT mice at this time point (**Figure 2.9a, b**). In addition, a higher level of STIM1 protein expression in nNOS$^{-/-}$ cerebella was determined by western blot at PD7 (**Figure 2.9c**).

STIM1 expression remained elevated in the PNs of nNOS$^{-/-}$ mice at 2W, evidenced by significantly more immunoreactive STIM1 clusters within PN somata (**Figure 2.9d, e**). Additionally, a higher level of STIM1 protein expression in the nNOS$^{-/-}$ cerebellum when compared with WT cerebella was determined by western blot (**Figure 2.9f**).

The elevated STIM1 clustering and expression in the PNs of nNOS$^{-/-}$ mice continued in 7W nNOS$^{-/-}$ cerebella, determined by immunohistochemistry and western blotting (**Figure 2.9g–i**). Elevated STIM1 expression and clustering suggests altered calcium dynamics within the PNs of the nNOS$^{-/-}$ mice.

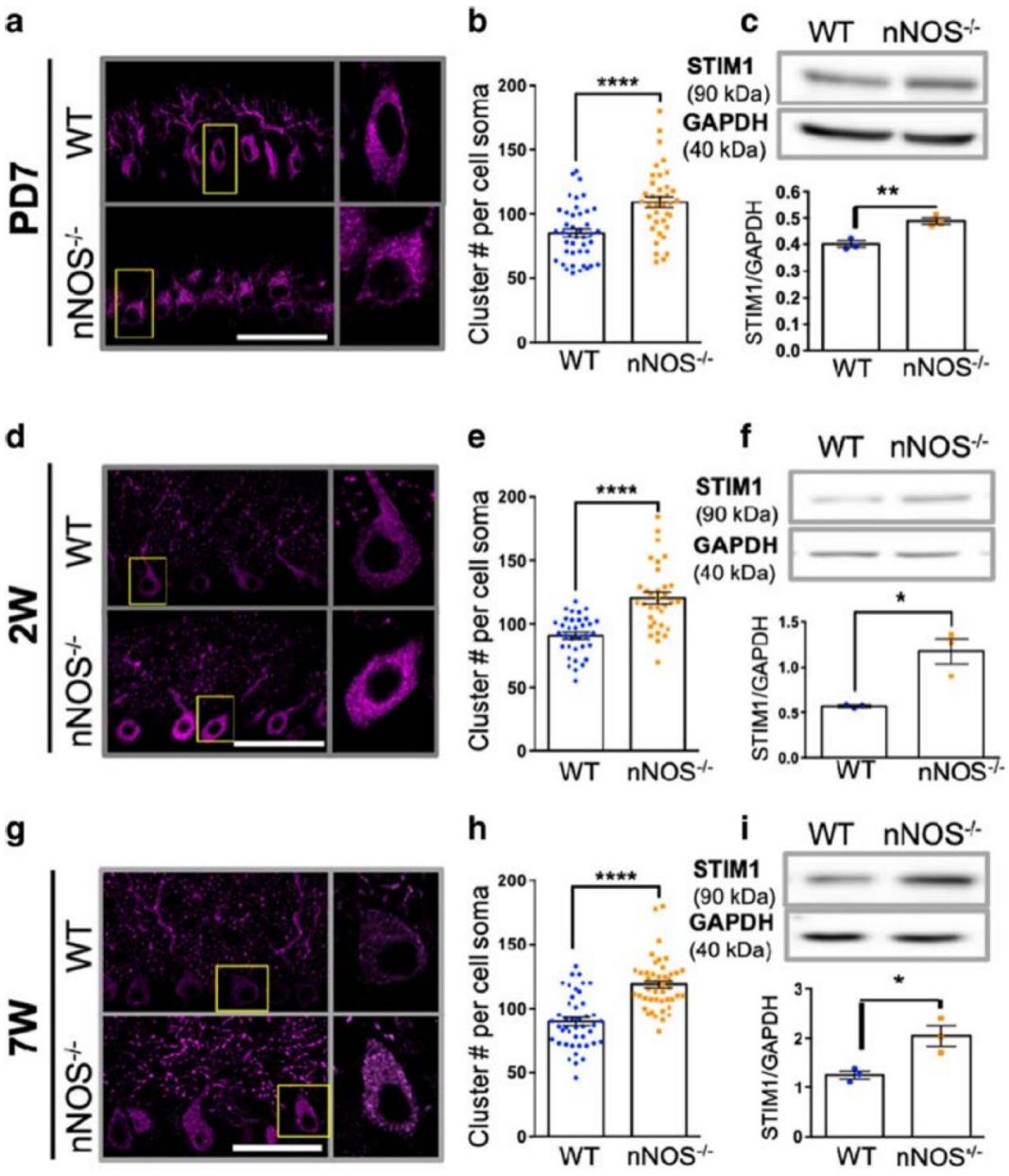

**** Figure legend on next page ****

Figure 2.9 STIM1 expression is increased in PD7, 2W, and 7W nNOS$^{-/-}$ cerebella.

A) Representative confocal images of PD7 WT and nNOS$^{-/-}$ PNs that show STIM1 (magenta) localization. Scale bar represents 50 μm. **B**) Bar graph represents number of STIM1 clusters per PN soma at PD7. N = 4 biological replicates per group; WT n =42 cells, nNOS$^{-/-}$ n = 37 cells. P < 0.0001. **C**) Representative western blot of STIM1 (90 kDa) protein expression of WT and nNOS$^{-/-}$ cerebellar tissue at PD7. STIM1 protein expression was normalized to GAPDH (40 kDa). Bar graph represents N = 3 biological replicates per group. P = 0.0065. **D**) Representative confocal images of 2W WT and nNOS$^{-/-}$ PNs that show STIM1 (magenta) localization. Scale bar represents 50 μm. **E**) Bar graph represents number of STIM1 clusters per PN soma at 2W. N = 4 biological replicates per group; WT n = 34 cells, nNOS$^{-/-}$ n = 33 cells. P < 0.0001. **F**) Representative western bot of STIM1 protein expression of WT and nNOS$^{-/-}$ cerebellar tissue at 2W. STIM1 protein expression was normalized to GAPDH. Bar graph represents N = 3 biological replicates per group. P = 0.0129. **G**) Representative confocal images of 7W WT and nNOS$^{-/-}$ PNs that show STIM1 (magenta) localization. Scale bar represents 50 μm. **H**) Bar graph represents number of STIM1 clusters per PN soma at 7W. N = 4 biological replicates per group; WT n =44 cells, nNOS$^{-/-}$ n = 44 cells. P < 0.0001. **I**) Representative western blot of STIM1 protein expression of WT and nNOS$^{-/-}$ cerebellar tissue at 7W. STIM1 protein expression was normalized to GAPDH expression. Bar graph represents N = 3 biological replicates per group. P = 0.0229. All data are represented as mean ± SEM.

2.4.6 Increased Calpain-1 Expression Corresponds with a Decrease in β-III-spectrin in Both Young and Adult nNOS$^{-/-}$ Cerebella.

Considering that STIM1 activity is crucial in regulating calcium influx into the PN, we therefore explored the potential consequences of aberrant calcium signaling that could alter PN morphology. Calpains are important calcium-dependent proteases that, when activated, are responsible for the cleavage of proteins involved in neuronal structural integrity(Suzuki, Hata, Kawabata, & Sorimachi, 2004). Western blots for calpain-1 at PD7, 2W, and 7W all demonstrated significantly elevated levels of calpain-1 within the cerebella of nNOS$^{-/-}$ mice (**Figure 2.10a–c**). To ensure localization of calpain-1 with PNs specifically, we have also made immunofluorescent stains for calpain-1, which showed global calpain-1 presence, with relatively high expression within PN somata and dendrites in both WT and nNOS$^{-/-}$ cerebella (**Figure 2.10d**). A measurement of calpain-1 integrated density with-in the PN somata revealed significantly increased calpain-1 expression within nNOS$^{-/-}$ PNs compared with WT at 7W, mirroring the western blot data (**Figure 2.10e**). In accordance with this upregulation of calpain-1, levels of β-III-spectrin, a calpain substrate and an important PN-specific structural protein, were decreased at 7W in nNOS$^{-/-}$ mice compared with age-matched WT controls (**Figure 2.10f**).

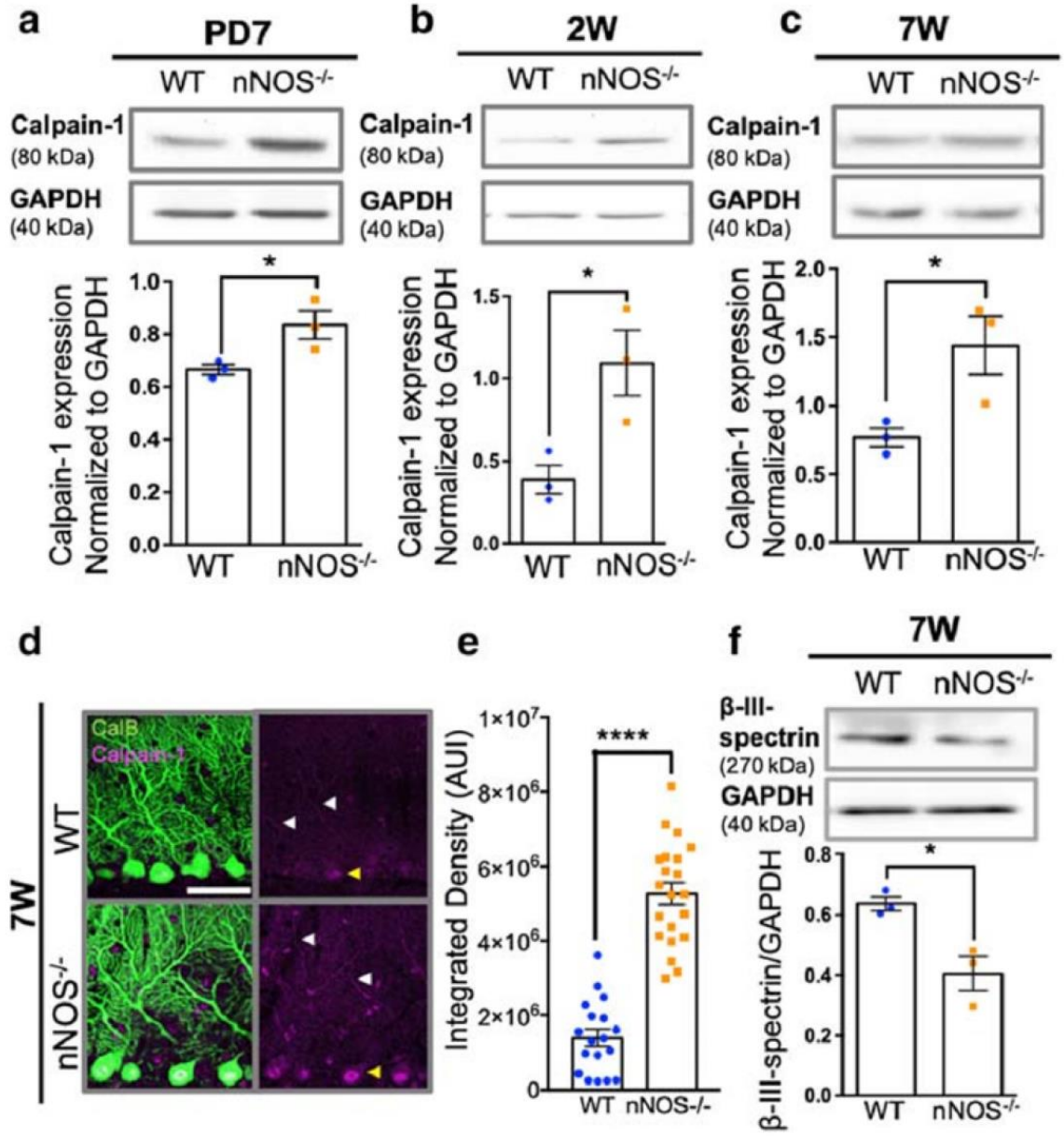

**** Figure legend on next page ****

Figure 2.10 Calpain-1 protein expression is upregulated, while β-III-spectrin is downregulated in nNOS$^{-/-}$ cerebella.

A) Representative western blot depicting protein expression of calpain-1 (80 kDa) in PD7 WT and nNOS$^{-/-}$ cerebella, along with bar graph representing N = 3 biological replicates per group. Calpain-1 protein bands were normalized to total GAPDH (40 kDa) expression. P = 0.0436. **B**) Representative western blot showing calpain-1 expression in 2W WT and nNOS$^{-/-}$ cerebellar tissue, along with bar graph representing N = 3 biological replicates per group. Calpain-1 protein was normalized to GAPDH expression. P =0.0351. **C**) Representative western blot depicting calpain-1 protein expression in 7W WT and nNOS$^{-/-}$ cerebella, along with bar graph representing N =3 biological replicates per group. Calpain-1 bands were normalized to total GAPDH expression. P = 0.0398. **D**) Representative confocal images of 7W WT and nNOS$^{-/-}$ PNs that show calpain-1 (magenta) localization, along with an overlay of CalB (green). Scale bar represents 50 μm. White arrowheads point to PN dendritic localization of calpain-1, while yellow arrowheads point to PN soma localization of calpain-1. **E**) Bar graph depicting calpain-1 integrated density represented as arbitrary units of intensity (AUIs) of the fluorescence images in 7W WT and nNOS$^{-/-}$ PN somata, representing N = 4 biological replicates per group; WT n = 18 cells, nNOS$^{-/-}$ n =21 cells. P < 0.0001. **F**) Representative western blot depicting expression of β-III-spectrin (270 kDa) in 7W WT and nNOS$^{-/-}$ cerebella, along with bar graph representing N = 3 biological replicates per group. Expression of β-III-spectrin was normalized to total GAPDH expression. P = 0.0193. All data are represented as mean ± SEM.

2.4.7 NO Signaling Regulates the mGluR1-Dependent Expression of Calpain-1 in nNOS$^{-/-}$ Organotypic Cerebellar Slice Cultures.

To determine whether the changes in morphology and protein expression in nNOS$^{-/-}$ PNs were a consequence of a lack of NO signaling within the cerebellum, we established ex vivo organotypic cultures of cerebellar slices and treated the cultured slices with various compounds. Treating WT cerebellar slices with either L-NAME, a NOS inhibitor, or with DHPG, an mGluR1 agonist, seemed to greatly decrease dendritic branching of PNs in cultured slices compared with controls (**Figure 2.11a**). In accordance with the observed detrimental effects on dendritic morphology, L-NAME and DHPG significantly increased the level of calpain-1 protein expression in WT slices when compared with their controls (**Figure 2.11a**). In contrast, treating WT slices with LY367385, an mGluR1 antagonist, did not seem to alter the dendritic morphology nor the level of calpain-1 expression in comparison with the control (**Figure 2.11a**).

Likewise, organotypic cultures of nNOS$^{-/-}$ slices were treated with either the slow release NO donor NOC-18, DHPG, or LY367385. Notably, NOC-18 treatment seemed to increase dendritic branching while significantly decreasing calpain-1 expression compared with the control (**Figure 2.11b**). Interestingly, DHPG treatment had no effect on calpain-1 levels, while LY367385 treatment seemed to increase dendritic branching while significantly decreasing calpain-1 expression when compared with controls (**Figure 2.11b**).

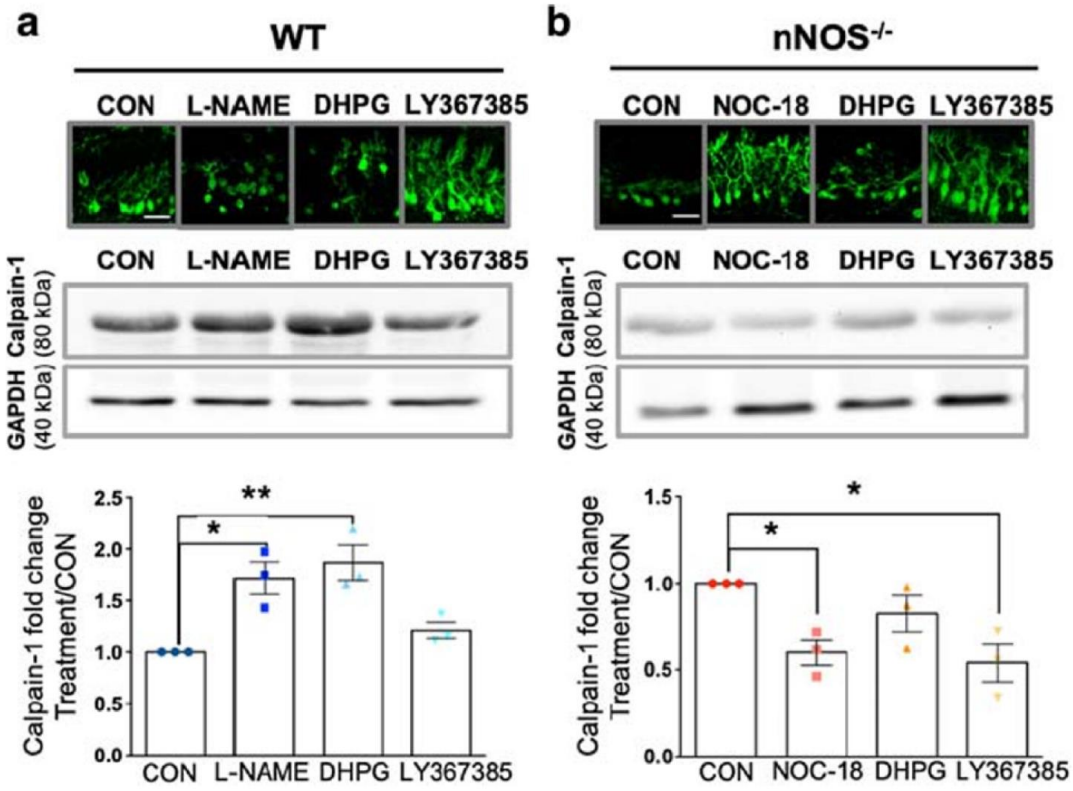

Figure 2.11 mGluR1-mediated expression of calpain-1 expression is modulated by NO signaling in ex vivo organotypic cerebellar slice cultures.

A) Representative confocal images of WT DIV7 ex vivo organotypic cerebellar slice cultures treated with L-NAME, DHPG, or LY367385 and stained with CalB (green). Scale bar represents 50 μm. **B**) Representative western blot of calpain-1 (80 kDa) expression in WT slices treated with L-NAME (100 μM), DHPG (10 μM), or LY367385 (10 μM). Calpain-1 expression was normalized to GAPDH (40 kDa). Bar graph represents N = 3 experimental replicates. Each replicate used n = 10–12 WT pups. $F(3, 8) = 11.36$, $P = 0.003$, ANOVA. **C**) Representative confocal images of $nNOS^{-/-}$ DIV7 ex vivo organotypic slice cultures treated with NOC-18, DHPG, or LY367385 and stained with CalB (green). Scale bar represents 50 μm. **D**) Representative western blot of calpain-1 expression in $nNOS^{-/-}$ slices treated with NOC-18 (300 μM), DHPG (10 μM), or LY367385 (10 μM). Calpain-1 expression was normalized to total GAPDH. Bar graph represents N = 3 experimental replicates. Each replicate used n =10–12 $nNOS^{-/-}$ pups. $F(3, 8) = 6.212$, $P = 0.0174$, ANOVA. All data are represented as mean ± SEM.

2.5 Discussion

Although the nNOS$^{-/-}$ mouse model experiences behavioral deficits associated with movement coordination and balance(Kriegsfeld et al., 1999; Nelson et al., 1995), a general morphological characterization of the principle cerebellar neurons generating motor output responses had not been fully conducted in this mouse strain. The present study is the first to report distinct alterations in PN morphology of nNOS$^{-/-}$ mice from early postnatal ages to adult. Specifically, our analyses showed that the morphological differences in dendritic branching were accompanied with decreased total mGluR1 expression, along with increased STIM1 expression, and vGluT2 expression only at 7W. Importantly, these changes were associated with increased calpain-1 protein expression in nNOS$^{-/-}$ mice, suggesting aberrant pathway activity and calcium influx. Additionally, modulation of NO as well as mGluR1 signaling affected both PN dendritic branching and calpain-1 expression levels in an ex vivo model.

2.5.1 Dendritic Abnormalities Are Present Within the PNs of nNOS$^{-/-}$ Mice.

One of the significant discoveries found by this study is the decrease in PN dendritic branching in nNOS$^{-/-}$ mice from postnatal ages to adulthood. This morphological deficit was expected, considering the importance of NO as a neurotransmitter within the cerebellum(Bal-Price, Moneer, & Brown, 2002; Kakizawa, Yamazawa, & Iino, 2013). In the cerebellum, NO is produced in an activity-dependent manner from PFs/granule cells and GABAergic interneurons(Wang et al., 2014), and such activity-dependent NO signaling is essential for the induction of PF-PN synaptic LTD (Boxall & Garthwaite, 1996; Lev-Ram, Jiang, Wood, Lawrence, & Tsien, 1997; Lev-Ram et al., 1995), which contributes to spine morphology and calcium regulation within dendrites(Lee, Jung, Arii, Imoto, & Rhyu, 2007). While normal neurite growth relies on optimal levels of calcium influx during development, chronically increased calcium suppresses neurite elongation and growth cone movement(Mattson & Kater, 1987). Therefore, a lack of NO signaling may affect intracellular calcium transients within the PN and contribute to the dendritic deficits seen in nNOS$^{-/-}$ cerebella during early development.

Altered intracellular calcium signaling within nNOS$^{-/-}$ PNs may also underlie the dramatic shift in dendritic spine type—from mushroom to thin-type spines at 7W. It is reported that mushroom spines are considered “memory spines,” har-boring features such as larger postsynaptic densities that accommodate more glutamate receptors and better local regulation of calcium influx, leading to functionally stronger synapse formation(Bourne & Harris, 2007; Mahmmoud et al., 2015). In contrast, thin spines or “learning spines” are transient and unstable, harboring smaller postsynaptic densities that either increase in strength or weaken and degrade(Bourne & Harris, 2007; Dumitriu et al., 2010). Changes from mushroom spines to thin spines may rely on the size and time course of calcium dynamics within the nNOS$^{-/-}$ PN, which is an area that warrants investigation in future studies.

2.5.2 Synaptic Alterations Exist Within the PNs of nNOS$^{-/-}$ Mice.

Appropriate glutamatergic synapse function is critical in maintaining PN output and motor activity, and this is achieved in part through activation of mGluR1(Coesmans et al., 2003; Kishimoto et al., 2002). Results from this study showed that total mGluR1 protein was significantly decreased in nNOS$^{-/-}$ mice at PD7, 2W, and 7W. Since mGluR1 is predominately located within PN spine heads, decreased total mGluR1 protein expression may be due to de-creased dendritic puncta. In addition, decreased PN spine head diameter in nNOS$^{-/-}$ animals can lead to smaller postsynaptic densities and less total synaptic mGluR1 protein accommodation within the PN dendritic spine (Ganeshina, Berry, Petralia, Nicholson, & Geinisman, 2004; Santamaria, Wils, De Schutter, & Augustine, 2006). It is important to note that PM expression of mGluR1 is indeed higher in nNOS$^{-/-}$ cerebella compared with WT at 7W, while no changes to the GluR1 subunit of the AMPA receptor are seen within this study. The significant increase of mGluR1 on the surface of PNs in nNOS$^{-/-}$ mice might allude to a feedback regulation mechanism, in which a total downregulation of mGluR1 is compensated by an upregulation of mGluR1 on the PM of the dendritic spine. In terms of synaptogenesis, activation of mGluR1 leads to protein kinase-C-γ (PKCγ) activity, and subsequent phosphorylation of calmodulin-dependent protein kinase-2β (CaMKIIβ), which has been shown to repress spine synaptogenesis on PNs(Sugawara, Hisatsune, Miyamoto, Ogawa, & Mikoshiba, 2017). Interestingly, a

previous study reported that overstimulation of mGluR1 on cultured hippocampal neurons resulted in prominent dendritic spine elongation into thin spines(Vanderklish & Edelman, 2002).

Consistent with the changes in dendritic branching and mGluR1 expression in nNOS$^{-/-}$ PNs, vGluT1 expression in PFs was also lower in nNOS$^{-/-}$ mice at PD7. Interestingly, this deficit in vGluT1 expression was not noticeable in 2W or 7W nNOS$^{-/-}$ mice, suggesting the importance of NO signaling on PF maturation during the early postnatal development period. Accordingly, granule cell migration and PF maturation relies on NO production(Takatsuru et al., 2006), which may explain the delay in vGluT1 protein expression levels at PD7 in nNOS$^{-/-}$ mice. Our results suggest that NO plays an age-dependent role during development, contributing to PF development in younger ages, while not being the main modulator of PF terminal maintenance into adulthood. This topic concerning the development of PF terminals in relation to NO signaling has not yet been elucidated and warrants further investigation.

In comparison with age-matched WT, the cerebellum of nNOS$^{-/-}$ mice at 7W showed an increase in vGluT2 protein expression, suggestive of increased CF boutons, and therefore more CF-PN synapses. Increased CF-PN innervation can result in motor deficits such as tremor and motor dyscoordination, both in animal models and in a clinical setting(Kuo et al., 2017; Pan, Ni, Wu, Li, & Kuo, 2018; Smeets & Verbeek, 2016). Given that increases in vGluT2 were only apparent at 7W and not at PD7 or 2W, the late phase of CF synapse elimination is most likely to be impaired in nNOS$^{-/-}$ mice(Kano, Watanabe, Uesaka, & Watanabe, 2018). Elimination of weak CF synapses in the late phase is governed by mGluR1-mediated PKCγ activation(Kano et al., 1997; Offermanns et al., 1997). Specifically, in mice lacking either mGluR1 or PKCγ protein expression, CF elimination is significantly impaired(Kano et al., 1995, 1997). Moreover, mGluR1-deficient mice result in a PN morphology similar to the nNOS$^{-/-}$ PN morphology reported in our study(Kano et al., 1997). However, according to Kano et al., dendritic morphology does not necessarily dictate the amount of CF innervation, while mGluR1/PKC seems to be the predominant influence(Kano et al., 1997). Therefore, increased CF innervation within nNOS$^{-/-}$ mice may be attributed to the total decreases in mGluR1 expression noted in nNOS$^{-/-}$ mice, rather

than thicker PN branches, as reported within this study. In addition, increases in vGluT2 seem to arise from the infiltration of vGluT2 clusters into the upper 20% of the molecular layer— a largely PF-dominated area(Lin et al., 2014). Numerous articles have reported the consequences of extensive CF innervation, which can be found in disorders such as essential tremor in humans(Lin et al., 2014), and have related excessive or mislocalized CF innervation with altered calcium homeostasis, leading to excitotoxicity(Hashimoto et al., 2001; Slemmer, De Zeeuw, & Weber, 2005).

Along with the increased PM expression of mGluR1 in nNOS$^{-/-}$ mice, significant increases in STIM1 protein expression and clustering were found at PD7, 2W, and 7W. It is known that following mGluR1 activation, STIM1 proteins oligomerize and control store-operated calcium entry through TRPC3 channels(Hartmann et al., 2008, 2014). Therefore, changes in expression levels and oligomerization patterns of STIM1 are indicative of calcium dysregulation(Klejman et al., 2009). Our results displayed increased STIM1 clustering in nNOS$^{-/-}$ PNs, alluding to aberrant calcium entry through a store-operated calcium entry mechanism. Indeed, a recent study noted the interaction between STIM1 and NO via S-nitrosylation, resulting in the prevention of STIM1 oligomerization and further reduction of store-operated calcium entry(Gui et al., 2018). The absence of NO/S-nitrosylation of STIM1 may result in elevated calcium entry through STIM1-gated TRPC3 channels in PNs, initiated by increased PM expression of mGluR1 in nNOS$^{-/-}$ mice.

2.5.3 Calpain-1 Is Increased in the PNs of nNOS$^{-/-}$ Mice.

Considering the importance of STIM1 as a regulator of intracellular calcium, we assessed the potential outcome of dysregulated calcium influx by measuring calpain-1 in the cerebellum of WT and nNOS$^{-/-}$ mice. As calcium-dependent cysteine proteases, calpains in neuronal cells are crucial for the regulation of synaptic plasticity, morphology, and neurodegeneration(Sorimachi, Ishiura, & Suzuki, 1997). Calpain activity can induce degradation of neuronal cytoskeletal proteins(Rami, Ferger, & Krieglstein, 1997; Schumacher, Siman, & Fehlings, 2002), including α-and β-spectrins (Löfvenberg & Backman, 1999) as well as IP3 receptors (Vosler, Brennan, & Chen, 2008), implicated in the progression of multiple SCAs (Avery, Thomas, & Hays, 2017; Hubener et al., 2013; Tada, Nishizawa, & Onodera, 2016). Results from immunohistochemical assays showed

that calpain-1 was globally expressed in cells of the cerebellar cortex, with a particularly higher expression within PN somata and dendrites. Notably, we revealed a significant increase in calpain-1 expression across all time points using western blotting, along with a decrease in β-III-spectrin expression in adult nNOS$^{-/-}$ mice. β-III-Spectrin is crucial in regulating glutamate transport in PNs and is consequently implicated in SCA5(Avery et al., 2017; Gao et al., 2011). Given that β-III-spectrin is necessary for the formation of mushroom-like dendritic spines(Efimova et al., 2017), the reduction of β-III-spectrin in the cerebellum may explain the alterations in dendritic structures and synapses in nNOS$^{-/-}$ PNs.

2.5.4 NO Supplementation Can Rectify Deficits in Ex Vivo nNOS$^{-/-}$ Cerebella.

Results from ex vivo experiments in this study showed that modulation of NO signaling significantly altered calpain-1 protein expression in both WT and nNOS$^{-/-}$ cerebellar slices. Specifically, inhibition of endogenous NOS activity by L-NAME appeared to hinder PN dendritic branching and significantly increased calpain-1 expression in WT cerebellar tissues. The L-NAME treatment was similar to the effect of DHPG on WT slices, known to cause elevated calcium levels and PN dendritic deficits in previous studies(Hasegawa, Sakuragi, Tominaga-Yoshino, & Ogura, 2015; Sirzen-Zelenskaya, Zeyse, & Kapfhammer, 2006), as well as affect calpain-1 expression and activity(Xu et al., 2007). Accordingly, NOC-18 and LY367385 mitigated the appearance of PN dendritic deficits and decreased the levels of calpain-1 in nNOS$^{-/-}$ cerebellar slices. These results indicate a critical role for NO signaling in the regulation of PN morphology and function by decreasing calpain-1 levels within the cerebellum.

It is important to note that mGluR1 blockade alone in nNOS$^{-/-}$ slices significantly decreased levels of calpain-1 expression, while activation of mGluR1 showed no significant differences in calpain-1 expression compared with the control. These results suggest that basal mGluR1 activity is upregulated in nNOS$^{-/-}$ cerebella, likely due to increased PM mGluR1 expression on the PNs of nNOS$^{-/-}$ mice. Although nNOS$^{-/-}$ cerebella displayed decreased total mGluR1 expression in vivo, vGluT1 expression remained similar, while vGluT2 expression significantly increased. This imbalance of presynaptic and postsynaptic compartments in vivo may result in an overload of glutamate within PF-

PN and CF-PN synaptic clefts, leading to further overexcitation of mGluR1 receptors and overload of intracellular calcium of PNs in $NOS^{-/-}$ cerebella. Characterization of this potential excitotoxic effect should be considered for future studies.

In summary, results from this study indicate that nNOS/NO signaling critically controls PN morphological development by regulating mGluR1 signaling. As depicted in **Figure 2.12**, mGluR1 activation causes ER calcium efflux, STIM1 oligomerization, and consequently calcium entry through STIM1-gated TRPC channels(Hartmann et al., 2008, 2014). We propose that under physiological conditions, nNOS/NO signaling maintains calcium homeostasis within PNs by attenuating mGluR1-mediated calcium influx(Gui et al., 2018). In contrast, the lack of NO signaling in $nNOS^{-/-}$ mice results in overactivation of mGluR1 leading to elevated expression of calcium-dependent proteases such as calpains, increasing degradation of structural proteins such as β-III-spectrin, and resulting in PN structural malformations. Further analysis of the PN phenotype in $nNOS^{-/-}$ mice will provide novel insight into the role of NO signaling in PN development and morphogenesis, along with a potential new mechanism and model of cerebellar ataxia.

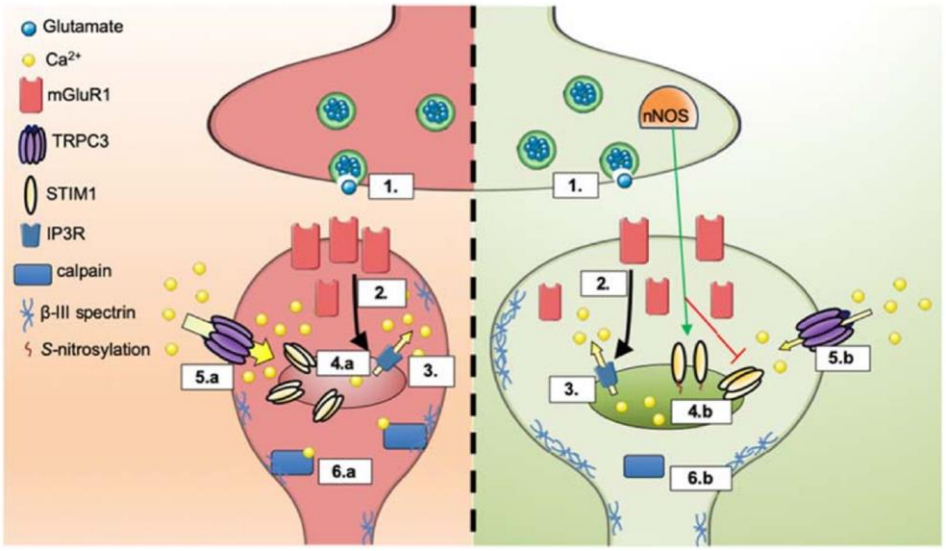

Figure 2.12 Schematic representation of the mGluR1 signaling cascade in relation to NO signaling.

The left side of this figure depicts a glutamatergic PN synapse in the absence of nNOS-derived NO signaling, while the right depicts a physiological glutamatergic PN synapse with nNOS expression and NO production. (**1**) Glutamate is released from the presynaptic terminal and binds to mGluR1 receptors on PN dendritic spines. (**2**) Through a Gq signaling cascade, mGluR1 activation stimulates the production of IP3 in PNs, leading to activation of the IP3R on the ER.(**3**) IP3R activation causes a calcium efflux from internal ER stores to the PN cytosol. *Left side* ($nNOS^{-/-}$) (**4.a**) Excessive mGluR1 activation results in ER calcium depletion and causing STIM1 oligomerization. (**5.a**) Chronically oligomerized STIM1 proteins interact and gate the opening of TRPC3 channels on the PN membrane, causing elevated calcium in-flux into the PN cytosol. (**6.a**) Chronically elevated calcium levels within the PN activates calcium-dependent proteases such as calpain-1, which cleaves integral structural proteins such as β-III-spectrin, leading to changes in PN dendritic morphology. *Right side* (WT): (**4.b**) NO release from the presynaptic terminal induces S-nitrosylation of STIM1, restricting its oligomerization and limiting calcium entry through TRPC3 channels. (**5.b**) Limited calcium entry through TRPC3 channels replenishes ER calcium stores. (**6.b**) Physiological concentrations of intracellular calcium controls calpain-1 protease activity, therefore maintaining the integrity of PN dendritic spines.

2.6 Acknowledgements

This work was supported by the Canadian Institutes of Health Research (MOP-133504) awarded to W-Y L. VT, and MJEM were awarded Ontario Graduate Scholarships.

2.7 References

Abbott, L. C., & Nahm, S. (2004). Neuronal nitric oxide synthase expression in cerebellar mutant mice. *Cerebellum (London, England)*, *3*(3), 141–151. https://doi.org/10.1080/14734220410031927

Avery, A. W., Thomas, D. D., & Hays, T. S. (2017). β-III-spectrin spinocerebellar ataxia type 5 mutation reveals a dominant cytoskeletal mechanism that underlies dendritic arborization. *Proceedings of the National Academy of Sciences of the United States of America*, *114*(44), E9376–E9385. https://doi.org/10.1073/pnas.1707108114

Bal-Price, A., Moneer, Z., & Brown, G. C. (2002). Nitric oxide induces rapid, calcium-dependent release of vesicular glutamate and ATP from cultured rat astrocytes. *Glia*, *40*(3), 312–323. https://doi.org/10.1002/glia.10124

Blanco, S., Molina, F. J., Castro, L., Del Moral, M. L., Hernandez, R., Jimenez, A., … Peinado, M. A. (2010). Study of the nitric oxide system in the rat cerebellum during aging. *BMC Neuroscience*, *11*, 78. https://doi.org/10.1186/1471-2202-11-78

Bourne, J., & Harris, K. M. (2007). Do thin spines learn to be mushroom spines that remember? *Current Opinion in Neurobiology*, *17*(3), 381–386. https://doi.org/10.1016/j.conb.2007.04.009

Boxall, A. R., & Garthwaite, J. (1996). Long-Term Depression in Rat Cerebellum Requires both NO Synthase and NO-sensitive Guanylyl Cyclase. *European Journal of Neuroscience*, *8*(10), 2209–2212. https://doi.org/10.1111/j.1460-9568.1996.tb00743.x

Coesmans, M., Smitt, P. A. S., Linden, D. J., Shigemoto, R., Hirano, T., Yamakawa, Y., … de Zeeuw, C. I. (2003). Mechanisms underlying cerebellar motor deficits due to mGluR1-autoantibodies. *Annals of Neurology*, *53*(3), 325–336. https://doi.org/10.1002/ana.10451

Conquet, F., Bashir, Z. I., Davies, C. H., Daniel, H., Ferraguti, F., Bordi, F., … Condé, F. (1994). Motor deficit and impairment of synaptic plasticity in mice lacking mGluR1. *Nature*, *372*(6503), 237–243. https://doi.org/10.1038/372237a0

Daniel, H., Levenes, C., & Crépel, F. (1998). Cellular mechanisms of cerebellar LTD. *Trends in Neurosciences*, *21*(9), 401–407. https://doi.org/10.1016/S0166-2236(98)01304-6

Dumitriu, D., Hao, J., Hara, Y., Kaufmann, J., Janssen, W. G. M., Lou, W., … Morrison, J. H. (2010). Selective Changes in Thin Spine Density and Morphology in Monkey Prefrontal Cortex Correlate with Aging-Related Cognitive Impairment. *Journal of Neuroscience*, *30*(22), 7507–7515. https://doi.org/10.1523/JNEUROSCI.6410-09.2010

Efimova, N., Korobova, F., Stankewich, M. C., Moberly, A. H., Stolz, D. B., Wang, J., … Svitkina, T. (2017). βIII Spectrin Is Necessary for Formation of the Constricted Neck of Dendritic Spines and Regulation of Synaptic Activity in Neurons. *The Journal of Neuroscience*, *37*(27), 6442–6459. https://doi.org/10.1523/JNEUROSCI.3520-16.2017

Fogel, B. L., Hanson, S. M., & Becker, E. B. E. (2015). Do mutations in the murine ataxia gene TRPC3 cause cerebellar ataxia in humans? *Movement Disorders : Official Journal of the Movement Disorder Society*, *30*(2), 284–286. https://doi.org/10.1002/mds.26096

Ganeshina, O., Berry, R. W., Petralia, R. S., Nicholson, D. A., & Geinisman, Y. (2004). Synapses with a segmented, completely partitioned postsynaptic density express more AMPA receptors than other axospinous synaptic junctions. *Neuroscience*, *125*(3), 615–623. https://doi.org/10.1016/J.NEUROSCIENCE.2004.02.025

Gao, Y., Perkins, E. M., Clarkson, Y. L., Tobia, S., Lyndon, A. R., Jackson, M., & Rothstein, J. D. (2011). β-III spectrin is critical for development of purkinje cell dendritic tree and spine morphogenesis. *The Journal of Neuroscience : The Official Journal of the Society for Neuroscience*, *31*(46), 16581–16590. https://doi.org/10.1523/JNEUROSCI.3332-11.2011

Gui, L., Zhu, J., Lu, X., Sims, S. M., Lu, W.-Y., Stathopulos, P. B., & Feng, Q. (2018). S-Nitrosylation of STIM1 by neuronal nitric oxide synthase inhibits store-operated Ca^{2+} entry. *Journal of Molecular Biology*. https://doi.org/10.1101/304022

Hartmann, J., Dragicevic, E., Adelsberger, H., Henning, H. A., Sumser, M., Abramowitz, J., … Konnerth, A. (2008). TRPC3 Channels Are Required for Synaptic Transmission and Motor Coordination. *Neuron*, *59*(3), 392–398. https://doi.org/10.1016/j.neuron.2008.06.009

Hartmann, J., Henning, H. A., & Konnerth, A. (2011). mGluR1/TRPC3-mediated synaptic transmission and calcium signaling in mammalian central neurons. *Cold Spring Harbor Perspectives in Biology*, *3*(4), 1–16. https://doi.org/10.1101/cshperspect.a006726

Hartmann, J., Karl, R. M., Alexander, R. P. D., Adelsberger, H., Brill, M. S., Rühlmann, C., … Konnerth, A. (2014). STIM1 Controls Neuronal Ca^{2+} Signaling, mGluR1-Dependent Synaptic Transmission, and Cerebellar Motor Behavior. *Neuron*, *82*(3), 635–644. https://doi.org/10.1016/J.NEURON.2014.03.027

Hasegawa, S., Sakuragi, S., Tominaga-Yoshino, K., & Ogura, A. (2015). Dendritic spine dynamics leading to spine elimination after repeated inductions of LTD. *Scientific Reports*, *5*. https://doi.org/10.1038/srep07707

Hashimoto, K., Ichikawa, R., Takechi, H., Inoue, Y., Aiba, A., Sakimura, K., … Kano, M. (2001). Roles of Glutamate Receptor δ2 Subunit (GluRδ2) and Metabotropic Glutamate Receptor Subtype 1 (mGluR1) in Climbing Fiber Synapse Elimination during Postnatal Cerebellar Development. *The Journal of Neuroscience*, *21*(24), 9701–9712. https://doi.org/10.1523/JNEUROSCI.21-24-09701.2001

Huang, P. L., Dawson, T. M., Bredt, D. S., Snyder, S. H., & Fishman, M. C. (1993). Targeted disruption of the neuronal nitric oxide synthase gene. *Cell*, *75*(7), 1273–1286. https://doi.org/10.1016/0092-8674(93)90615-w

Hubener, J., Weber, J. J., Richter, C., Honold, L., Weiss, A., Murad, F., … Nguyen, H. P. (2013). Calpain-mediated ataxin-3 cleavage in the molecular pathogenesis of

spinocerebellar ataxia type 3 (SCA3). *Human Molecular Genetics*, *22*(3), 508–518. https://doi.org/10.1093/hmg/dds449

Jin, Y., Kim, S. J., Kim, J., Worley, P. F., & Linden, D. J. (2007). Long-Term Depression of mGluR1 Signaling. *Neuron*, *55*(2), 277–287. https://doi.org/10.1016/j.neuron.2007.06.035

Kakizawa, S., Yamazawa, T., & Iino, M. (2013). Nitric oxide-induced calcium release. *Channels*, *7*(1), 1–5. https://doi.org/10.4161/chan.22555

Kano, M., Hashimoto, K., Chen, C., Abeliovich, A., Aiba, A., Kurihara, H., … Tonegawa, S. (1995). Impaired synapse elimination during cerebellar development in PKCγ mutant mice. *Cell*, *83*(7), 1223–1231. https://doi.org/10.1016/0092-8674(95)90147-7

Kano, M., Hashimoto, K., Kurihara, H., Watanabe, M., Inoue, Y., Aiba, A., & Tonegawa, S. (1997). Persistent Multiple Climbing Fiber Innervationof Cerebellar Purkinje Cellsin Mice Lacking mGluR1. *Neuron*, *18*(1), 71–79. https://doi.org/10.1016/S0896-6273(01)80047-7

Kano, M., Watanabe, T., Uesaka, N., & Watanabe, M. (2018). Multiple Phases of Climbing Fiber Synapse Elimination in the Developing Cerebellum. *Cerebellum (London, England)*, *17*(6), 722–734. https://doi.org/10.1007/s12311-018-0964-z

Kasumu, A., & Bezprozvanny, I. (2012). Deranged calcium signaling in purkinje cells and pathogenesis in spinocerebellar ataxia 2 (SCA2) and other ataxias. *Cerebellum*, *11*(3), 630–639. https://doi.org/10.1007/s12311-010-0182-9

Kishimoto, Y., Fujimichi, R., Araishi, K., Kawahara, S., Kano, M., Aiba, A., & Kirino, Y. (2002). mGluR1 in cerebellar Purkinje cells is required for normal association of temporally contiguous stimuli in classical conditioning. *The European Journal of Neuroscience*, *16*(12), 2416–2424. https://doi.org/10.1046/j.1460-9568.2002.02407.x

Klejman, M. E., Gruszczynska-Biegala, J., Skibinska-Kijek, A., Wisniewska, M. B., Misztal, K., Blazejczyk, M., … Kuznicki, J. (2009). Expression of STIM1 in brain and puncta-like co-localization of STIM1 and ORAI1 upon depletion of Ca^{2+} store in neurons. *Neurochemistry International*, *54*(1), 49–55.

https://doi.org/10.1016/j.neuint.2008.10.005

Kriegsfeld, L. J., Eliasson, M. J., Demas, G. E., Blackshaw, S., Dawson, T. M., Nelson, R. J., & Snyder, S. H. (1999). Nocturnal motor coordination deficits in neuronal nitric oxide synthase knock-out mice. *Neuroscience*, *89*(2), 311–315. https://doi.org/S0306-4522(98)00614-9 [pii]

Kuo, S.-H., Lin, C.-Y., Wang, J., Sims, P. A., Pan, M.-K., Liou, J.-Y., … Faust, P. L. (2017). Climbing fiber-Purkinje cell synaptic pathology in tremor and cerebellar degenerative diseases. *Acta Neuropathologica*, *133*(1), 121–138. https://doi.org/10.1007/s00401-016-1626-1

Lee, K. J., Jung, J. G., Arii, T., Imoto, K., & Rhyu, I. J. (2007). Morphological changes in dendritic spines of Purkinje cells associated with motor learning. *Neurobiology of Learning and Memory*, *88*(4), 445–450. https://doi.org/10.1016/J.NLM.2007.06.001

Lev-Ram, V., Jiang, T., Wood, J., Lawrence, D. S., & Tsien, R. Y. (1997). Synergies and Coincidence Requirements between NO, cGMP, and Ca^{2+} in the Induction of Cerebellar Long-Term Depression. *Neuron*, *18*(6), 1025–1038. https://doi.org/10.1016/S0896-6273(00)80340-2

Lev-Ram, V., Makings, L. R., Keitz, P. F., Kao, J. P. Y., & Tsien, R. Y. (1995). Long-term depression in cerebellar Purkinje neurons results from coincidence of nitric oxide and depolarization-induced Ca^{2+} transients. *Neuron*, *15*(2), 407–415. https://doi.org/10.1016/0896-6273(95)90044-6

Lin, C. Y., Louis, E. D., Faust, P. L., Koeppen, A. H., Vonsattel, J. P. G., & Kuo, S. H. (2014). Abnormal climbing fibre-Purkinje cell synaptic connections in the essential tremor cerebellum. *Brain*, *137*(12), 3149–3159. https://doi.org/10.1093/brain/awu281

Liu, J., Tang, T.-S., Tu, H., Nelson, O., Herndon, E., Huynh, D. P., … Bezprozvanny, I. (2009). Deranged calcium signaling and neurodegeneration in spinocerebellar ataxia type 2. *The Journal of Neuroscience : The Official Journal of the Society for Neuroscience*, *29*(29), 9148–9162. https://doi.org/10.1523/JNEUROSCI.0660-09.2009

Löfvenberg, L., & Backman, L. (1999). Calpain-induced proteolysis of β-spectrins. *FEBS Letters*, *443*(2), 89–92. https://doi.org/10.1016/S0014-5793(98)01697-4

Mahmmoud, R. R., Sase, S., Aher, Y. D., Sase, A., Gröger, M., Mokhtar, M., … Lubec, G. (2015). Spatial and Working Memory Is Linked to Spine Density and Mushroom Spines. *PLOS ONE*, *10*(10), e0139739. https://doi.org/10.1371/journal.pone.0139739

Mattson, M., & Kater, S. (1987). Calcium regulation of neurite elongation and growth cone motility. *The Journal of Neuroscience*, *7*(12), 4034–4043. https://doi.org/10.1523/JNEUROSCI.07-12-04034.1987

Nelson, R., Demas, G., Huang, P., Fishman, M., Dawson, V., Dawson, T., & Snyder, S. (1995). Behavioural abnormalities in male mice lacking neuronal nitric oxide synthase. *Nature*, *378*(6555), 383–386. https://doi.org/10.1038/378383a0

Offermanns, S., Hashimoto, K., Watanabe, M., Sun, W., Kurihara, H., Thompson, R. F., … Simon, M. I. (1997). Impaired motor coordination and persistent multiple climbing fiber innervation of cerebellar Purkinje cells in mice lacking G q. *Proceedings of the National Academy of Sciences*, *94*(25), 14089–14094. https://doi.org/10.1073/pnas.94.25.14089

Pan, M.-K., Ni, C.-L., Wu, Y.-C., Li, Y.-S., & Kuo, S.-H. (2018). Animal Models of Tremor: Relevance to Human Tremor Disorders. *Tremor and Other Hyperkinetic Movements (New York, N.Y.)*, *8*, 587. https://doi.org/10.7916/D89S37MV

Power, E. M., Morales, A., & Empson, R. M. (2016). Prolonged Type 1 Metabotropic Glutamate Receptor Dependent Synaptic Signaling Contributes to Spino-Cerebellar Ataxia Type 1. *The Journal of Neuroscience*, *36*(18), 4910–4916. https://doi.org/10.1523/JNEUROSCI.3953-15.2016

Rami, A., Ferger, D., & Krieglstein, J. (1997). Blockade of calpain proteolytic activity rescues neurons from glutamate excitotoxicity. *Neuroscience Research*, *27*(1), 93–97. https://doi.org/10.1016/S0168-0102(96)01123-6

Rossi, P. I. A., Vaccari, C. M., Terracciano, A., Doria-Lamba, L., Facchinetti, S., Priolo, M., … Puliti, A. (2010). The metabotropic glutamate receptor 1, GRM1: evaluation

as a candidate gene for inherited forms of cerebellar ataxia. *Journal of Neurology*, *257*(4), 598–602. https://doi.org/10.1007/s00415-009-5380-3

Santamaria, F., Wils, S., De Schutter, E., & Augustine, G. J. (2006). Anomalous Diffusion in Purkinje Cell Dendrites Caused by Spines. *Neuron*, *52*(4), 635–648. https://doi.org/10.1016/j.neuron.2006.10.025

Schilling, K., Schmidt, H. H., & Baader, S. L. (1994). Nitric oxide synthase expression reveals compartments of cerebellar granule cells and suggests a role for mossy fibers in their development. *Neuroscience*, *59*(4), 893–903.

Schindelin, J., Arganda-Carreras, I., Frise, E., Kaynig, V., Longair, M., Pietzsch, T., … Cardona, A. (2012). Fiji: an open-source platform for biological-image analysis. *Nature Methods*, *9*(7), 676–682. https://doi.org/10.1038/nmeth.2019

Schumacher, P. A., Siman, R. G., & Fehlings, M. G. (2002). Pretreatment with Calpain Inhibitor CEP-4143 Inhibits Calpain I Activation and Cytoskeletal Degradation, Improves Neurological Function, and Enhances Axonal Survival After Traumatic Spinal Cord Injury. *Journal of Neurochemistry*, *74*(4), 1646–1655. https://doi.org/10.1046/j.1471-4159.2000.0741646.x

Sirzen-Zelenskaya, A., Zeyse, J., & Kapfhammer, J. P. (2006). Activation of class I metabotropic glutamate receptors limits dendritic growth of Purkinje cells in organotypic slice cultures. *European Journal of Neuroscience*, *24*(11), 2978–2986. https://doi.org/10.1111/j.1460-9568.2006.05196.x

Slemmer, J. E., De Zeeuw, C. I., & Weber, J. T. (2005). Don’t get too excited: Mechanisms of glutamate-mediated Purkinje cell death. *Progress in Brain Research*, *148*, 367–390. https://doi.org/10.1016/S0079-6123(04)48029-7

Smeets, C. J. L. M., & Verbeek, D. S. (2016). Climbing fibers in spinocerebellar ataxia: A mechanism for the loss of motor control. *Neurobiology of Disease*, *88*, 96–106. https://doi.org/10.1016/j.nbd.2016.01.009

Sorimachi, H., Ishiura, S., & Suzuki, K. (1997). Structure and physiological function of calpains. *Biochemical Journal*, *328*(3), 721–732. https://doi.org/10.1042/bj3280721

Sugawara, T., Hisatsune, C., Miyamoto, H., Ogawa, N., & Mikoshiba, K. (2017). Regulation of spinogenesis in mature Purkinje cells via mGluR/PKC-mediated phosphorylation of CaMKIIβ. *Proceedings of the National Academy of Sciences of the United States of America*, *114*(26), E5256–E5265. https://doi.org/10.1073/pnas.1617270114

Suzuki, K., Hata, S., Kawabata, Y., & Sorimachi, H. (2004). Structure, Activation, and Biology of Calpain. *Diabetes*, *53*(Supplement 1), S12–S18. https://doi.org/10.2337/diabetes.53.2007.S12

Tada, M., Nishizawa, M., & Onodera, O. (2016). Roles of inositol 1,4,5-trisphosphate receptors in spinocerebellar ataxias. *Neurochemistry International*, *94*, 1–8. https://doi.org/10.1016/J.NEUINT.2016.01.007

Takatsuru, Y., Takayasu, Y., Iino, M., Nikkuni, O., Ueda, Y., Tanaka, K., & Ozawa, S. (2006). Roles of glial glutamate transporters in shaping EPSCs at the climbing fiber-Purkinje cell synapses. *Neuroscience Research*, *54*(2), 140–148. https://doi.org/10.1016/j.neures.2005.11.002

Toru, S., Murakoshi, T., Ishikawa, K., Saegusa, H., Fujigasaki, H., Uchihara, T., … Tanabe, T. (2000). Spinocerebellar ataxia type 6 mutation alters P-type calcium channel function. *The Journal of Biological Chemistry*, *275*(15), 10893–10898. https://doi.org/10.1074/jbc.275.15.10893

van de Leemput, J., Chandran, J., Knight, M. A., Holtzclaw, L. A., Scholz, S., Cookson, M. R., … Singleton, A. B. (2007). Deletion at ITPR1 underlies ataxia in mice and spinocerebellar ataxia 15 in humans. *PLoS Genetics*, *3*(6), e108. https://doi.org/10.1371/journal.pgen.0030108

Vanderklish, P. W., & Edelman, G. M. (2002). Dendritic spines elongate after stimulation of group 1 metabotropic glutamate receptors in cultured hippocampal neurons. *Proceedings of the National Academy of Sciences*, *99*(3), 1639–1644. https://doi.org/10.1073/pnas.032681099

Vosler, P. S., Brennan, C. S., & Chen, J. (2008). Calpain-mediated signaling mechanisms

in neuronal injury and neurodegeneration. *Molecular Neurobiology*, *38*(1), 78–100. https://doi.org/10.1007/s12035-008-8036-x

Wang, D.-J., Su, L.-D., Wang, Y.-N., Yang, D., Sun, C.-L., Zhou, L., … Shen, Y. (2014). Long-Term Potentiation at Cerebellar Parallel Fiber-Purkinje Cell Synapses Requires Presynaptic and Postsynaptic Signaling Cascades. *Journal of Neuroscience*, *34*(6), 2355–2364. https://doi.org/10.1523/JNEUROSCI.4064-13.2014

Willard, S. S., & Koochekpour, S. (2013). Glutamate, glutamate receptors, and downstream signaling pathways. *International Journal of Biological Sciences*, *9*(9), 948–959. https://doi.org/10.7150/ijbs.6426

Xu, W., Wong, T. P., Chery, N., Gaertner, T., Wang, Y. T., & Baudry, M. (2007). Calpain-Mediated mGluR1α Truncation: A Key Step in Excitotoxicity. *Neuron*. https://doi.org/10.1016/j.neuron.2006.12.020

Yoshida, T., Inoue, R., Morii, T., Takahashi, N., Yamamoto, S., Hara, Y., … Mori, Y. (2006). Nitric oxide activates TRP channels by cysteine S-nitrosylation. *Nature Chemical Biology*, *2*(11), 596–607. https://doi.org/10.1038/nchembio821

Chapter 3

3 The Expression and Function of GLAST in Bergmann Glia Are Critically Regulated by Neuronal Nitric Oxide Synthase-Derived Nitric Oxide

3.1 Abstract

Bergmann glia (BG) predominantly use glutamate/aspartate transporters (GLAST) for glutamate uptake in the cerebellum. Recently, nitric oxide (NO) treatment has been shown to upregulate GLAST function and increase glutamate uptake *in vitro*. We previously discovered that neuronal nitric oxide synthase knockout ($nNOS^{-/-}$) mice displayed structural and functional neuronal abnormalities in the cerebellum during development, in addition to previously reported motor deficits. Although these developmental deficits have been identified in the $nNOS^{-/-}$ cerebellum, it is unknown whether BG morphology and GLAST expression are also affected in the absence of nNOS in vivo. This study is the first to characterize BG morphological abnormalities and GLAST expression during development in $nNOS^{-/-}$ mice using immunohistochemistry and western blotting across postnatal development. Results showed that BG in $nNOS^{-/-}$ mice exhibited abnormal morphology and decreased GLAST expression compared to wildtype (WT) mice across postnatal development. Treating *ex vivo* WT cerebellar slices with the NOS inhibitor L-NAME decreased GLAST expression, while treating $nNOS^{-/-}$ slices with the slow-release NO-donor NOC-18 increased GLAST expression when compared to their respective controls. In addition, treating primary BG isolated from WT mice with the selective nNOS inhibitor 7N decreased the membrane expression of GLAST and Ca^{2+}/Na^{+} influx, while treating $nNOS^{-/-}$ BG with SNAP increased the membrane expression of GLAST and Ca^{2+}/Na^{+} influx. Moreover, the effects of SNAP on GLAST expression and Ca^{2+}/Na^{+} influx in $nNOS^{-/-}$ BGs were significantly reduced by a PKG inhibitor. Together, these results reveal a novel role for nNOS/NO signaling in BG development, regulated by a PKG-mediated mechanism.

3.2 Introduction

The cerebellum is known for its role in fine motor control and coordination, and more recently has been recognized for its role in cognition and executive function (Koziol, Budding, & Chidekel, 2012; Manto et al., 2012). To execute these motor functions, Purkinje neurons (PNs) in the cerebellar cortex integrate and relay synaptic inputs from both inhibitory and excitatory neurons, sending inhibitory projections to deep cerebellar nuclei. PNs form dense synapses with glutamatergic parallel fibers (PFs) and climbing fibers (CFs) that are closely ensheathed by fine processes belonging to Bergmann glia (BG), specialized radial astrocytes specific to the cerebellum. Along with their more common role of uptaking and recycling glutamate from the synaptic cleft of excitatory PF- and CF-PN synapses, BG play an important role during granule cell and PN development by guiding immature granule neurons from the external granular layer (EGL) to the inner granular layer (IGL) and providing a scaffold for PN dendritic growth during development(Altman, 1972; Ango et al., 2008; Lordkipanidze & Dunaevsky, 2005; Xu et al., 2013).

These excitatory synapses, in particular the PF-PN synapse, are major sites for synaptic plasticity and are heavily regulated by nitric oxide (NO)(Contestabile, 2012; Matyash, Filippov, Mohrhagen, & Kettenmann, 2001; D.-J. Wang et al., 2014). The cerebellum is one of the few sites in the central nervous system (CNS) that abundantly expresses neuronal nitric oxide synthase (nNOS) – more so than any other region of the brain(Bredt, Hwang, & Snyder, 1990; Campese et al., 2006). The localization of nNOS in the cerebellum is specific to granule cells, with some localization in stellate cells, basket cells, and to some degree BG(Ihara et al., 2006; Tiburcio-Félix et al., 2019). Available evidence shows that the presence of NO in the cerebellum is crucial for the development of fine motor control and movement memory, particularly by modulating the long-term depression (LTD) profile in PNs(Daniel, Levenes, & Crépel, 1998; D.-J. Wang et al., 2014). NO also contributes to a normal movement phenotype, as studies in $nNOS^{-/-}$ mice showed behavioural deficits typical of ataxia when compared to age-matched wildtype (WT) mice(Huang, Dawson, Bredt, Snyder, & Fishman, 1993; Kriegsfeld et al., 1999; Nelson et al., 1995). More recently, our group reported that $nNOS^{-/-}$ mice exhibit PN

dendritic deficits that begin early in development and persist into adulthood. Specifically, we noted that mGluR1 overexpression in the nNOS$^{-/-}$ mouse resulted in increased calcium-dependent protease activity, which lead to dendritic deficits in PNs and excitotoxicity(Tellios, Maksoud, Xiang, & Lu, 2020).

Importantly, the effects of NO are not limited to neurons within the cerebellum, as supporting cells such as BG are also under the influence of NO signaling. Specifically, NO regulates BG glutamate uptake from the synaptic cleft, which is an important process that combats excitotoxicity. Specialized radial astrocytes such as BG abundantly express glutamate/aspartate transporters (GLAST/EAAT1), a notable difference compared to common cortical astrocytes that express glutamate transporter-1 (GLT-1/EAAT2)(Perego et al., 2000). In particular, GLAST has a 6-fold greater expression level relative to GLT-1, making it the predominant glutamate transporter in the cerebellum(Lehre & Danbolt, 1998; Takatsuru et al., 2006). GLAST functions as a homotrimer on the PM of BG, where it transports one molecule of glutamate, as well as L-/D- aspartate by co-transporting three Na^+ and one H^+ into the cytosol, while transporting one K^+ to the extracellular space(Bauer et al., 2012). Recent studies have determined that increases in NO concentrations are proportional to increases in both nNOS expression as well as GLAST functionality of cultured cerebellar BG, measured as relative D-aspartate uptake(Balderas et al., 2014; Tiburcio-Félix et al., 2019). Despite these reports, it is still unknown whether nNOS/NO signaling directly influences GLAST expression and functionality in BG during development.

Considering the importance of nNOS/NO signaling in the dendritic development of the cerebellar PNs as we previously reported(Tellios et al., 2020), along with previous studies that found a link between GLAST functionality and NO supplementation(Balderas et al., 2014; Tiburcio-Félix et al., 2019), this study sought to examine potential differences in GLAST expression and functionality in a murine model comparing WT and nNOS$^{-/-}$ cerebella across postnatal development. Specifically, the present study aimed to delineate potential changes in BG morphology and expression across development, along with functional changes of GLAST in vitro using immunocytochemistry, western blotting, dual calcium and sodium imaging, and L-aspartate uptake activity.

3.3 Materials and Methods

3.3.1 Animals

WT (C57/BL6, Stock No: 000664) and nNOS$^{-/-}$ mice (B6.129S4-Nos1^{tm1Plh}, Stock No: 002986) were purchased from the Jackson Laboratory. All experiments were conducted in accordance with Animal Use Protocol (#2018-106) approved by the Animal Care and Veterinary Services at the University of Western Ontario.

3.3.2 Immunohistochemical Preparation

Intact brains from postnatal day 3 (PD3), postnatal day 7 (PD7), 2 weeks (2W) and 7 weeks (7W) old male mice were isolated from WT and nNOS$^{-/-}$ mice and immediately placed in 4% paraformaldehyde (PFA) for 48 hrs. Brains were subsequently transferred to a 30% sucrose solution for at least 48 hrs and then sagittally sectioned at a thickness of 80 μm using a vibratome, placed in a cryoprotectant solution, and stored in -20^{o}C until stained. Slices were first washed with PBS, then permeabilized using a 0.25% Triton-X solution for 5 mins. Free-floating slices were then blocked with a 10% normal donkey serum (NDS) solution for 1 hr and incubated with the following primary antibodies overnight in 4^{o}C: 1:500 goat anti-calbindin (CalB) (Santa Cruz Biotechnology, Dallas, TX, Catalogue #: sc-7691); 1:500 guinea pig anti-GLAST (Synaptic Systems, Goettingen, Germany, Catalogue #: 250 114). Slices were washed and then incubated with the appropriate secondary antibodies for 2 hrs: 1:1000 anti-goat AlexaFluor 488, or 1:500 anti-guinea pig Cy3 (Jackson Immunoresearch, Burlington, ON). After incubation with the nuclear stain DAPI, slices were mounted on cover glass using Fluoromount-G (Electron Microscopy Solutions, Hatfield, PA) and images were taken using the Olympus FV1000 confocal microscope at 60x magnification using an oil-immersion objective.

3.3.3 Primary Cerebellar Astrocyte Cultures

WT and nNOS$^{-/-}$ pups (PD 0-4) were used for acquiring primary BG cell cultures. First, pups were decapitated, and brains were quickly removed and placed in ice-cold Leibowitz L-15 media that contained 100 mg/mL bovine serum albumin and 1x penicillin/streptomycin (P/S) antibiotics (ThermoFischer Scientific, Waltham MA).

Murine cerebella were carefully dissected and then homogenized by serial pipetting, first through a 10 mL pipette, then 1 mL pipette, and finally with a 200 µL pipette. Homogenized cerebella were then filtered through a 70 µm nylon filter. The filtrate was centrifuged at 900 g for 4 min at room temperature. The resulting cells were resuspended in Dulbecco's modified eagle's medium (DMEM) that contained 1x P/S and 10% fetal bovine serum (FBS) (ThermoFischer Scientific, Waltham, MA). The cells were seeded in T-75 flasks containing approximately 5-7 cerebella per flask. Culture media was replaced 5 days after initial plating, and subsequently every 3 days until a confluent astrocyte monolayer was present. T-75 flasks were then placed on a shaker for 2 hrs at 36 ^{o}C and 200 rpm to dislodge any microglial cells present. After shaking, culture media and dislodged microglia were removed, and the cerebellar astrocyte monolayer was incubated with 3 mL trypsin for 5 mins. After, 7 mL of DMEM supplemented with 1x P/S and 10% FBS was used to neutralize the trypsin, and cells were centrifuged at 900g for 4 mins at room temperature and resuspended in fresh culture media. Isolated cerebellar astrocytes were plated at 5 x 104 cells/mL in various culture dishes for experiments. The resulting astrocytes were primarily BG, as 90% of astrocytes within the cerebellum are identified as being BG(Martínez-Lozada, Hernández-Kelly, Aguilera, López-Bayghen, & Ortega, 2011). Specifically, BG were identified based on culture morphology and intensity of GLAST staining.

3.3.4 Immunocytochemistry

Cerebellar astrocytes were seeded on poly-$_{D}$-lysine coated coverglass placed in 24-well plates. Thirty minutes after specific treatments, culture media was removed and cells were fixed using 4% PFA and washed once with 0.1 M glycine, then followed by two washes with PBS for 10 min, each. Fixed cells were permeabilized using a 0.1% Triton-X solution for 5 min. Cells were blocked with 5% NDS solution for 1 hr and then incubated with 1:500 guinea pig anti-GLAST overnight. Primary antibodies were washed three times with PBS for 10 min each and then incubated with 1:500 anti-guinea pig AlexaFluor 488 (Jackson Immunoresearch, Burlington, ON) for 45 min. Secondary antibodies were washed out 3 times with PBS and then incubated with DAPI for 15 min at room temperature. Cells were then washed twice with PBS, and Fluoromount-G was applied to each coverglass and

then mounted onto a glass slide for imaging. Images were taken using the Olympus FV1000 confocal microscope at 60x magnification using an oil-immersion objective.

3.3.5 Live Cell Calcium and Sodium Imaging

For conducting calcium and sodium imaging in cultured cerebellar astrocytes, culture media was washed out and replaced with a bath solution containing (in mM): 130 NaCl, 5 KCl, 3 MgCl2, 2 CaCl2, 5 glucose, and 10 4-(2-hydroxyethyl)-1-piperazineethanesulfonic acid (HEPES). Rhod-4AM (AAT Bioquest, Sunnyvale, CA, Catalogue #: 21122) and Sodium Green^{TM} tetraacetate (ThermoFischer Scientific, Waltham, MA, Catalogue #: S6901) were equilibrated to room temperature for 1 hr before incubation with cerebellar astrocyte cultures. Each culture well was incubated with 3 uL of the calcium fluorescence indicator rhod-4AM and 3 μL of the sodium fluorescence indicator Sodium Green tetraacetate(Lo, Leake, & Berry, 2006) under normal cell culture conditions for 1 hr. Both fluorescent indicators were then washed out using bath solution after incubation.

Thirty minutes before fluorescent imaging, astrocyte cultures were pre-treated with the following drug preparations – WT: 50 nM 7N; for nNOS$^{-/-}$: 250 μM SNAP; for both: 10 μM arginyl-lysyl-arginyl-alanyl-arginyl-lysyl-glutamic acid (PKG_i)(Maksoud, Tellios, Xiang, & Lu, 2020), 1 μM 2-Amino-5,6,7,8-tetrahydro-4-(4-methoxyphenyl)-7-(naphthalen-1-yl)-5-oxo-4H-chromene-3-carbonitrile (UCPH-101, selective EAAT1 inhibitor)(Liang et al., 2014), 1 μM SEA 0400 (NCX inhibitor)(Matsuda et al., 2001). Simultaneous Ca^{2+} and Na^{+} imaging was then performed using the EVOS FL Auto 2 system under 20x magnification, with images documented every 10 s. Baseline Ca^{2+} and Na^{+} levels were recorded for at least 3 min before application of 100 μM D-aspartate to stimulate GLAST activity(Balderas et al., 2014). The ratio of calcium to sodium influx was determined in order to adjust for Na^{+} transients associated with the Na^{+}/Ca^{2+} exchanger(Rose, Ziemens, & Verkhratsky, 2020). Cellular Ca^{2+}/Na^{+} responses for each cell were normalized to their respective average baseline level using FIJI open source software and plotted across time using GraphPad Prism 8.

3.3.6 Western Blotting

Cerebella were isolated from WT and nNOS$^{-/-}$ mice and stored at -80 ºC. Cerebellar lysates were obtained by homogenizing the cerebellar tissues using a glass homogenizer in radioimmunoprecipitation assay (RIPA) lysis buffer, supplemented with 0.1% apoprotein and 0.1% leupeptin. Once homogenized, lysates were centrifuged for 30 mins at 4 ºC. The supernatant was collected, and protein was measured using a Bradford reagent mix (Bio-Rad, Hercules, CA). Samples were later prepared using 2x sample buffer and loaded onto 8% or 10% polyacrylamide gels for electrophoresis and run for 2 hrs at 100V. Gels were then wet-transferred onto nitrocellulose membranes for 2 hrs at 80V. Blots were blocked in 5% bovine serum albumin (BSA) for 1 hr before incubated with the following primary antibodies overnight: 1:1000 guinea pig anti-GLAST (62 kDa). For total protein comparisons, 1:10000 anti-glyceraldehyde-3-phosphate dehydrogenase (GAPDH, 40 kDa) (Abcam, Toronto, ON, Catalogue #: ab9482) was used as a housekeeping protein. After 3 washes in tris-buffered saline solution, the appropriate secondary horseradish-peroxidase antibodies (Jackson Immunoresearch, Burlington, ON) were incubated on the membranes for 1.5 hrs. Protein was visualized using enhanced chemiluminescence substrate (Bio-Rad, Hercules, CA) and imaged using the Bio-Rad VersaDoc system. All proteins were normalized to their respective GAPDH levels. Densitometric analyses were quantified using FIJI open source software.

3.3.7 Ex Vivo Organotypic Slice Cultures

Cerebella were isolated from 10-12 postnatal day 0 WT and nNOS$^{-/-}$ pups in Hank's balanced salt solution (HBSS) containing: 15 mM 4-(2-hydroxyehtyl)-1-piperazineethanesulfonic acid (HEPES), 0.5% glucose, 2% sucrose, and maintained at pH 7.3 and 315 mOsm. Isolated cerebella were sliced at a thickness of 350 μm using a tissue chopper and plated on 35 mm membrane inserts (Milipore Ltd., Etobicoke, ON). The bottom half of the insert was exposed to minimum essential medium (MEM) supplemented with 5 mg/ml glucose, 25% heat-inactivated horse serum, 25 mM HEPES, 1 mM glutamine, and 100 U/ml penicillin and streptomycin. Cultures were maintained for 7 days in vitro (DIV7). Half of the medium was refreshed every 2 days. WT slices were treated with 100 μM NOS inhibitor N(G)-Nitro-L-arginine methyl ester (L-NAME) (Santa Cruz

Biotechnology, Dallas, TX), while nNOS$^{-/-}$ slices were treated with slow NO-donor, 300 μM diethylenetriamine NONOate (NOC-18) (Santa Cruz Biotechnology, Dallas, TX). The cultured cerebellar slices were then used for western blotting.

3.3.8 Aspartate Uptake Assay

Primary cerebellar astrocytes were cultured as previous described. To perform the aspartate uptake assay, culture medium was replaced with serum-free culture medium for at least 2 hrs. Drug pre-treatments (for WT: 50nM 7N; for nNOS$^{-/-}$: 250uM SNAP; for both: 10uM PKG$_i$) were applied for 30 min prior to application of 100 μM $_L$-aspartate for another 30 mins. After treatment, cells were lysed and aspartate levels were measured using the Aspartate Assay Kit (Sigma-Aldrich, Darmstedt, Germany, Catalogue #: MAK095) and performed in accordance with the manufacturer's instructions.

3.3.9 Image Analysis

3.3.9.1 BG Lamellar Process Thickness Quantification

BG lamellar process thickness reports the diameter of largest smooth radial processes, visualized using GLAST fluorescent staining, that are visible in the EGL, present in PD3 and PD7 WT and nNOS$^{-/-}$ mice. Briefly, the 10 largest processes were identified per image and measured in micrometers (μm) using the straight line tool on FIJI. BG lamellar process thickness was averaged from multiple images across four biological replicates.

3.3.9.2 Colocalization Analysis

Immunohistochemical images stained with both GLAST and CalB were converted separately into masks using FIJI open source software. Next, the GLAST mask was overlayed onto the CalB mask, and the image was subtracted to reveal the area of GLAST + CalB per 60x image taken. This area of overlap consisting of GLAST + CalB was then normalized to the total area of GLAST staining to obtain a percent area (% area) of GLAST colocalizing to CalB. The resulting % areas were graphed using GraphPad Prism 8.

3.3.9.3 Immunocytochemistry PM/Cytosol Expression Quantification

To determine changes in PM and cytosolic localization of GLAST across a variety of pharmacological treatments, an image analysis protocol as detailed in a previous report (Maksoud, Tellios, An, Xiang, & Lu, 2019) was adapted for cultured BG. Briefly, GLAST fluorescent staining was used to determine the outer borders of each BG in culture. The GLAST stain was then thresholded and converted into a mask using FIJI. Entire cell regions of interest (ROIs) were obtained corresponding to each cell within the imaged culture well, and each ROI was further eroded to create an ROI denoting the BG cytosol(Maksoud et al., 2019). A PM mask for each cell was then made from subtracting the cytosol mask from the entire cell mask. The PM and cytosol mask of each cell was then overlayed onto the GLAST fluorescent image, and the integrated density of each region was measured to determine a PM/cytosol ratio for each cell. The PM/cytosol ratio of GLAST fluorescence for all individual cells per treatment group were averaged and graphed using GraphPad Prism 8.

3.3.10 Statistical Analysis

Statistical analyses were performed using an unpaired, two-tailed t-test for all results comparing WT to $nNOS^{-/-}$ mice. Results obtained from immunocytochemistry PM expression were analyzed using a one-way ANOVA corrected with a Tukey's post hoc test. Significance was determined using a threshold of $p = 0.05$. All values are reported as mean ± standard error of the mean (SEM).

3.4 Results

3.4.1 nNOS Regulates BG Morphology and GLAST Expression in the Cerebella of Mice During Postnatal Development.

GLAST is highly expressed in specialized radial astrocytes and is a biomarker for cerebellar BG. Therefore, we first investigated whether the morphology of BG as well as the expression and localization of GLAST are altered during postnatal development in $nNOS^{-/-}$ cerebella by comparing to age-matched WT mice. Immunohistochemical analysis from WT and $nNOS^{-/-}$ cerebella at PD3 revealed GLAST expression within the IGL and

the EGL. GLAST-expressing BG processes surrounded the cell bodies and sparse dendritic processes of PNs, marked by CalB staining, and BG lamellar processes were easily visible (**Figure 3.1a**). To further examine BG morphology, we analyzed the percent of GLAST coverage to CalB staining between WT and nNOS$^{-/-}$ cerebella. Our analyses revealed more GLAST-PN coverage in WT cerebella compared to nNOS$^{-/-}$ cerebella at PD3 (**Figure 3.1b**). Additionally, nNOS$^{-/-}$ BG displayed thicker lamellar processes when compared to WT BG at PD3 (**Figure 3.1c**). Our western blot analysis for GLAST expression in cerebellar tissues revealed a significant downregulation of GLAST protein expression in nNOS$^{-/-}$ cerebella when compared to WT cerebella at PD3 (**Figures 3.1d**).

At PD7, cerebellar cortex organization was more apparent and PN dendritic processes were more visible. It is important to note that PN dendrites at this developmental time point differ significantly between WT and nNOS$^{-/-}$, as described in prior experiments from our group(Tellios et al., 2020). GLAST staining of BG extended to all layers of the cerebellar cortex in PD7 mice (**Figure 3.2a**). However, the majority of GLAST expression remained close to the cell bodies and dendrites of PNs. Image analyses showed that the percentage of GLAST-CalB overlay was significantly lower in nNOS $^{-/-}$ cerebella compared to WT cerebella at PD7 (**Figure 3.2b**). BG lamellar processes were prominent in both WT and nNOS$^{-/-}$ BG at PD7, however, significantly thicker processes were observed in nNOS$^{-/-}$ BG compared to age matched WT BG (**Figure 3.2c**). Our western blot analysis revealed significantly less GLAST expression in nNOS$^{-/-}$ cerebella compared to WT cerebella at PD7 (**Figure 3.2d**).

At 2W, the structural organization of the cerebellum is similar to the organization of the mature cerebellar cortex – the lamellar processes are functionally dissolved along with the EGL, and the IGL is now referred to as the granular cell layer. Immunohistochemical assays showed that nearly all GLAST expression was localized to the PN layer and the molecular layer, with little to no staining present in the granular cell layer (**Figure 3.3a**). Similar to earlier timepoints, our imaging analyses showed a significant decrease in the percent of GLAST-CalB colocalization in nNOS$^{-/-}$ cerebella compared to WT cerebella at 2W (**Figure 3.3b**). At this time point, total GLAST protein

expression was significantly decreased in nNOS$^{-/-}$ cerebella compared to WT cerebella, evidenced by our western blot analyses (**Figure 3.3c**).

The majority of GLAST expression in 7W mice cerebella was concentrated to the PN layer and the molecular layer, with little to no GLAST immunofluorescence observed in the granular cell layer (**Figure 3.4a**). The percent of GLAST-CalB colocalization was significantly lower in nNOS$^{-/-}$ cerebella compared to age matched WT cerebella (**Figure 3.4b**). Western blotting in nNOS$^{-/-}$ cerebella at 7W revealed a significant decrease in GLAST protein expression when compared to age-matched WT cerebella (**Figure 3.4c**). Together, results from our immunohistochemical and biochemical analyses showed that the absence of nNOS critically regulates BG morphology and decreases GLAST protein expression during postnatal development.

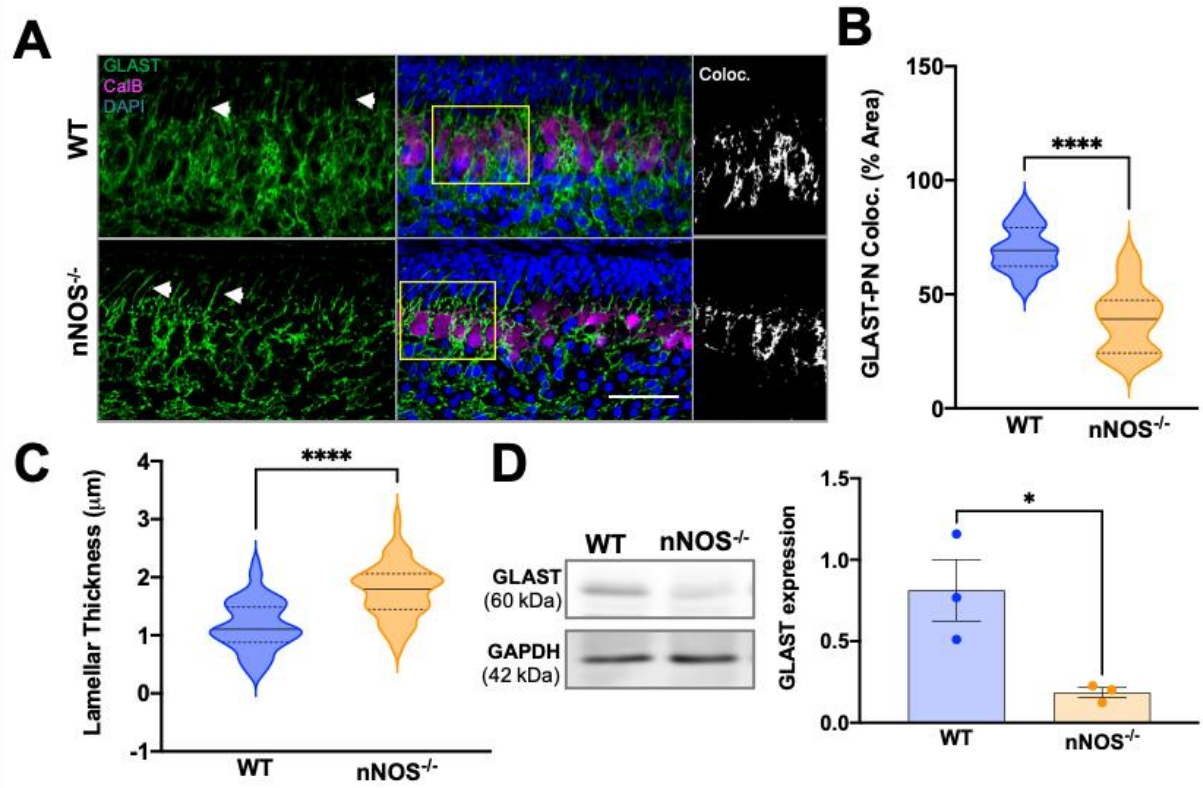

Figure 3.1 BG-PN colocalization and total GLAST expression decreased at PD3 in nNOS$^{-/-}$ cerebella compared to WT.

(**A**) Representative confocal images of WT and nNOS$^{-/-}$ cerebella showing GLAST (green) in BG, CalB (magenta) in PNs, and nuclei stained with DAPI (blue). White arrows point to BG lamellar processes. Scale bar represents 50 µm. Depicted in the third panel are representative images of GLAST-CalB colocalization analysis, with white representing the area of GLAST+CalB overlay. (**B**) Violin plots represent the area of GLAST+CalB overlay in relation to total CalB staining within a consistent ROI size, presented as % Area. N = 4 biological replicates per group; WT n = 20 ROIs, nNOS$^{-/-}$ n = 12 ROIs. P < 0.0001. (**C**) Violin plots represent lamellar process thickness, measured in µm. N = 4 biological replicates per group. WT n = 58 processes, nNOS$^{-/-}$ n = 79 processes. P < 0.0001. (**D**) Representative western blot of total GLAST protein expression for PD3 WT and nNOS$^{-/-}$ cerebella and the housekeeping protein GAPDH. Bar graph reports GLAST expression normalized to GAPDH. N = 3 biological replicates per group. P = 0.0302.

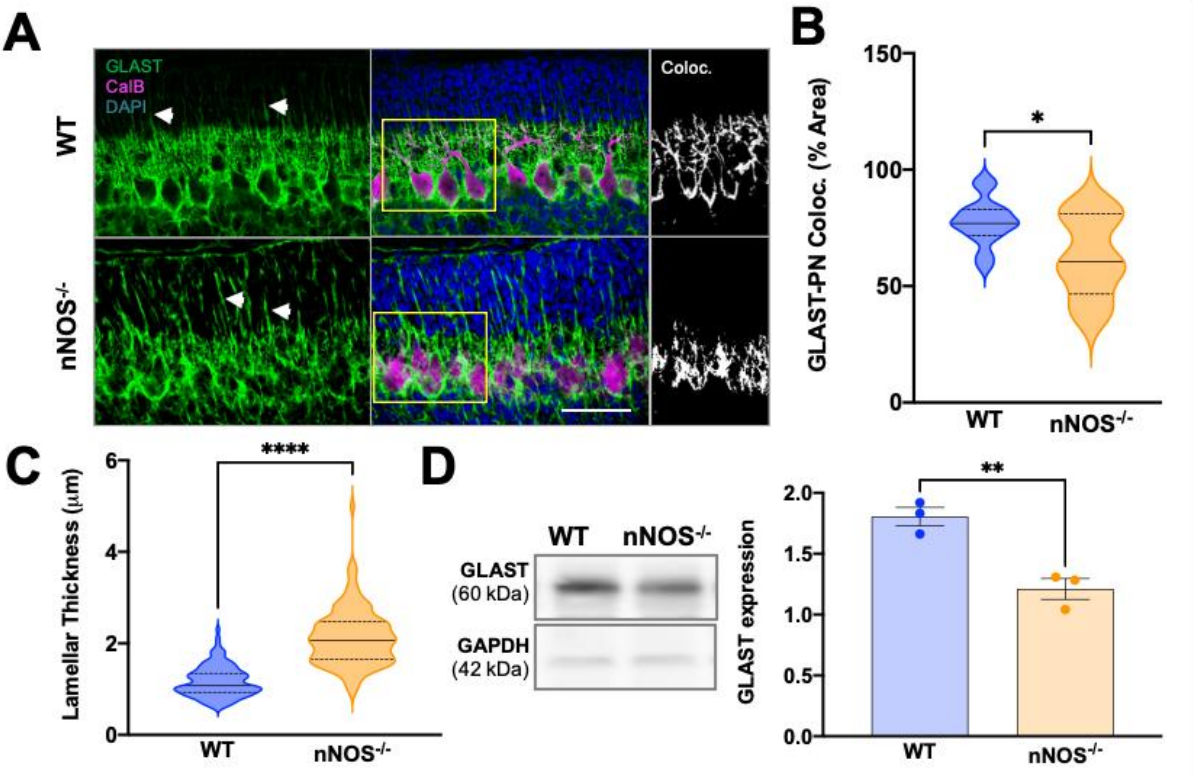

Figure 3.2 BG-PN colocalization and total GLAST expression decreased at PD7 in nNOS$^{-/-}$ cerebella compared to WT.

(**A**) Representative confocal images of WT and nNOS$^{-/-}$ cerebella showing GLAST (green), CalB (magenta), and nuclei stained with DAPI (blue). White arrows highlight BG lamellar processes. Scale bar represents 50 µm. Depicted in the third panel are representative images of GLAST-CalB colocalization analysis with white representing the overlay of GLAST+CalB staining. (**B**) Violin plots represent the area of GLAST+CalB staining in relation to total CalB staining within a consistent ROI, represented as % Area. N = 4 biological replicates per group; WT n = 14 ROIs, nNOS$^{-/-}$ n = 8 ROIs. P = 0.0161. (**C**) Violin plots represent lamellar process thickness, measured in µm. N = 4 biological replicates per group. WT n = 125 processes, nNOS$^{-/-}$ n = 112 processes. P < 0.0001. (**D**) Representative western blot of total GLAST protein expression for PD7 WT and nNOS$^{-/-}$ cerebella and housekeeping protein GAPDH. Bar graph represents GLAST protein expression normalized to GAPDH. N = 3 biological replicates per group. P = 0.0065.

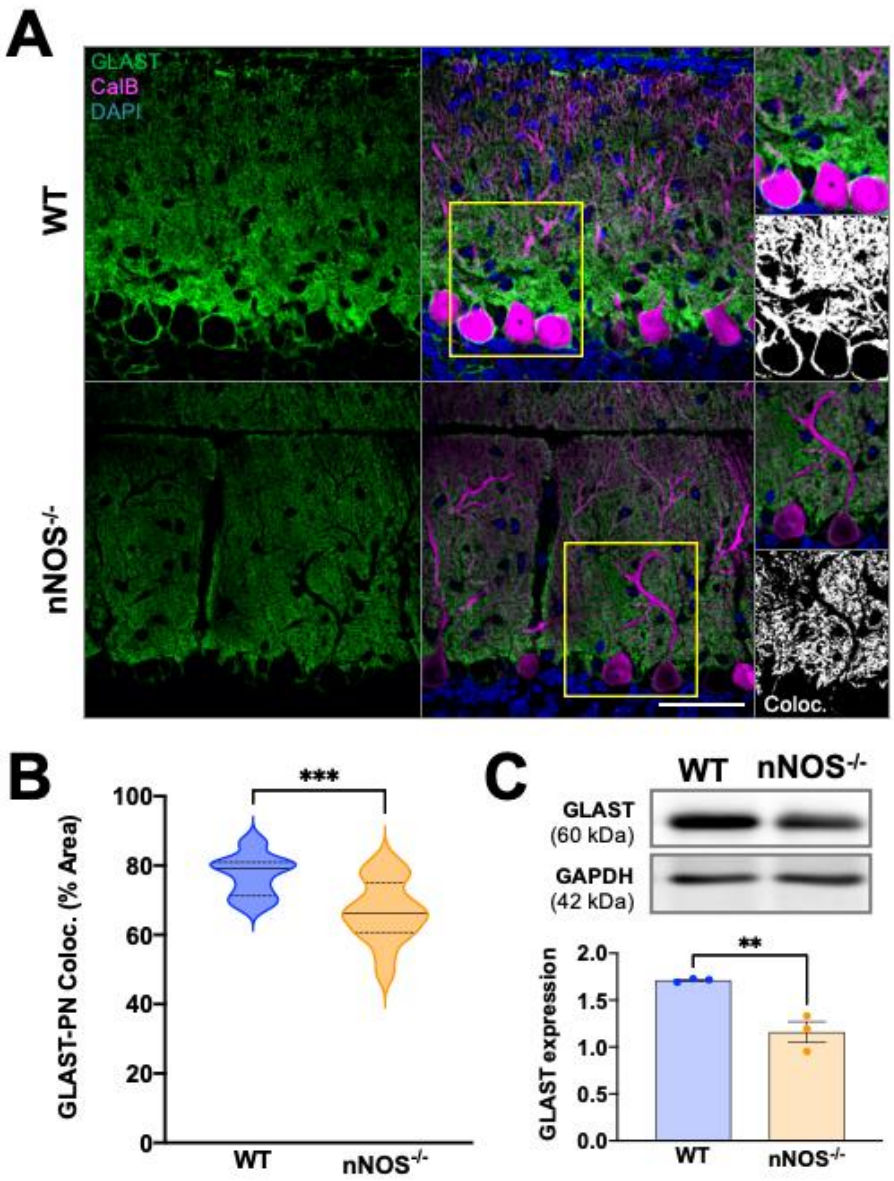

**** Figure legend on next page ****

Figure 3.3 BG-PN colocalization and total GLAST expression is decreased in 2W nNOS$^{-/-}$ cerebella compared to WT.

(**A**) Representative confocal images of GLAST (green) and CalB (magenta) expression in WT and nNOS$^{-/-}$ cerebella with nuclei stained by DAPI (blue). Scale bar represents 50 μm. Representative image of GLAST-CalB colocalization analysis depicted in third panel, with white representing the area of GLAST+CalB overlay. (**B**) Violin plots represent the area of GLAST+CalB overlay in relation to the total area of CalB staining within a consistent ROI, represented as % Area. $N = 4$ biological replicates per group; WT $n = 14$ ROIs, nNOS$^{-/-}$ $n = 16$ ROIs. $P = 0.0009$. (**C**) Representative western blot of total GLAST protein expression in 2W WT and nNOS$^{-/-}$ cerebella and housekeeping protein GAPDH, along with bar graph presenting GLAST expression normalized to GAPDH. $N = 3$ biological replicates per group. $P = 0.0077$.

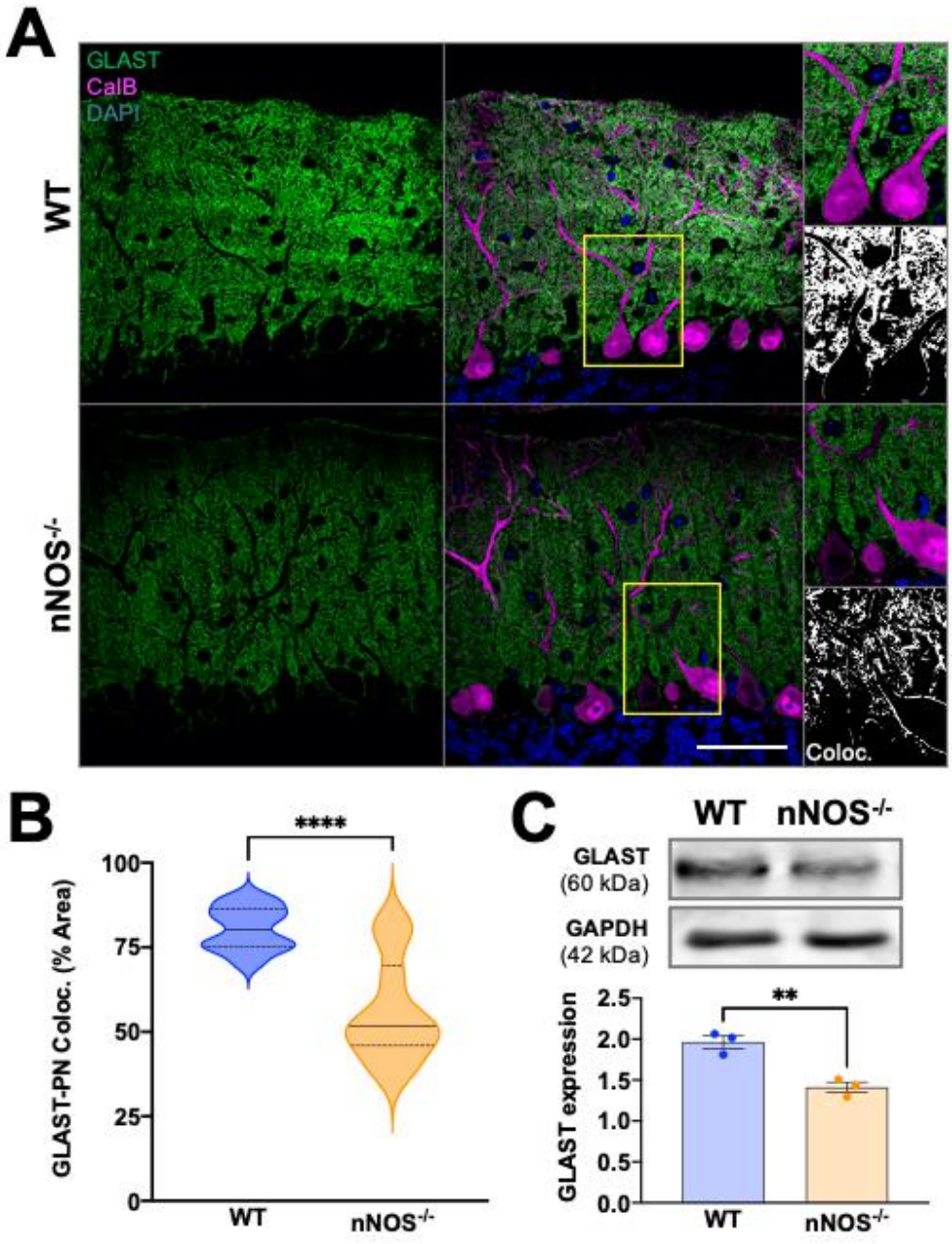

**** Figure legend on next page ****

Figure 3.4 BG-PN colocalization and total GLAST expression is decreased in 7W nNOS$^{-/-}$ cerebella compared to WT.

(**A**) Representative confocal images of WT and nNOS$^{-/-}$ cerebella expressing GLAST (green) and CalB (magenta) with nuclei stained with DAPI (blue). Scale bar represents 50 μm. Representative image of GLAST-CalB colocalization analysis are depicted in the third panel, with white representing common GLAST+CalB overlay. (**B**) Violin plots represent the area of GLAST+CalB overlay in relation to the total area of CalB staining within a consistent ROI, represented as % Area. N = 4 biological replicates per group; WT n = 12 ROIs, nNOS$^{-/-}$ n = 10 ROIs. $P < 0.0001$. (**C**) Representative western blot of total GLAST protein expression for 7W WT and nNOS$^{-/-}$ cerebella and the housekeeping protein GAPDH, along with bar graph representing GLAST expression normalized to GAPDH. N = 3 biological replicates per group. $P = 0.0053$.

3.4.2 NO Upregulates GLAST Expression in Organotypic Cerebellar Slice Cultures and Facilitates L-Aspartate Uptake in Cultured BG.

To determine whether NO regulates the expression level of GLAST in a functional paradigm, we established *ex vivo* organotypic cultures of cerebellar slices from PD0 WT and nNOS$^{-/-}$ mice. After treating the WT or nNOS$^{-/-}$ cerebellar slice cultures for 7 days with pharmacological agents that would either inhibit NO production or increase NO concentration respectively, the expression of GLAST protein was assayed using western blot. Results showed that after treatment with L-NAME, the expression level of GLAST in WT cerebellar slice cultures was significantly decreased compared to control WT slice cultures (**Figure 3.5a**). On the other hand, nNOS$^{-/-}$ slices treated with slow-release NO-donor NOC-18 showed a significant increase in GLAST expression when compared to control nNOS$^{-/-}$ slice cultures (**Figure 3.5b**). These results demonstrated that NO regulates the expression level of GLAST in cerebellar astrocytes.

To examine whether nNOS/NO regulates the function of GLAST in BG, we cultured primary astrocytes and measured L-aspartate uptake between WT and nNOS$^{-/-}$ cultures. Our assay showed that 30 min after treatment with 100 μM L-aspartate, nNOS$^{-/-}$ BG exhibited a significantly lower level of cytosolic L-aspartate compared to WT BG (**Figure 3.5c**).

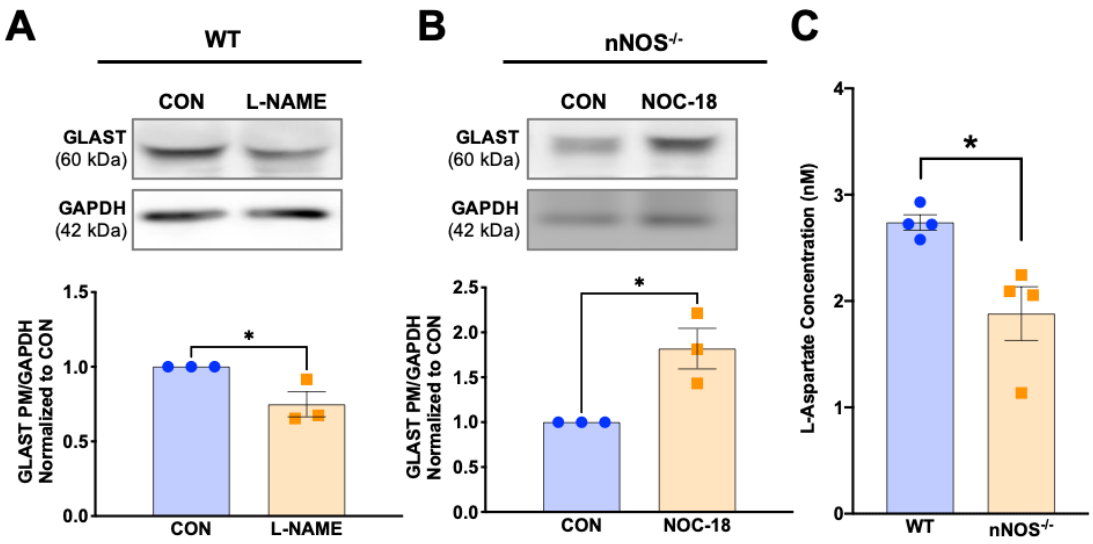

Figure 3.5 Nitric oxide modulates GLAST expression in an ex vivo model, and BG from nNOS$^{-/-}$ mice display deficits in GLAST functionality.

(**A**) Representative western blot of total GLAST expression in WT slices that were left untreated (CON) or treated with 100 µM L-NAME. Bar graph represents N = 3 experimental replicates. P = 0.0403. (**B**) Representative western blot of total GLAST expression in nNOS$^{-/-}$ slices that were left untreated (CON) or treated with 300 µM NOC-18. Bar graph represents N = 3 experimental replicates. P = 0.0222. (**C**) Bar graph represents the concentration of L-aspartate taken up by WT and nNOS$^{-/-}$ astrocyte cultures after 30 mins of L-aspartate treatment. N = 4 experimental replicates. P = 0.0172.

3.4.3 PM GLAST Expression Can Be Modulated by NO Production In Vitro

Considering that NO signals mainly through the classical PKG pathway, we next investigated whether NO-PKG signaling regulates the expression and subcellular localization of GLAST in cultured WT and nNOS$^{-/-}$ BG. Specifically, WT cells were either left untreated (CON), or treated with either 50 nM 7N or with 10 μM PKG$_i$. BG were identified based on their intense staining of GLAST. WT CON BG exhibited GLAST fluorescence that was localized to the PM (**Figure 3.6a**). In contrast, 7N treatment significantly decreased GLAST fluorescence on the PM and increased GLAST internalization when compared to WT CON cells (**Figure 3.6a**). Treatment of PKG$_i$ did not affect PM localization of GLAST when compared to WT CON BG (**Figure 3.6a**). Similarly, western blot assays revealed a significant decrease in GLAST protein expression in 7N treated WT BG when compared to CON WT and PKG$_i$-treated WT BG (**Figure 3.6b**).

nNOS$^{-/-}$ BG were either left untreated (CON) or treated with either 250 μM SNAP or with a combination of SNAP and PKG$_i$ (SNAP+PKG$_i$). The nNOS$^{-/-}$ CON BG had considerably less GLAST fluorescence localized near the PM in comparison to the WT CON cultures. Importantly, SNAP-treated nNOS$^{-/-}$ BG had significantly more GLAST localized on the PM than the CON nNOS$^{-/-}$ BG. Notably, nNOS$^{-/-}$ cells treated with SNAP+PKG$_i$ showed a similar amount of GLAST localization on the PM when compared to CON nNOS$^{-/-}$ BG, but significantly less PM localization of GLAST when compared to SNAP-treated nNOS$^{-/-}$ BG (**Figure 3.7a**). Western blotting of GLAST protein in nNOS$^{-/-}$ BG revealed an increase in GLAST expression within the SNAP-treated BG when compared to CON and SNAP+PKG$_i$-treated nNOS$^{-/-}$ BG (**Figure 3.7b**).

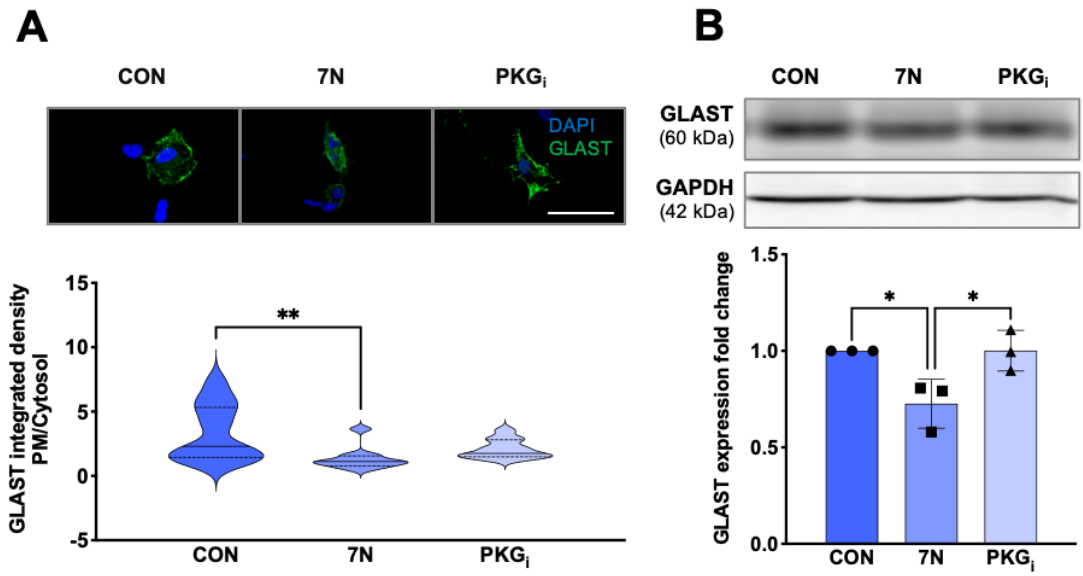

Figure 3.6 PM localization and total expression of GLAST is decreased in WT BG that were treated with a nNOS inhibitor.

(**A**) Representative confocal images of GLAST (green) and nuclear staining DAPI (blue) fluorescence in WT BG that were untreated (CON) or treated with either 50 nM 7N or 10 μM PKG_i. Scale bar represents 50 μm. Violin plots represent the ratio of PM-localized GLAST immunofluorescence to cytosol-localized GLAST immunofluorescence. N = 4 experimental replicates per group; CON n = 18 cells, 7N n = 10 cells, PKG_i n = 11 cells. $F(2, 36) = 5.532$; $P = 0.0080$. (**B**) Representative western blot of GLAST expression in WT astrocyte cultures that were untreated (CON) or treated with 7N or PKG_i. Bar graph represents GLAST expression normalized to the housekeeping protein GAPDH. N = 3 biological replicates per group. $F(2, 6) = 8.282$; $P = 0.0188$.

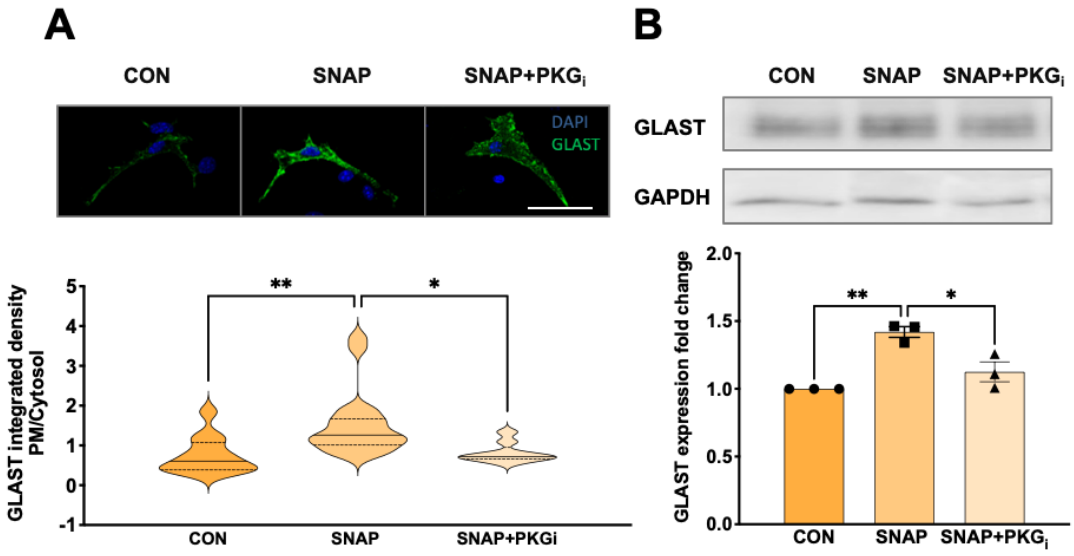

Figure 3.7 PM localization and total expression of GLAST is increased by NO application in nNOS$^{-/-}$ BG.

(**A**) Representative confocal images of GLAST (green) and nuclear staining DAPI (blue) fluorescence in nNOS$^{-/-}$ BG that were left untreated (CON) or treated with either 250 μM SNAP or a combination of SNAP and 10 μM PKG$_i$ (SNAP+PKG$_i$). Scale bar represents 50 μm. Violin plots represent a ratio of PM-localized GLAST immunofluorescence to cytosol-localized GLAST immunofluorescence. N = 4 experimental replicates per group; CON n = 12 cells, SNAP n = 19 cells, SNAP+PKG$_i$ n = 9 cells. $F(2, 37) = 7.022$; $P = 0.0026$. (**B**) Representative western blot of GLAST expression in nNOS$^{-/-}$ astrocyte cultures left untreated (CON) or treated with SNAP or SNAP+PKG$_i$. Bar graph represents GLAST expression normalized to the housekeeping protein GAPDH. N = 3 biological replicates per group. $F(2, 6) = 20.24$; $P = 0.0022$.

3.4.4 NO Influences the D-Aspartate Evoked Ca^{2+}/Na^{+} Dynamics in Cultured WT and $nNOS^{-/-}$ BG.

The function of GLAST is tightly coupled to the sodium-calcium exchanger (NCX) reverse-mode activity(Sergei Kirischuk, Kettenmann, & Verkhratsky, 2007), and thus cytosolic changes in the concentrations of Ca^{2+} and Na^{+} in BGs are indicators of overall NCX-GLAST functionality. We performed live-cell imaging on WT and $nNOS^{-/-}$ cerebellar astrocytes to measure simultaneous changes of Na^{+} and Ca^{2+} fluorescence in response to application of 100 μM D-aspartate, a compound that is known to activate GLAST(Balderas et al., 2014).

WT BG were left untreated (CON) or treated with either 50 nM 7N, 10 μM PKG_i, 1 μM UCPH, or 1 μM NCX_i. Application of D-aspartate to CON WT cells evoked an influx of Ca^{2+} relative to Na^{+} that peaked within the first minute after D-aspartate application, and this ratio of Ca^{2+}/Na^{+} remained elevated for the entire trace (**Figures 3.8a-d**). Notably, application of D-aspartate to WT cells pretreated with 7N significantly decreased the influx of Ca^{2+} relative to Na^{+} when compared to WT CON trace (**Figure 3.8a and e**). Treating WT BG with PKG_i showed a similar Ca^{2+}/Na^{+} response to D-aspartate as the WT CON BG (**Figure 3.8b**), while pretreatment with UCPH (**Figure 3.8c**) or NCX_i (**Figure 3.8d**) significantly decreased the influx of Ca^{2+} relative to Na^{+} when compared to the WT CON trace (**Figure 3.8e**). These results confirm that endogenous nNOS activity in cerebellar BG regulates NCX-coupled GLAST activity.

As well, $nNOS^{-/-}$ BG were left untreated (CON), or were treated with either 250 μM SNAP, a combination of SNAP and PKGi (SNAP+PKG_i), UCPH, or NCX_i. Application of D-aspartate to CON $nNOS^{-/-}$ BG evoked an influx of Ca^{2+} relative to Na^{+} within the first 2 minutes after D-aspartate application, and this ratio of Ca^{2+}/Na^{+} dropped to baseline levels after 2 minutes before slowly increasing for the remainder of the trace (**Figures 3.9a**). Importantly, pre-treatment with SNAP evoked a significantly larger Ca^{2+}/Na^{+} influx in response to D-aspartate when compared to CON $nNOS^{-/-}$ BG (**Figure 3.9a**). As well, pre-treatment of SNAP+PKG_i on $nNOS^{-/-}$ BG evoked a Ca^{2+}/Na^{+} response similar to CON $nNOS^{-/-}$ BG, abolishing the observed effect from SNAP treatment alone (**Figure 3.9b and e**). In response to D-aspartate, both UCPH (**Figure 3.9c**) and NCX_i (**Figure 3.9d**) pre-

treatment showed similar Ca^{2+}/Na^{+} kinetics as CON nNOS$^{-/-}$ BG, which was significantly smaller than nNOS$^{-/-}$ BG in the presence of SNAP (**Figure 3.9e**). These results confirm NO can recover NCX-coupled GLAST activity in nNOS$^{-/-}$ BG.

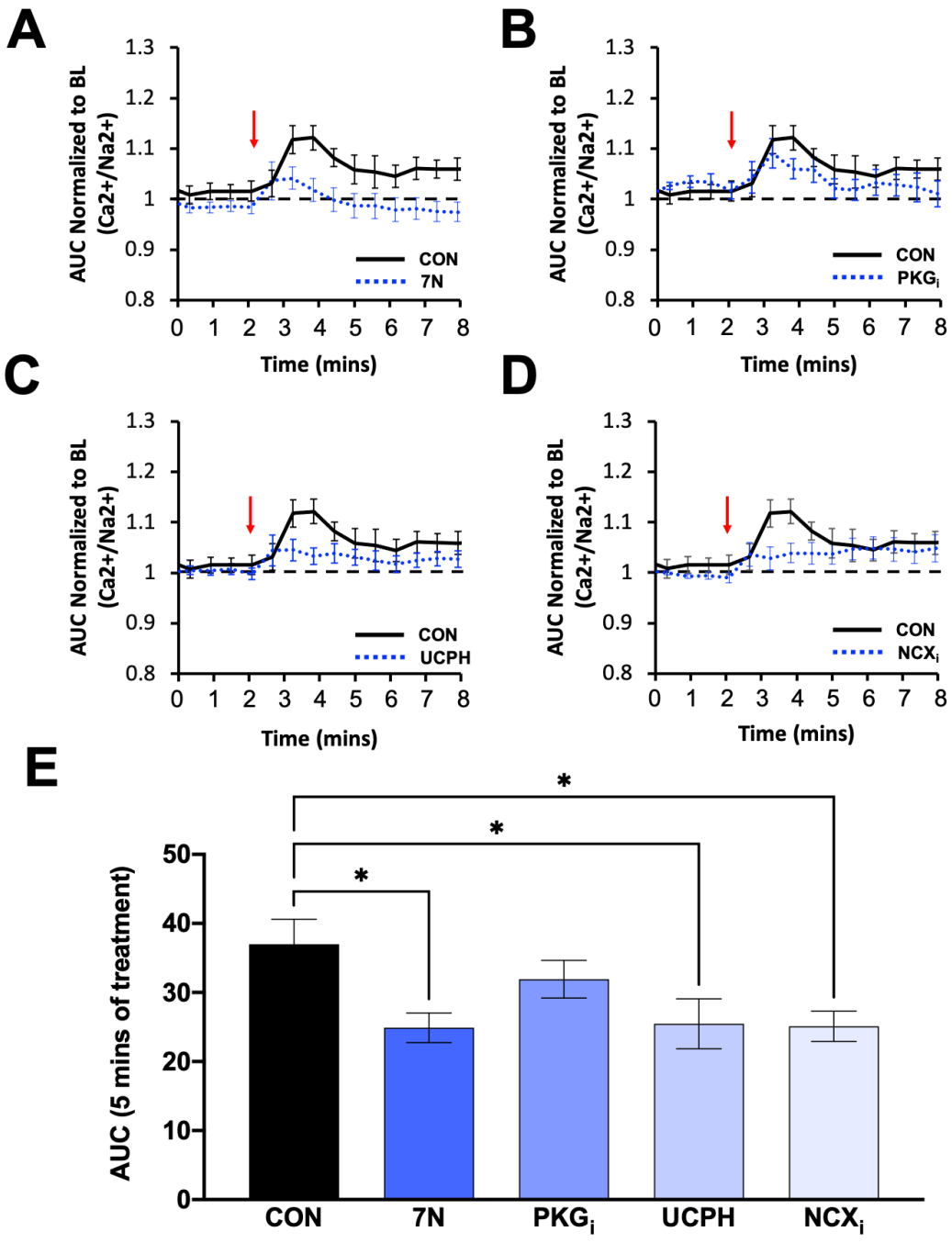

**** Figure legend on next page ****

Figure 3.8 Ca^{2+}/Na^{+} influx is downregulated by nNOS blockade in WT BG.

(**A-D**) Representative time course of Ca^{2+}/Na^{+} influx in response to application of D-aspartate, denoted by the red arrow. The black line represents the Ca^{2+}/Na^{+} influx of WT BGs without a pre-treatment (CON), while the blue line either represents WT BGs pre-treated with 7N (**A**), PKG_i (**B**), UCPH (**C**), or NCX_i (**D**). Black, dashed line represents baseline Ca^{2+}/Na^{+} conductance. (E) Bar graph represents the area under the curve (AUC) for each pre-treatment visualized in A-D after 5 mins of D-aspartate treatment. N = 3 experimental replicates. CON n = 25 cells, 7N n = 24 cells, PKG_i n = 24 cells, UCPH n = 27 cells, NCX_i n = 21 cells. $F(4, 130) = 3.408$; $P = 0.0110$.

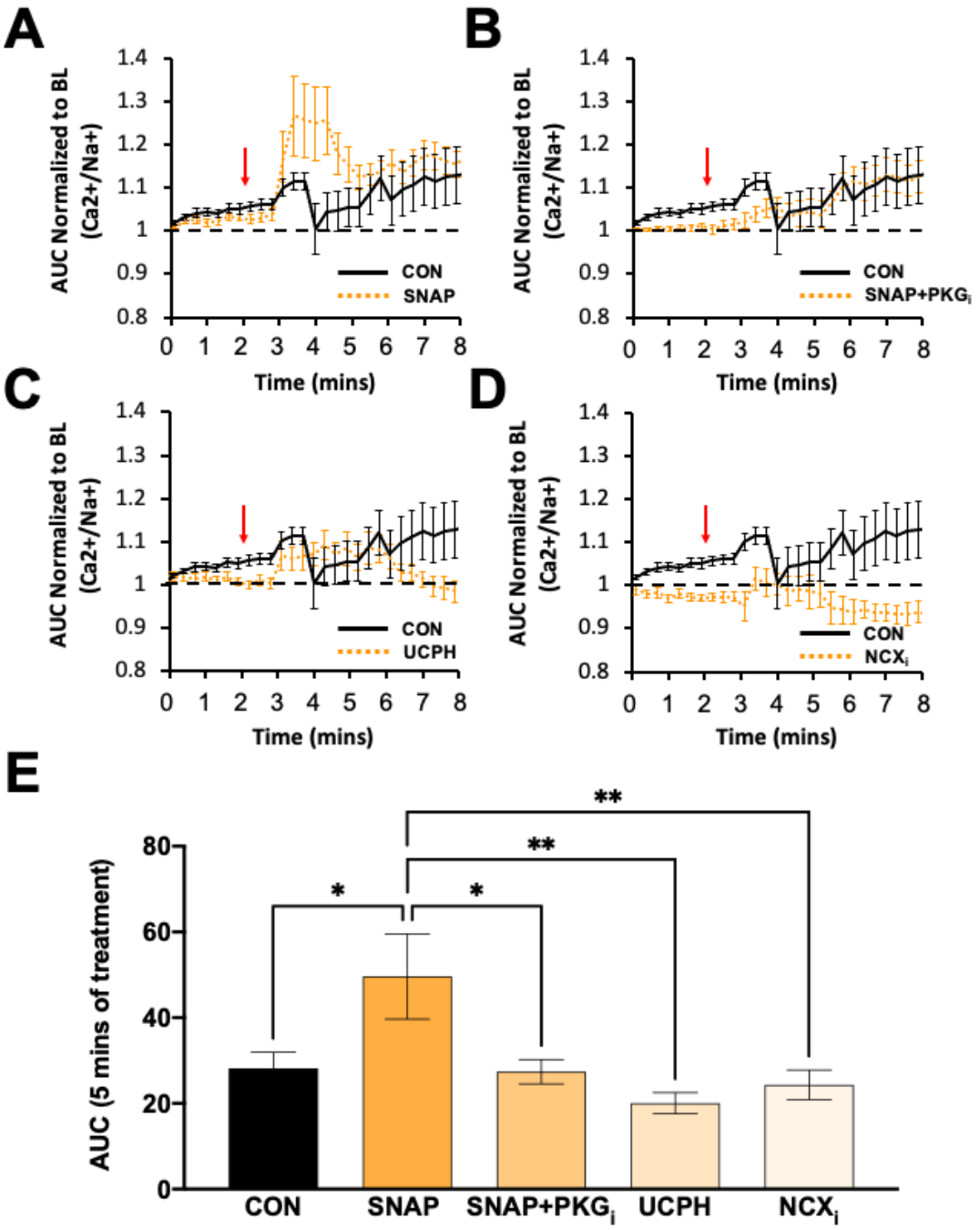

**** Figure legend on next page ****

Figure 3.9 Ca^{2+}/Na^{+} influx is downregulated by NO application in $nNOS^{-/-}$ BG.

(**A-D**) Representative time course of Ca^{2+}/Na^{+} influx in response to application of D-aspartate, denoted by the red arrow. The black line represents the Ca^{2+}/Na^{+} influx of $nNOS^{-/-}$ BGs without a pre-treatment (CON), while the orange line either represents $nNOS^{-/-}$ BGs pre-treated with SNAP (**A**), SNAP+PKG_i (**B**), UCPH (**C**), or NCX_i (**D**). Black, dashed line represents baseline Ca^{2+}/Na^{+} conductance. (E) Bar graph represents the area under the curve (AUC) for each pre-treatment visualized in A-D after 5 mins of D-aspartate treatment. N = 3 experimental replicates. CON n = 23 cells, SNAP n = 20 cells, SNAP+PKG_i n = 26 cells, UCPH n = 25 cells, NCX_i n = 25 cells. $F(4, 130) = 4.723$; $P = 0.0014$.

3.5 Discussion

In the cerebellum, the relatively high concentration of nNOS-derived NO is crucial for the development of PN dendritic arborization and PN calcium homeostasis(Tellios et al., 2020). Although some evidence suggests that NO regulates GLAST function in the cerebellum(Balderas et al., 2014; Tiburcio-Félix et al., 2019), this study is the first to thoroughly characterize the role of nNOS/NO signaling on the regulation of GLAST expression, localization and functionality of cerebellar BGs using WT and nNOS$^{-/-}$ mice. Specifically, this study is the first to report two novel findings. First, BG morphology and GLAST expression across early murine postnatal stages are regulated by nNOS signaling. Second, the PM localization of GLAST is regulated by NO, which facilitates the GLAST coupled to the reverse mode NCX activity to mobilize calcium and sodium ions in BG.

3.5.1 Morphological Abnormalities Are Present in BG of Young nNOS$^{-/-}$ Mice.

It has previously been reported that BG serve as important mediators of both granule cell differentiation and migration from the EGL to the IGL, as well as PN dendritic and synaptic growth from the PN layer to the pial surface(Altman, 1972; Ango et al., 2008; Lordkipanidze & Dunaevsky, 2005; Xu et al., 2013). During early postnatal development (PD0 – PD10), BG morphology transitions from distinct smooth lamellar processes that radiate towards the pial surface, to rough radial processes that contain outgrowths that work to ensheath PN synaptic connections with PFs and stellate cells(Lippman, Lordkipanidze, Buell, Yoon, & Dunaevsky, 2008; Yamada et al., 2000). In the present study, our group discovered abnormally thick lamellar processes in nNOS$^{-/-}$ cerebella during PD3 and PD7 when compared to WT. An earlier study that explored BG morphology in the weaver cerebellar mutant mouse reported a similar BG morphology with abnormally thick lamellar processes, which this group denoted was the cause of PN and granule cell degeneration that presented later in life(Bignami & Dahl, 1974). Similarly, we have found stark PN dendritic deficits in the nNOS$^{-/-}$ mouse, specifically at PD7(Tellios et al., 2020). This finding, when taken into consideration with the BG morphological changes noted in this study, is not surprising as BG lamellar processes work to guide and promote PN dendritic growth towards the pial surface(Lordkipanidze & Dunaevsky, 2005).

BG lamellar processes guide the direction of PN dendritic growth by interacting closely with the tips of dendritic branches. Moreover, BG are able to influence PN dendritic growth and PN firing through a mechanism involving GLAST activity(Miyazaki et al., 2017; Perkins et al., 2018). In the present study, we observed a notable decrease in GLAST colocalization with CalB in nNOS$^{-/-}$ cerebella compared to WT. This finding implies a reduced ensheathment of PN dendritic spines and synapses by BG. As BG lamellar processes mature, radial outgrowths wrap around PN dendritic spines and protect synapses from excitotoxic damage(Lippman et al., 2008; Yamada et al., 2000). We previously showed that in adult nNOS$^{-/-}$ mice, there was an overall decrease in PN spine number compared to WT, and the majority of PN dendritic spines take the form of thin-type spines, as opposed to the predominant mushroom-type spine found on WT PNs(Tellios et al., 2020). Therefore, the PN deficits reported in nNOS$^{-/-}$ mice may be the result of aberrant BG growth, which is supported by multiple studies that report BG-specific deficits lead to the degeneration and loss of PNs(Takatsuru et al., 2006; X. Wang, Imura, Sofroniew, & Fushiki, 2011). Likewise, it is known that nNOS is expressed in supporting cells such as BGs, and not PNs(Ihara et al., 2006; Kugler & Drenckhahn, 1996; Tiburcio-Félix et al., 2019), therefore, it is possible that the structural and functional deficits of PNs in the nNOS$^{-/-}$ mice are at least partially the result of aberrant BG growth.

3.5.2 GLAST Protein Expression is Decreased in the Cerebella of nNOS$^{-/-}$ Mice.

The morphological changes observed in nNOS$^{-/-}$ BG are associated with a decrease in GLAST protein expression in the cerebella of nNOS$^{-/-}$ mice across all time points in this study. Being the predominant transporter on BG, GLAST plays a crucial role in protecting PN synapses from excitotoxic damage. Although it has previously been reported that nNOS expression is upregulated in cultured BG following exposure to glutamate(Tiburcio-Félix et al., 2019) and that nNOS-derived NO signaling enhances glutamate uptake in BG (Balderas et al., 2014), our study is the first to report decreased GLAST expression from a lack of nNOS-derived NO production in vivo. Specifically, our assays revealed a decreased expression of GLAST protein in nNOS$^{-/-}$ cerebella across postnatal time points when compared to WT cerebella. In addition, inhibition of the enzymatic activity of NOS in ex

vivo WT cerebellar slices by LNAME or in cultured WT BG by 7N, significantly reduced GLAST expression. It is known that GLAST is an important modulator of synaptic function in the cerebellum, as it is crucial in regulating glutamate levels within the synaptic cleft. As well, decreased GLAST expression on astrocytes is a major factor that propagates a host of neurological disorders involving excitotoxic damage, including but not limited to, episodic ataxia, Alzheimer's disease, and retinal degeneration(Jen, Wan, Palos, Howard, & Baloh, 2005; Yanagisawa et al., 2020; Zoia et al., 2004). Decreased GLAST expression has been related not only to PN morphological deficits, but deficits in spontaneous PN firing and spike activity(Perkins et al., 2018; Takatsuru et al., 2006). GLAST downregulation can happen for various reasons, including genetic causes such as expression of polynucleotide expansion of ataxin-7 as seen in spinocerebellar ataxia 7(Custer et al., 2006), or as a result of external factors such as high concentrations of extracellular glutamate (Lopez-Bayghen & Ortega, 2004).

Importantly, our study also found that exogenous supplementation of NO significantly increased GLAST expression in ex vivo nNOS /- cerebellar slices and in cultured $nNOS^{-/-}$ BG. This is in line with our previous report that discovered more PN branching in $nNOS^{-/-}$ cerebellar slices treated with NOC-18, (Tellios et al., 2020). As well, a crucial study has noted that decreased GLAST expression may be a result of overactive group 1 mGluRs(Gegelashvili, Dehnes, Danbolt, & Schousboe, 2000). Interestingly, the $nNOS^{-/-}$ mouse itself may be a model of mGluR1 excitotoxicity, as this mouse line exhibits high levels of calcium-dependent protease activity, similar to levels experienced with WT slices treated with group 1 mGluR agonist, DHPG(Tellios et al., 2020).

3.5.3 NO Increases L-Aspartate Uptake and Upregulates GLAST Expression on the PM of BG Through a PKG Mechanism.

To examine the functional activity of GLAST, we examined L-aspartate uptake in cultured WT and $nNOS^{-/-}$ BG. Our study noted lower cytosolic concentrations of L-aspartate in $nNOS^{-/-}$ BGs compared to WT BG, which is associated with the lower level of GLAST protein expression that was observed in $nNOS^{-/-}$ BG when compared to WT BG. Importantly, Balderas et al., noted higher levels of D-aspartate uptake in cerebellar BG treated with NO-donor sodium nitroprusside as well as with treatment of cGMP analogue,

dbcGMP(Balderas et al., 2014). This study by Balderas et al., highlighted the importance of the NO-cGMP-PKG pathway in upregulating GLAST activity in vitro.

We further examined if GLAST localization in cultured WT and nNOS$^{-/-}$ BG was regulated by NO-PKG signaling. Notably, our assays detected a decrease in GLAST fluorescence on the PM of WT BG that were treated with nNOS inhibitor when compared to control WT BG. Importantly, treatment with PKG_i on WT BG did not elicit any significant changes in GLAST localization when compared to control WT BG. Although, many studies have reported that the activation of PKG results in an upregulation of GLAST expression and functionality in WT BGs(Balderas et al., 2014; Cabrera-Pastor, Arenas, Taoro-Gonzalez, Montoliu, & Felipo, 2019), our results demonstrated that inhibition of PKG activity does not result in the internalization of GLAST, which must be regulated by an alternative mechanism.

Alternatively, NO-donor increased GLAST fluorescence at the PM in nNOS$^{-/-}$ BGs when compared to control nNOS$^{-/-}$ BG. Indeed, inhibiting PKG activity abolished the increased PM localization of GLAST observed from NO-donor treatment. In this case, it is apparent that NO signals through PKG to facilitate GLAST trafficking to the PM. All these available data indicate that, NO facilitates GLAST localization to the PM of BGs via activation of the PKG pathway.

3.5.4 NO Regulates the Function of GLAST Coupled to NCX Activity in the Reverse Mode.

GLAST is a cotransporter utilizing the concentration gradient of Na^+ to bring glutamate into the cell. Importantly, GLAST activity is balanced by NCX activity, which transports 3 Na^+ in the opposite direction of 1 Ca^{2+}(Bauer et al., 2012). In resting astrocytes, 3 Na^+ are shuttled into the cell while 1 Ca^{2+} is transported to the extracellular space by NCX activity in the forward mode. However, when GLAST is activated in the presence of glutamate, L-aspartate, or D-aspartate, the NCX functions in the reverse mode to combat the sudden Na^+ influx from GLAST by ejecting Na^+ to the extracellular space and mobilizing Ca^{2+} into the cell(S Kirischuk, Ketfenmann, & Verkhratsky, 2007; Rojas et al., 2007). Considering this coupling action of GLAST and NCX, we utilized dual calcium and

sodium fluorescent imaging to examine ion mobilization from NCX in response to D-aspartate activation of GLAST in cultures of WT and nNOS$^{-/-}$ BG.

Our assays revealed that control WT traces resulted in peak Ca^{2+} entry and Na^{+} efflux within the first minute after application of D-aspartate, which was followed by a smaller, sustained increase in Ca^{2+}/Na^{+} influx above baseline. Application of either UCPH or NCX_i eliminated the peak influx of Ca^{2+}/Na^{+} in response to D-aspartate and confirmed previous reports suspecting glutamate transporters such as GLAST are coupled to NCX activity, which may be required for GLAST activity in BG(Ibáñez, Bartolomé-Martín, Piniella, Giménez, & Zafra, 2019; S Kirischuk et al., 1997; Piccirillo et al., 2020).

Notably, inhibiting endogenous nNOS activity in WT BG resulted in a significant decrease in the Ca^{2+}/Na^{+} ratio when compared to control WT BG, while supplementing NO to the nNOS$^{-/-}$ BG significantly elevated the Ca^{2+}/Na^{+} influx when compared to control nNOS$^{-/-}$ BG, confirming that NO critically controls the coupled activity of GLAST and NCX. Interestingly, treating WT BG with PKGi did not affect the Ca^{2+}/Na^{+} ratio in response D-aspartate when compared to WT controls, while treating nNOS$^{-/-}$ BG with PKG_i¬ significantly abolished the Ca^{2+}/Na^{+} ratio observed from nNOS$^{-/-}$ BG that had NO supplemented in their culture conditions. These trends noted from live cell imaging of calcium and sodium fluorescence in response to D-aspartate are substantiated by the fluorescent localization of GLAST protein on the PM in WT and nNOS$^{-/-}$BG cultures. PKG inhibition on WT BG displayed no change in either PM localization of GLAST or Ca^{2+}/Na^{+} ratio when compared to WT control BG while PKG inhibition on nNOS$^{-/-}$ BG that had NO supplemented in their culture conditions displayed both reduced PM localization of GLAST as well as reduced Ca^{2+}/Na^{+} ratio when compared to nNOS$^{-/-}$ BG that had NO supplemented in their culture conditions. These data further demonstrate that NO signaling regulates the function of GLAST coupled to NCX activity in the reverse mode, possibly through GLAST trafficking to the PM in a PKG dependent mechanism. Further analysis of the coupling between GLAST and the NCX in relation to NO signaling would provide insight into novel therapeutic options for glutamate transporter dysfunction.

In general, Ca^{2+} influx is critical for BG to maintain appropriate physiological growth and functionality. Specialized Ca^{2+}-permeable AMPA receptors are found on BG and are stimulated by glutamate but not by L- or D-aspartate (Lopez-Bayghen & Ortega, 2004; Metea & Newman, 2006). A previous study noted that viral delivery of the GluR2 gene into BG caused their Ca^{2+}-permeable AMPA receptors to become Ca^{2+}-impermeable, which resulted in retraction of BG processes and less PN ensheathment(Iino et al., 2001), similar to what we observed in $nNOS^{-/-}$ BG. Furthermore, overexpression of Ca^{2+}-permeable receptors on BG resulted in BG process growth and extension(Ishiuchi et al., 2007). Therefore, the reduced Ca^{2+} influx and aberrant phenotype that we noted in $nNOS^{-/-}$ BG aligns well with previous findings that reports Ca^{2+} signaling is important for the function and activity of BG.

In summary, results from this study demonstrate a novel role for nNOS-derived NO signaling in regulating BG morphological development, GLAST expression, and GLAST functionality. As depicted in **Figure 3.10**, we propose that under physiological conditions, BG express GLAST to remove excessive glutamate that is released from PFs. During this process, NO derived from nNOS located in PFs and BG leads to an upregulation of GLAST expression and functionality through NO-cGMP-PKG pathway. As well, NO influences the activity of GLAST coupled to the NCX channel working in the reverse mode to shuttle calcium into BG, which is a common indicator of GLAST function(Nashida et al., 2011). Under the regulation of NO, BG ensheath PN synapses whereby expression of GLAST can remove excessive glutamate from the synaptic cleft to combat excitotoxicity on PN during development. However, a lack of nNOS-derived NO, results in less BG ensheathment of PNs, less GLAST expression, less glutamate uptake, and more mGluR1 stimulation on PNs that leads to excitotoxicity during development(Tellios et al., 2020). Further analysis of the coupling between GLAST and the NCX in relation to NO would provide insight into novel therapeutic options for glutamate transporter dysfunction.

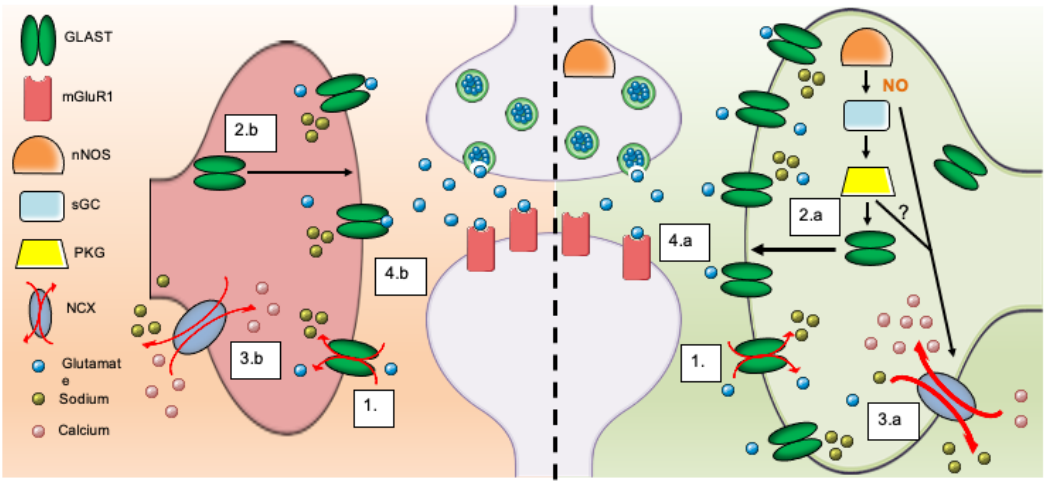

Figure 3.10 Schematic representation of GLAST regulation in relation to nNOS/NO signaling.

The left side of the figure depicts a glutamatergic PN synapse in the absence of nNOS-derived NO signaling, while the right side depicts a physiological glutamatergic synapse with nNOS expression and NO production. (**1.**) Glutamate released by PFs/CFs are taken up by GLAST and co-transported with 3 Na^+ ions into the BG cytosol. *Right side:* (**2.a**) NO produced by PF terminals and BG will activate PKG through the common NO-cGMP-PKG pathway, causing transport of GLAST to the BG PM. (**3.a**) Additionally, the increased Na^+ influx through GLAST activity, along with the presence of NO, causes a reversal of the NCX, allowing for Na^+ to be shuttled outside of the BG and causing an influx of Ca^{2+} into the BG. (**4.a**) As a result, appropriate glutamate clearance from the synaptic cleft occurs, contributing to the normal function of PNs in the cerebellum. *Left side:* (**2.b**) In the absence of nNOS/NO signaling, there is less activation of PKG and therefore less transport of GLAST to the BG PM. (**3.b**) Additionally, the lack of NO and lower Na^+ from active GLAST transporters results in lower activity of the NCX in reverse mode, leading to less Ca^{2+} influx into the BG cytosol, which can cause BG process retraction and less BG ensheathment of the synaptic cleft. (**4.b**) As a result, the lower efficiency of glutamate uptake will lead to an overload of glutamate in the synaptic cleft, leading to PN excitotoxicity.

3.6 Acknowledgements

This work was supported by the Canadian Institutes of Health Research (MOP-133504) awarded to W-Y L. VT, and MJEM were awarded Ontario Graduate Scholarships.

3.7 References

Altman, J. (1972). Postnatal Development of the Cerebellar Cortex in the Rat I. *The Journal of Comparative Neurology*, *145*(3), 353–398.

Ango, F., Wu, C., Van Der Want, J. J., Wu, P., Schachner, M., & Huang, Z. J. (2008). Bergmann glia and the recognition molecule CHL1 organize GABAergic axons and direct innervation of Purkinje cell dendrites. *PLoS Biology*, *6*(4), 739–756. https://doi.org/10.1371/journal.pbio.0060103

Balderas, A., Guillem, A. M., Martínez-Lozada, Z., Hernández-Kelly, L. C., Aguilera, J., & Ortega, A. (2014). GLAST/EAAT1 regulation in cultured Bergmann glia cells: Role of the NO/cGMP signaling pathway. *Neurochemistry International*, *73*(1), 139–145. https://doi.org/10.1016/j.neuint.2013.10.011

Bauer, D. E., Jackson, J. G., Genda, E. N., Montoya, M. M., Yudkoff, M., & Robinson, M. B. (2012). The glutamate transporter, GLAST, participates in a macromolecular complex that supports glutamate metabolism. *Neurochemistry International*, *61*(4), 566–574. https://doi.org/10.1016/j.neuint.2012.01.013

Bignami, A., & Dahl, D. (1974). The development of bergmann glia in mutant mice with cerebellar malformations: Reeler, staggerer and weaver. Immunofluorescence study with antibodies to the glial fibrillary acidic protein. *The Journal of Comparative Neurology*, *155*(2), 219–229. https://doi.org/10.1002/cne.901550207

Bredt, D. S., Hwang, P. M., & Snyder, S. H. (1990). Localization of nitric oxide synthase indicating a neural role for nitric oxide. *Nature*, *347*(6295), 768–770.

https://doi.org/10.1038/347768a0

Cabrera-Pastor, A., Arenas, Y. M., Taoro-Gonzalez, L., Montoliu, C., & Felipo, V. (2019). Chronic hyperammonemia alters extracellular glutamate, glutamine and GABA and membrane expression of their transporters in rat cerebellum. Modulation by extracellular cGMP. *Neuropharmacology*, *161*, 107496. https://doi.org/10.1016/j.neuropharm.2019.01.011

Campese, V. M., Sindhu, R. K., Ye, S., Bai, Y., Vaziri, N. D., & Jabbari, B. (2006). Regional expression of NO synthase , NAD (P) H oxidase and superoxide dismutase in the rat brain. *Brain Research*, *1134*, 27–32. https://doi.org/10.1016/j.brainres.2006.11.067

Contestabile, A. (2012). Role of nitric oxide in cerebellar development and function: Focus on granule neurons. *Cerebellum*, *11*(1), 50–61. https://doi.org/10.1007/s12311-010-0234-1

Custer, S. K., Garden, G. A., Gill, N., Rueb, U., Libby, R. T., Schultz, C., … La Spada, A. R. (2006). Bergmann glia expression of polyglutamine-expanded ataxin-7 produces neurodegeneration by impairing glutamate transport. *Nature Neuroscience*, *9*(10), 1302–1311. https://doi.org/10.1038/nn1750

Daniel, H., Levenes, C., & Crépel, F. (1998). Cellular mechanisms of cerebellar LTD. *Trends in Neurosciences*, *21*(9), 401–407. https://doi.org/10.1016/S0166-2236(98)01304-6

Gegelashvili, G., Dehnes, Y., Danbolt, N. C., & Schousboe, A. (2000). The high-affinity glutamate transporters GLT1, GLAST, and EAAT4 are regulated via different signalling mechanisms. *Neurochemistry International*, *37*(2–3), 163–170.

https://doi.org/10.1016/S0197-0186(00)00019-X

Huang, P. L., Dawson, T. M., Bredt, D. S., Snyder, S. H., & Fishman, M. C. (1993). Targeted disruption of the neuronal nitric oxide synthase gene. *Cell*, *75*(7), 1273–1286. https://doi.org/10.1016/0092-8674(93)90615-w

Ibáñez, I., Bartolomé-Martín, D., Piniella, D., Giménez, C., & Zafra, F. (2019). Activity dependent internalization of the glutamate transporter GLT-1 requires calcium entry through the NCX sodium/calcium exchanger. *Neurochemistry International*, *123*, 125–132. https://doi.org/10.1016/j.neuint.2018.03.012

Ihara, H., Kuwamura, M., Atsuta, M., Nihonmatsu, I., Okada, T., Mukamoto, M., & Kozaki, S. (2006). Expression of neuronal nitric oxide synthase variant, nNOS-μ, in rat brain. *Nitric Oxide - Biology and Chemistry*, *15*(1), 13–19. https://doi.org/10.1016/j.niox.2005.11.011

Iino, M., Goto, K., Kakegawa, W., Okado, H., Sudo, M., Ishiuchi, S., … Ozawa, S. (2001). Glia-synapse interaction through Ca^{2+}-permeable AMPA receptors in Bergmann glia. *Science*, *292*(5518), 926–929. https://doi.org/10.1126/science.1058827

Ishiuchi, S., Yoshida, Y., Sugawara, K., Aihara, M., Ohtani, T., Watanabe, T., … Ozawa, S. (2007). Ca^{2+}-permeable AMPA receptors regulate growth of human glioblastoma via Akt activation. *Journal of Neuroscience*, *27*(30), 7987–8001. https://doi.org/10.1523/JNEUROSCI.2180-07.2007

Jen, J. C., Wan, J., Palos, T. P., Howard, B. D., & Baloh, R. W. (2005). Mutation in the glutamate transporter EAAT1 causes episodic ataxia, hemiplegia, and seizures. *Neurology*, *65*(4), 529–534. https://doi.org/10.1212/01.WNL.0000172638.58172.5a

Kirischuk, S, Kettenmann, H., & Verkhratsky, A. (1997). Na^{+}/Ca^{2+} exchanger modulates

kainate-triggered Ca $^{2+}$ signaling in Bergmann glial cells in situ. *The FASEB Journal*, *11*(7), 566–572. https://doi.org/10.1096/fasebj.11.7.9212080

Kirischuk, Sergei, Kettenmann, H., & Verkhratsky, A. (2007). Membrane currents and cytoplasmic sodium transients generated by glutamate transport in Bergmann glial cells. *Pflugers Archiv : European Journal of Physiology*, *454*(2), 245–252. https://doi.org/10.1007/s00424-007-0207-5

Koziol, L. F., Budding, D. E., & Chidekel, D. (2012). From Movement to Thought: Executive Function, Embodied Cognition, and the Cerebellum. *The Cerebellum*, *11*(2), 505–525. https://doi.org/10.1007/s12311-011-0321-y

Kriegsfeld, L. J., Eliasson, M. J., Demas, G. E., Blackshaw, S., Dawson, T. M., Nelson, R. J., & Snyder, S. H. (1999). Nocturnal motor coordination deficits in neuronal nitric oxide synthase knock-out mice. *Neuroscience*, *89*(2), 311–315. https://doi.org/S0306-4522(98)00614-9 [pii]

Kugler, P., & Drenckhahn, D. (1996). Astrocytes and Bergmann glia as an important site of nitric oxide synthase I. *Glia*, *16*(2), 165–173. https://doi.org/10.1002/(SICI)1098-1136(199602)16:2<165::AID-GLIA8>3.0.CO;2-2

Lehre, K. P., & Danbolt, N. C. (1998). The Number of Glutamate Transporter Subtype Molecules at Glutamatergic Synapses: Chemical and Stereological Quantification in Young Adult Rat Brain. *The Journal of Neuroscience*, *18*(21), 8751–8757. https://doi.org/10.1523/JNEUROSCI.18-21-08751.1998

Liang, J., Chao, D., Sandhu, H. K., Yu, Y., Zhang, L., Balboni, G., … Xia, Y. (2014). δ-Opioid receptors up-regulate excitatory amino acid transporters in mouse astrocytes. *British Journal of Pharmacology*, *171*(23), 5417–5430.

https://doi.org/10.1111/bph.12857

Lippman, J. J., Lordkipanidze, T., Buell, M. E., Yoon, S. O., & Dunaevsky, A. (2008). Morphogenesis and regulation of Bergmann glial processes during Purkinje cell dendritic spine ensheathment and synaptogenesis. *GLIA*, *56*(13), 1463–1477. https://doi.org/10.1002/glia.20712

Lo, C. J., Leake, M. C., & Berry, R. M. (2006). Fluorescence measurement of intracellular sodium concentration in single Escherichia coli cells. *Biophysical Journal*, *90*(1), 357–365. https://doi.org/10.1529/biophysj.105.071332

Lopez-Bayghen, E., & Ortega, A. (2004). Glutamate-dependent transcriptional regulation of GLAST: role of PKC. *Journal of Neurochemistry*, *91*(1), 200–209. https://doi.org/10.1111/j.1471-4159.2004.02706.x

Lordkipanidze, T., & Dunaevsky, A. (2005). Purkinje cell dendrites grow in alignment with Bergmann glia. *Glia*, *51*(3), 229–234. https://doi.org/10.1002/glia.20200

Maksoud, M. J. E., Tellios, V., An, D., Xiang, Y.-Y., & Lu, W.-Y. (2019). Nitric oxide upregulates microglia phagocytosis and increases transient receptor potential vanilloid type 2 channel expression on the PM. *GLIA*, *67*(12). https://doi.org/10.1002/glia.23685

Maksoud, M. J. E., Tellios, V., Xiang, Y.-Y., & Lu, W.-Y. (2020). Nitric oxide signaling inhibits microglia proliferation by activation of protein kinase-G. *Nitric Oxide - Biology and Chemistry*, *94*. https://doi.org/10.1016/j.niox.2019.11.005

Manto, M., Bower, J. M., Conforto, A. B., Delgado-García, J. M., da Guarda, S. N. F., Gerwig, M., … Timmann, D. (2012). Consensus Paper: Roles of the Cerebellum in Motor Control—The Diversity of Ideas on Cerebellar Involvement in Movement. *The*

Cerebellum, *11*(2), 457–487. https://doi.org/10.1007/s12311-011-0331-9

Martínez-Lozada, Z., Hernández-Kelly, L. C., Aguilera, J., López-Bayghen, E., & Ortega, A. (2011). Signaling through EAAT-1/GLAST in cultured Bergmann glia cells. *Neurochemistry International*, *59*(6), 871–879. https://doi.org/10.1016/j.neuint.2011.07.015

Matsuda, T., Arakawa, N., Takuma, K., Kishida, Y., Kawasaki, Y., Sakaue, M., … Baba, A. (2001). SEA0400, a novel and selective inhibitor of the Na^+-Ca^{2+} exchanger, attenuates reperfusion injury in the in vitro and in vivo cerebral ischemic models. *The Journal of Pharmacology and Experimental Therapeutics*, *298*(1), 249–256. Retrieved from http://www.ncbi.nlm.nih.gov/pubmed/11408549

Matyash, V., Filippov, V., Mohrhagen, K., & Kettenmann, H. (2001). Nitric oxide signals parallel fiber activity to Bergmann glial cells in the mouse cerebellar slice. *Molecular and Cellular Neuroscience*, *18*(6), 664–670. https://doi.org/10.1006/mcne.2001.1047

Metea, M. R., & Newman, E. A. (2006). Calcium signaling in specialized glial cells. *Glia*, *54*(7), 650–655. https://doi.org/10.1002/glia.20352

Miyazaki, T., Yamasaki, M., Hashimoto, K., Kohda, K., Yuzaki, M., Shimamoto, K., … Watanabe, M. (2017). Glutamate transporter GLAST controls synaptic wrapping by Bergmann glia and ensures proper wiring of Purkinje cells. *Proceedings of the National Academy of Sciences of the United States of America*, *114*(28), 7438–7443. https://doi.org/10.1073/pnas.1617330114

Nashida, T., Takuma, K., Fukuda, S., Kawasaki, T., Takahashi, T., Baba, A., … Matsuda, T. (2011). The specific Na^+/Ca^{2+} exchange inhibitor SEA0400 prevents nitric oxide-induced cytotoxicity in SH-SY5Y cells. *Neurochemistry International*, *59*(1), 51–58.

https://doi.org/10.1016/j.neuint.2011.03.026

Nelson, R., Demas, G., Huang, P., Fishman, M., Dawson, V., Dawson, T., & Snyder, S. (1995). Behavioural abnormalities in male mice lacking neuronal nitric oxide synthase. *Nature*, *378*(6555), 383–386. https://doi.org/10.1038/378383a0

Perego, C., Vanoni, C., Bossi, M., Massari, S., Basudev, H., Longhi, R., & Pietrini, G. (2000). The GLT-1 and GLAST glutamate transporters are expressed on morphologically distinct astrocytes and regulated by neuronal activity in primary hippocampal cocultures. *Journal of Neurochemistry*, *75*(3), 1076–1084. https://doi.org/10.1046/j.1471-4159.2000.0751076.x

Perkins, E. M., Clarkson, Y. L., Suminaite, D., Lyndon, A. R., Tanaka, K., Rothstein, J. D., … Jackson, M. (2018). Loss of cerebellar glutamate transporters EAAT4 and GLAST differentially affects the spontaneous firing pattern and survival of Purkinje cells. *Human Molecular Genetics*, *27*(15), 2614–2627. https://doi.org/10.1093/hmg/ddy169

Piccirillo, S., Magi, S., Castaldo, P., Preziuso, A., Lariccia, V., & Amoroso, S. (2020). NCX and EAAT transporters in ischemia: At the crossroad between glutamate metabolism and cell survival. *Cell Calcium*, *86*, 102160. https://doi.org/10.1016/j.ceca.2020.102160

Rojas, H., Colina, C., Ramos, M., Benaim, G., Jaffe, E. H., Caputo, C., & DiPolo, R. (2007). Na^+ entry via glutamate transporter activates the reverse Na^+/Ca^{2+} exchange and triggers Cai^{2+} -induced Ca^{2+} release in rat cerebellar Type-1 astrocytes. *Journal of Neurochemistry*, *100*(5), 1188–1202. https://doi.org/10.1111/j.1471-4159.2006.04303.x

Rose, C. R., Ziemens, D., & Verkhratsky, A. (2020). On the special role of NCX in astrocytes: Translating Na^+-transients into intracellular Ca^{2+} signals. *Cell Calcium*, *86*, 102154. https://doi.org/10.1016/j.ceca.2019.102154

Takatsuru, Y., Takayasu, Y., Iino, M., Nikkuni, O., Ueda, Y., Tanaka, K., & Ozawa, S. (2006). Roles of glial glutamate transporters in shaping EPSCs at the climbing fiber-Purkinje cell synapses. *Neuroscience Research*, *54*(2), 140–148. https://doi.org/10.1016/j.neures.2005.11.002

Tellios, V., Maksoud, M. J. E., Xiang, Y. Y., & Lu, W. Y. (2020). Nitric Oxide Critically Regulates Purkinje Neuron Dendritic Development Through a Metabotropic Glutamate Receptor Type 1–Mediated Mechanism. *Cerebellum*, *19*(4), 510–526. https://doi.org/10.1007/s12311-020-01125-7

Tiburcio-Félix, R., Cisneros, B., Hernández-Kelly, L. C. R., Hernández-Contreras, M. A., Luna-Herrera, J., Rea-Hernández, I., … Ortega, A. (2019). Neuronal Nitric Oxide Synthase in Cultured Cerebellar Bergmann Glia: Glutamate-Dependent Regulation. *ACS Chemical Neuroscience*, *10*(6), 2668–2675. https://doi.org/10.1021/acschemneuro.8b00656

Wang, D.-J., Su, L.-D., Wang, Y.-N., Yang, D., Sun, C.-L., Zhou, L., … Shen, Y. (2014). Long-Term Potentiation at Cerebellar Parallel Fiber-Purkinje Cell Synapses Requires Presynaptic and Postsynaptic Signaling Cascades. *Journal of Neuroscience*, *34*(6), 2355–2364. https://doi.org/10.1523/JNEUROSCI.4064-13.2014

Wang, X., Imura, T., Sofroniew, M. V., & Fushiki, S. (2011). Loss of adenomatous polyposis coli in Bergmann glia disrupts their unique architecture and leads to cell nonautonomous neurodegeneration of cerebellar Purkinje neurons. *Glia*, *59*(6), 857–

868. https://doi.org/10.1002/glia.21154

Xu, H., Yang, Y., Tang, X., Zhao, M., Liang, F., Xu, P., … Fan, X. (2013). Bergmann glia function in granule cell migration during cerebellum development. *Molecular Neurobiology*, *47*(2), 833–844. https://doi.org/10.1007/s12035-013-8405-y

Yamada, K., Fukaya, M., Shibata, T., Kurihara, H., Tanaka, K., Inoue, Y., & Watanabe, M. (2000). Dynamic transformation of Bergmann glial fibers proceeds in correlation with dendritic outgrowth and synapse formation of cerebellar Purkinje cells. *The Journal of Comparative Neurology*, *418*(1), 106–120. https://doi.org/10.1002/(SICI)1096-9861(20000228)418:1<106::AID-CNE8>3.0.CO;2-N

Yanagisawa, M., Namekata, K., Aida, T., Katou, S., Takeda, T., Harada, T., … Tanaka, K. (2020). EAAT1 variants associated with glaucoma. *Biochemical and Biophysical Research Communications*, *529*(4), 943–949. https://doi.org/10.1016/j.bbrc.2020.06.099

Zoia, C., Cogliati, T., Tagliabue, E., Cavaletti, G., Sala, G., Galimberti, G., … Ferrarese, C. (2004). Glutamate transporters in platelets: EAAT1 decrease in aging and in Alzheimer's disease. *Neurobiology of Aging*, *25*(2), 149–157. https://doi.org/10.1016/S0197-4580(03)00085-X

Chapter 4

4 Neuronal Nitric Oxide Synthase Critically Regulates the Endocannabinoid Pathway in the Murine Cerebellum During Postnatal Development.

4.1 Abstract

The cerebellum is a major site of endocannabinoid (eCB) production and signaling. The predominant eCB within the cerebellum, 2-arachadonylglycerol (2-AG), is produced by a metabotropic glutamate receptor type 1 (mGluR1)-initiated signaling cascade within Purkinje neurons (PNs). 2-AG retroactively stimulates cannabinoid 1 receptors (CB1Rs) located on presynaptic terminals. The activated CB1R decreases neurotransmitter release and leads to the production of nitric oxide (NO), a gaseous molecule. Recently, our group discovered that during development in mice lacking neuronal nitric oxide synthase (nNOS$^{-/-}$), PNs display an excitotoxic phenotype associated with overactivated mGluR1. Considering the importance of mGluR1 in 2-AG synthesis, the present study explored the role of nNOS-derived NO in regulating the eCB pathway within the cerebella of wildtype (WT) and nNOS$^{-/-}$ mice at postnatal day 7 (PD7), 2 weeks (2W), and 7 weeks (7W). Our analysis showed that diacylglycerol lipase α, the enzyme that catalyzes 2-AG production, was elevated at early postnatal ages, and followed by elevated levels of 2-AG in nNOS$^{-/-}$ cerebella compared to WT. CB1R expression in nNOS$^{-/-}$ cerebella was upregulated at PD7 but decreased at 2W and 7W when compared to age-matched WT mice cerebella. Importantly, treating organotypic nNOS$^{-/-}$ cerebellar slice cultures with an NO-donor attenuated CB1R levels after 7 days in vitro. In addition, expression of the eCB hydrolases fatty acid amide hydrolase and monoacylglycerol lipase were significantly downregulated in nNOS$^{-/-}$ cerebella compared to WT cerebella at 7W. Together, these results reveal a novel role for nNOS/NO in regulating eCB signaling in the cerebellum.

4.2 Introduction

The cerebellum is a highly organized brain region commonly associated with motor coordination, locomotion, fine motor control, and spatial navigation, which works to fine tune the commands from the motor cortex(Koziol, Budding, & Chidekel, 2012; Manto et al., 2012). Unlike the cerebral cortex, the cerebellar cortex is divided into 3 distinct layers; the granule cell layer, the Purkinje neuron (PN) layer, and the molecular layer. PNs represent the sole output response of the cerebellum, and therefore are subject to heavy synaptic regulation by neighbouring glutamatergic and GABAergic innervations, including parallel fibers (PFs), basket cells (BCs), and stellate cells (SCs).

A major component of synaptic regulation within the cerebellum involves nitric oxide (NO), a gaseous neurotransmitter produced by the catalytic activity of neuronal nitric oxide synthase (nNOS) that is abundantly expressed within the cerebellum, more so than any other region of the brain(Bredt, Hwang, & Snyder, 1990; Campese et al., 2006). NO is a major modulator of synaptic transmission and subsequently motor learning throughout development(Matyash, Filippov, Mohrhagen, & Kettenmann, 2001; Shibuki & Okada, 1991; Wang et al., 2014). Recently, our group discovered that the absence of nNOS ($nNOS^{-/-}$) in mice resulted in major PN dendritic deficits, beginning early within postnatal development and persisting into adulthood(Tellios, Maksoud, Xiang, & Lu, 2020). Additionally, a significant component affected within the PN of $nNOS^{-/-}$ mice involves the metabotropic glutamate 1 receptor (mGluR1) pathway(Tellios et al., 2020). Metabotropic GluR1 is a Gq protein coupled receptor that catalyzes the production of inositol triphosphate (IP3) and diacylglycerol (DAG) from phosphatidylinositol 4,5-biphosphate (PIP2) via phospholipase-C activity(Willard & Koochekpour, 2013). The mGluR1-initiated production of IP3 activates receptors on the endoplasmic reticulum to initiate store-operated calcium entry (SOCE) within the PNs(Hartmann, Henning, & Konnerth, 2011; Ryu et al., 2017; Takashi Yoshida et al., 2006). Our group discovered that mGluR1-initiated SOCE in PNs is overactivated in $nNOS^{-/-}$ mice when compared to normal wildtype (WT) mice, which results in calcium-dependent degradation of PN dendrites(Tellios et al., 2020).

In addition to the activation of SOCE by IP3, the mGluR1-initiated production of DAG is involved with the synthesis of cerebellar endocannabinoids (eCBs). Specifically, DAG is enzymatically converted by DAG lipase α (DAGLα) into 2-arachidonoylglycerol (2-AG), a prominent eCB within the cerebellum(Maejima et al., 2005; Richardson, Ortori, Chapman, Kendall, & Barrett, 2007; Savinainen, Järvinen, Laine, & Laitinen, 2001; Su, Wang, Yang, Shen, & Hu, 2013). Once produced, 2-AG signals retroactively to cannabinoid-1 receptors (CB1Rs) located on presynaptic terminals, predominately PFs, BCs, and SCs(Kawamura, 2006). CB1Rs are Gi protein-coupled receptors that are abundantly expressed within the molecular layer of the cerebellum. CB1R activation inhibits adenylyl cyclase and cAMP production(Howlett, 1987), suppresses the release of neurotransmitters such as GABA and glutamate from interneurons and PFs, respectively(Carey et al., 2011; P. Safo, Cravatt, & Regehr, 2006). Additionally, CB1R activity also induces morphological changes in neurons, specifically though cAMP-dependent pathways(Tapia et al., 2017). Interestingly, chronic activation of CB1Rs can result in decreased nNOS expression and NO production through inhibition of voltage-gated calcium channels, as CB1R-deficient mice exhibit greater NOS activity within the cerebrum compared to WT mice(Sun et al., 2006). However, evidence suggests that CB1R activation increases NO production in specific cell types. For example, N18TG2 neuroblastoma cells demonstrated elevated NO production in the presence of CB1R agonists(Jones, Carney, Vrana, Norford, & Howlett, 2008). Importantly, there is little evidence that delineates the interaction between NO and CB1R within the cerebellum and it remains unclear how, or if, a lack of NO signaling during development can affect the maturation of the CB1R pathway in the cerebellum.

Considering the already demonstrated, but not fully elucidated, interdependence between eCBs/CB1Rs and nNOS/NO production(Carney et al., 2009), along with our recent demonstration of the link between NO production and mGluR1 signaling in the cerebellum(Tellios et al., 2020), this study sought to characterize components of the eCB/CB1R pathway in the cerebellum of $nNOS^{-/-}$ mice across development. Specifically, the present study aimed to identify differences in the production of 2-AG, protein expression of eCB hydrolases, as well as the protein localization and expression of CB1R across postnatal ages between WT and $nNOS^{-/-}$ mice.

4.3 Materials and Methods

4.3.1 Animals

WT (C57/BL6, Stock No: 000664) and nNOS$^{-/-}$ mice (B6.129S4-Nos1^{tm1Plh}, Stock No: 002986) were obtained from the Jackson Laboratory. All the experiments within this study were conducted in accordance with Animal Use Protocol (#2018-106) approved by the Animal Care and Veterinary Services at the University of Western Ontario. The timepoints for cerebellar tissue collection occurred at postnatal day 7 (PD7), 2 weeks (2W) and 7 weeks (7W) of age using male mice.

4.3.2 2-AG ELISA

Whole, intact cerebella from WT and nNOS$^{-/-}$ mice were harvested and stored at –80 ^{o}C until use. To perform the 2-AG ELISA, samples were homogenized in PBS and centrifuged at 3000 rpm for 20 mins and the supernatant was collected. After homogenization, 2-AG levels within WT and nNOS$^{-/-}$ supernatants were measured using the Mouse 2-AG ELISA kit (MyBioSoure, San Diego, CA, Catalogue #: MBS1601288) and performed in accordance with the manufacturer's instructions.

4.3.3 Immunohistochemical Preparation

Whole, intact brains were isolated from WT and nNOS$^{-/-}$ mice and immediately placed in 4% paraformaldehyde (PFA) for 48 hrs. Fixed brains were then transferred to a 30% sucrose solution for a minimum of 48 hrs. Brains were sagittally sectioned at a thickness of 40 μm using a vibratome, and later placed in a cryoprotectant solution and stored in -20^{o}C until immunohistochemical preparation. Slices were washed with PBS then permeabilized using a 0.25% Triton-X solution for 5 mins. Slices were then incubated in 10% normal donkey serum (NDS) solution for 1 hr and later incubated with the following primary antibodies overnight in 4^{o}C: 1:500 guinea pig anti-calbindin (CalB) (Synaptic Systems, Goettingen, Germany, Catalogue #: 214005); 1:500 goat anti-DAGLα (Novus Biologicals, Toronto, ON, Catalogue #: NBP1-20905); 1:500 rabbit anti-CB1R (Abcam, Toronto, ON, Catalogue #: ab23703). Slices were then washed and incubated with the appropriate secondary antibodies for 2 hrs: anti-rabbit Cy3, anti-guinea pig AlexaFluor

488, or anti-goat AlexaFluor 647 (Jackson Immunoresearch, Burlington, ON). After incubation with the nuclear stain DAPI, slices were mounted on cover glass using Fluoromount-G (Electron Microscopy Solutions, Hatfield, PA) and images were taken using the Olympus FV1000 confocal microscope at 60x magnification using an oil-immersion objective.

4.3.4 Western Blotting

Whole, intact cerebella were isolated from WT and nNOS$^{-/-}$ mice and stored at -80 ^{o}C. Cerebellar tissues were homogenized using a glass homogenizer in radioimmunoprecipitation assay (RIPA) lysis buffer, supplemented with 0.1% apoprotein and 0.1% leupeptin. Once homogenized, cerebellar lysates were centrifuged for 30 mins at 4 ^{o}C. The supernatant was collected, and protein was measured using a Bradford reagent mix (Bio-Rad, Hercules, CA). Samples were later prepared using 2x sample buffer and loaded onto 10% or 12% polyacrylamide gels for electrophoresis and run for 2 hrs at 100V. Gels were then wet-transferred onto nitrocellulose membranes for 2 hrs at 80V. Blots were then incubated in 5% bovine serum albumin (BSA) for 1 hr before incubated with the following primary antibodies overnight: 1:500 goat anti-DAGLα (62 kDa); 1:1000 rabbit anti-CB1R (53 kDa); 1:1000 mouse anti-fatty acid amide hydrolase (FAAH) (67 kDa) (Santa Cruz Biotechnology, Dallas, TX, Catalogue #: sc-100739); 1:500 rabbit anti-monoacylglycerol lipase (MGL) (33 kDa) (ThermoFischer Scientific, Waltham MA, Catalogue #: PA5-27915). For total protein comparisons, 1:10000 anti-glyceraldehyde-3-phosphate dehydrogenase (GAPDH, 40 kDa) (Abcam, Toronto, ON) was used. After 3 washes in tris-buffered saline solution, the appropriate secondary horseradish-peroxidase antibodies (Jackson Immunoresearch, Burlington, ON) were incubated on the membranes for 1.5 hrs. Protein was visualized using enhanced chemiluminescence substrate (Bio-Rad, Hercules, CA) and imaged using the Bio-Rad VersaDoc system. All proteins were normalized to the housekeeping protein GAPDH. Densitometric analyses were quantified using FIJI open-source software.

4.3.5 Ex Vivo Organotypic Slice Cultures

Cerebella were obtained from 10-12 PD0 WT and nNOS$^{-/-}$ pups in Hank's balanced salt solution (HBSS) containing: 15 mM 4-(2-hydroxyehtyl)-1-piperazineethanesulfonic acid (HEPES), 0.5% glucose, 2% sucrose, and maintained at pH 7.3 and 315 mOsm. Cerebella were then sliced using a tissue chopper set to 350 μM thickness and carefully plated on 35 mm membrane inserts (Milipore Ltd., Etobicoke, ON). The bottom of the membrane insert was exposed to cerebellar slice culture media that contained minimum essential medium (MEM) supplemented with 5 mg/ml glucose, 25% heat-inactivated horse serum, 25 mM HEPES, 1 mM glutamine, and 100 U/ml penicillin and streptomycin. Cultures were maintained for 7 days in vitro (DIV7) and every 2 days, half of the medium was replaced. Slices from WT cultures were treated with 100 μM NOS inhibitor N(G)-Nitro-L-arginine methyl ester (L-NAME) (Santa Cruz Biotechnology, Dallas, TX), while nNOS$^{-/-}$ cultures were treated with the slow NO-donor, 300 μM diethylenetriamine NONOate (NOC-18) (Santa Cruz Biotechnology, Dallas, TX). Cultured cerebellar slices were then prepared for western blotting.

4.3.6 Image Analysis

4.3.6.1 Integrated Density

CB1R fluorescence intensity across all timepoints in WT and nNOS$^{-/-}$ cerebella was measured using FIJI. For PD7 and 2W CB1R measurements, a consistent ROI of the PN dendritic region, determined using the CalB stain, was made and overlayed on the corresponding DAGLα image. For 7W CB1R measurements, a consistent ROI of the PN dendritic region and the PN axon hillock region (distal and proximal measurements, respectively) were made and overlayed o the corresponding CB1R image. Then, integrated density — measured in arbitrary units of intensity (AUIs) — was graphed for each WT and nNOS$^{-/-}$ CB1R ROI. Integrated density was averaged from multiple images across four biological replicates.

4.3.7 Statistical Analysis

Statistical analyses were performed using an unpaired, two-tailed t-test for all results comparing WT to nNOS$^{-/-}$ mice. Significance was determined using a threshold of $p = 0.05$. All values are reported as mean ± standard error of the mean (SEM).

4.4 Results

4.4.1 2-AG Production is Higher in the Cerebella of nNOS$^{-/-}$ Mice at Later Postnatal Ages.

Our group first investigated whether the basal levels of 2-AG differed between WT and nNOS$^{-/-}$ cerebella across postnatal development using a 2-AG ELISA kit. At PD7, the levels of 2-AG were not significantly different between WT and nNOS$^{-/-}$ cerebellar tissues (WT = 124.99 ± 6.68 ng/mL; nNOS$^{-/-}$ = 112.11 ± 8.14 ng/mL) (**Figure 4.1a**). In contrast, nNOS$^{-/-}$ cerebellar tissues had significantly elevated levels of 2-AG at 2W when compared to age-matched WT cerebellar tissues (WT = 90.82 ± 6.86 ng/mL; nNOS$^{-/-}$ = 126.09 ± 5.47 ng/mL) (**Figure 4.1b**). A significant upregulation of 2-AG was also detected in nNOS$^{-/-}$ cerebellar tissues at 7W when compared to age-matched WT cerebellar tissue (WT = 109.97 ± 1.54 ng/mL; nNOS$^{-/-}$ = 138.08 ± 9.36 ng/mL) (**Figure 4.1c**).

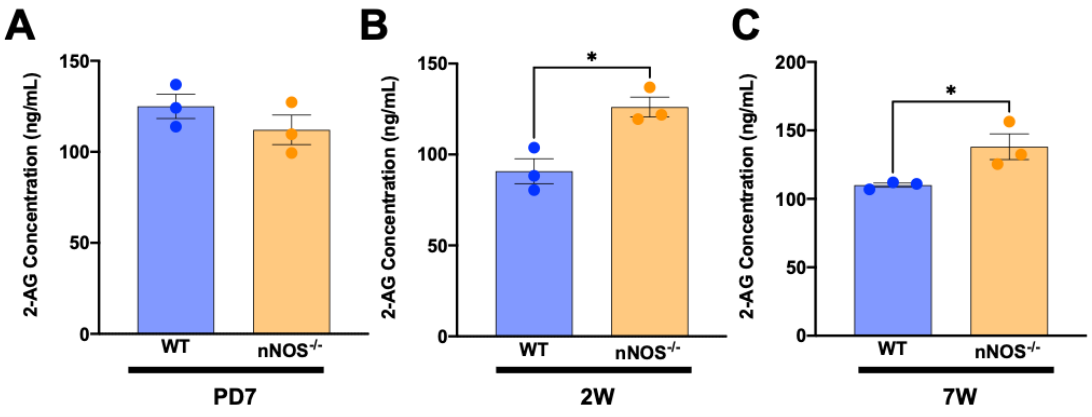

Figure 4.1 2-AG concentrations are significantly elevated in the cerebella of 2W and 7W nNOS$^{-/-}$ mice compared to age-matched WT mice.

Bar graphs represent concentrations of 2-AG in cerebellar tissues from WT and nNOS$^{-/-}$ mice at (**A**) PD7 (P = 0.2884), (**B**) 2W (P = 0.0158), and (**C**) 7W (P = 0.0415). N = 3 biological replicates per group.

4.4.2 DAGLα Expression is Upregulated in the Cerebella of nNOS$^{-/-}$ Mice at Early Postnatal Ages.

DAGLα is an enzyme predominantly localized to the PN, responsible for cerebellar 2-AG synthesis(Yoshida, Takayuki et al., 2006). Next, our group examined the expression and localization of DAGLα in the cerebella of WT and nNOS$^{-/-}$ mice across postnatal development. Immunohistochemical analyses showed that at PD7 CalB staining of PNs revealed some dendritic branches that colocalized to DAGLα fluorescence. Specifically, DAGLα fluorescence was located in the cytosol of both the cell body and dendrites of PNs, with intense staining near the PN cell border (**Figure 4.2a**). Western blot analyses revealed a significantly higher protein expression of DAGLα in nNOS$^{-/-}$ cerebellar tissues at PD7 when compared to age-matched WT cerebella (**Figure 4.2b**).

At 2W, CalB staining revealed complex dendritic arborizations of the PNs. Notably, fluorescence of DAGLα is heavily localized to the dendrites of PNs and to a lesser degree in the soma of PNs (**Figure 4.3a**). Similar to the PD7 timepoint, western blot analyses showed a significant increase in DAGLα protein expression in nNOS$^{-/-}$ cerebellar tissues at 2W when compared to age-matched WT cerebellar tissues (**Figure 4.3b**).

At 7W, CalB staining of PNs in both WT and nNOS$^{-/-}$ cerebella displayed more complex dendritic arborization. Fluorescence of DAGLα was localized primarily in the PN dendrites, with little staining in the PN soma of both WT and nNOS$^{-/-}$ cerebella at 7W (**Figure 4.4a**). Interestingly, western blot analyses revealed no significant difference in DAGLα protein expression between WT and nNOS$^{-/-}$ cerebellar tissues at 7W (**Figure 4.4b**).

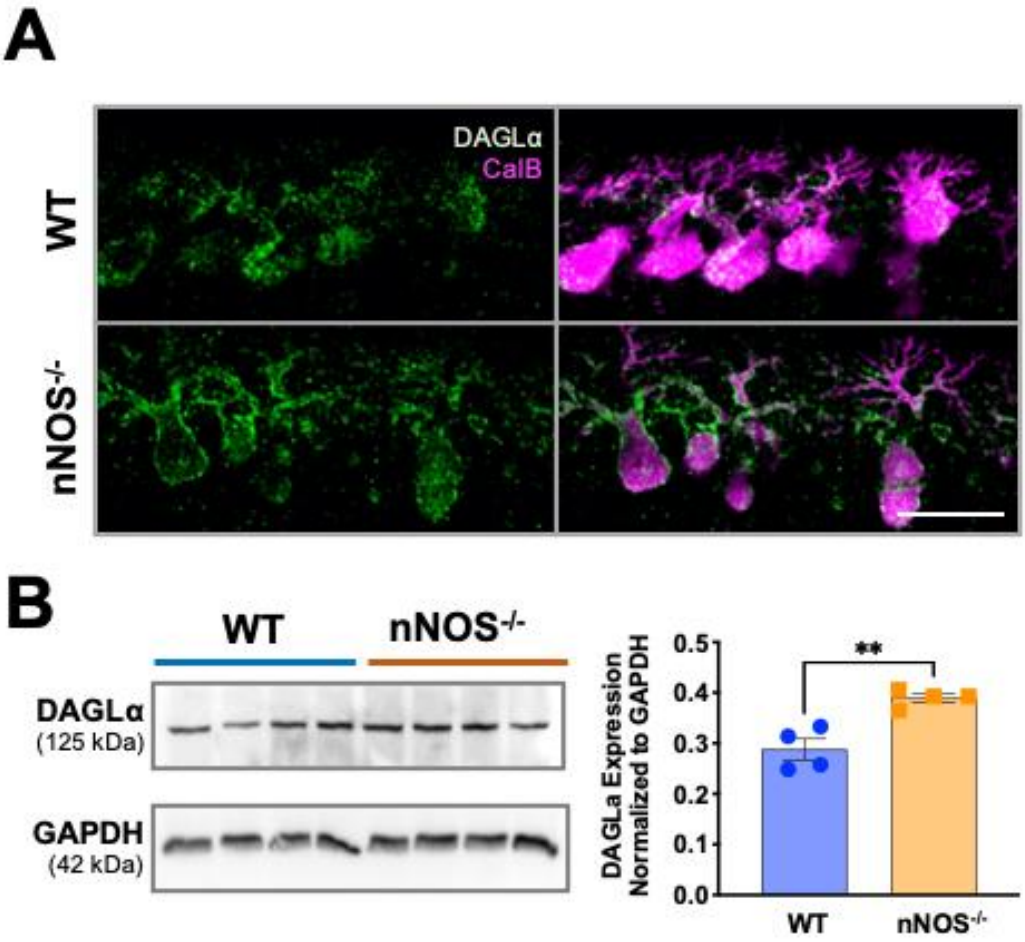

Figure 4.2 DAGLα expression is significantly upregulated in PD7 nNOS$^{-/-}$ cerebella compared to WT cerebella.

(**A**) Representative confocal microscopy images of DAGLα (green) and CalB (magenta) immunofluorescence in the cerebella of WT and nNOS$^{-/-}$ mice at PD7. Scale bar represents 50 μm. (**B**) Representative western blot of total DAGLα protein expression for WT and nNOS$^{-/-}$ cerebella at PD7. The housekeeping protein GAPDH was used as the loading control. Bar graph (right) represents the ratio of total DAGLα protein normalized to GAPDH protein. N = 4 biological replicates per group. P = 0.0041.

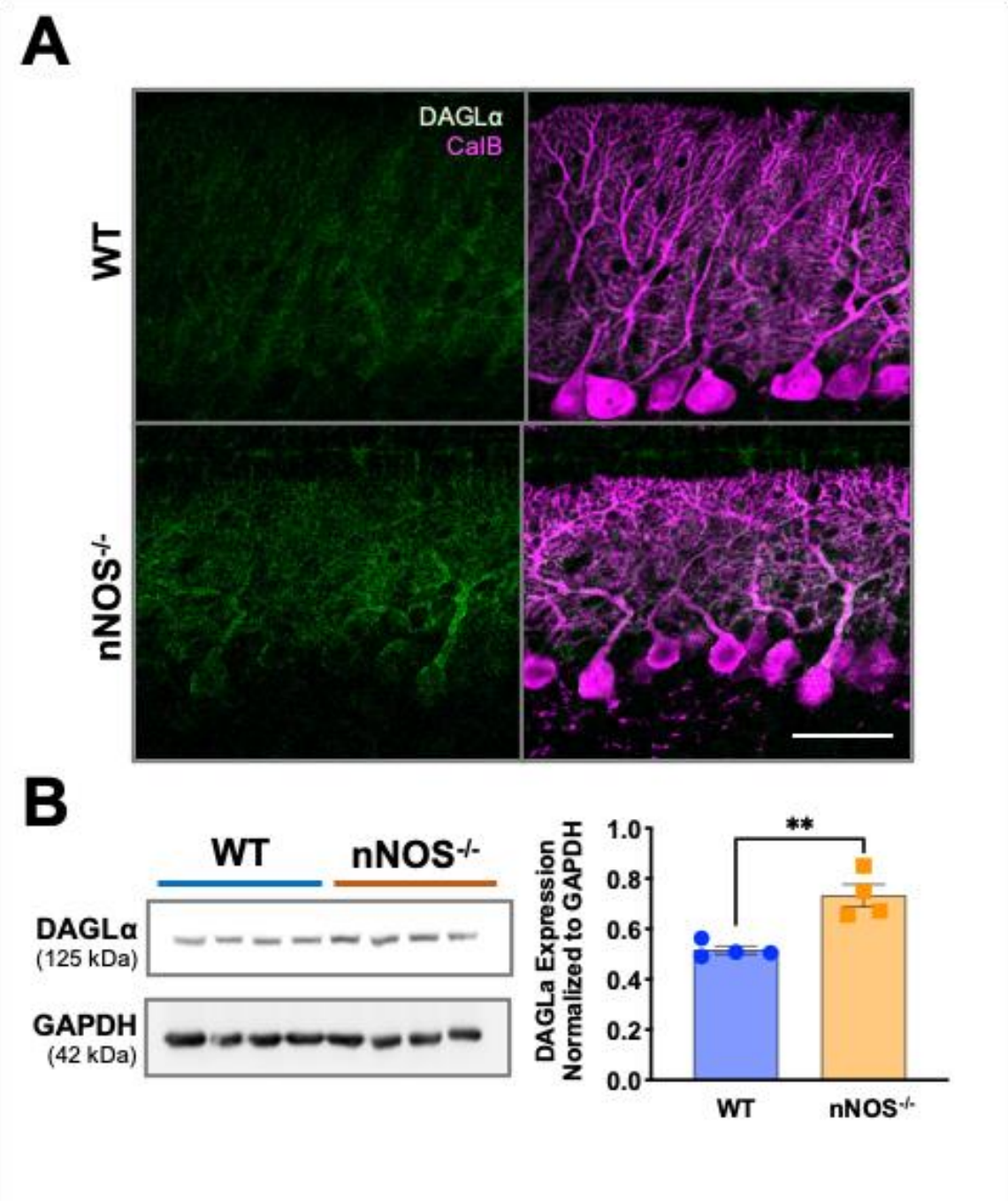

**** Figure legend on next page ****

Figure 4.3 DAGLα expression is significantly upregulated in 2W nNOS$^{-/-}$ cerebella compared to WT cerebella.

(**A**) Representative confocal microscopy images of DAGLα (green) and CalB (magenta) immunofluorescence in the cerebella of WT and nNOS$^{-/-}$ mice at 2W. Scale bar represents 50 μm. (**B**) Representative western blot of total DAGLα protein expression for WT and nNOS$^{-/-}$ cerebella at 2W. The housekeeping protein GAPDH was used as a loading control. Bar graph (right) represents the ratio of DAGLα protein normalized to GAPDH protein. N = 4 biological replicates per group. P = 0.0039.

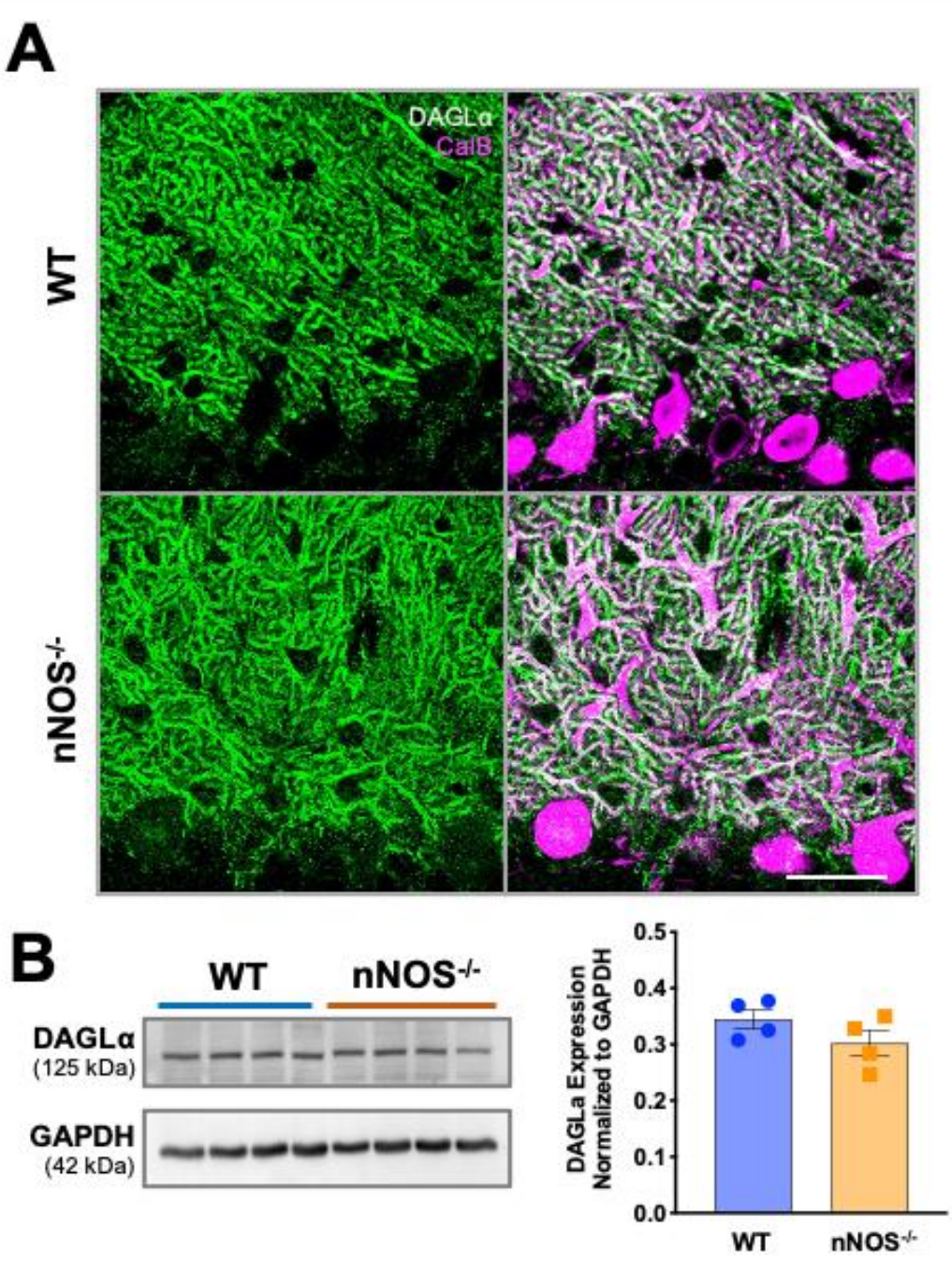

**** Figure legend on next page ****

Figure 4.4 DAGLα expression is not significantly different between 7W WT and nNOS$^{-/-}$ cerebella.

(**A**) Representative confocal microscopy images of DAGLα (green) and CalB (magenta) immunofluorescence in the cerebella of WT and nNOS$^{-/-}$ mice at 7W. Scale bar represents 50 μm. (**B**) Representative western blot of total DAGLα protein expression for WT and nNOS$^{-/-}$ cerebella at 7W. The housekeeping protein GAPDH was used as a loading control. Bar graph (right) represents the ratio of DAGLα protein normalized to GAPDH protein. *N* = 4 biological replicates per group. *P* = 0.1875.

4.4.3 CB1R Expression and Localization are Differentially Regulated at Different Postnatal Timepoints in nNOS$^{-/-}$ Cerebella.

In the cerebellum, CB1Rs are located on the presynaptic terminals and are the main target for retrograde eCB signaling. To understand the impact of nNOS/NO signaling on eCB signaling in the cerebella, our group characterized potential differences in CB1R expression and localization between WT and nNOS$^{-/-}$ mice cerebella. At PD7, immunofluorescence of CB1R was predominantly localized to the molecular layer of the cerebellum, surrounding the PN dendrites (**Figure 4.5a**). An analysis of integrated density revealed significantly more CB1R fluorescence in nNOS$^{-/-}$ cerebella compared to age-matched WT cerebella (**Figure 4.5b**). Similarly, western blot analyses revealed significantly more CB1R protein expression in nNOS$^{-/-}$ cerebellar tissue compared to WT cerebellar tissue at PD7 (**Figure 4.5c**).

At 2W, immunofluorescence of CB1R was heavily localized in the molecular layer of both WT and nNOS$^{-/-}$ cerebella. At this timepoint, immunofluorescence of CB1R also began to boarder the soma and axon hillock of PNs in both WT and nNOS$^{-/-}$ cerebella (**Figure 4.6a**). Integrated density analyses at this timepoint revealed significantly lower immunofluorescence of CB1R staining in nNOS$^{-/-}$ cerebella compared to WT cerebellar tissues (**Figure 4.6b**). Similarly, western blot analyses revealed significantly less CB1R protein levels in nNOS$^{-/-}$ cerebellar tissues when compared to age-matched WT cerebellar tissues (**Figure 4.6c**).

The localization of CB1R fluorescence at 7W was similar to that of 2W cerebella, with intense staining in the molecular layer. However, fluorescence of CB1R was also concentrated and localized around the soma and axon hillock of PNs, which was more prominent at 7W than at 2W (**Figure 4.7a**). Analyses of integrated density revealed significantly less CB1R immunofluorescence in the molecular layer (or the distal region) of nNOS$^{-/-}$ tissues compared to WT tissues at 7W (**Figure 4.7b**). Similarly, significantly less CB1R immunofluorescence in the proximal region containing the axon hillock of PNs was observed in nNOS$^{-/-}$ cerebella compared to WT cerebella at 7W (**Figure 4.7b**).

Western blot analyses revealed significantly less CB1R protein levels in nNOS$^{-/-}$ cerebella at 7W compared to age-matched WT cerebella (**Figure 4.7c**).

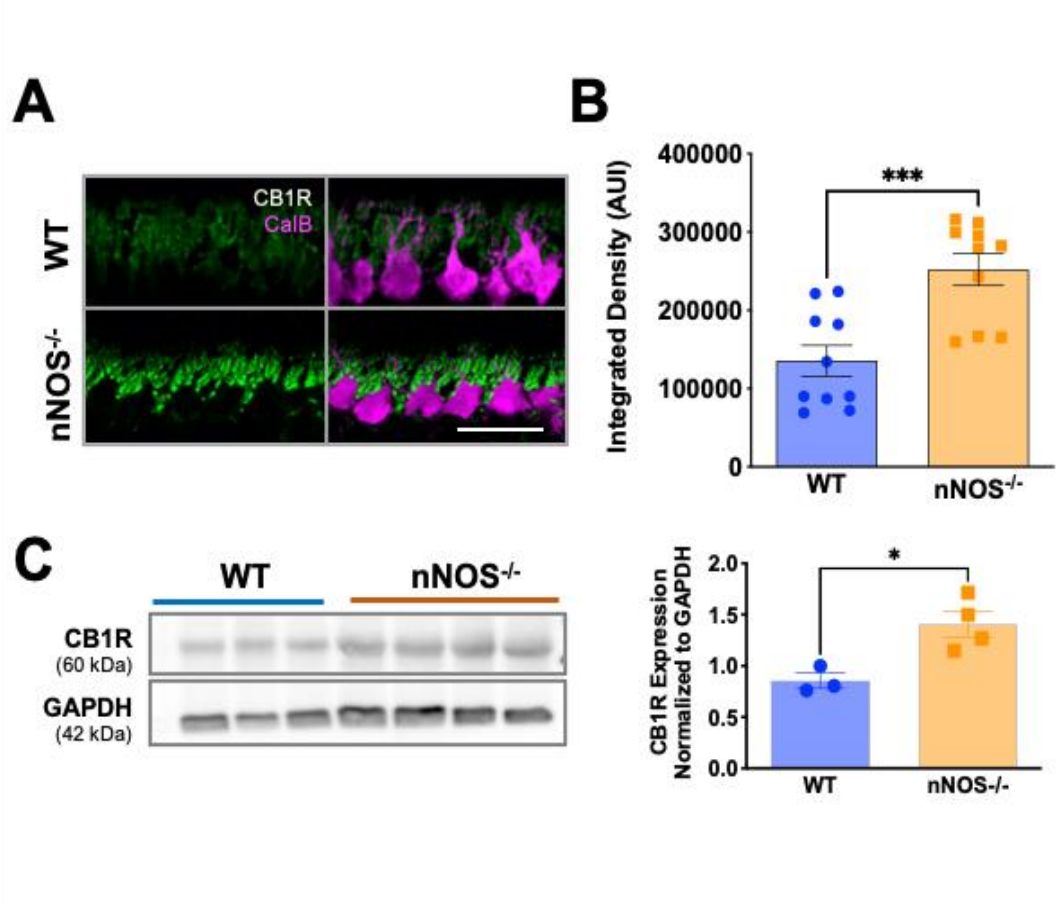

Figure 4.5 CB1R expression is significantly upregulated in PD7 nNOS$^{-/-}$ cerebella compared to WT cerebella.

(**A**) Representative confocal microscopy images of CB1R (green) and CalB (magenta) immunofluorescence in the cerebella of WT and nNOS$^{-/-}$ mice at PD7. Scale bar represents 50 μm. (**B**) Bar graph represents the integrated density of CB1R fluorescence. N = 4 biological replicates per group. WT n = 10 ROIs, nNOS$^{-/-}$ = 10 ROIs. P = 0.0006. (**C**) Representative western blot of total CB1R protein expression and the housekeeping protein GAPDH for WT and nNOS$^{-/-}$ cerebella at PD7. Bar graph (right) represents the ratio of CB1R protein normalized to GAPDH protein. N = 3 biological replicates for WT; N = 4 biological replicates for nNOS$^{-/-}$. P = 0.0187.

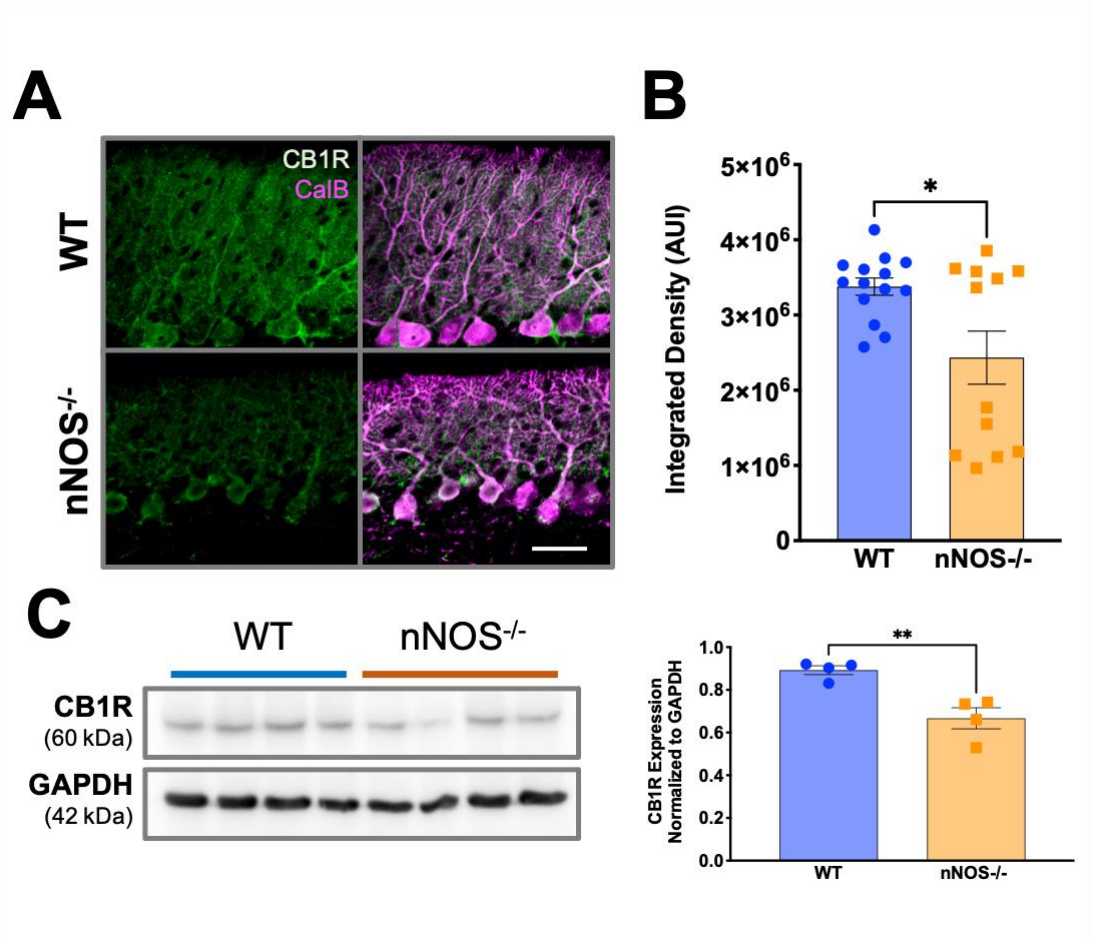

Figure 4.6 CB1R expression is significantly downregulated in 2W nNOS$^{-/-}$ cerebella compared to WT cerebella.

(**A**) Representative confocal microscopy images of CB1R (green) and CalB (magenta) immunofluorescence in the cerebella of WT and nNOS$^{-/-}$ mice at 2W. Scale bar represents 50 μm. (**B**) Bar graph represents the integrated density of CB1R fluorescence. *N* = 4 biological replicates per group. WT n = 14 ROIs, nNOS$^{-/-}$ = 12 ROIs. *P* = 0.0121. (**C**) Representative western blot of total CB1R protein and the housekeeping protein GAPDH WT and nNOS$^{-/-}$ cerebella at 2W. Bar graph represents CB1R protein normalized to GAPDH protein. *N* = 4 biological replicates per group. *P* = 0.0057.

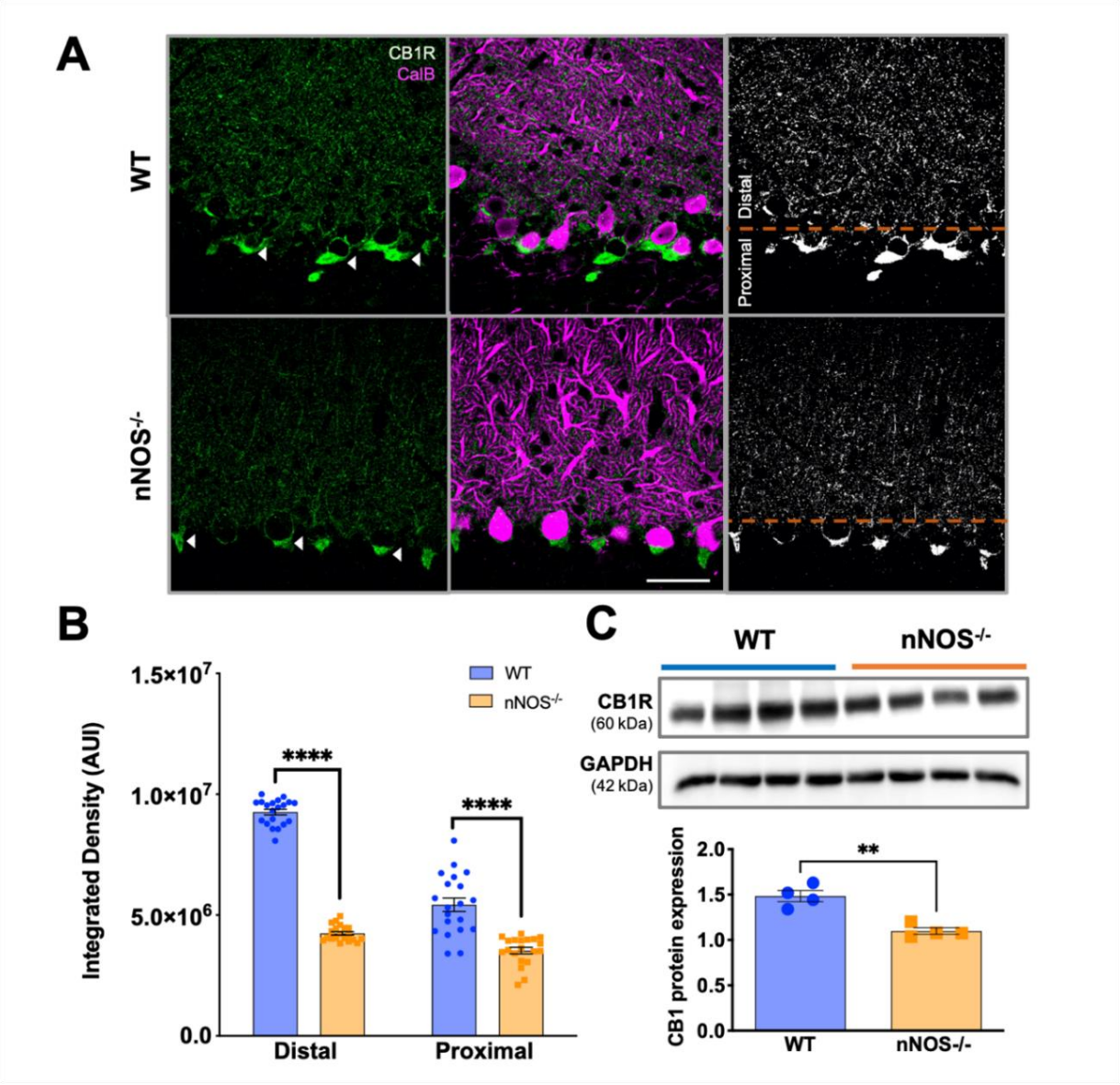

**** Figure legend on next page ****

Figure 4.7 CB1R expression is significantly downregulated in 7W nNOS$^{-/-}$ cerebella compared to WT cerebella.

(**A**) Representative confocal images of CB1R (green) and CalB (magenta) immunofluorescence in the cerebella of WT and nNOS$^{-/-}$ mice at 7W. Scale bar represents 50 μm. The right panel depicts a thresholded image of CB1R fluorescence and denotes the distal region that contains the PN dendrites in the ML and the proximal region that contains the PN soma and axon hillock, which were separated for image analyses. (**B**) Bar graph represents the integrated density of CB1R fluorescence in the distal and proximal regions. $N = 4$ biological replicates per group. WT (distal and proximal) n = 20 ROIs, nNOS$^{-/-}$ (distal and proximal) = 20 ROIs. $P < 0.0001$ for both distal and proximal comparisons. (**C**) Representative western blot of total CB1R protein and the housekeeping protein GAPDH for WT and nNOS$^{-/-}$ cerebella at 7W. Bar graph represents the ratio of CB1R protein normalized to GAPDH protein. $N = 4$ biological replicates per group. $P = 0.0016$.

4.4.4 Both FAAH and MGL Protein Expression Are Downregulated in Adult nNOS$^{-/-}$ Cerebella.

The breakdown of eCBs in the cerebellum is primarily facilitated by enzymatic activity of FAAH and MGL. Therefore, our group characterized the expression levels of these proteins in the cerebella of WT and nNOS$^{-/-}$ mice across different postnatal ages. At PD7, western blot analyses revealed less FAAH protein levels in nNOS$^{-/-}$ cerebella compared to age-matched WT cerebella, although this difference was not significant (**Figure 4.8a**). At 2W, no significant differences in FAAH protein levels were noted between WT and nNOS$^{-/-}$ cerebella (**Figure 4.8b**). Notably, western blot analyses revealed a significant decrease in FAAH protein levels in nNOS$^{-/-}$ cerebella at 7W compared to age-matched WT mouse cerebella (**Figure 4.8c**).

Western blot analyses detected significantly less MGL protein expression in nNOS$^{-/-}$ cerebella at 7D compared to age-matched WT mouse cerebella (**Figure 4.9a**). At 2W, there were no significant differences in MGL protein expression between WT and nNOS$^{-/-}$ cerebella (**Figure 4.9b**). Finally, western blot analyses detected a significant decrease in MGL protein expression in nNOS$^{-/-}$ cerebella at 7W compared to age-matched WT cerebella (**Figure 4.9c**).

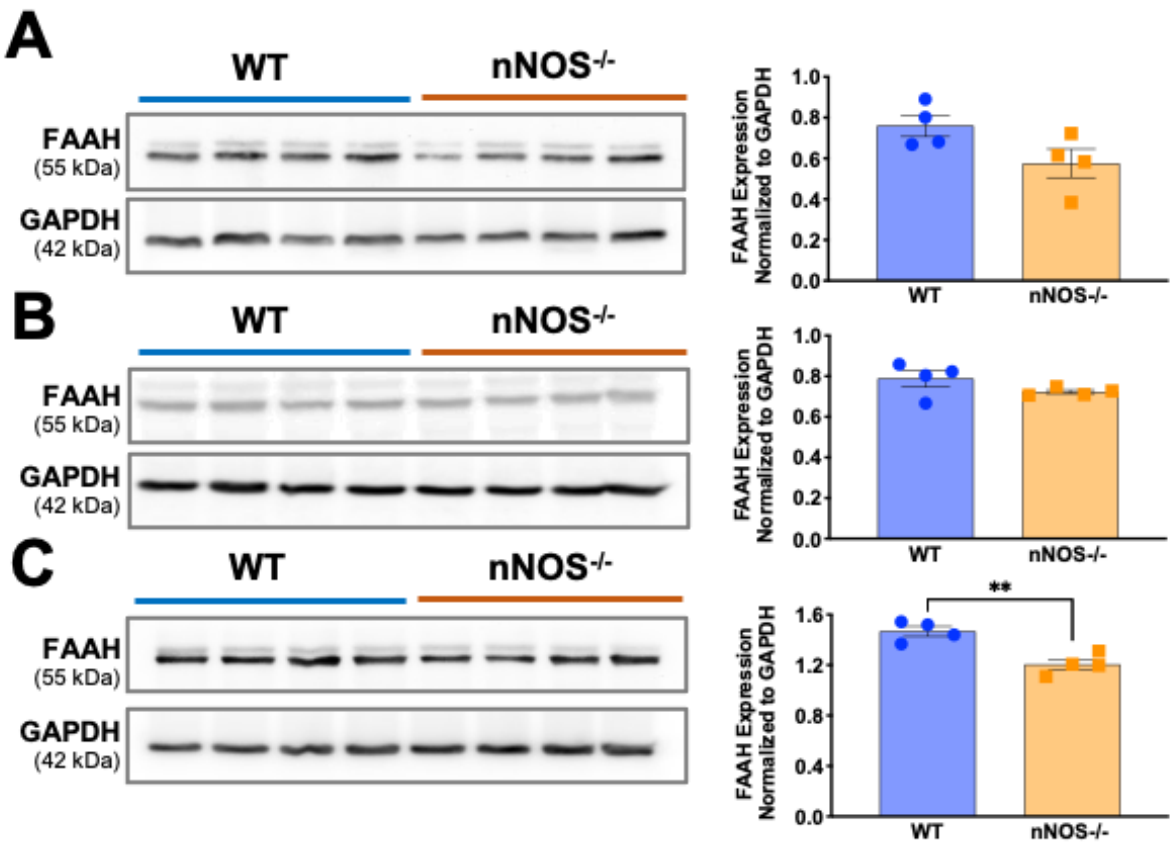

Figure 4.8 FAAH protein expression is significantly decreased in 7W nNOS$^{-/-}$ cerebella compared to WT cerebella.

(**A**) Representative western blot of total FAAH and GAPDH protein for PD7 WT and nNOS$^{-/-}$ cerebella. Bar graph represents the ratio of FAAH protein normalized to GAPDH. *N* = 4 biological replicates per group. *P* = 0.0814. (**B**) Representative western blot of total FAAH and GAPDH protein for 2W WT and nNOS$^{-/-}$ cerebella. Bar graph represents the ratio of FAAH protein normalized to GAPDH. *N* = 4 biological replicates per group. *P* = 0.1829. (**C**) Representative western blot of total FAAH and GAPDH protein for 7W WT and nNOS$^{-/-}$ cerebella. Bar graph represents the ratio of FAAH protein normalized to GAPDH. *N* = 4 biological replicates per group. *P* = 0.0097.

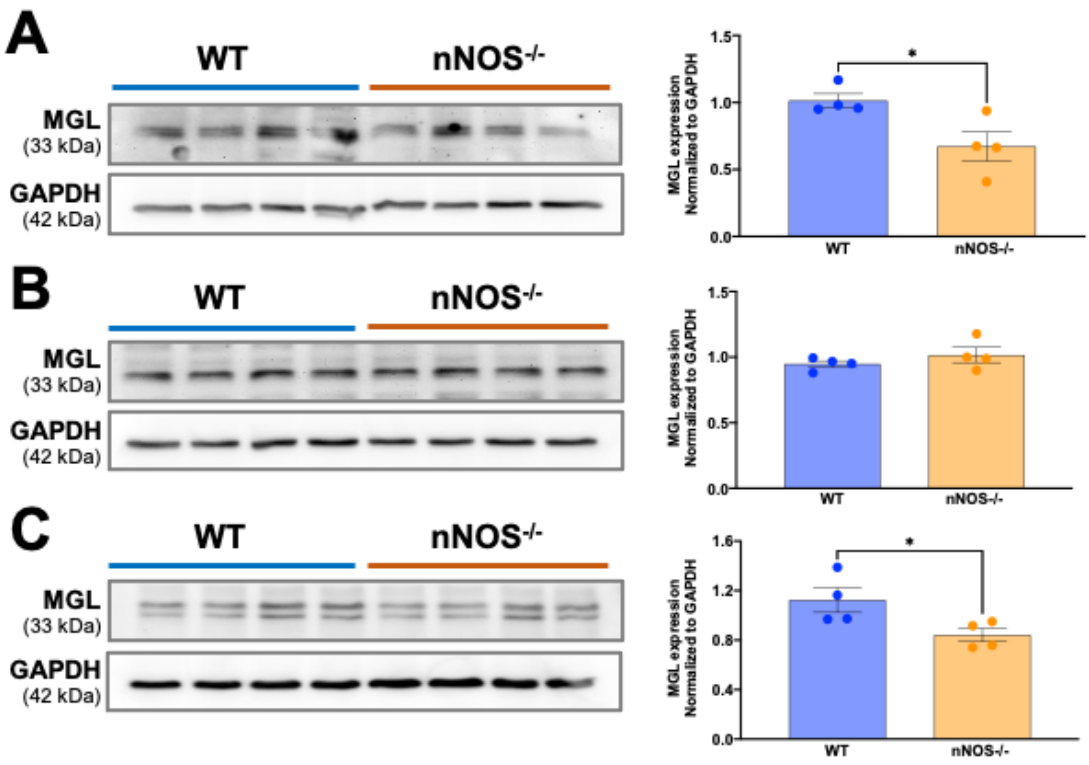

Figure 4.9 MGL protein expression is significantly decreased in PD7 and 7W nNOS$^{-/-}$ cerebella compared to WT cerebella.

(**A**) Representative western blot of total MGL and GAPDH protein for PD7 WT and nNOS$^{-/-}$ cerebella. Bar graph represents the ratio of MGL protein normalized to GAPDH. N = 4 biological replicates per group. P = 0.0287. (**B**) Representative western blot of total MGL and GAPDH protein for 2W WT and nNOS$^{-/-}$ cerebella. Bar graph represents the ratio of MGL protein normalized to GAPDH. N = 4 biological replicates per group. P = 0.3196. (**C**) Representative western blot of total MGL and GAPDH protein for 7W WT and nNOS$^{-/-}$ cerebella. Bar graph represents the ratio of MGL protein expression normalized to GAPDH. N = 4 biological replicates per group. P = 0.0096.

4.4.5 NO Signaling Regulates CB1R Expression in WT and nNOS$^{-/-}$ Organotypic Cerebellar Slice Cultures.

To determine whether nNOS/NO signaling influences the expression of CB1R in the cerebellum of mice, we compared the protein expression of CB1R in untreated organotypic slice cultures of WT or nNOS$^{-/-}$ cerebella to organotypic slice cultures of WT or nNOS$^{-/-}$ cerebella treated with the NOS inhibitor L-NAME or the slow-release NO-donor NOC-18 respectively, for 7 days in vitro (DIV7). Western blot analyses revealed that blocking NOS activity in WT organotypic slice cultures caused significantly more CB1R protein expression when compared to control organotypic WT cerebellar cultures (**Figure 4.10a**). Furthermore, western blotting revealed that supplementing NO onto nNOS$^{-/-}$ cerebellar slices significantly decreased CB1R protein expression in nNOS$^{-/-}$ organotypic cerebellar cultures when compared to control organotypic nNOS$^{-/-}$ cerebellar cultures (**Figure 4.10b**).

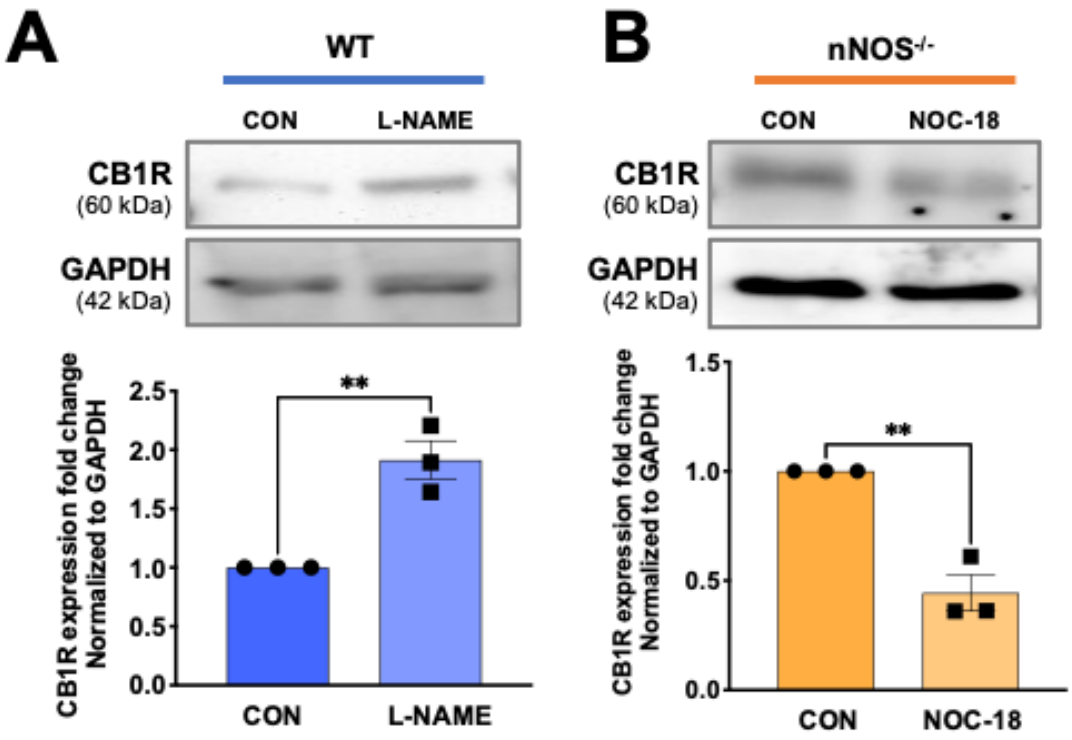

Figure 4.10 CB1R expression in the cerebella of WT and nNOS$^{-/-}$ mice is modulated by NO signaling in an ex vivo model.

(**A**) Representative western blot of total CB1R and GAPDH protein in WT cerebellar slices that were left untreated (CON) or treated with 100 μM L-NAME for 7 days. Bar graph represents the ratio of CB1R protein normalized to GAPDH from N = 3 experimental replicates. P = 0.0050. (**B**) Representative western blot of total CB1R and GAPDH protein in nNOS$^{-/-}$ cerebellar slices that were left untreated (CON) or treated with 300 μM NOC-18. Bar graph represents the ratio of CB1R protein normalized to GAPDH from N = 3 experimental replicates. P = 0.0026.

4.5 Discussion

The cerebellum is a brain region that has one of the highest concentrations of 2-AG, which makes the eCB pathway a crucial component in regulating cerebellar function(Richardson et al., 2007; Su et al., 2013). Although there is evidence of CB1R activity interacting with the NO signaling pathway, it is currently unknown whether alterations in the nNOS-derived NO pathway elicits changes in the eCB pathway within the cerebellum. This study is the first to determine changes in the eCB pathway in the cerebellum during postnatal development of $nNOS^{-/-}$ mice. The major findings of this study are summarized in Table 1.

Table 4.1 Summary of alterations in the eCB pathway components in the cerebella of $nNOS^{-/-}$ mice during cerebellar development.

eCB Pathway Components	Alterations at Postnatal Developmental Timepoints		
	7D	**2W**	**7W**
2-AG	—	↑	↑
DAGL*α*	↑↑	↑↑	—
CB1R	↑	↓↓	↓↓
FAAH	—	—	↓↓
MGL	↓	—	↓

4.5.1 A Lack of nNOS/NO Signaling in the Cerebellum Increases the Basal Concentrations of 2-AG During Postnatal Development.

2-AG is an important neurotransmitter responsible for the activation of CB1Rs and at physiological levels, 2AG induces long term depression at the PF-PN synapse(Lévénès, Daniel, Soubrié, & Crépel, 1998; P. K. Safo & Regehr, 2005; Takayuki Yoshida et al., 2002). Likewise, the presence of nNOS/NO signaling is crucial in regulating long term depression at the PF-PN synapse through a mechanism that involves mGluR1-mediated calcium mobilization within PNs(Daniel, Levenes, & Crépel, 1998; Tellios et al., 2020). We previously discovered that a lack of NO within the cerebellum of $nNOS^{-/-}$ mice resulted in an overactivation of mGluR1(Tellios et al., 2020). Importantly, activation of mGluR1 increases the synthesis and release of eCBs such as 2-AG within the cerebellum(Kyriakatos & El Manira, 2007). Aligning with this understanding, our present study revealed that the cerebella from $nNOS^{-/-}$ mice contain significantly elevated levels of 2-AG at 2W and 7W when compared to the cerebella from age-matched WT mice. Interestingly, it was reported that chronic alcohol exposure, a known mediator of nNOS inhibition(Karadayian et al., 2015), also elevates 2-AG levels in humans(Basavarajappa & Hungund, 2005). These results further confirm that deficient NO signaling enhances 2-AG synthesis in the cerebellum during development.

4.5.2 A Lack of nNOS/NO Signaling in the Cerebellum Decreases the Expression of 2-AG Hydrolyzing Enzymes and Increases the Expression of DAGLα

The eCBs in the CNS are hydrolyzed by two prominent enzymes: FAAH and MGL. Cerebellar localization of FAAH and MGL are complementary, such that FAAH is predominantly located in the soma and dendrites of PNs, while MGL is localized within presynaptic terminals within the molecular layer(Gulyas et al., 2004). Interestingly, our assays revealed a significant downregulation of both FAAH and MGL at 7W, while only MGL was downregulated at PD7 in $nNOS^{-/-}$ cerebella compared to age-matched WT cerebella.

The decreased protein expression of MGL in nNOS$^{-/-}$ cerebella at PD7 aligns well with our previous study that noted a decreased expression of the presynaptic terminal marker, vesicular glutamate transporter-1 (vGluT1), in PD7 nNOS$^{-/-}$ cerebella when compared to age-matched WT cerebella(Tellios et al., 2020). Specifically, the decreased protein expression of MGL in nNOS$^{-/-}$ cerebella at this timepoint is likely attributed to structural differences such as a reduction of PF-PN synapses within nNOS$^{-/-}$ cerebella.

At 7W, both MGL and FAAH protein expression was decreased in nNOS$^{-/-}$ cerebella compared to WT cerebella. It is known that blockade of MGL, either using pharmacological inhibitors or MGL$^{-/-}$ models, elevates 2-AG levels in vivo(Donatelli, 2015; Pan et al., 2011; Schlosburg et al., 2010). On the other hand, FAAH is commonly associated with the hydrolysis of N-arachidonoylethanolamide (AEA), the second most common eCB within the CNS. Although 2-AG is the predominant eCB within the cerebellum, others have noted the unusually high expression of FAAH within the cerebellum may play a role in 2-AG hydrolysis in vivo(Di Marzo & Maccarrone, 2008; Goparaju, Ueda, Yamaguchi, & Yamamoto, 1998). Specifically, downregulation or inhibition of FAAH has been shown to increase levels of both 2-AG and AEA(Hohmann et al., 2005). It is important for future studies to consider the delicate balance between FAAH, AEA, and 2-AG when examining changes in these eCBs.

DAGLα is the dominant enzymatic isoform that catalyzes 2-AG synthesis in the nervous system and is responsible for about 80% of 2-AG production in the brain(Gao et al., 2010). In the cerebellum, DAGLα is expressed specifically in PNs, and its activity is downstream of the mGluR1 signaling cascade(Maejima et al., 2005). In this study, we found a significant increase in DAGLα expression in nNOS$^{-/-}$ cerebella at PD7 and 2W but not at 7W when compared to age-matched WT cerebella. Considering that DAGLα converts the compound DAG into 2-AG, the elevated protein expression of DAGLα observed in the nNOS$^{-/-}$ cerebella at 2W correlates well with our findings that demonstrate elevated 2-AG in nNOS$^{-/-}$ cerebella at 2W when compared to age-matched WT cerebella. Furthermore, overactive mGluR1 receptors in the nNOS$^{-/-}$ mouse is a likely contributor to the increased expression of DAGLα protein observed at PD7 and 2W(Tellios et al., 2020). However, DAGLα protein expression at 7W of age was unchanged in the nNOS$^{-/-}$ cerebella

despite an increase of 2-AG at this timepoint in comparison to WT cerebella. This observed phenomenon may be the result of decreases in 2-AG hydrolyzing enzymes such as FAAH and MGL in nNOS$^{-/-}$ cerebella at 7W. Furthermore, the enzymatic activity of DAGLα has been reported to depend on calcium/calmodulin dependent protein kinase II activity(Shonesy et al., 2013), which may be altered in the nNOS$^{-/-}$ cerebella at this timepoint. Another potential factor that may influence 2-AG production is the lack of transient receptor potential vanilloid type 1 ion channel activity, which can promote glutathione-dependent 2-AG synthesis as described by a previous group(Maccarrone et al., 2008). In order to further characterize the compensatory effects occurring in the eCB pathway of the nNOS$^{-/-}$ mouse cerebella, future studies should examine the regulatory mechanisms surrounding DAGLα expression and activation.

4.5.3 A Lack of nNOS/NO Signaling Alters CB1R Expression During Postnatal Development

CB1R is abundant in the cerebellum and specifically located on pre-synaptic terminals including PFs, BCs, and SCs(P. K. Safo & Regehr, 2005). Our assays found that at PD7, the expression of CB1R was significantly upregulated in nNOS$^{-/-}$ cerebella compared to WT cerebella. It is important to note that at PD7, BC innervation specifically at the axon hillock has yet to form. Although inhibitory interneurons such as BCs and stellate cells express CB1Rs to a high degree in the cerebellum, inhibitory interneuron migration to the molecular layer occurs between PD1 – 2W, while these cells functionally innervate PNs at around PD10(Pouzat & Hestrin, 1997). Therefore, the CB1R expression measured at PD7 is likely associated with PF terminals. Interestingly, our previous study revealed a significant downregulation of vGluT1, a marker for PF terminals, in PD7 nNOS$^{-/-}$ cerebella compared to WT(Tellios et al., 2020). Previous literature has demonstrated that activation of CB1R at vGluT1-positive terminals led to a decrease in excitatory synaptic transmission, which may also account for the decrease in vGluT1 expression in the cerebella of nNOS$^{-/-}$ mice at PD7(Castillo, Younts, Chávez, & Hashimotodani, 2012).

Our group noted significant decreases in CB1R fluorescent intensity and protein expression in nNOS$^{-/-}$ cerebella compared to WT cerebella at both 2W and 7W. Previous studies have identified a compensatory mechanism where chronically elevated levels of 2-

AG can result in CB1R internalization and inactivation over time(Wu et al., 2008). As our study noted elevated levels of 2-AG at both 2W and 7W of age, it is likely that chronic 2-AG elevation within the nNOS$^{-/-}$ cerebellum results in the downregulation of CB1R expression at these postnatal timepoints. It could also be the case that a lack of nNOS/NO signaling may differentially affect CB1Rs on glutamatergic and GABAergic synaptic terminals. As previously mentioned, inhibitory interneurons such as BCs and stellate cells begin to innervate PNs at around 2W, and axon terminals from BCs form pinceau synapses that surround the axon hillock of PNs at this time point(Pouzat & Hestrin, 1997). We specifically discovered a striking difference in CB1R expression specifically on pinceau synapses that are localized to the PN axon hillock at 7W in nNOS$^{-/-}$ cerebella, which may contribute to the overall downregulate of CB1Rs at this timepoint. Future studies should explore whether retrograde eCB signaling is different between the glutamatergic and GABAergic neurons that exist in the cerebellum.

4.5.4 Modulation of the NO Pathway Can Regulate CB1R Expression in an Ex Vivo Model.

To determine whether expression of CB1R protein in the cerebella of mice is dependent on nNOS/NO signaling, we blocked nNOS activity in organotypic WT cerebella slices and supplemented exogenous NO to organotypic nNOS$^{-/-}$ cerebella slices in an ex vivo model. The ex vivo cerebellar tissues were from PD0 WT and nNOS$^{-/-}$ pups and harvested for western blotting after DIV7. Collecting the ex vivo organotypic slices after 7 days allowed us to compare trends to the cerebella isolated from PD7 WT and nNOS$^{-/-}$ mice(Rakotomamonjy & Guemez-Gamboa, 2019). Firstly, our western blot analyses revealed similar trends in CB1R protein expression from the ex vivo environment when compared to the in vivo environment, in that protein expression of CB1R was higher in the absence of nNOS/NO signaling. Specifically, treatment of L-NAME onto organotypic WT cerebellar slices increased the protein expression level of CB1R, which was similar to the trend observed in the nNOS$^{-/-}$ cerebella at PD7 in vivo. Similarly, treatment of the slow-release NO donor NOC-18 onto organotypic nNOS$^{-/-}$ cerebellar slices decreased the protein expression level of CB1R, which was similar to the observed trend in the WT cerebella to PD7 in vivo. These results confirm a key role of nNOS/NO signaling in the regulation of

eCB signaling components and indicates that the absence of nNOS/NO signaling in the cerebella alters CB1R expression. Our previous study examined ex vivo cerebellar slices prepared from $nNOS^{-/-}$ and WT mice and showed that deficiency in nNOS/NO signaling caused morphological alterations of the PF-PN synapses through mGluR1 activation and calcium overload at DIV7(Tellios et al., 2020). Likewise, NO from PFs may indirectly regulate CB1R expression by indirectly exerting its effects on the mGluR1 pathway. The possibility that NO regulates CB1R expression in glutamatergic and GABAergic terminals should be examined in the future.

In summary, our group noted a significant dysregulation of various components of the eCB pathway in the cerebellum of $nNOS^{-/-}$ mice when compared to WT mice across development. Specifically, the absence of nNOS/NO signaling resulted in increased DAGLα protein expression at early developmental timepoints and a downregulation of the eCB hydrolyzing enzymes FAAH and MGL in adulthood, which could both be responsible for the increased synthesis of 2-AG at older developmental timepoints. Importantly, a consequence of chronically elevated 2-AG levels is internalization and decreased protein expression of CB1Rs(Wu et al., 2008), which was also observed in the absence of nNOS/NO signaling. The changes in the eCB pathway components in the absence of nNOS/NO signaling may be the result of structural changes or compensatory mechanisms from altered glutamatergic and GABAergic terminals within the cerebellum. Understanding the interaction between the eCB signaling pathway and NO production in the cerebellum is foundational for discovering the therapeutic potential of cannabis for patients with cerebellar ataxia.

4.6 Acknowledgements

This work was supported by the Canadian Institutes of Health Research (MOP-133504) awarded to W-Y L. VT, and MJEM were awarded Ontario Graduate Scholarships.

4.7 References

Basavarajappa, B. S., & Hungund, B. L. (2005). Role of the endocannabinoid system in the development of tolerance to alcohol. *Alcohol and Alcoholism (Oxford, Oxfordshire)*, *40*(1), 15–24. https://doi.org/10.1093/alcalc/agh111

Bredt, D. S., Hwang, P. M., & Snyder, S. H. (1990). Localization of nitric oxide synthase indicating a neural role for nitric oxide. *Nature*, *347*(6295), 768–770. https://doi.org/10.1038/347768a0

Campese, V. M., Sindhu, R. K., Ye, S., Bai, Y., Vaziri, N. D., & Jabbari, B. (2006). Regional expression of NO synthase , NAD (P) H oxidase and superoxide dismutase in the rat brain. *Brain Research*, *1134*, 27–32. https://doi.org/10.1016/j.brainres.2006.11.067

Carey, M. R., Myoga, M. H., McDaniels, K. R., Marsicano, G., Lutz, B., Mackie, K., & Regehr, W. G. (2011). Presynaptic CB1 Receptors Regulate Synaptic Plasticity at Cerebellar Parallel Fiber Synapses. *Journal of Neurophysiology*, *105*(2), 958–963. https://doi.org/10.1152/jn.00980.2010

Carney, S. T., Lloyd, M. L., MacKinnon, S. E., Newton, D. C., Jones, J. D., Howlett, A. C., & Norford, D. C. (2009). Cannabinoid regulation of nitric oxide synthase i (nNOS) in neuronal cells. *Journal of Neuroimmune Pharmacology*, *4*(3), 338–349. https://doi.org/10.1007/s11481-009-9153-7

Castillo, P. E., Younts, T. J., Chávez, A. E., & Hashimotodani, Y. (2012). Endocannabinoid signaling and synaptic function. *Neuron*, *76*(1), 70–81. https://doi.org/10.1016/j.neuron.2012.09.020

Daniel, H., Levenes, C., & Crépel, F. (1998). Cellular mechanisms of cerebellar LTD. *Trends in Neurosciences*, *21*(9), 401–407. https://doi.org/10.1016/S0166-2236(98)01304-6

Di Marzo, V., & Maccarrone, M. (2008). FAAH and anandamide: is 2-AG really the odd one out? *Trends in Pharmacological Sciences*, *29*(5), 229–233. https://doi.org/10.1016/j.tips.2008.03.001

Gao, Y., Vasilyev, D. V, Goncalves, M. B., Howell, F. V, Hobbs, C., Reisenberg, M., … Doherty, P. (2010). Loss of Retrograde Endocannabinoid Signaling and Reduced Adult Neurogenesis in Diacylglycerol Lipase Knock-out Mice. *Journal of Neuroscience*, *30*(6), 2017–2024. https://doi.org/10.1523/JNEUROSCI.5693-09.2010

Goparaju, S. K., Ueda, N., Yamaguchi, H., & Yamamoto, S. (1998). Anandamide amidohydrolase reacting with 2-arachidonoylglycerol, another cannabinoid receptor ligand. *FEBS Letters*, *422*(1), 69–73. https://doi.org/10.1016/S0014-5793(97)01603-7

Gulyas, A. I., Cravatt, B. F., Bracey, M. H., Dinh, T. P., Piomelli, D., Boscia, F., & Freund, T. F.

(2004). Segregation of two endocannabinoid-hydrolyzing enzymes into pre- and postsynaptic compartments in the rat hippocampus, cerebellum and amygdala. *European Journal of Neuroscience*, *20*(2), 441–458. https://doi.org/10.1111/j.1460-9568.2004.03428.x

Hartmann, J., Henning, H. A., & Konnerth, A. (2011). mGluR1/TRPC3-mediated synaptic transmission and calcium signaling in mammalian central neurons. *Cold Spring Harbor Perspectives in Biology*, *3*(4), 1–16. https://doi.org/10.1101/cshperspect.a006726

Hohmann, A. G., Suplita, R. L., Bolton, N. M., Neely, M. H., Fegley, D., Mangieri, R., … Piomelli, D. (2005). An endocannabinoid mechanism for stress-induced analgesia. *Nature*, *435*(7045), 1108–1112. https://doi.org/10.1038/nature03658

Howlett, A. C. (1987). Cannabinoid inhibition of adenylate cyclase: relative activity of constituents and metabolites of marihuana. *Neuropharmacology*, *26*(5), 507–512. https://doi.org/10.1016/0028-3908(87)90035-9

Imperatore, R., Morello, G., Luongo, L., Taschler, U., Romano, R., De Gregorio, D., … Cristino, L. (2015). Genetic deletion of monoacylglycerol lipase leads to impaired cannabinoid receptor CB 1 R signaling and anxiety-like behavior. *Journal of Neurochemistry*, *135*(4), 799–813. https://doi.org/10.1111/jnc.13267

Jones, J. D., Carney, S. T., Vrana, K. E., Norford, D. C., & Howlett, A. C. (2008). Cannabinoid receptor-mediated translocation of NO-sensitive guanylyl cyclase and production of cyclic GMP in neuronal cells. *Neuropharmacology*, *54*(1), 23–30. https://doi.org/10.1016/j.neuropharm.2007.06.027

Karadayian, A. G., Bustamante, J., Czerniczyniec, A., Lombardi, P., Cutrera, R. A., & Lores-Arnaiz, S. (2015). Alcohol hangover induces mitochondrial dysfunction and free radical production in mouse cerebellum. *Neuroscience*, *304*, 47–59. https://doi.org/10.1016/j.neuroscience.2015.07.012

Kawamura, Y. (2006). The CB1 Cannabinoid Receptor Is the Major Cannabinoid Receptor at Excitatory Presynaptic Sites in the Hippocampus and Cerebellum. *Journal of Neuroscience*, *26*(11), 2991–3001. https://doi.org/10.1523/JNEUROSCI.4872-05.2006

Koziol, L. F., Budding, D. E., & Chidekel, D. (2012). From Movement to Thought: Executive Function, Embodied Cognition, and the Cerebellum. *The Cerebellum*, *11*(2), 505–525. https://doi.org/10.1007/s12311-011-0321-y

Kyriakatos, A., & El Manira, A. (2007). Long-term plasticity of the spinal locomotor circuitry mediated by endocannabinoid and nitric oxide signaling. *The Journal of Neuroscience : The Official Journal of the Society for Neuroscience*, *27*(46), 12664–12674. https://doi.org/10.1523/JNEUROSCI.3174-07.2007

Lévénès, C., Daniel, H., Soubrié, P., & Crépel, F. (1998). Cannabinoids decrease excitatory synaptic transmission and impair long-term depression in rat cerebellar Purkinje cells. *Journal of Physiology*, *510*(3), 867–879. https://doi.org/10.1111/j.1469-7793.1998.867bj.x

Maccarrone, M., Rossi, S., Bari, M., De Chiara, V., Fezza, F., Musella, A., … Centonze, D. (2008). Anandamide inhibits metabolism and physiological actions of 2-arachidonoylglycerol in the striatum. *Nature Neuroscience*, *11*(2), 152–159. https://doi.org/10.1038/nn2042

Maejima, T., Oka, S., Hashimotodani, Y., Ohno-Shosaku, T., Aiba, A., Wu, D., … Kano, M. (2005). Synaptically driven endocannabinoid release requires Ca^{2+}-assisted metabotropic glutamate receptor subtype 1 to phospholipase Cbeta4 signaling cascade in the cerebellum. *The Journal of Neuroscience : The Official Journal of the Society for Neuroscience*, *25*(29), 6826–6835. https://doi.org/10.1523/JNEUROSCI.0945-05.2005

Manto, M., Bower, J. M., Conforto, A. B., Delgado-García, J. M., da Guarda, S. N. F., Gerwig, M., … Timmann, D. (2012). Consensus Paper: Roles of the Cerebellum in Motor Control—The Diversity of Ideas on Cerebellar Involvement in Movement. *The Cerebellum*, *11*(2), 457–487. https://doi.org/10.1007/s12311-011-0331-9

Matyash, V., Filippov, V., Mohrhagen, K., & Kettenmann, H. (2001). Nitric oxide signals parallel fiber activity to Bergmann glial cells in the mouse cerebellar slice. *Molecular and Cellular Neuroscience*, *18*(6), 664–670. https://doi.org/10.1006/mcne.2001.1047

Pan, B., Wang, W., Zhong, P., Blankman, J. L., Cravatt, B. F., & Liu, Q. -s. (2011). Alterations of Endocannabinoid Signaling, Synaptic Plasticity, Learning, and Memory in Monoacylglycerol Lipase Knock-out Mice. *Journal of Neuroscience*, *31*(38), 13420–13430. https://doi.org/10.1523/JNEUROSCI.2075-11.2011

Pouzat, C., & Hestrin, S. (1997). Developmental Regulation of Basket/Stellate Cell→Purkinje Cell Synapses in the Cerebellum. *The Journal of Neuroscience*, *17*(23), 9104–9112. https://doi.org/10.1523/JNEUROSCI.17-23-09104.1997

Rakotomamonjy, J., & Guemez-Gamboa, A. (2019). Purkinje cell survival in organotypic

cerebellar slice cultures. *Journal of Visualized Experiments*, *2019*(154), 60353. https://doi.org/10.3791/60353

Richardson, D., Ortori, C. A., Chapman, V., Kendall, D. A., & Barrett, D. A. (2007). Quantitative profiling of endocannabinoids and related compounds in rat brain using liquid chromatography-tandem electrospray ionization mass spectrometry. *Analytical Biochemistry*, *360*(2), 216–226. https://doi.org/10.1016/j.ab.2006.10.039

Ryu, C., Jang, D. C., Jung, D., Kim, Y. G., Shim, H. G., Ryu, H.-H., … Kim, S. J. (2017). STIM1 regulates somatic Ca^{2+} signals and intrinsic firing properties of cerebellar Purkinje neurons. *The Journal of Neuroscience*, *37*(37), 3973–16. https://doi.org/10.1523/JNEUROSCI.3973-16.2017

Safo, P., Cravatt, B., & Regehr, W. (2006). Retrograde endocannabinoid signaling in the cerebellar cortex. *The Cerebellum*, *5*(2), 134–145. https://doi.org/10.1080/14734220600791477

Safo, P. K., & Regehr, W. G. (2005). Endocannabinoids control the induction of cerebellar LTD. *Neuron*, *48*(4), 647–659. https://doi.org/10.1016/j.neuron.2005.09.020

Savinainen, J. R., Järvinen, T., Laine, K., & Laitinen, J. T. (2001). Despite substantial degradation, 2-arachidonoylglycerol is a potent full efficacy agonist mediating CB 1 receptor-dependent G-protein activation in rat cerebellar membranes. *British Journal of Pharmacology*, *134*(3), 664–672. https://doi.org/10.1038/sj.bjp.0704297

Schlosburg, J. E., Blankman, J. L., Long, J. Z., Nomura, D. K., Kinsey, S. G., Nguyen, P. T., … Cravatt, B. F. (2010). Chronic monoacylglycerol lipase blockade causes functional antagonism of the endocannabinoid system. *Nature Publishing Group*, *13*(9). https://doi.org/10.1038/nn.2616

Shibuki, K., & Okada, D. (1991). Endogenous nitric oxide release required for long-term synaptic depression in the cerebellum. *Nature*, *349*(6307), 326–328. https://doi.org/10.1038/349326a0

Shonesy, B. C., Wang, X., Rose, K. L., Ramikie, T. S., Cavener, V. S., Rentz, T., … Colbran, R. J. (2013). CaMKII regulates diacylglycerol lipase-α and striatal endocannabinoid signaling. *Nature Neuroscience*, *16*(4), 456–463. https://doi.org/10.1038/nn.3353

Su, L.-D., Wang, D.-J., Yang, D., Shen, Y., & Hu, Y.-H. (2013). Retrograde cPLA2α/arachidonic acid/2-AG signaling is essential for cerebellar depolarization-induced suppression of

excitation and long-term potentiation. *Cerebellum (London, England)*, *12*(3), 297–299. https://doi.org/10.1007/s12311-012-0444-9

Sun, H. K., Seok, J. W., Xiao, O. M., Ledent, C., Jin, K., & Greenberg, D. A. (2006). Role for neuronal nitric-oxide synthase in cannabinoid-induced neurogenesis. *Journal of Pharmacology and Experimental Therapeutics*, *319*(1), 150–154. https://doi.org/10.1124/jpet.106.107698

Tapia, M., Dominguez, A., Zhang, W., Puerto, A. Del, Ciorraga, M., Benitez, M. J., … Garrido, J. J. (2017). Cannabinoid receptors modulate neuronal morphology and ankyring density at the axon initial segment. *Frontiers in Cellular Neuroscience*, *11*, 5. https://doi.org/10.3389/fncel.2017.00005

Tellios, V., Maksoud, M. J. E., Xiang, Y. Y., & Lu, W. Y. (2020). Nitric Oxide Critically Regulates Purkinje Neuron Dendritic Development Through a Metabotropic Glutamate Receptor Type 1–Mediated Mechanism. *Cerebellum*, *19*(4), 510–526. https://doi.org/10.1007/s12311-020-01125-7

Wang, D.-J., Su, L.-D., Wang, Y.-N., Yang, D., Sun, C.-L., Zhou, L., … Shen, Y. (2014). Long-Term Potentiation at Cerebellar Parallel Fiber-Purkinje Cell Synapses Requires Presynaptic and Postsynaptic Signaling Cascades. *Journal of Neuroscience*, *34*(6), 2355–2364. https://doi.org/10.1523/JNEUROSCI.4064-13.2014

Willard, S. S., & Koochekpour, S. (2013). Glutamate, glutamate receptors, and downstream signaling pathways. *International Journal of Biological Sciences*, *9*(9), 948–959. https://doi.org/10.7150/ijbs.6426

Wu, D.-F., Yang, L.-Q., Goschke, A., Stumm, R., Brandenburg, L.-O., Liang, Y.-J., … Koch, T. (2008). Role of receptor internalization in the agonist-induced desensitization of cannabinoid type 1 receptors. *Journal of Neurochemistry*, *104*(4), 1132–1143. https://doi.org/10.1111/j.1471-4159.2007.05063.x

Yoshida, Takashi, Inoue, R., Morii, T., Takahashi, N., Yamamoto, S., Hara, Y., … Mori, Y. (2006). Nitric oxide activates TRP channels by cysteine S-nitrosylation. *Nature Chemical Biology*, *2*(11), 596–607. https://doi.org/10.1038/nchembio821

Yoshida, Takayuki, Hashimoto, K., Zimmer, A., Maejima, T., Araishi, K., & Kano, M. (2002). The Cannabinoid CB1 Receptor Mediates Retrograde Signals for Depolarization-Induced

Suppression of Inhibition in Cerebellar Purkinje Cells. *The Journal of Neuroscience*, *22*(5), 1690–1697. https://doi.org/10.1523/JNEUROSCI.22-05-01690.2002

Yoshida, Takayuki, Fukaya, M., Uchigashima, M., Miura, E., Kamiya, H., Kano, M., & Watanabe, M. (2006). Localization of diacylglycerol lipase-alpha around postsynaptic spine suggests close proximity between production site of an endocannabinoid, 2-arachidonoylglycerol, and presynaptic cannabinoid CB1 receptor. *The Journal of Neuroscience, 26*(18), 4740-4751.

Chapter 5 Discussion

5 nNOS/NO signaling regulates neuronal and glial morphology as well as network formation in murine cerebella.

NO derived from nNOS is a key component of cerebellar synaptic plasticity in the form of LTD and has also been implicated in a wide variety of functions related to cerebellar homeostasis, including synaptic transmission and physiological development. Despite the important role of nNOS-derived NO signaling in cerebellar functions, previous studies using $nNOS^{-/-}$ mice have not reported gross anatomical deficits with regards to the morphology of cerebellar cells, despite studies that report behavioural and motor deficits in this mouse model and has since remained largely uncharacterized(Huang, Dawson, Bredt, Snyder, & Fishman, 1993; Kriegsfeld et al., 1999; Nelson et al., 1995). Previous reports have also determined a link between NO production and ataxic behaviours in mutant mouse models of cerebellar ataxia, which report decreases in NO concentrations or NOS activity in association with PN loss or degeneration(Abbott & Nahm, 2004; Rhyu et al., 2003). In addition, the association between neurodegenerative processes and intracellular calcium levels has been heavily established, as chronic increases in intracellular calcium often result in neurodegeneration. Although both NO levels and intracellular calcium levels have been implicated in ataxic behaviours and neurodegeneration, the link between NO production and intracellular calcium regulation is not entirely known. My dissertation focused on characterizing crucial differences within the cerebellum of the $nNOS^{-/-}$ mouse across development. Here, I will discuss my work surrounding nNOS-derived NO signaling on cerebellar neuron and glia development and function, while examining the implications of this work on cerebellar pathologies and excitotoxic disorders.

5.1 Absence of nNOS/NO production during development results in delayed PN dendritic arborization and aberrant mGluR1 signaling.

Although the nNOS$^{-/-}$ mouse displays behavioural deficits associated with movement coordination and balance (Kriegsfeld et al., 1999; Nelson et al., 1995), a general morphological characterization of PNs had not been fully conducted in this mouse strain. We are the first to report distinct alterations in PN morphology of nNOS$^{-/-}$ mice across three developmental time points. Specifically, analyses reported in Chapter 2 showed that the morphological differences in PN dendritic branching were accompanied with decreased total mGluR1 expression, along with alterations associated with the downstream pathway of mGluR1-initiated SOCE.

5.1.1 A lack of NO signaling delays PN dendritic development

One of the significant discoveries found by this study is the robust decrease in PN dendritic branching in nNOS$^{-/-}$ mice specifically at PD7 compared to WT (**Figure 2.3**). In the cerebellum, NO is produced in an activity-dependent manner from PFs/GNs as well as GABAergic interneurons, although at PD7 the latter are not fully developed (D.-J. Wang et al., 2014). The activity-dependent production of NO is essential for the induction of PF-PN synaptic LTD (Boxall & Garthwaite, 1996; Lev-Ram, Jiang, Wood, Lawrence, & Tsien, 1997; Lev-Ram, Makings, Keitz, Kao, & Tsien, 1995), which contributes to spine morphology (Lee, Jung, Arii, Imoto, & Rhyu, 2007). While normal neurite growth relies on optimal levels of calcium influx during development, chronically increased calcium suppresses neurite elongation and growth cone movement, as discovered in culture (Mattson & Kater, 1987). Therefore, a lack of NO signaling may affect intracellular calcium transients within the PN and contribute to the dendritic deficits during the early phase of PN dendritic development.

The early phase of PN dendritic development is characterized by an increase in PN-CF innervation, which decreases within the late phase of PN development until only one CF interacts with one PN(Hashimoto, Ichikawa, Kitamura, Watanabe, & Kano, 2009;

Mason, Christakos, & Catalano, 1990). While my analyses showed no difference in CF innervation at PD7 between WT and nNOS$^{-/-}$ cerebella, increased CF innervation persisted in nNOS$^{-/-}$ mice at 7W when compared to age-matched WT mice (**Figure 2.8**), which may suggest impairments in the late phase of CF synapse elimination during the late phase of development. Elimination of weak CF synapses in the late phase is controlled by mGluR1-mediated PKCγ activation (Kano et al., 1997; Offermanns et al., 1997). Specifically, in mice lacking either mGluR1 or PKCγ protein expression, CF elimination is significantly impaired (Kano et al., 1995, 1997). Moreover, mGluR1-deficient mice result in an abnormal PN morphology similar to that of nNOS$^{-/-}$ PNs reported in my studies (Kano et al., 1997).

In older nNOS$^{-/-}$ cerebella it was noted that PN dendritic spines appeared to have less mushroom-type dendritic spines and more thin-type spines in relation to WT cerebella (**Figure 2.4**). Mushroom spines are often considered to be "memory spines", while thin spines or "learning spines" are transient and unstable, with smaller post-synaptic densities that either increase in strength or degrade completely (Bourne & Harris, 2007; Dumitriu et al., 2010; Mahmmoud et al., 2015). Changes from mushroom spines to thin spines may rely on the size and time-course of calcium dynamics within the synapse, as aberrant connectivity can lead to an accumulation of thin-type spines (Bourne & Harris, 2007).

5.1.2 A lack of NO production results in greater PN calcium entry through mGluR1-initiated SOCE.

My analyses in Chapter 2 uncovered significantly more protein expression of calpain-1, a calcium-dependent protease, in nNOS$^{-/-}$ cerebella – particularly within PNs – compared to WT (**Figure 2.10**). Additionally, calpain-1 expression in WT ex vivo slices was elevated by inhibiting NOS activity via L-NAME or by agonizing mGluR1 via DHPG (**Figure 2.11**). Furthermore, additional experiments revealed greater calcium influx in WT PNs pretreated with the selective nNOS inhibitor 7N when exposed to DHPG, while nNOS$^{-/-}$ PNs pretreated with SNAP attenuated the calcium influx associated with DHPG treatment (**Figure 6.A1**). Elevated intracellular calcium levels with PNs can result in altered dendrite and spine morphology via calcium-dependent activation of calpain. Calpains in neuronal

cells are crucial for the regulation of synaptic plasticity, morphology, and neurodegeneration (Sorimachi, Ishiura, & Suzuki, 1997). Notably, my analyses revealed a significant decrease in β-III-spectrin expression in the cerebella of adult nNOS$^{-/-}$ mice, along with increased calpain-1 expression when compared to cerebella from age-matched WT mice (**Figure 2.10**). Given that β-III-spectrin is necessary for the formation of mushroom-like dendritic spines (Efimova et al., 2017), the reduction of β-III-spectrin in the cerebellum may explain the alterations in dendritic structures and synapses in PNs of nNOS$^{-/-}$ mice.

5.1.3 A lack of NO production results in altered mGluR1 signaling within PNs.

My results reported in Chapter 2 showed that mGluR1 protein expression was significantly decreased in nNOS$^{-/-}$ mice at PD7, 2W and 7W, while PM protein expression of mGluR1 was significantly increased in 7W nNOS$^{-/-}$ cerebella compared to age-matched WT mice (**Figures 2.5, 2.6**). Since mGluR1 is predominately located on PN spine heads, decreased total mGluR1 protein expression may be due to decreased dendritic puncta, noted earlier in Chapter 2 (**Figure 2.4**). As well, decreased PN spine head diameter in nNOS$^{-/-}$ animals can lead to smaller post-synaptic densities and less synaptic mGluR1 protein accommodation within the dendritic spine (Ganeshina, Berry, Petralia, Nicholson, & Geinisman, 2004; Santamaria, Wils, De Schutter, & Augustine, 2006). However, the increased PM localization of mGluR1 in nNOS$^{-/-}$ cerebella appropriately explains the increase in mGluR1-initiated SOCE in comparison to WT (**Figure 6.A1**). In terms of synaptogenesis, activation of mGluR1 leads to the initiation of calcium-dependent protein kinase-C-γ (PKCγ) activity, and subsequent phosphorylation of calmodulin-dependent protein kinase-2β (CaMKIIβ), which has been shown to repress spine synaptogenesis on PNs (Sugawara, Hisatsune, Miyamoto, Ogawa, & Mikoshiba, 2017). Interestingly, a previous study reported that over-stimulation of mGluR1 on cultured hippocampal neurons resulted in prominent dendritic spine elongation into thin spines (Vanderklish & Edelman, 2002).

The changes in mGluR1 protein expression resulted in protein changes downstream of mGluR1, including STIM1 and TRPC3 (**Figures 2.9, 6.A3**). Along with increased PM protein expression of mGluR1 in nNOS$^{-/-}$ mice, significant increases in STIM1 protein expression and clustering were also found at PD7, 2W and 7W (**Figure 2.9**). Following mGluR1 activation, STIM1 proteins oligomerize gate calcium influx through TRPC3 channels (Hartmann et al., 2008, 2014). Therefore, changes in expression levels and oligomerization patterns of STIM1 are indicative of calcium dysregulation (Klejman et al., 2009). Our results displayed increased STIM1 clustering in nNOS$^{-/-}$ PNs, alluding to aberrant calcium entry through a SOCE mechanism. Indeed, a recent study noted the interaction between STIM1 and NO via *S*-nitrosylation results in the prevention of STIM1 oligomerization and further reduction of SOCE (Gui et al., 2018). The absence of NO/*S*-nitrosylation of STIM1 may result in elevated calcium entry through STIM1-gated TRPC3 channels in nNOS$^{-/-}$ PNs, despite decreases in mGluR1 protein expression. As well, my analyses also revealed a significant decrease in TRPC3 protein expression at 7W in nNOS$^{-/-}$ mice compared to WT (**Figure 6.A3**). This decrease may be a result of a negative feedback regulation, which works to adjust calcium entry despite overactivation of mGluR1. A study revealed that TRPC3 can be regulated independently of STIM1, which may explain why TRPC3 does not increase in accordance with STIM1(Dehaven et al., 2009).

5.2 Implications of mGluR1 dysfunction in SCAs.

In human SCAs, mutations within the mGluR1 pathway, including *SPTBN2*, *ITPR1* and *TRPC3* – genes that encode β-III-spectrin, IP3 receptors, and TRPC3 – are affected in SCA5, 15 and 41 respectively, and are crucial in maintaining PN viability and functionality(Armbrust et al., 2014; Becker, 2014; Coutelier et al., 2015; Cvetanovic, 2015; Jin, Kim, Kim, Worley, & Linden, 2007; Kim et al., 2012). Specifically, these gene mutations are similar in that they alter calcium ion dynamics within the PN and result in PN degeneration and loss(Kasumu & Bezprozvanny, 2012; Reitstetter & Yool, 1998; Yang & Lisberger, 2014). Results from Chapter 2 indicate that the nNOS$^{-/-}$ mouse model also harbours similar features to those discovered in human SCAs, including decreased protein expression of β-III-spectrin and TRPC3 (**Figures 2.10, 6.A3**). It is understood that calpain

activity can induce degradation of neuronal cytoskeletal proteins, including α- and β-spectrins, as well as IP3 receptors, which are implicated in the progression of multiple SCAs (Avery, Thomas, & Hays, 2017; Hubener et al., 2013; Löfvenberg & Backman, 1999; Rami, Ferger, & Krieglstein, 1997; Schumacher, Siman, & Fehlings, 2002; Tada, Nishizawa, & Onodera, 2016; Vosler, Brennan, & Chen, 2008). Therefore, the knowledge that nNOS-derived NO signaling may mimic a similar phenotype to that of human SCAs could provide foundational knowledge in better understand the progression of SCA progression as well as other movement disorders associated with the cerebellum.

5.3 nNOS/NO production increases glutamate uptake via GLAST activity on BG.

Our results reported in Chapter 2 indicated that the normal expression of nNOS, and subsequently nNOS-derived NO, is important for the development of PN dendritic arborization and PN calcium homeostasis(Tellios, Maksoud, Xiang, & Lu, 2020). In Specifically, my analyses reported in Chapter 2 revealed that the $nNOS^{-/-}$ mouse exhibits a decrease in mGluR1 protein expression but an overactivation of mGluR1 downstream signaling. These results imply that mGluR1 in PNs is overstimulated by excessive extracellular glutamate. To further understand the cause of mGluR1 overactivation, results from Chapter 3 focused on the relationship between NO production and astrocytic glutamate uptake. Although some evidence suggests that NO regulates GLAST function in the cerebellum(Balderas et al., 2014; Tiburcio-Félix et al., 2019), my thesis work is the first to thoroughly characterize the role of nNOS/NO signaling on GLAST expression and localization, in addition to functionality of cerebellar BGs using WT and $nNOS^{-/-}$ mice. Specifically, Chapter 3 reports two novel findings. First, both BG morphology and GLAST expression across early murine postnatal ages are regulated by nNOS signaling. Second, the PM localization of GLAST is regulated by NO, which facilitates GLAST coupling to the reverse mode NCX activity to mobilize calcium and sodium ions in BG.

5.3.1 nNOS$^{-/-}$ mice display altered BG morphology across postnatal development.

It has previously been reported that BG serve as important mediators of both granule cell differentiation and migration from the EGL to the IGL, in addition to PN dendritic and synaptic growth from the PN layer to the pial surface(Altman, 1972; Ango et al., 2008; Lordkipanidze & Dunaevsky, 2005; Xu et al., 2013). During early postnatal development (PD0 – PD10), BG morphology transitions from distinct smooth lamellar processes that radiate towards the pial surface, to rough radial processes that contain outgrowths that work to ensheath PN synaptic connections with PFs and stellate cells(Lippman, Lordkipanidze, Buell, Yoon, & Dunaevsky, 2008; Yamada et al., 2000). In Chapter 3, my analyses revealed abnormally thick lamellar processes in nNOS$^{-/-}$ cerebella during PD3 and PD7 in comparison to WT (**Figures 3.1, 3.2**). An early study that explored BG morphology in the *weaver* cerebellar mutant mouse reported similarly thick BG lamellar processes, which this group denoted to be the reason behind PN and granule cell degeneration(Bignami & Dahl, 1974). Likewise, the nNOS$^{-/-}$ mouse presents with stark PN dendritic deficits, specifically at PD7(Tellios et al., 2020).

BG are able to influence PN dendritic growth and PN firing through a mechanism involving GLAST activity(Miyazaki et al., 2017; Perkins et al., 2018). In the present study, we observed a notable decrease in GLAST colocalization with PNs in nNOS$^{-/-}$ cerebella compared to WT cerebella (**Figures 3.1-4**). This finding implies the BG ensheathment of PN dendritic spines and synapses by BG is reduced in nNOS$^{-/-}$ cerebella. As BG lamellar processes mature, radial outgrowths wrap around PN dendritic spines and protect synapses from glutamate-induced excitotoxic damage(Lippman et al., 2008; Yamada et al., 2000). Less colocalization between BG processes and PN dendrites in nNOS$^{-/-}$ cerebella might be a driver for the overall decrease in PN mushroom-type spines and overall spine number when compared to WT cerebella(Tellios et al., 2020). Therefore, the PN deficits reported in nNOS$^{-/-}$ mice may be exacerbated by aberrant BG growth, which is supported by multiple studies that report BG-specific deficits lead to the degeneration and loss of PNs(Takatsuru et al., 2006; X. Wang, Imura, Sofroniew, & Fushiki, 2011). Likewise, it is known that nNOS is expressed in supporting cells such as BG and GNs, and not PNs(Ihara

et al., 2006; Kugler & Drenckhahn, 1996; Tiburcio-Félix et al., 2019), therefore, it is possible that the structural and functional deficits of PNs in the nNOS$^{-/-}$ mice are at least partially the result of aberrant BG growth.

5.3.2 NO signaling in necessary for GLAST function.

To examine the functional activity of GLAST, I examined L-aspartate uptake in cultures of WT and nNOS$^{-/-}$ BG and discovered lower levels of both GLAST protein expression and cytosolic concentrations of L-aspartate in nNOS$^{-/-}$ BGs compared to WT BG (**Figure 3.5**). Importantly, Balderas et al., noted higher levels of D-aspartate uptake in cerebellar BG treated with the NO-donor sodium nitroprusside as well as with treatment of the cGMP analogue, dbcGMP(Balderas et al., 2014). This study by Balderas et al., highlighted the importance of the NO-cGMP-PKG pathway in upregulating GLAST activity in vitro. Results from Chapter 3 demonstrated that SNAP treatment on cultured nNOS$^{-/-}$ BG increased the PM expression of GLAST on BG, which was abolished with the blockade of PKG (**Figure 3.7**). However, PKG blockade alone in WT BG did not significantly alter PM expression of GLAST (**Figure 3.6**). In this case, it is apparent that NO signals through PKG to facilitate GLAST trafficking to the PM but does not have a prominent role in the internalizing of GLAST.

5.4 Implications of BG and GLAST dysfunction on excitotoxic neurological disorders.

GLAST is localized to almost all astrocytes of the CNS but has the highest expression in astrocytes of the cerebellum, retina, and hippocampus(Schmitt, Asan, Püschel, & Kugler, 1997). As such, GLAST activity plays an important role in regulating synaptic activity and preventing excitotoxic insults to neurons. In fact, dysfunction of GLAST has been linked to motor disorders such as Parkinson's disease and retinal degeneration(Iovino, Tremblay, & Civiero, 2020; Yanagisawa et al., 2015). This next section will describe the role of GLAST in neurodegenerative disorders such as ataxia and glaucoma.

5.4.1 GLAST dysfunction and ataxia progression.

Both SCA and EA progression are affected by changes to BG and GLAST expression and functionality. Although SCA1 is caused by a mutation in the *ATXN1* gene, reports have shown the loss of the protein ataxin-1 can negatively affect the morphology of BG, while analyses of humans with SCA1 revealed overall less BG compared to healthy controls, which suggests that stimulating BG activity and proliferation might be beneficial for treating this form of SCA(Cvetanovic, 2015; Shiwaku, Yagishita, Eishi, & Okazawa, 2013). Similar to SCAs, EA is a neurological condition originating in the cerebellum that transiently affects movement coordination (Orsucci, Raglione, Mazzoni, & Vista, 2019). Like SCAs, there are multiple types of EAs that present with various genetic mutations, in particular SLC1A3 – a gene that encodes EAAT1 in humans and leads to the progression of EA6 (Iwama et al., 2018; Jen & Wan, 2018). Although the severity of the PN deficit is currently unclear in clinical cases of EA6, characterization of the GLAST$^{-/-}$ mouse model showed a large detriment to PN synaptic transmission and development(Miyazaki et al., 2017). Understanding the relationship between NO and GLAST functionality may bring to light novel ways to increase BG activity and GLAST expression to ameliorate motor deficits seen in various ataxias.

5.4.2 GLAST dysfunction and glaucoma progression.

Glaucoma is the second leading cause of irreversible blindness worldwide, projected to affect nearly 112 million people by 2040, with no known cause or cure(Tham et al., 2014). As a progressive optic neuropathy, glaucoma results in retinal ganglion cell (RGC) death along with optic nerve degeneration, and leads to progressive vision loss(Weinreb, Aung, & Medeiros, 2014). Despite being a neurodegenerative disease, current glaucoma treatments do not target neuronal dysfunction. One potential overlooked mechanism of onset for glaucoma lists glutamate excitotoxicity as a cause of RGC death(Gupta & Yücel, 2007). In this case, overstimulated glutamate receptors on neurons can lead to cell death and progressive vision loss characteristic of glaucoma(Guo et al., 2006; Gupta & Yücel, 2007). Similar to the cerebellum, the retina also contains specialized radial astrocytes similar to BG, termed Müller glia (MG) that control glutamate uptake via GLAST and maintain RGC functionality(Harada et al., 2007). A recent study focused on

ways to upregulate GLAST protein expression in MG in order to reduce the excessive amount of free glutamate within the synaptic cleft and combat RGC degeneration that is prevalent in the retina of GLAST$^{+/-}$ mice(Yanagisawa et al., 2015). However, a clinical study had shown that mutations in the GLAST gene across patients with glaucoma are not significantly different than control subjects(Nishisako et al., 2016). Despite no common alteration in gene structure, post-mortem immunohistological analyses of human glaucomatous eyes revealed less GLAST immunostaining on the MG membrane compared to control samples(Naskar, Vorwerk, & Dreyer, 2000). Therefore, investigating potential upstream regulators of GLAST protein function and localization, such as NO, rather than gene expression could reveal potential targets for future glaucoma medications.

Interestingly, NO levels are decreased both with age as well as within glaucomatous eyes(Doganay, Evereklioglu, Turkoz, & Er, 2002). With the rise of NO-donating glaucoma treatments within the pharmaceutical industry, it is important to determine the potential neurological effect of NO treatment on the retina(Cavet, Vittitow, Impagnatiello, Ongini, & Bastia, 2014). Understanding the full potential of NO beyond its already established vasodilating effects may help to broaden the scope of current glaucoma therapies, which only target intraocular pressure symptoms, to therapies that may remedy the neurodegeneration ubiquitously present across all glaucomatous patients.

5.5 NO production regulates eCB synthesis in the cerebellum via the mGluR1 pathway.

In addition to initiating SOCE signaling, mGluR1 activation is concurrently responsible for 2-AG production in the cerebellum. Importantly, my analyses in Chapter 4 revealed a significant increase in basal levels of 2-AG in 2W and 7W nNOS$^{-/-}$ cerebella compared to age-matched WT cerebella (**Figure 4.1**). 2-AG is an important neurotransmitter responsible for the activation of CB1Rs and at physiological levels, 2-AG works to induce LTD within the PN in addition to termination of synaptic transmission at the PF-PN synapse(Lévénès, Daniel, Soubrié, & Crépel, 1998; Safo & Regehr, 2005; Yoshida et al., 2002). Likewise, NO has been shown to be crucial in regulating PN LTD,

specifically by affecting calcium transients within the PN, particularly via mGluR1-initiated SOCE(Tellios et al., 2020). In Chapter 2, my thesis work revealed that a lack of NO within the cerebellum resulted in an overactivation of mGluR1, which leads to increased calcium entry into the PN and activation of calcium-dependent proteases such as calpain-1 (**Figure 2.10**). Therefore, a lack of NO production during development affects both SOCE and eCB production primarily through the mGluR1 pathway. To further corroborate this information, my analyses revealed a significant increase in DAGLα expression – an enzyme responsible for 2-AG synthesis downstream of mGluR1 activation – in nNOS$^{-/-}$ cerebella at PD7 and 2W timepoints compared to age-matched WT cerebella (**Figures 4.2-4**). Interestingly, the increase in 2-AG levels in nNOS$^{-/-}$ cerebella can also be attributed to the decrease in 2-AG hydrolyzing enzymes such as FAAH and MGL at 7W when compared to WT cerebella (**Figures 4.8, 4.9**).

5.6 Implications of the eCB pathway on cerebellar dysfunction.

Chronic increases in eCBs, as we noted in the nNOS$^{-/-}$ mouse model, have been previously shown to result in an internalization of CB1Rs and likewise, my analyses in Chapter 4 revealed a similar trend, where CB1R expression was significantly decreased in 2W and 7W nNOS$^{-/-}$ cerebella compared to age-matched WT cerebella (**Figures 4.6, 4.7**). As a prominent control of the overall output of the cerebellar cortex, CB1Rs could act as a good therapeutic site for synaptic modulation. However, the effects of CB1R antagonism/agonism in treating symptoms of ataxia have been equivocal within the literature. The next section will discuss the current literature on the role of the eCB pathway in movement disorders.

5.6.1 Using the eCB pathway as a potential therapeutic in treating motor disorders.

Anecdotal evidence points to the use of cannabis as a useful agent in alleviating symptoms of various movement disorders such as ataxia, tremors, and pain. Preclinical studies have shown that overactivation of CB1Rs within the cerebellum can lead to an

ataxic phenotype that can be modulated via CB1R antagonists(DeSanty & Dar, 2001; Patel & Hillard, 2001). Interestingly, $CB1R^{-/-}$ mice display a progressive ataxic phenotype, in which younger animals do not present with behavioural deficits, while older mice display deficits in motor function and coordination, which suggests that long term loss of CB1R expression may contribute to the ataxic phenotype(Bilkei-Gorzo et al., 2005; Kishimoto & Kano, 2006). This finding is particularly interesting, as my analyses on CB1R expression in $nNOS^{-/-}$ cerebella showed a similar progressive loss of CB1Rs at older developmental timepoints (**Figures 4.6, 4.7**). However, the clinical data associated with cannabis use to treat ataxic symptoms remains inconclusive. Some clinical data suggest that oral THC or inhaled cannabis compounds improved motor coordination in patients with multiple sclerosis, while post-mortem studies of SCA patients revealed an increase in postsynaptic CB1R expression, attributed to increased PN degeneration(Fernández-Ruiz et al., 2011; Hill, Williams, Whalley, & Stephens, 2012; Rodríguez-Cueto et al., 2014). In the early phases of Parkinson's disease progression, CB1R protein expression is low, while late phases of Parkinson's disease progression is presented with elevated levels of CB1R protein expression(Arjmand et al., 2015; García-Arencibia et al., 2009). The sensitivity of CB1Rs during the time course of different neuropathologies with similar symptoms suggests that the use of cannabis as a therapeutic for motor disorders should be considered on a neuropathology-specific basis. It is important to observe the eCB system as being in a delicate balance, as both increases as well as decreases in eCB signaling within the cerebellum may lead to the progression of symptoms of ataxia.

5.7 Known limitations to this study.

Although the work presented in this dissertation uncovered new information on the $nNOS^{-/-}$ mouse model with regards to postnatal development of the cerebellum, it is important to acknowledge certain shortcomings associated with the methodology and the experimental design. First, it is important to note that the $nNOS^{-/-}$ mouse model used throughout this dissertation is a global knockout of the nNOS gene. Due to this design, it was difficult for our group to discern the effects of one specific component to the rest of the cerebellar network. To combat this, conditional knockout models of the nNOS gene in

GNs or BG would be helpful in determining each cell's supporting role in PN growth and development.

Secondly, the experiments within this dissertation measured differences in protein expression using western blotting techniques; however, we understand that a difference in protein expression alone does not equate to differences in activity level of the protein. To address this limitation, enzymatic activity assays (particularly in the case of calpain-1 and DAGLα) can be conducted to determine whether increases in protein expression can be equated to increases in the function of these enzymes. Following closely to this limitation, it is also important to note that some proteins assayed within this dissertation are not cell specific; rather, proteins such as STIM1 and calpain-1 are abundantly expressed in PN, yet also ubiquitously expressed by other cerebellar cells. Therefore, localizing one specific protein and its expression to a specific cell type in vivo can be difficult. In these cases, we worked to increase the specificity of our data to the cell type of interest by comparing total cerebellar expression of a protein with immunohistochemical analyses within a certain cell type, such as the PN. However, future studies can address this concern by creating conditional knockouts of specific proteins within specific cerebellar cell types to determine its effect on cerebellar and PN growth and development.

5.8 Concluding remarks and future directions.

PNs comprise the sole output response of the cerebellum, and as such, they are crucial in regulating cerebellar function and motor coordination in conjunction with the cerebral cortex. Results from my studies revealed that global deletion of the gene responsible for nNOS expression disrupts normal cerebellar development by delaying PN dendritic growth and disrupting calcium homeostasis via overactivation of mGluR1. Overactivation of mGluR1 resulted in elevated levels of intracellular calcium within the PN via mGluR1-initiated SOCE. Increases in intracellular calcium levels within $nNOS^{-/-}$ PNs was associated with increases in calpain-1, leading to PN dendritic degeneration across all developmental time points assayed in my studies.

The relative overactivation of mGluR1 in nNOS$^{-/-}$ cerebella is complimented with a decrease in GLAST expression on BG across all studied time points. A decrease in GLAST corresponded to a decrease in glutamate uptake in an in vitro environment. Likewise, application of exogenous NO was able to increase GLAST expression in nNOS$^{-/-}$ cerebella in an ex vivo model.

Overactivation of mGluR1 was found to have repercussions on both the SOCE component of the signaling cascade as well as 2-AG synthesis. Chronic elevations of 2-AG within the nNOS$^{-/-}$ cerebellum resulted in less CB1R expression in relation to WT in adult ages. Overall, this thesis is the first to thoroughly characterize the cerebellar microenvironment of nNOS$^{-/-}$ mice across development. A summary of these findings can be found in **Figure 5.1**. The findings within these studies point to the nNOS$^{-/-}$ mouse model as a potential cerebellar ataxia model. The foundational work presented in this thesis implicates NO as a critical regulator of mGluR1 activity, but some questions remain that may be examined in future cerebellar research, which will be discussed in the sections to follow.

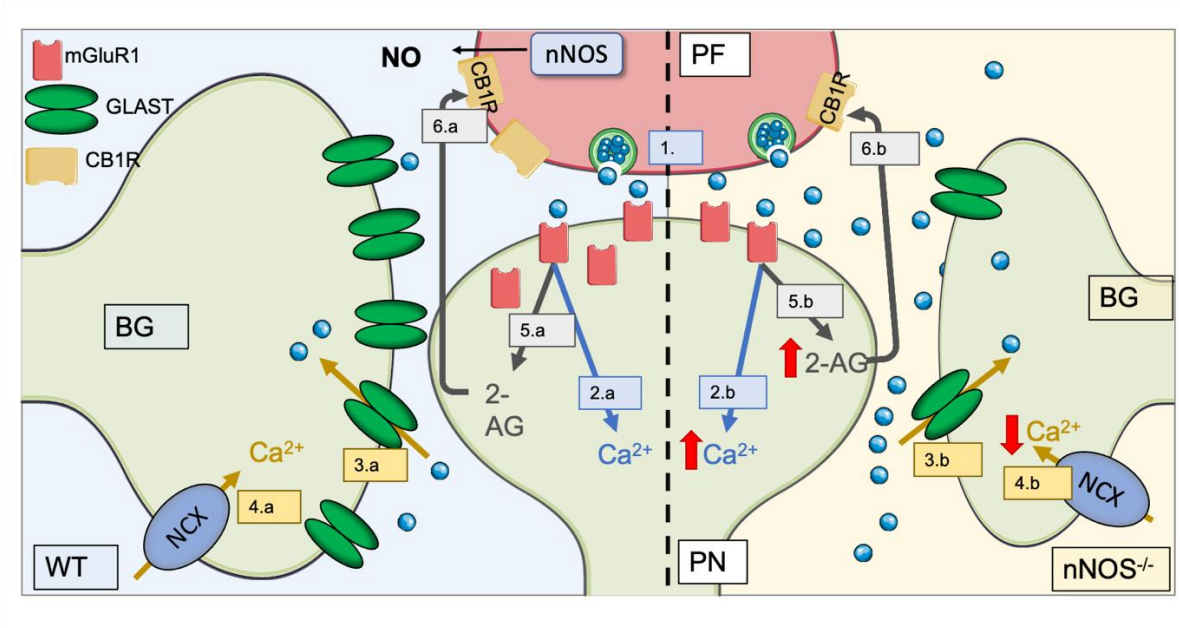

**** Figure legend on next page ****

Figure 5.1 Summary schematic of PF-PN dynamics between WT and nNOS$^{-/-}$ mice.

The left side of this figure depicts a WT glutamatergic tripartite synapse consisting of the presynaptic PF, postsynaptic PN, and BG, while the right side depicts an nNOS$^{-/-}$ tripartite synapse. (**1**) Glutamate is released from the PF and binds to mGluR1 receptors on PNs. *Left side (WT):* (**2.a**) Through a Gq signaling cascade, mGluR1 activation stimulates the production of IP3 in PNs, leading to IP3R activation and subsequent calcium efflux from internal ER stores to the PN cytosol. (**3.a**) Glutamate within the PF-PN synaptic cleft is then taken up by BG via GLAST activity. (**4.a**) Glutamate transporter via GLAST triggers reversal of the NCX, leading to increases in calcium within the BG cytosol. (**5.a**) In addition to mGluR1-initated SOCE, mGluR1 activation also triggers the production of 2-AG. (**6.a**) 2-AG retroactively signals to CB1Rs, a Gi protein-coupled receptor, which works to inhibit glutamate release in the presynaptic terminal. *Right side (nNOS$^{-/-}$)*: (**2.b**) Excessive mGluR1 activation results in ER calcium depletion, increased STIM1 oligomerization, and overall increases in PN SOCE in mice lacking nNOS expression. (**3.b**) Overactivation of mGluR1 is exacerbated by excess glutamate within the PF-PN synaptic cleft, as a result of decreased BG GLAST expression and decreased glutamate uptake by nNOS$^{-/-}$ BG. (**4.b**) As a result of the lack of NO as well as decreased glutamate uptake, the NCX transports less calcium into the BG cytosol in nNOS$^{-/-}$ mice. (**5.b**) Overactivation of mGluR1 also contributes to elevated 2-AG levels within older ages of nNOS$^{-/-}$ mice. (**6.b**) Excessive 2-AG may contribute to lower CB1R expression within nNOS$^{-/-}$ mice, and therefore perpetuating the cycle of mGluR1 overaction within the PF-PN synapse.

5.8.1 Does PN dendritic arborization affect supporting cell morphology?

The results presented within Chapters 2 and 3 revealed morphological deficits in both PN dendrites and synapses, as well as BG lamellar processes. Considering the close interaction between PN and supporting glia during cerebellar development, a question remains as to whether glial deficits result in PN morphological delays, PN deficits cause glial morphological abnormalities, or whether both deficits occur independently of each other. As BG lamellar processes mature, radial outgrowths wrap around PN dendritic spines and protect synapses from excitotoxic damage(Lippman et al., 2008; Yamada et al., 2000). My analyses from Chapter 2 showed that in adult nNOS$^{-/-}$ mice, there was an overall decrease in PN spine number as well as mushroom-type spines in comparison to WT mice(Tellios et al., 2020). Therefore, it may be the case that PN deficits reported in nNOS$^{-/-}$ mice may be the consequence of aberrant BG growth, which is supported by multiple studies that report BG-specific deficits led to the degeneration and loss of PNs(Takatsuru et al., 2006; X. Wang et al., 2011). Likewise, it is known that nNOS is expressed in supporting cells such as BGs, and not PNs(Ihara et al., 2006; Kugler & Drenckhahn, 1996; Tiburcio-Félix et al., 2019), therefore, it is possible that the structural and functional deficits of PNs in the nNOS$^{-/-}$ mice may be at least partially the result of aberrant BG growth. Future studies should explore whether the absence of nNOS-derived NO production negatively affects PN morphology independently or as a consequence of aberrant BG development.

5.8.2 Is glutamate uptake in PNs also altered in nNOS$^{-/-}$ mice and does this correspond to differences in GABA production?

Results from Chapter 3 revealed a novel role for NO in regulating glutamate uptake via GLAST on BG. Although glutamate uptake via GLAST makes up around 90% of the total glutamate uptake within the cerebellum, neuronal glutamate uptake also plays a unique role in synaptic transmission regulation(Martínez-Lozada, Hernández-Kelly, Aguilera, López-Bayghen, & Ortega, 2011). In particular, EAAT4 is a PN-specific glutamate transporter that is responsible for the remaining 10% of glutamate clearance

within the cerebellum(Martínez-Lozada et al., 2011). Located in the perisynaptic region of PN dendritic spines, EAAT4 is responsible for preventing any spill-over of glutamate outside of the synaptic cleft that may occur, thereby containing synaptic transmission within a particular synaptic cleft. Although the deficits observed in EAAT4$^{-/-}$ mice are not as severe as EAAT1$^{-/-}$ mice, EAAT4$^{-/-}$ PNs display aberrant PN firing, specifically within the mGluR1-mediated EPSC(Nikkuni, Takayasu, Iino, Tanaka, & Ozawa, 2007; Perkins et al., 2018). In particular, this group noted that EAAT4$^{-/-}$ PNs exhibit larger mGluR1 activation compared to WT mice, similar to the mGluR1 overactivation demonstrated in nNOS$^{-/-}$ mice(Nikkuni et al., 2007). Furthermore, a crucial cytoskeletal protein involved in anchoring EAAT4 to the PN cell membrane is β-III-spectrin, which results from Chapter 2 revealed to be significantly downregulated in nNOS$^{-/-}$ mice compared to WT (**Figure 2.10**). The consequences of reduced EAAT4 activity in PNs may result in an overall decrease in GABA output via less conversion of intracellular glutamate, which may be another factor that can affect movement output(Nanri et al., 2013). Future studies should identify whether PN-specific glutamate uptake is altered in nNOS$^{-/-}$ mice, and whether changes in EAAT4 expression result in overall changes in PN GABA production.

5.8.3 How is the activity of GLAST coupled to the activity of the NCX in the reverse mode in BG?

Previous reports discuss the relationship between GLAST and NCX activity(S Kirischuk, Kettenmann, & Verkhratsky, 1997; Sergei Kirischuk, Kettenmann, & Verkhratsky, 2007; Rose, Ziemens, & Verkhratsky, 2020). As described in Chapter 3, inhibiting endogenous nNOS activity in WT BG resulted in a significant decrease in the Ca^{2+}/Na^{+} ratio when compared to control WT BG, while supplementing NO to the nNOS$^{-/-}$ BG significantly elevated the Ca^{2+}/Na^{+} influx when compared to control nNOS$^{-/-}$ BG (**Figures 3.8, 3.9**). Although these results confirm that NO critically controls the coupled activity of GLAST and NCX, it remains unknown how this coupling occurs, as well as the role NO has in facilitating this GLAST-NCX coupled activity. A previous study noted the characteristic calcium influx induced by the co-transport of either glutamate or D-aspartate with sodium leads to the activation of the NCX(Takuma, Ago, & Matsuda, 2013). Furthermore, it is known that NO can affect the direction of NCX activity from the forward

to the reverse mode, allowing calcium entry into BG(Asano et al., 2002; Secondo et al., 2011). It has been speculated that the NO-cGMP-PKG pathway is implicated in the reversal of the channel however, whether NO production occurs prior to NCX reversal or as a result of NCX reversal remains unknown(Takuma et al., 2013). Further analysis of the coupling between GLAST and the NCX in relation to NO signaling would provide insight into novel therapeutic options for glutamate transporter dysfunction.

5.8.4 Are CB1Rs differentially regulated in glutamatergic and GABAergic presynaptic terminals?

As described in Chapter 4, CB1R expression in nNOS$^{-/-}$ mice is differentially regulated according to postnatal developmental timepoint. Specifically, my analyses in Chapter 4 revealed increased CB1R expression at PD7 in nNOS$^{-/-}$ cerebella compared to WT cerebella, while 2W and 7W nNOS$^{-/-}$ cerebella showed decreased CB1R expression compared to age-matched WT cerebella (**Figures 4.6, 4.7**). Although inhibitory interneurons such as BCs and SCs express CB1Rs within the cerebellum, this inhibitory interneuron innervation PNs only occurs at around PD10(Pouzat & Hestrin, 1997). Therefore, the CB1R expression measured at PD7 is likely associated with PF terminals. Interestingly, results from Chapter 2 revealed a significant downregulation of vGluT1, a marker for PF terminals, in PD7 nNOS$^{-/-}$ cerebella compared to age-matched WT cerebella(Tellios et al., 2020). Previous literature has demonstrated that activation of CB1R at glutamatergic terminals led to a decrease in excitatory synaptic transmission, which may also account for the decrease in vGluT1 expression in the cerebella of nNOS$^{-/-}$ mice at PD7(P. E. Castillo, Younts, Chávez, & Hashimotodani, 2012).

As our group noted elevated levels of 2-AG at both 2W and 7W of age, it is likely that chronic 2-AG elevation within nNOS$^{-/-}$ cerebella results in downregulation of CB1R protein expression at these timepoints. It could also be the case that a lack of nNOS/NO signaling may differentially affect CB1Rs on glutamatergic and GABAergic synaptic terminals. As previously mentioned, inhibitory interneurons such as BCs and stellate cells begin to innervate PNs at around 2W, and axon terminals from BCs form pinceau synapses that surround the axon hillock of PNs at this time point(Pouzat & Hestrin, 1997). We

specifically discovered a striking difference in CB1R expression specifically on pinceau synapses that are localized to the PN axon hillock at 7W in nNOS$^{-/-}$ cerebella, which may contribute to the overall downregulate of CB1Rs at this timepoint (**Figures 4.6, 4.7**). As CB1R expression is mostly associated with inhibitory interneuron terminals, global decreases in cerebellar CB1R expression at 2W and 7W in nNOS$^{-/-}$ mice may not accurately depict individual changes in glutamatergic and GABAergic terminals. Future studies should explore whether retrograde eCB signaling is different between glutamatergic and GABAergic neurons within the cerebellum.

5.8.5 Is NO supplementation a feasible therapeutic in treating cerebellar disorders?

Taken together, results from my thesis work revealed deficits in cerebellar network formation as a result of a global lack of nNOS-derived NO production. NO is a hotly disputed molecule in terms of its role in physiological and pathological contexts. In general, chronically elevated NO concentrations have proven detrimental in a variety of neurological pathologies, such as stroke, multiple sclerosis, and glaucoma(J. Castillo, Rama, & Dávalos, 2000; Eliasson et al., 1999; Lu, Chen, Chang, Chiang, & Yao, 2014; Neufeld, 1999). In pathologies such as stroke, NO levels increase as a result of excitotoxicity and subsequently results in decreased neuron survival. Specifically, NO as a free radical can oxidize and form reactive oxygen and nitrogen species in high concentrations that are detrimental to cell metabolism, and eventually induce apoptosis(Osborne, 2010). In excitotoxic environments within the cerebral cortex, NMDARs are coupled with the production of NO via nNOS, in that overactivation of NMDARs on neurons results in a chronic influx of calcium, consequently causing the overactivation of nNOS and the overproduction of NO(Prilloff, Noblejas, Chedhomme, & Sabel, 2007; Sucher, Lei, & Lipton, 1991). Additionally, stressed or dying cells can release cytokines such as TNF-α, which can trigger the expression and activation of iNOS within neurons and supporting cells(Tezel, 2008). NO production via iNOS activity occurs as a burst effect, releasing higher levels of NO in a shorter period of time, and has often been deemed the culprit of pathologically elevated NO levels(Colasanti & Suzuki, 2000).

Despite the detrimental effect NO may have at pathologically high concentrations, physiological levels of NO are crucial in maintaining normal neuronal structure and function. Importantly, a lack of NO can produce effects that are equally as harmful to neuronal homeostasis as an excess of NO, as demonstrated by my work characterizing $nNOS^{-/-}$ mice, as well as in neuropathologies such as Huntington's disease and to some degree schizophrenia and depression(Norris, Waldvogel, Faull, Love, & Emson, 1996; Xing, Chavko, Zhang, Yang, & Post, 2002). In the cerebellum specifically, PNs have the added benefit of not expressing NMDARs on their cell membranes, which may alleviate the detrimental effects of excess NO production in these cells. However, maintaining physiologically appropriate levels of NO via exogenous application may be difficult, as NO is a highly diffusible and transient molecule. Although there have been recent advances in optimizing the slow release of NO for neurological targets, using NO as a widescale therapeutic may be tricky(Horton et al., 2018). As mentioned previously, multiple animal models of SCA have identified a decrease in cerebellar NOS activity, highlighting a common deficit associated with this pathology(Abbott & Nahm, 2004; Rhyu et al., 2003). In order to avoid the unpredictability of exogenous NO supplementation, clinical therapeutics often target downstream effectors of NO, such as cGMP or PKG, in order to elicit similar effects. Gaining a better understanding of what interacts with NO in the cerebellum is the first step in conceptualizing therapeutics to combat motor deficits. Future studies should determine the efficacy of targeting cGMP analogues or PKG modulators as a potential therapeutic in cerebellar disorders.

5.9 References

Abbott, L. C., & Nahm, S. (2004). Neuronal nitric oxide synthase expression in cerebellar mutant mice. *Cerebellum (London, England)*, *3*(3), 141–151. https://doi.org/10.1080/14734220410031927

Altman, J. (1972). Postnatal Development of the Cerebellar Cortex in the Rat I. *The Journal of Comparative Neurology*, *145*(3), 353–398.

Ango, F., Wu, C., Van Der Want, J. J., Wu, P., Schachner, M., & Huang, Z. J. (2008). Bergmann glia and the recognition molecule CHL1 organize GABAergic axons and direct innervation of Purkinje cell dendrites. *PLoS Biology*, *6*(4), 739–756. https://doi.org/10.1371/journal.pbio.0060103

Arjmand, S., Vaziri, Z., Behzadi, M., Abbassian, H., Stephens, G. J., & Shabani, M. (2015, October 1). Cannabinoids and Tremor Induced by Motor-related Disorders: Friend or Foe? *Neurotherapeutics*. Springer New York LLC. https://doi.org/10.1007/s13311-015-0367-5

Armbrust, K. R., Wang, X., Hathorn, T. J., Cramer, S. W., Chen, G., Zu, T., … Ranum, L. P. W. (2014). Mutant β-III spectrin causes mGluR1α mislocalization and functional deficits in a mouse model of spinocerebellar ataxia type 5. *The Journal of Neuroscience : The Official Journal of the Society for Neuroscience*, *34*(30), 9891–9904. https://doi.org/10.1523/JNEUROSCI.0876-14.2014

Asano, S., Matsuda, T., Takuma, K., Kim, H. S., Sato, T., Nishikawa, T., & Baba, A. (2002). Nitroprusside and Cyclic GMP Stimulate Na^{+}-Ca^{2+} Exchange Activity in Neuronal Preparations and Cultured Rat Astrocytes. *Journal of Neurochemistry*, *64*(6), 2437–2441. https://doi.org/10.1046/j.1471-4159.1995.64062437.x

Avery, A. W., Thomas, D. D., & Hays, T. S. (2017). β-III-spectrin spinocerebellar ataxia type 5 mutation reveals a dominant cytoskeletal mechanism that underlies dendritic arborization. *Proceedings of the National Academy of Sciences of the United States of America*, *114*(44), E9376–E9385. https://doi.org/10.1073/pnas.1707108114

Balderas, A., Guillem, A. M., Martínez-Lozada, Z., Hernández-Kelly, L. C., Aguilera, J., & Ortega, A. (2014). GLAST/EAAT1 regulation in cultured Bergmann glia cells: Role of the NO/cGMP signaling pathway. *Neurochemistry International*, *73*(1), 139–145. https://doi.org/10.1016/j.neuint.2013.10.011

Becker, E. B. E. (2014). The Moonwalker Mouse: New Insights into TRPC3 Function, Cerebellar Development, and Ataxia. *Cerebellum*, *13*(5), 628–636. https://doi.org/10.1007/s12311-014-0564-5

Bignami, A., & Dahl, D. (1974). The development of bergmann glia in mutant mice with cerebellar malformations: Reeler, staggerer and weaver. Immunofluorescence study with antibodies to the glial fibrillary acidic protein. *The Journal of Comparative Neurology*, *155*(2), 219–229. https://doi.org/10.1002/cne.901550207

Bilkei-Gorzo, A., Racz, I., Valverde, O., Otto, M., Michel, K., Sarstre, M., & Zimmer, A. (2005). Early age-related cognitive impairment in mice lacking cannabinoid CB1 receptors. *Proceedings of the National Academy of Sciences of the United States of America*, *102*(43), 15670–15675. https://doi.org/10.1073/pnas.0504640102

Bourne, J., & Harris, K. M. (2007). Do thin spines learn to be mushroom spines that remember? *Current Opinion in Neurobiology*, *17*(3), 381–386. https://doi.org/10.1016/j.conb.2007.04.009

Boxall, A. R., & Garthwaite, J. (1996). Long-Term Depression in Rat Cerebellum Requires both NO Synthase and NO-sensitive Guanylyl Cyclase. *European Journal of Neuroscience*, *8*(10), 2209–2212. https://doi.org/10.1111/j.1460-9568.1996.tb00743.x

Castillo, J., Rama, R., & Dávalos, A. (2000). Nitric Oxide–Related Brain Damage in Acute Ischemic Stroke. *Stroke*, *31*(4), 852–857. https://doi.org/10.1161/01.STR.31.4.852

Castillo, P. E., Younts, T. J., Chávez, A. E., & Hashimotodani, Y. (2012). Endocannabinoid signaling and synaptic function. *Neuron*, *76*(1), 70–81. https://doi.org/10.1016/j.neuron.2012.09.020

Cavet, M. E., Vittitow, J. L., Impagnatiello, F., Ongini, E., & Bastia, E. (2014). Nitric Oxide (NO): An Emerging Target for the Treatment of Glaucoma. *Investigative Opthalmology & Visual Science*, *55*(8), 5005. https://doi.org/10.1167/iovs.14-14515

Colasanti, M., & Suzuki, H. (2000). The dual personality of NO. *Trends in Pharmacological Sciences*, *21*(7), 249–252. https://doi.org/10.1016/S0165-6147(00)01499-1

Coutelier, M., Blesneac, I., Monteil, A., Monin, M. L., Ando, K., Mundwiller, E., … Stevanin, G. (2015). A recurrent mutation in CACNA1G alters Cav3.1 T-type calcium-channel conduction and causes autosomal-dominant cerebellar ataxia. *American Journal of Human Genetics*, *97*(5), 726–737. https://doi.org/10.1016/j.ajhg.2015.09.007

Cvetanovic, M. (2015). Decreased Expression of Glutamate Transporter GLAST in Bergmann Glia Is Associated with the Loss of Purkinje Neurons in the Spinocerebellar Ataxia Type 1. *Cerebellum*, *14*(1), 8–11. https://doi.org/10.1007/s12311-014-0605-0

Dehaven, W. I., Jones, B. F., Petranka, J. G., Smyth, J. T., Tomita, T., Bird, G. S., & Putney, J. W. (2009). TRPC channels function independently of STIM1 and Orai1. *Journal of Physiology*, *587*(10), 2275–2298. https://doi.org/10.1113/jphysiol.2009.170431

DeSanty, K. P., & Dar, M. S. (2001). Cannabinoid-induced motor incoordination through the cerebellar CB1 receptor in mice. *Pharmacology Biochemistry and Behavior*, *69*(1–2), 251–259. https://doi.org/10.1016/S0091-3057(01)00539-1

Doganay, S., Evereklioglu, C., Turkoz, Y., & Er, H. (2002). Decreased Nitric Oxide Production in Primary Open-Angle Glaucoma. *European Journal of Ophthalmology*, *12*(1), 44–48. https://doi.org/10.1177/112067210201200109

Dumitriu, D., Hao, J., Hara, Y., Kaufmann, J., Janssen, W. G. M., Lou, W., … Morrison, J. H. (2010). Selective Changes in Thin Spine Density and Morphology in Monkey Prefrontal Cortex Correlate with Aging-Related Cognitive Impairment. *Journal of Neuroscience*, *30*(22), 7507–7515. https://doi.org/10.1523/JNEUROSCI.6410-

09.2010

Efimova, N., Korobova, F., Stankewich, M. C., Moberly, A. H., Stolz, D. B., Wang, J., … Svitkina, T. (2017). βIII Spectrin Is Necessary for Formation of the Constricted Neck of Dendritic Spines and Regulation of Synaptic Activity in Neurons. *The Journal of Neuroscience*, *37*(27), 6442–6459. https://doi.org/10.1523/JNEUROSCI.3520-16.2017

Eliasson, M. J., Huang, Z., Ferrante, R. J., Sasamata, M., Molliver, M. E., Snyder, S. H., & Moskowitz, M. A. (1999). Neuronal nitric oxide synthase activation and peroxynitrite formation in ischemic stroke linked to neural damage. *The Journal of Neuroscience : The Official Journal of the Society for Neuroscience*, *19*(14), 5910–5918. Retrieved from http://www.ncbi.nlm.nih.gov/pubmed/10407030

Fernández-Ruiz, J., Moreno-Martet, M., Rodríguez-Cueto, C., Palomo-Garo, C., Gõmez-Cañas, M., Valdeolivas, S., … Ramos, J. A. (2011, August). Prospects for cannabinoid therapies in basal ganglia disorders. *British Journal of Pharmacology*. Wiley-Blackwell. https://doi.org/10.1111/j.1476-5381.2011.01365.x

Ganeshina, O., Berry, R. W., Petralia, R. S., Nicholson, D. A., & Geinisman, Y. (2004). Synapses with a segmented, completely partitioned postsynaptic density express more AMPA receptors than other axospinous synaptic junctions. *Neuroscience*, *125*(3), 615–623. https://doi.org/10.1016/J.NEUROSCIENCE.2004.02.025

García-Arencibia, M., García, C., Kurz, A., Rodríguez-Navarro, J. A., Gispert-Sánchez, S., Mena, M. A., … Fernández-Ruiz, J. (2009). Cannabinoid CB1 receptors are early DownRegulated followed by a further UpRegulation in the basal Ganglia of mice with deletion of specific park genes. *Journal of Neural Transmission, Supplementa*, (73), 269–275. https://doi.org/10.1007/978-3-211-92660-4_22

Gui, L., Zhu, J., Lu, X., Sims, S. M., Lu, W.-Y., Stathopulos, P. B., & Feng, Q. (2018). S-Nitrosylation of STIM1 by neuronal nitric oxide synthase inhibits store-operated Ca^{2+} entry. *Journal of Molecular Biology*. https://doi.org/10.1101/304022

Guo, L., Salt, T. E., Maass, A., Luong, V., Moss, S. E., Fitzke, F. W., & Cordeiro, M. F. (2006). Assessment of Neuroprotective Effects of Glutamate Modulation on Glaucoma-Related Retinal Ganglion Cell Apoptosis In Vivo. *Investigative Opthalmology & Visual Science*, *47*(2), 626. https://doi.org/10.1167/iovs.05-0754

Gupta, N., & Yücel, Y. H. (2007). Glaucoma as a neurodegenerative disease. *Current Opinion in Ophthalmology*, *18*(2), 110–114. https://doi.org/10.1097/ICU.0b013e3280895aea

Harada, T., Harada, C., Nakamura, K., Quah, H.-M. A., Okumura, A., Namekata, K., … Tanaka, K. (2007). The potential role of glutamate transporters in the pathogenesis of normal tension glaucoma. *Journal of Clinical Investigation*, *117*(7), 1763–1770. https://doi.org/10.1172/JCI30178

Hartmann, J., Dragicevic, E., Adelsberger, H., Henning, H. A., Sumser, M., Abramowitz, J., … Konnerth, A. (2008). TRPC3 Channels Are Required for Synaptic Transmission and Motor Coordination. *Neuron*, *59*(3), 392–398. https://doi.org/10.1016/j.neuron.2008.06.009

Hartmann, J., Karl, R. M., Alexander, R. P. D., Adelsberger, H., Brill, M. S., Rühlmann, C., … Konnerth, A. (2014). STIM1 Controls Neuronal Ca^{2+} Signaling, mGluR1-Dependent Synaptic Transmission, and Cerebellar Motor Behavior. *Neuron*, *82*(3), 635–644. https://doi.org/10.1016/J.NEURON.2014.03.027

Hashimoto, K., Ichikawa, R., Kitamura, K., Watanabe, M., & Kano, M. (2009). Translocation of a "Winner" Climbing Fiber to the Purkinje Cell Dendrite and Subsequent Elimination of "Losers" from the Soma in Developing Cerebellum. *Neuron*, *63*(1), 106–118. https://doi.org/10.1016/j.neuron.2009.06.008

Hill, A. J., Williams, C. M., Whalley, B. J., & Stephens, G. J. (2012). Phytocannabinoids as novel therapeutic agents in CNS disorders. *Pharmacology and Therapeutics*. Elsevier Inc. https://doi.org/10.1016/j.pharmthera.2011.09.002

Horton, A., Nash, K., Tackie-Yarboi, E., Kostrevski, A., Novak, A., Raghavan, A., …

Schiefer, I. T. (2018). Furoxans (Oxadiazole-4 N-oxides) with Attenuated Reactivity are Neuroprotective, Cross the Blood Brain Barrier, and Improve Passive Avoidance Memory. *Journal of Medicinal Chemistry*, *61*(10), 4593–4607. https://doi.org/10.1021/acs.jmedchem.8b00389

Huang, P. L., Dawson, T. M., Bredt, D. S., Snyder, S. H., & Fishman, M. C. (1993). Targeted disruption of the neuronal nitric oxide synthase gene. *Cell*, *75*(7), 1273–1286. https://doi.org/10.1016/0092-8674(93)90615-w

Hubener, J., Weber, J. J., Richter, C., Honold, L., Weiss, A., Murad, F., … Nguyen, H. P. (2013). Calpain-mediated ataxin-3 cleavage in the molecular pathogenesis of spinocerebellar ataxia type 3 (SCA3). *Human Molecular Genetics*, *22*(3), 508–518. https://doi.org/10.1093/hmg/dds449

Ihara, H., Kuwamura, M., Atsuta, M., Nihonmatsu, I., Okada, T., Mukamoto, M., & Kozaki, S. (2006). Expression of neuronal nitric oxide synthase variant, nNOS-μ, in rat brain. *Nitric Oxide - Biology and Chemistry*, *15*(1), 13–19. https://doi.org/10.1016/j.niox.2005.11.011

Iwama, K., Iwata, A., Shiina, M., Mitsuhashi, S., Miyatake, S., Takata, A., … Matsumoto, N. (2018). A novel mutation in SLC1A3 causes episodic ataxia. *Journal of Human Genetics*, *63*(2), 207–211. https://doi.org/10.1038/s10038-017-0365-z

Jen, J. C., & Wan, J. (2018). Episodic ataxias. In *Handbook of Clinical Neurology* (Vol. 155, pp. 205–215). Elsevier B.V. https://doi.org/10.1016/B978-0-444-64189-2.00013-5

Jin, Y., Kim, S. J., Kim, J., Worley, P. F., & Linden, D. J. (2007). Long-Term Depression of mGluR1 Signaling. *Neuron*, *55*(2), 277–287. https://doi.org/10.1016/j.neuron.2007.06.035

Kano, M., Hashimoto, K., Chen, C., Abeliovich, A., Aiba, A., Kurihara, H., … Tonegawa, S. (1995). Impaired synapse elimination during cerebellar development in PKCγ mutant mice. *Cell*, *83*(7), 1223–1231. https://doi.org/10.1016/0092-8674(95)90147-7

Kano, M., Hashimoto, K., Kurihara, H., Watanabe, M., Inoue, Y., Aiba, A., & Tonegawa, S. (1997). Persistent Multiple Climbing Fiber Innervationof Cerebellar Purkinje Cellsin Mice Lacking mGluR1. *Neuron*, *18*(1), 71–79. https://doi.org/10.1016/S0896-6273(01)80047-7

Kasumu, A., & Bezprozvanny, I. (2012). Deranged calcium signaling in purkinje cells and pathogenesis in spinocerebellar ataxia 2 (SCA2) and other ataxias. *Cerebellum*, *11*(3), 630–639. https://doi.org/10.1007/s12311-010-0182-9

Kim, Y., Wong, A. C. Y., Power, J. M., Tadros, S. F., Klugmann, M., Moorhouse, A. J., … Housley, G. D. (2012). Alternative Splicing of the TRPC3 Ion Channel Calmodulin/IP3 Receptor-Binding Domain in the Hindbrain Enhances Cation Flux. *Journal of Neuroscience*, *32*(33), 11414–11423. https://doi.org/10.1523/JNEUROSCI.6446-11.2012

Kirischuk, S, Kettenmann, H., & Verkhratsky, A. (1997). Na^{+}/Ca^{2+} exchanger modulates kainate-triggered Ca^{2+} signaling in Bergmann glial cells in situ. *The FASEB Journal*, *11*(7), 566–572. https://doi.org/10.1096/fasebj.11.7.9212080

Kirischuk, Sergei, Kettenmann, H., & Verkhratsky, A. (2007). Membrane currents and cytoplasmic sodium transients generated by glutamate transport in Bergmann glial cells. *Pflugers Archiv : European Journal of Physiology*, *454*(2), 245–252. https://doi.org/10.1007/s00424-007-0207-5

Kishimoto, Y., & Kano, M. (2006). Endogenous cannabinoid signaling through the CB1 receptor is essential for cerebellum-dependent discrete motor learning. *Journal of Neuroscience*, *26*(34), 8829–8837. https://doi.org/10.1523/JNEUROSCI.1236-06.2006

Klejman, M. E., Gruszczynska-Biegala, J., Skibinska-Kijek, A., Wisniewska, M. B., Misztal, K., Blazejczyk, M., … Kuznicki, J. (2009). Expression of STIM1 in brain and puncta-like co-localization of STIM1 and ORAI1 upon depletion of Ca^{2+} store in neurons. *Neurochemistry International*, *54*(1), 49–55. https://doi.org/10.1016/J.NEUINT.2008.10.005

Kriegsfeld, L. J., Eliasson, M. J., Demas, G. E., Blackshaw, S., Dawson, T. M., Nelson, R. J., & Snyder, S. H. (1999). Nocturnal motor coordination deficits in neuronal nitric oxide synthase knock-out mice. *Neuroscience*, *89*(2), 311–315. https://doi.org/S0306-4522(98)00614-9 [pii]

Kugler, P., & Drenckhahn, D. (1996). Astrocytes and Bergmann glia as an important site of nitric oxide synthase I. *Glia*, *16*(2), 165–173. https://doi.org/10.1002/(SICI)1098-1136(199602)16:2<165::AID-GLIA8>3.0.CO;2-2

Lee, K. J., Jung, J. G., Arii, T., Imoto, K., & Rhyu, I. J. (2007). Morphological changes in dendritic spines of Purkinje cells associated with motor learning. *Neurobiology of Learning and Memory*, *88*(4), 445–450. https://doi.org/10.1016/J.NLM.2007.06.001

Lev-Ram, V., Jiang, T., Wood, J., Lawrence, D. S., & Tsien, R. Y. (1997). Synergies and Coincidence Requirements between NO, cGMP, and Ca^{2+} in the Induction of Cerebellar Long-Term Depression. *Neuron*, *18*(6), 1025–1038. https://doi.org/10.1016/S0896-6273(00)80340-2

Lev-Ram, V., Makings, L. R., Keitz, P. F., Kao, J. P. Y., & Tsien, R. Y. (1995). Long-term depression in cerebellar Purkinje neurons results from coincidence of nitric oxide and depolarization-induced Ca^{2+} transients. *Neuron*, *15*(2), 407–415. https://doi.org/10.1016/0896-6273(95)90044-6

Lévénès, C., Daniel, H., Soubrié, P., & Crépel, F. (1998). Cannabinoids decrease excitatory synaptic transmission and impair long-term depression in rat cerebellar Purkinje cells. *Journal of Physiology*, *510*(3), 867–879. https://doi.org/10.1111/j.1469-7793.1998.867bj.x

Lippman, J. J., Lordkipanidze, T., Buell, M. E., Yoon, S. O., & Dunaevsky, A. (2008). Morphogenesis and regulation of Bergmann glial processes during Purkinje cell dendritic spine ensheathment and synaptogenesis. *GLIA*, *56*(13), 1463–1477. https://doi.org/10.1002/glia.20712

Löfvenberg, L., & Backman, L. (1999). Calpain-induced proteolysis of β-spectrins. *FEBS*

Letters, *443*(2), 89–92. https://doi.org/10.1016/S0014-5793(98)01697-4

Lordkipanidze, T., & Dunaevsky, A. (2005). Purkinje cell dendrites grow in alignment with Bergmann glia. *Glia*, *51*(3), 229–234. https://doi.org/10.1002/glia.20200

Lu, D.-W., Chen, Y.-H., Chang, C.-J., Chiang, C.-H., & Yao, H.-Y. (2014). Nitric oxide levels in the aqueous humor vary in different ocular hypertension experimental models. *The Kaohsiung Journal of Medical Sciences*, *30*(12), 593–598. https://doi.org/10.1016/j.kjms.2014.09.004

Mahmmoud, R. R., Sase, S., Aher, Y. D., Sase, A., Gröger, M., Mokhtar, M., … Lubec, G. (2015). Spatial and Working Memory Is Linked to Spine Density and Mushroom Spines. *PLOS ONE*, *10*(10), e0139739. https://doi.org/10.1371/journal.pone.0139739

Martínez-Lozada, Z., Hernández-Kelly, L. C., Aguilera, J., López-Bayghen, E., & Ortega, A. (2011). Signaling through EAAT-1/GLAST in cultured Bergmann glia cells. *Neurochemistry International*, *59*(6), 871–879. https://doi.org/10.1016/j.neuint.2011.07.015

Mason, C. A., Christakos, S., & Catalano, S. M. (1990). Early climbing fiber interactions with Purkinje cells in the postnatal mouse cerebellum. *Journal of Comparative Neurology*, *297*(1), 77–90. https://doi.org/10.1002/cne.902970106

Mattson, M., & Kater, S. (1987). Calcium regulation of neurite elongation and growth cone motility. *The Journal of Neuroscience*, *7*(12), 4034–4043. https://doi.org/10.1523/JNEUROSCI.07-12-04034.1987

Miyazaki, T., Yamasaki, M., Hashimoto, K., Kohda, K., Yuzaki, M., Shimamoto, K., … Watanabe, M. (2017). Glutamate transporter GLAST controls synaptic wrapping by Bergmann glia and ensures proper wiring of Purkinje cells. *Proceedings of the National Academy of Sciences of the United States of America*, *114*(28), 7438–7443. https://doi.org/10.1073/pnas.1617330114

Nanri, K., Niwa, H., Mitoma, H., Takei, A., Ikeda, J., Harada, T., … Mizusawa, H. (2013). Low-Titer Anti-GAD-Antibody-Positive Cerebellar Ataxia.

https://doi.org/10.1007/s12311-012-0411-5

Naskar, R., Vorwerk, C. K., & Dreyer, E. B. (2000). Concurrent downregulation of a glutamate transporter and receptor in glaucoma. *Investigative Ophthalmology & Visual Science*, *41*(7), 1940–1944. Retrieved from http://www.ncbi.nlm.nih.gov/pubmed/10845620

Nelson, R., Demas, G., Huang, P., Fishman, M., Dawson, V., Dawson, T., & Snyder, S. (1995). Behavioural abnormalities in male mice lacking neuronal nitric oxide synthase. *Nature*, *378*(6555), 383–386. https://doi.org/10.1038/378383a0

Neufeld, A. H. (1999). Nitric Oxide. *Survey of Ophthalmology*, *43*(6 SUPPL.), S129–S135. https://doi.org/10.1016/S0039-6257(99)00010-7

Nikkuni, O., Takayasu, Y., Iino, M., Tanaka, K., & Ozawa, S. (2007). Facilitated activation of metabotropic glutamate receptors in cerebellar Purkinje cells in glutamate transporter EAAT4-deficient mice. *Neuroscience Research*, *59*(3), 296–303. https://doi.org/10.1016/j.neures.2007.07.006

Nishisako, M., Meguro, A., Nomura, E., Yamane, T., Takeuchi, M., Ota, M., … Mizuki, N. (2016). SLC1A1 Gene Variants and Normal Tension Glaucoma: An Association Study. *Ophthalmic Genetics*, *37*(2), 194–200. https://doi.org/10.3109/13816810.2015.1028649

Norris, P. J., Waldvogel, H. J., Faull, R. L. M., Love, D. R., & Emson, P. C. (1996). Decreased neuronal nitric oxide synthase messenger RNA and somatostatin messenger RNA in the striatum of Huntington's disease. *Neuroscience*, *72*(4), 1037–1047. https://doi.org/10.1016/0306-4522(95)00596-X

Offermanns, S., Hashimoto, K., Watanabe, M., Sun, W., Kurihara, H., Thompson, R. F., … Simon, M. I. (1997). Impaired motor coordination and persistent multiple climbing fiber innervation of cerebellar Purkinje cells in mice lacking G q. *Proceedings of the National Academy of Sciences*, *94*(25), 14089–14094. https://doi.org/10.1073/pnas.94.25.14089

Orsucci, D., Raglione, L. M., Mazzoni, M., & Vista, M. (2019). Therapy of episodic ataxias: case report and review of the literature. *Drugs in Context*, *8*, 1–6. https://doi.org/10.7573/dic.212576

Osborne, N. N. (2010). Mitochondria: Their role in ganglion cell death and survival in primary open angle glaucoma. *Experimental Eye Research*, *90*(6), 750–757. https://doi.org/10.1016/j.exer.2010.03.008

Patel, S., & Hillard, C. J. (2001). Cannabinoid CB1 Receptor Agonists Produce Cerebellar Dysfunction in Mice. *Journal of Pharmacology and Experimental Therapeutics*, *297*(2).

Perkins, E. M., Clarkson, Y. L., Suminaite, D., Lyndon, A. R., Tanaka, K., Rothstein, J. D., … Jackson, M. (2018). Loss of cerebellar glutamate transporters EAAT4 and GLAST differentially affects the spontaneous firing pattern and survival of Purkinje cells. *Human Molecular Genetics*, *27*(15), 2614–2627. https://doi.org/10.1093/hmg/ddy169

Pouzat, C., & Hestrin, S. (1997). Developmental Regulation of Basket/Stellate Cell→Purkinje Cell Synapses in the Cerebellum. *The Journal of Neuroscience*, *17*(23), 9104–9112. https://doi.org/10.1523/JNEUROSCI.17-23-09104.1997

Prilloff, S., Noblejas, M. I., Chedhomme, V., & Sabel, B. A. (2007). Two faces of calcium activation after optic nerve trauma: life or death of retinal ganglion cells in vivo depends on calcium dynamics. *European Journal of Neuroscience*, *25*(11), 3339–3346. https://doi.org/10.1111/j.1460-9568.2007.05550.x

Rami, A., Ferger, D., & Krieglstein, J. (1997). Blockade of calpain proteolytic activity rescues neurons from glutamate excitotoxicity. *Neuroscience Research*, *27*(1), 93–97. https://doi.org/10.1016/S0168-0102(96)01123-6

Reitstetter, R., & Yool, A. J. (1998). Morphological consequences of altered calcium-dependent transmembrane signaling on the development of cultured cerebellar Purkinje neurons. *Developmental Brain Research*, *107*(1), 165–167.

https://doi.org/10.1016/S0165-3806(98)00017-0

Rhyu, I. J., Nahm, S. S., Hwang, S. J., Kim, H., Suh, Y. S., Oda, S. I., … Abbott, L. C. (2003). Altered neuronal nitric oxide synthase expression in the cerebellum of calcium channel mutant mice. *Brain Research*, *977*(2), 129–140. https://doi.org/10.1016/S0006-8993(03)02403-X

Rodríguez-Cueto, C., Benito, C., Romero, J., Hernández-Gálvez, M., Gómez-Ruiz, M., & Fernández-Ruiz, J. (2014). Endocannabinoid-hydrolysing enzymes in the post-mortem cerebellum of humans affected by hereditary autosomal dominant ataxias. *Pathobiology*, *81*(3), 149–159. https://doi.org/10.1159/000358127

Rose, C. R., Ziemens, D., & Verkhratsky, A. (2020). On the special role of NCX in astrocytes: Translating Na^+-transients into intracellular Ca^{2+} signals. *Cell Calcium*, *86*, 102154. https://doi.org/10.1016/j.ceca.2019.102154

Safo, P. K., & Regehr, W. G. (2005). Endocannabinoids control the induction of cerebellar LTD. *Neuron*, *48*(4), 647–659. https://doi.org/10.1016/j.neuron.2005.09.020

Santamaria, F., Wils, S., De Schutter, E., & Augustine, G. J. (2006). Anomalous Diffusion in Purkinje Cell Dendrites Caused by Spines. *Neuron*, *52*(4), 635–648. https://doi.org/10.1016/j.neuron.2006.10.025

Schumacher, P. A., Siman, R. G., & Fehlings, M. G. (2002). Pretreatment with Calpain Inhibitor CEP-4143 Inhibits Calpain I Activation and Cytoskeletal Degradation, Improves Neurological Function, and Enhances Axonal Survival After Traumatic Spinal Cord Injury. *Journal of Neurochemistry*, *74*(4), 1646–1655. https://doi.org/10.1046/j.1471-4159.2000.0741646.x

Secondo, A., Molinaro, P., Pannaccione, A., Esposito, A., Cantile, M., Lippiello, P., … Annunziato, L. (2011). Nitric oxide stimulates NCX1 and NCX2 but inhibits NCX3 isoform by three distinct molecular determinants. *Molecular Pharmacology*, *79*(3), 558–568. https://doi.org/10.1124/mol.110.069658

Shiwaku, H., Yagishita, S., Eishi, Y., & Okazawa, H. (2013). Bergmann glia are reduced

in spinocerebellar ataxia type 1. *NeuroReport*, *24*(11), 620–625. https://doi.org/10.1097/WNR.0b013e32836347b7

Sorimachi, H., Ishiura, S., & Suzuki, K. (1997). Structure and physiological function of calpains. *Biochemical Journal*, *328*(3), 721–732. https://doi.org/10.1042/bj3280721

Sucher, N. J., Lei, S. Z., & Lipton, S. A. (1991). Calcium channel antagonists attenuate NMDA receptor-mediated neurotoxicity of retinal ganglion cells in culture. *Brain Research*, *551*(1–2), 297–302. https://doi.org/10.1016/0006-8993(91)90944-Q

Sugawara, T., Hisatsune, C., Miyamoto, H., Ogawa, N., & Mikoshiba, K. (2017). Regulation of spinogenesis in mature Purkinje cells via mGluR/PKC-mediated phosphorylation of CaMKIIβ. *Proceedings of the National Academy of Sciences of the United States of America*, *114*(26), E5256–E5265. https://doi.org/10.1073/pnas.1617270114

Tada, M., Nishizawa, M., & Onodera, O. (2016). Roles of inositol 1,4,5-trisphosphate receptors in spinocerebellar ataxias. *Neurochemistry International*, *94*, 1–8. https://doi.org/10.1016/J.NEUINT.2016.01.007

Takatsuru, Y., Takayasu, Y., Iino, M., Nikkuni, O., Ueda, Y., Tanaka, K., & Ozawa, S. (2006). Roles of glial glutamate transporters in shaping EPSCs at the climbing fiber-Purkinje cell synapses. *Neuroscience Research*, *54*(2), 140–148. https://doi.org/10.1016/j.neures.2005.11.002

Takuma, K., Ago, Y., & Matsuda, T. (2013). The glial sodium-calcium exchanger: a new target for nitric oxide-mediated cellular toxicity. *Current Protein & Peptide Science*, *14*(1), 43–50. https://doi.org/10.2174/1389203711314010007

Tellios, V., Maksoud, M. J. E., Xiang, Y. Y., & Lu, W. Y. (2020). Nitric Oxide Critically Regulates Purkinje Neuron Dendritic Development Through a Metabotropic Glutamate Receptor Type 1–Mediated Mechanism. *Cerebellum*, *19*(4), 510–526. https://doi.org/10.1007/s12311-020-01125-7

Tezel, G. (2008). TNF-α signaling in glaucomatous neurodegeneration. In *Progress in*

Brain Research (Vol. 173, pp. 409–421). https://doi.org/10.1016/S0079-6123(08)01128-X

Tham, Y. C., Li, X., Wong, T. Y., Quigley, H. A., Aung, T., & Cheng, C. Y. (2014). Global prevalence of glaucoma and projections of glaucoma burden through 2040: A systematic review and meta-analysis. *Ophthalmology*, *121*(11), 2081–2090. https://doi.org/10.1016/j.ophtha.2014.05.013

Tiburcio-Félix, R., Cisneros, B., Hernández-Kelly, L. C. R., Hernández-Contreras, M. A., Luna-Herrera, J., Rea-Hernández, I., … Ortega, A. (2019). Neuronal Nitric Oxide Synthase in Cultured Cerebellar Bergmann Glia: Glutamate-Dependent Regulation. *ACS Chemical Neuroscience*, *10*(6), 2668–2675. https://doi.org/10.1021/acschemneuro.8b00656

Vanderklish, P. W., & Edelman, G. M. (2002). Dendritic spines elongate after stimulation of group 1 metabotropic glutamate receptors in cultured hippocampal neurons. *Proceedings of the National Academy of Sciences*, *99*(3), 1639–1644. https://doi.org/10.1073/pnas.032681099

Vosler, P. S., Brennan, C. S., & Chen, J. (2008). Calpain-mediated signaling mechanisms in neuronal injury and neurodegeneration. *Molecular Neurobiology*, *38*(1), 78–100. https://doi.org/10.1007/s12035-008-8036-x

Wang, D.-J., Su, L.-D., Wang, Y.-N., Yang, D., Sun, C.-L., Zhou, L., … Shen, Y. (2014). Long-Term Potentiation at Cerebellar Parallel Fiber-Purkinje Cell Synapses Requires Presynaptic and Postsynaptic Signaling Cascades. *Journal of Neuroscience*, *34*(6), 2355–2364. https://doi.org/10.1523/JNEUROSCI.4064-13.2014

Wang, X., Imura, T., Sofroniew, M. V., & Fushiki, S. (2011). Loss of adenomatous polyposis coli in Bergmann glia disrupts their unique architecture and leads to cell nonautonomous neurodegeneration of cerebellar Purkinje neurons. *Glia*, *59*(6), 857–868. https://doi.org/10.1002/glia.21154

Weinreb, R. N., Aung, T., & Medeiros, F. A. (2014). The Pathophysiology and Treatment

of Glaucoma. *JAMA*, *311*(18), 1901. https://doi.org/10.1001/jama.2014.3192

Xing, G., Chavko, M., Zhang, L. X., Yang, S., & Post, R. M. (2002). Decreased calcium-dependent constitutive nitric oxide synthase (cNOS) activity in prefrontal cortex in schizophrenia and depression. *Schizophrenia Research*, *58*(1), 21–30. https://doi.org/10.1016/S0920-9964(01)00388-7

Xu, H., Yang, Y., Tang, X., Zhao, M., Liang, F., Xu, P., … Fan, X. (2013). Bergmann glia function in granule cell migration during cerebellum development. *Molecular Neurobiology*, *47*(2), 833–844. https://doi.org/10.1007/s12035-013-8405-y

Yamada, K., Fukaya, M., Shibata, T., Kurihara, H., Tanaka, K., Inoue, Y., & Watanabe, M. (2000). Dynamic transformation of Bergmann glial fibers proceeds in correlation with dendritic outgrowth and synapse formation of cerebellar Purkinje cells. *The Journal of Comparative Neurology*, *418*(1), 106–120. https://doi.org/10.1002/(SICI)1096-9861(20000228)418:1<106::AID-CNE8>3.0.CO;2-N

Yanagisawa, M., Aida, T., Takeda, T., Namekata, K., Harada, T., Shinagawa, R., & Tanaka, K. (2015). Arundic acid attenuates retinal ganglion cell death by increasing glutamate/aspartate transporter expression in a model of normal tension glaucoma. *Cell Death & Disease*, *6*(3), e1693. https://doi.org/10.1038/cddis.2015.45

Yang, Y., & Lisberger, S. G. (2014). Purkinje-cell plasticity and cerebellar motor learning are graded by complex-spike duration. *Nature*, *510*(7506), 529–532. https://doi.org/10.1038/nature13282

Yoshida, T., Hashimoto, K., Zimmer, A., Maejima, T., Araishi, K., & Kano, M. (2002). The Cannabinoid CB1 Receptor Mediates Retrograde Signals for Depolarization-Induced Suppression of Inhibition in Cerebellar Purkinje Cells. *The Journal of Neuroscience*, *22*(5), 1690–1697. https://doi.org/10.1523/JNEUROSCI.22-05-01690.2002

Chapter 6

6 Appendix

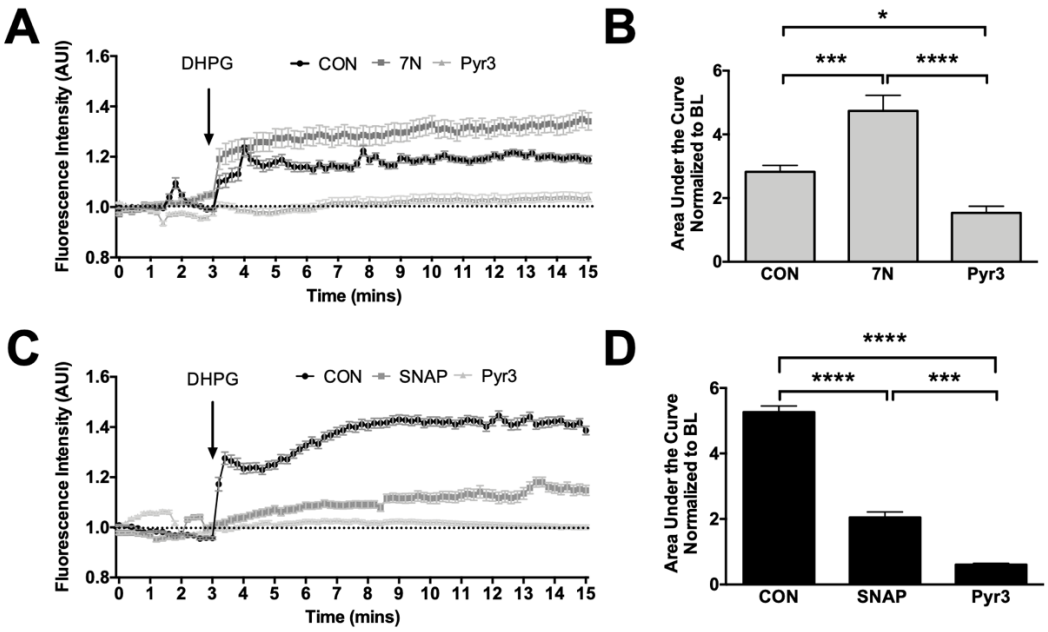

Figure 6.A1 NO modulation affects mGluR1-initiated calcium influx in WT and nNOS$^{-/-}$ PNs in culture.

(**A**) Representative time course of calcium influx in response to application of DHPG, denoted by the black arrow. The black line represents the calcium influx of WT PNs without a pre-treatment (CON), while the grey line represents WT PNs pre-treated with 7N and the light grey line represents TRPC3 inhibitor Pyr3. Black, dotted line represents baseline calcium conductance. (**B**) Bar graph represents the area under the curve (AUC) for each pre-treatment visualized in (**A**) after DHPG treatment. (**C**) Representative time course of calcium influx in response to application of DHPG, denoted by the black arrow. The black line represents the calcium influx of nNOS$^{-/-}$ PNs without a pre-treatment (CON), while the grey line represents nNOS$^{-/-}$ PNs pre-treated with SNAP and the light grey line represents Pyr3. Black, dotted line represents baseline calcium conductance. (**B**) Bar graph represents the area under the curve (AUC) for each pre-treatment visualized in (**A**) after DHPG treatment.

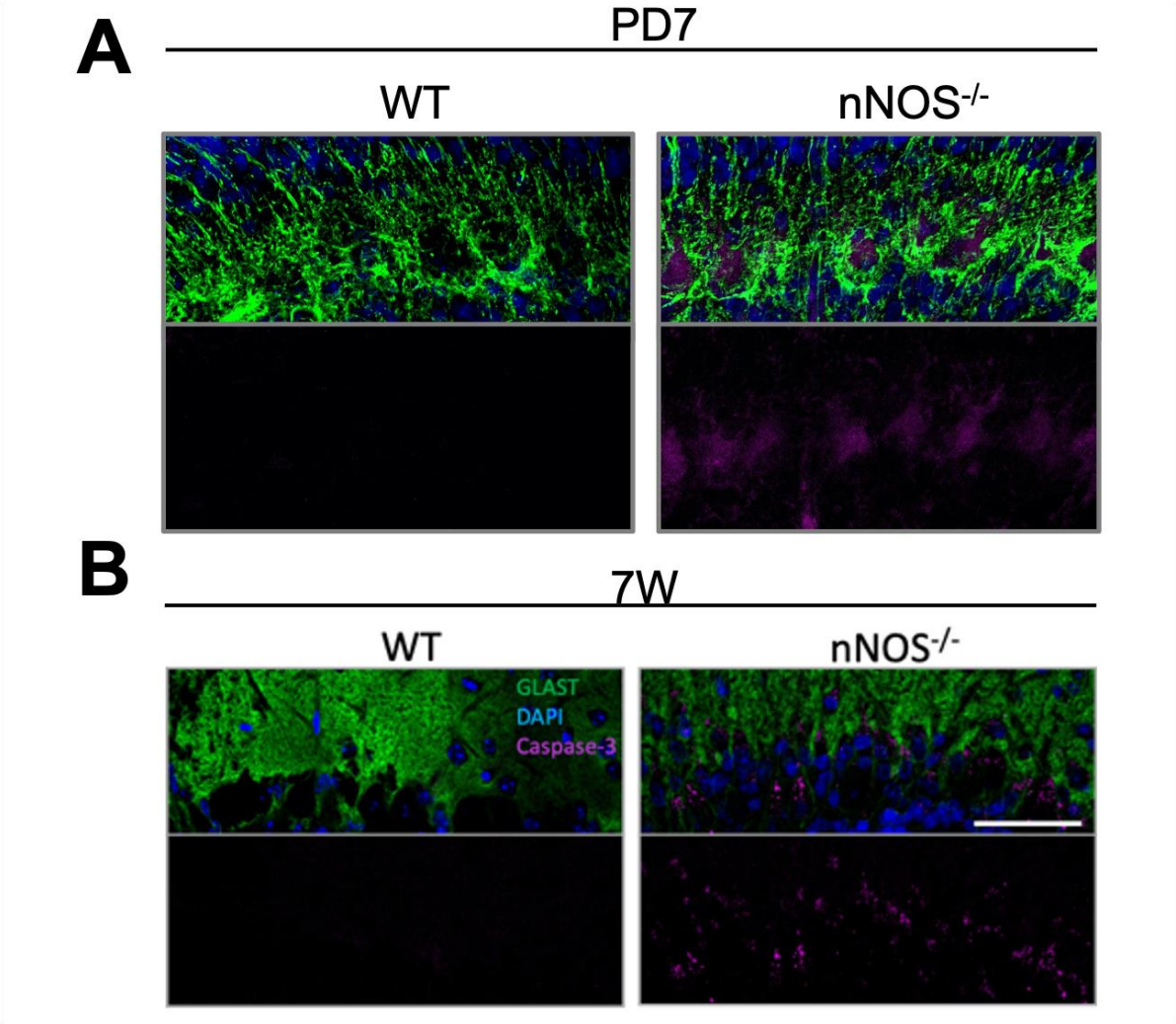

Figure 6.A2 nNOS$^{-/-}$ PN somata express caspase-3 expression at PD7 and 7W.

(**A**) Representative confocal images of PD7 WT and nNOS$^{-/-}$ cerebellar tissues stained with DAPI (blue), GLAST (green), and caspase-3 (magenta). (**B**) Representative confocal images of 7W WT and nNOS$^{-/-}$ cerebellar tissues stained with DAPI (blue), GLAST (green), and caspase-3 (magenta). Scale bar represents 50 µm.

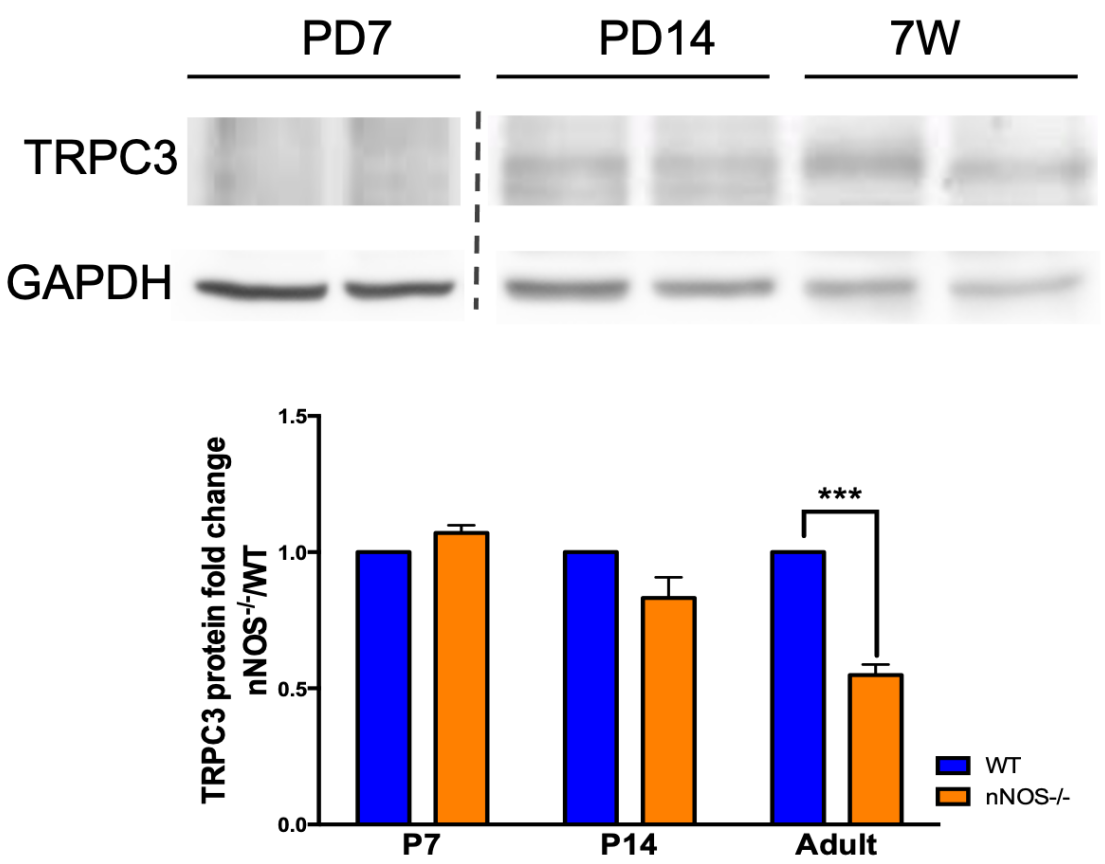

Figure 6.A3 TRPC3 expression is significantly decreased in 7W nNOS$^{-/-}$ cerebella compared to WT.

Representative western blot of total TRPC3 and GAPDH protein for PD7, PD14, and 7W WT and nNOS$^{-/-}$ cerebella. Bar graph represents the fold change of TRPC3 protein normalized to GAPDH. $N = 3$ biological replicates per group. $P < 0.001$.

7 Curriculum Vitae

VASILIKI TELLIOS

EDUCATION

The University of Western Ontario, London, ON

Doctor of Philosophy (Ph.D.) Neuroscience **2016 – 2021**

- The role of nNOS in the development of cerebellar networks in mice.
- Supervisor: Dr. Wei-Yang Lu

Honours Bachelor of Science (H.B.Sc.) **2016**

- Honours Specialization: Kinesiology
- Major: Classical Studies

PUBLICATIONS

Vasiliki Tellios[1], Matthew J.E. Maksoud, Ravneet Nagra, and Wei-Yang Lu, Neuronal nitric oxide synthase critically regulates the endocannabinoid pathway in the cerebellum during postnatal development. **In preparation.**

Vasiliki Tellios[1], Matthew J.E. Maksoud, and Wei-Yang Lu, The expression and function of GLAST in Bergmann glia are critically regulated by neuronal nitric oxide synthase-derived nitric oxide. **In preparation.**

Matthew J.E. Maksoud, **Vasiliki Tellios**, Yun-Yan Xiang, and Wei-Yang Lu, Nitric oxide displays a biphasic effect on calcium dynamics in microglia. *Nitric oxide.* (2021) 10.1016/j.niox.2021.01.0015.

Matthew J.E. Maksoud, **Vasiliki Tellios**, and Wei-Yang Lu, Nitric oxide attenuates murine microglia proliferation by sequentially facilitating calcium influx through TRPV2 channels, activating NFATC2, and increasing p21 transcription signaling. *Cell cycle*. (2021). 10.1080/15384101.2021.1877936.

Vasiliki Tellios[1], Matthew J.E. Maksoud, Yun-Yan Xiang, and Wei-Yang Lu, Nitric oxide is a critical regulator of Purkinje neuron dendritic morphology through a metabotropic glutamate receptor type-1 mediated mechanism. *The Cerebellum*. (2020). https://doi.org/10.1007/s12311-020-01125-7.

Matthew J.E. Maksoud, **Vasiliki Tellios**, Yun-Yan Xiang, and Wei-Yang Lu, Nitric oxide signaling inhibits microglia proliferation by activation of protein kinase-G, *Nitric Oxide.* 94 (2019) 125–134. https://doi.org/10.1016/j.niox.2019.11.005

Matthew J.E. Maksoud, **Vasiliki Tellios**, Dong An, Yun-Yan Xiang, and Wei-Yang Lu, Nitric Oxide upregulates microglia phagocytosis and increases transient receptor potential vanilloid type 2 channel expression on the plasma membrane, *Glia.* 67 (2019) 2294–2311. https://doi.org/10.1002/glia.23685

Nikoleta Tellios, Mary Feng, Nancy Chen, Hong Liu, **Vasiliki Tellios**, Mary Wang, Xiangji Li, Caitlin Chang, and Cindy Hutnik, Mechanical stretch upregulates connexin43 in human trabecular meshwork cells. *Clinical and experimental ophthalmology.* (2019). 10.1111/ceo.13492

Vasiliki Tellios[1], Hong Liu, Nikoleta Tellios, Xiangji Li, and Cindy Hutnik, Administration of nitric oxide through a novel copper-chitosan delivery system in human corneal and limbal epithelial cell injury. *Investigative ophthalmology and visual science*. (2018). 10.1167/iovs.17-23044

PUBLISHED ABSTRACTS

V. Tellios, M. J.-E. Maksoud, R. Nagra, W.-Y. Lu, Cannabinoid-1 receptor dysregulation during cerebellar development in nNOS$^{-/-}$ mice. Canadian Association for Neuroscience. 2020. **cancelled due to COVID-19*

V. Tellios, M. J.-E. Maksoud, Y.-Y. Xiang, W.-Y. Lu, Bergmann glia morphology and GLAST expression is downregulated in nNOS-/- cerebellum. Canadian Association for Neuroscience. 2019.

M. J.-E. Maksoud, V. Tellios, Y.-Y. Xiang, W.-Y. Lu, Nitric oxide production from iNOS inhibits microglia proliferation via TRPV2-mediated calcium influx. Canadian Association for Neuroscience. 2019

V. Tellios, M. J.-E. Maksoud, Y.-Y. Xiang, W.-Y. Lu., Neuronal nitric oxide synthase in the cerebellum: Implications on development of the parallel fiber-Purkinje neuron synapse in mice. Society for Neuroscience. 2018.

M. J.-E. Maksoud, V. Tellios, D. An, Y.-Y. Xiang, W.-Y. Lu, Nitric oxide regulates transient receptor potential vanilloid type 2 channel trafficking in microglia. Society for Neuroscience. 2018.

ACADEMIC AWARDS, Scholarships & Funding

Best 2020 Glaucoma Paper for a Graduate Student

Canadian Glaucoma Society

Awarded to the best paper published between 2019-2020 within the field of glaucoma research, $500.

Cayman Chemical Travel Award

Cayman Chemical Company.

In support for CAN 2019 travels (Toronto, ON), $250 USD. **2019**

In support for SFN 2018 travels (Sand Diego, CA), $300 USD. **2018**

Ontario Graduate Scholarship

The University of Western Ontario, London, ON

In support for graduate study in science and technology, $15,000. **2018**

Robarts Research Retreat Oral Presentation Award

The University of Western Ontario, London, ON

One of six oral presenters selected, $100. **2018**

Physiology & Pharmacology Research Day Poster Award

The University of Western Ontario, London, ON

Awarded to the best poster presentation, $200. **2017**

Robarts Research Retreat Poster Award

The University of Western Ontario, London, ON

Awarded to the best poster presentation, $200. **2017**

Department of Ophthalmology Award

The University of Western Ontario, London, ON

Awarded to the best undergraduate oral presentation, $1000. **2016**

Trainee Travel Award

Form and function in Ocular Disease Symposium, Halifax, NS

Awarded one of four national travel awards, $1500. **2016**

TEACHING EXPERIENCE

The University of Western Ontario, London, ON

Western Certificate in University Teaching and Learning. **2020**

Developed active learning techniques to engage students and promote learning.
Learned different methods to plan and facilitate discussions within the classroom.
Developed a syllabus and curriculum for a novel course: *Cerebellar Motor Disorders: Mechanisms and Pathogenesis.*
Revised current teaching strategies to develop a more constructive and effective student learning experience.

Head Teaching Assistant – Special Topics in Medical Sciences (MedSci 4930Z) **2020 - 2021**

Trained and assisted other TAs on ways to mark various assignments.
Organized grading sheets and ensured marks were released to students on time.
Worked closely with course professor to ensure efficiency and consistency across online platform.

Teaching Assistant – Special Topics in Medical Sciences (MedSci 4930F/G) **2016 - 2020**

Responsible for marking assignments and providing effective feedback.
Answered student emails addressing concerns about marks or course content.
Designed and presented various hot topic tutorials.

Project Supervisor Roles **2017 – 2021**

Supervised Students in wet lab research.
Developed & discussed research proposals while emphasizing previous literature.
Explained laboratory procedures & techniques with emphasis on safety protocols.
Managed students' progress and helped with technique troubleshooting.
Guided basic neuroanatomy learning on the weekly basis.

Project Supervisor – Physiology & Pharmacology Thesis (4980E; 5 Students) **2016 – 2020**

Anmol Gill – Project: Autocrine GABA signaling in SH-SY5Y cell differentiation. 2020

Donghyun Lee – Project: Regulation of TRPV channels in PC12 cells by nitric oxide. *Accepted to the Schulich School of Medicine Program at the University of Western Ontario*. 2018

Abdelheady Osman – Project: Nitric oxide critically regulates Bergmann glia morphology *in vivo*. 2017

Dong An – Project: Nitric oxide regulation of TRPV2 plasma membrane expression in BV2 cells. *Accepted to the University of Toronto Medical Program*. 2016

2016

Yimo Wang – Project: Autocrine GABA signaling in SH-SY5Y cells. *Accepted to the Physiotherapy Program at McMaster University*.

2019 – 2020

Project Supervisor – Neuroscience (4000E; 2 Students) 2020

Vlad Marinescu – Project: Examining changes in cerebellar microglia morphology according to nitric oxide synthase expression. 2019

Ravneet Nagra – Project: Regulation of the endocannabinoid system by nitric oxide in cerebellar Purkinje neurons.

2017 – 2019

Partners in Experiential Learning Supervisor – (Co-op; 4 Students) 2019

Katie Schornagel – Project: Changes in microglial morphology according to nitric oxide synthase expression. 2018

Sharisse Velasquez – Project: Changes in microglial morphology according to nitric oxide synthase expression 2017

Mridula Debnath – Project: Changes in microglial morphology according to nitric oxide synthase expression 2017

Ching Yuan – Project: Changes in microglial morphology according to nitric oxide synthase expression

2015

Teaching Assistant Training Program Certificate

Uncovered the basics behind effective lecture styles for science-specific teaching.